SISSA
Scuola Internazionale Superiore di Studi Avanzati

Neuroscience Area – PhD course in

Neurobiology

Cell-type specific gene delivery using chemically modified AAV vectors

Candidate:

Alessandro Barenghi

Advisor:

Prof. Paul A. Heppenstall

Co-advisors:

Prof. Anna Menini

Prof. Michele Giugliano

Prof. Nereo Kalebic

Prof. Ewan St. John Smith

Academic Year 2021-22

ABSTRACT

In the last years the use of Adeno-Associated Viruses (AAVs) as carriers for gene transfer became increasingly popular for both research and clinical applications. Besides their excellent safety profile, the existence of various AAV serotypes characterized by different proprieties is exploited in the context of gene therapy to target a broad range of diseases. However, currently used techniques to re-direct AAV tropism still present many drawbacks. With this project, we have developed a tool that could enable cell-type specific reprogramming of viral tropism based of post-production chemical modifications of the vectors. By using AAV2 as representative serotype, we patented a method to chemically coupling targeting ligands by exploiting naturally occurring functional groups present on viral capsid. In particular, we have employed different heterobifunctional crosslinker molecules to couple the lectins Wheat Germ Agglutinin (WGA) and Griffonia Simplicifolia Isolectin B4 (IB4), the protein Nerve Growth Factor (NGF) and the Protease-Activated Receptor 1 (PAR1) agonist peptide SFLLRN directly with the amine groups (-NH_2) present on lysine residues that compose AAV viral proteins (VPs). After in vitro validation and optimization of modified vectors, their efficiency and acquired specificity were assessed in a mouse model, where we were able to confirm correct re-targeting of viral tropism and acquired accurate cell-type specificity. Moreover, we have explored other possible applications of our tool, including boosting transduction efficiency of different AAV serotypes and conferring particular proprieties such as increased permeability for cellular barriers. Due to its versatility, the technology we have developed could be exploited in different fields of basic and applied research and could have a major impact on gene therapy approaches. Furthermore, being it based on simple click chemistry reactions, it could allow for streamlined modification of different class of viruses, thus offering a valid and more flexible alternative to currently used methods to re-direct viral tropism based on genetic modifications.

LIST OF ABBREVIATIONS

AAP - Assembly-Activating Protein

AAV - Adeno-Associated Virus

AAVR - Adeno-Associated Virus Receptor

AB - Antibody

AD - Adenovirus

ANS - Autonomic Nervous System

BBB - Blood Brain Barrier

BC - Basic Cluster

BG - Benzylguanine

BME - Betamercaptoethanol

BMEC - Brain Microvascular Endothelial Cells

CAG - CMV early enhancer/chicken β actin

CAR – Chimeric Antigen Receptor

CGRP - Calcitonin Gene Related Peptide

CMV - Cytomegalovirus

CNS – Central Nervous System

CSF - Cerebrospinal Fluid

DARPIN - Designed Ankyrin Repeat Proteins

DBCO - Dibenzocyclooctyne

DTT - Dithiothreitol

EDC - 1-Ethyl-3-(3-dimethylaminopropy)

GDNF - Glia ell-Derived Neurotrophic Factor

GLcNAc - N-acetylglucosamine

GLS - Griffonia Simplicifolia Lectin

GPR - G-protein Coupled Receptor

GTP – Guanosine Triphosphate

HRP - Horseradish Peroxidase

HSC – Hematopoietic Stem Cell

HSPG – Heparan Sulfate Proteoglycan

IB4 – Isolectin B4

IFN – Interferon

ITR – Inverted Terminal Repeat

LTR – Long Terminal Repeat

MMP - Matrix Metalloprotease

MOI – Multiplicity of Infection

MW – Molecular Weight

NGF – Nerve Growth Factor

NHS – N-Hydroxylsuccinimide

NLS – Nuclear Localization Signal

NPC - Nuclear Pore Complex

ORF – Open Reading Frame

PAR1 – Protease Activated Receptor 1

PDK - Polycystic Kidney Domain

PEG – Polyethylene Glycol

PEI - Polyethylenimine

PLL – Poly-L-Lysine

PLS - Phospholipase AV2

PNS – Peripheral Nervous System

RBE - Rep Binding Element

RC - Replication Competent

RD - Replication Defective

RRE - rev Responsive Element

RTC - Reverse Transcription Complex

scAAV - Self-Complementary AAV

SNS - Sympathetic Nervous System

SV40 - Simian Virus 40

TNG - Trans-Golgi Network

trkA - Tropomyosin Receptor Kinase A

TRS - Terminal Resolution Site

UAA - Unnatural Amino Acid

VG - Viral Genome

VP (1/2/3) - Viral Protein (1/2/3)

WGA – Wheat Germ Agglutinin

WPRE - Woodchuck Hepatitis Virus Posttranscriptional Regulatory Element

TABLE OF CONTENTS

1 INTRODUCTION

1.1 THE PERIPHERAL NERVOUS SYSTEM

To be able to perceive and to react to different stimuli coming from the outside or from the inside of our body is the basis of our ability to adapt and to survive. To date, the first neuronal cells have appeared more than 600 million years ago in the *cnidaria* phylum, and probably there was an initial outline of nervous system even before, in demosponges (Sakarya et al., 2007).

The peripheral nervous system (PNS) is the division of the nervous system that encompasses all the nervous tissues which lie outside of the central nervous system (CNS). Its main role is to connect the peripheral tissues and organs directly to the brain and the spinal cord, which compose the CNS. The PNS relays sensory information to the CNS and transmits all the impulses which are generated at

central level directly to the organs involved in different tasks, including voluntary movements and autonomic functions. Of note, even the easier task requires the integration of a lot of different sensory, motor and motivational stimuli, reason why all these functional pathways are organized in different and well-defined structures, called generically “nuclei”.

The study of the nervous system has its roots in a very old time, the ancient Greek: the word “nerve”, indeed, comes from Greek and means “tendon”. In the past, many people have tried to understand how the stimuli are transmitted through the body. The first theory comes from a roman physician, Galen, who believed that the nerves controlled the actions of muscles, and that the two main functions of the nervous system, sensation and motion, were governed by different fibers. Still, we need to wait until the Renaissance to have a better understanding of the nervous system, and the 1681 for the word “neurology” to appear in the English dictionary.

1.1.1 Organization of the peripheral nervous system

The PNS is made of two main components, which are the autonomic nervous system and the somatic nervous system.

The autonomic nervous system (ANS) – known also as vegetative nervous system, is the part of the nervous system that primarily controls and modulates the functions of the visceral organs. It innervates smooth muscle and glands, thereby regulating the functions of internal organs. The main functions of the ANS include the control of internal temperature, hearth and respiratory rate, digestion and sexual behaviour, plus eventually some reflex actions as vomit and sneezing (Principles of Neural Science. E. Kandel 2016). Even if the ANS is mainly involuntary, it is closely integrated with all the behaviors which are controlled by the voluntary somatic nervous system: every physical action we perform, such as running, expect complex metabolic needs and cause thermoregulatory modifications which are operated by the ANS through variation of the blood flow, cardiac output, ventilation and so on.

The ANS is, in turn, divided into three parts: sympathetic (“fight or flight”), parasympathetic (“rest and digest”) and enteric (gastrointestinal functions) nervous system.

The somatic Nervous System (SNS) – known also as voluntary nervous system or somatosensory system, it acts on skeletal muscles to drive voluntary control of body movements. It is composed of afferent sensory nerves which bring stimuli from the environment to the CNS and by efferent motor nerves which relay the commands from the CNS to the body, typically ending in muscular contraction.

The first step of sensory transduction, which is the transformation of the sensory stimulus into an action potential, is operated by sensory neurons, cells that are activated by sensory input from the environment**.** When we talk about somatosensation we usually think about the touch. However, this word is used to indicate a group of senses, which include temperature, itch, proprioception and, finally, pain. The first big difference between the somatosensory system and the other sensory pathways is at the level of the receptors. While for the other sensations the receptors are located in specific organs, the primary sensory neurons involved in somatosensation are distributed all over

the skin and inside the body (muscle and joint). Most of these receptors are specialized nerve endings, which are incapsulated in the cells of surrounding tissues and optimized for the different kind of stimuli. Moreover, all the different sensory modalities are perceived and processed by different pathways and specific cells. For example, talking about the touch, Merkel cells respond to sustained touch and pressure, Ruffini's end sense stretch, Pacini corpuscles sense fast vibration and deep pressure, Meissner's corpuscles are involved in slow vibration and hair follicles are triggered by light touch and air currents (Sadler & Stucky, 2019).

The typical somatosensory pathway is composed by three orders of neurons. Sensory neurons (first-order) are pseudounipolar neurons which have their cell body in the dorsal root ganglia (DRG) of the spinal nerve. Their peripheral axon innervates or directly form the peripheral sensory receptor, while the central axon reaches the spinal cord where synapses on the second-order neuron. The only exception is for the nerves innervating the parts of the head and neck not covered by cervical nerves, in which case they have their body in the trigeminal ganglia and not in the DRG. Second-order neurons lie in the spinal cord or in the brainstem, and they contact third-order neurons in different nuclei of the brain, depending on the particular stimulus.

As we have already mentioned, pain is one of the somatosensory modalities. Although pain is typically an effect of a physical extreme, such as temperature, it is not perceived by the normal receptors designed for that sensation, but by specialized nociceptors. These are bare free nerve endings which are placed all over the body, from the skin to the deeper internal organs. Although all cutaneous free nerve endings appear very similar morphologically, they are actually well specialized, responding to different kind of tissue injury, and classified according to their electrophysiological proprieties, structural features and markers expression. Aδ-nociceptor are, for example, myelinated neurons that express the tyrosine receptor kinase A (trkA) marker, neurofilament200 (NF200) and calcitonin gene-related peptide (CGRP). Unmyelinated C-fibres are small nociceptors which are typically divided in three populations, all expressing TrkA: peptidergic nociceptors (expressing peptides like CGRP and Substance P), non-peptidergic nociceptor (marked by the isolectin IB4) and silent nociceptors (Le Pichon & Chesler, 2014). These neurons control different modalities of pain, and they follow even separate pathways. For example, peptidergic nociceptors project to the first lamina of the dorsal horn in the spinal cord, while non-peptidergic nociceptors go directly to the second lamina.

1.1.2 Peripheral Nervous System disorders

As any other system in our body, the PNS can be subjected to a broad variety of disorders, which can be broadly divided into sensory or motor dysfunctions. Sensory neuron dysfunction results in abnormal or lost sensation, while motor neuron dysfunction leads to muscle weakness or paralysis. A typical symptom usually associated with PNS disorders is chronic pain, which can be labelled as "nociceptive" (caused by ongoing stimulation of pain receptors) and "neuropathic" (NP). Neuropathic pain is a chronic secondary condition caused by a lesion or disease of the somatosensory nervous system, which about the 10% of the global population (Jensen et al., 2011).

It is a really invalidating condition which unfortunately is still extremely complicated to treat, considering that most of the currently employed strategies target predominantly the clinical symptoms instead of the causes.

At the moment, physicians are treating chronic pain patients with both pharmacological and nonpharmacological approaches. First-line drugs include tricyclic antidepressants and serotonin-reuptake inhibitors, which are often not sufficient, thereby requiring the use of most effective opioids, like morphine and oxycodone (Szok et al., 2019). Even if these strong opioids are effective in a short-term scale, they present major side effects when administrated for a longer period. It is well known that analgesic tolerance, dependence and addiction are limiting the use of opioid in chronic pain patients. Tolerance causes the decrease of subjective and objective effect of the same dose of opioids over time, thereby requiring an increase of the amount of the drug to obtain the same effect (Szok et al., 2019). Other major and life-threatening side effects include gastrointestinal and nervous-system related disorders.

Seen the poor efficacy of the current treatments, new therapeutic strategies are explored constantly. In particular, in the last decade a new approach has been obtaining good outcomes. Gene therapy has already been validated as a powerful tool to treat a great number of diseases, including nervous system disorders and, potentially, chronic pain patients as well.

1.2 FROM GENETIC MANIPULATION TO GENE THERAPY

Genetic manipulation aims to introduce, replace or remove a particular genetic information to improve or to generate new feature in the cells and in the organism. Specifically, it is possible to deliver RNA or DNA into cells to generate a specific characteristic (transgenesis) or use the genetic material as a drug to treat a specific disease (gene therapy). In general, the gene delivery system is composed of two components which are a plasmid-based gene expression system that controls the function of a gene within the targeting cell and a gene delivery system that controls the delivery of the gene expression plasmid, which acts as a shuttle. Indeed, foreign genetic material must remain stable until it reaches the nucleus of the cell, in order to achieve efficient gene expression (Han et al., 2000). Genetic manipulation sees a large number of possible applications, not necessary clinic-related. Indeed, it is commonly used in industries for the production of biological molecules, from protein to vaccines (Rosano & Ceccarelli, 2014), but also in agriculture to ameliorate plants and vegetables, acting on their growth and survival potential (Singh et al., 2014).

Genetic manipulation has also had a huge impact on scientific research, thereby opening a whole new world of research opportunities. Genetic manipulation is a powerful tool to simply re-program cells to express the transgene of interest or to generate genetically modified animals and develop transgenic models. It is possible to exploit this technology to perform loss/gain of function experiments directly in animal models in order to study the function of a particular gene, to create specific pathologies models or simply to track and label the cells of interest (Boyle, 2008).

Anyhow, probably the most impactful outcomes based on genetic manipulation are found in medicine. Laboratories and companies commonly use genetic approaches to produce hybridomas to obtain, for example, monoclonal antibodies (Roque et al., 2004), but also for drug manufacturing,

including the production of recombinant hormones (Goeddel et al., 1979) and, obviously, to develop new therapies.

1.3 GENE THERAPY

1.3.1 An overview

Genetic material can be directly used as a drug to regulate, repair or replace dysfunctional genes therefore preventing or treating various diseases. Gene therapy can be performed either by direct in vivo administration of the therapeutic gene into the living organism (direct gene transfer) or by using ex vivo modified (stem) cells as vehicles for gene delivery, as reported in figure 1 (Melim et al., 2020).

- *"in vivo" delivery*

  With this method the genetic material is administrated directly into the patient's organism. The main advantage are the simplicity and quickness (compared to the ex vivo delivery), due to the absence of cell handling procedures such as isolation, culturing, genetic manipulation and transplantation. On the other hand, it is impossible to have the total spatial control of the administrated genetic material, thereby the risk to hit unintended structures rises. This, in turn, could lead to off target effects and less available genetic material for the actual target. In the case of viruses as delivery vectors, other drawbacks are the occurrence of host immune reactions or the possible presence of pre-existing immunity against the vector used.

- "ex vivo" delivery

  This technique is based on the genetic modification of cells outside of the body to produce therapeutic factors and subsequent transplantation back into patients. In this case the main advantage it is precise control and accuracy from both spatial and biological point of views. Indeed, in vitro culturing allows a strict control of the number of cells required but also of the genetical modification procedures applied. It is possible to act at every level of the procedure and to select only for the successfully modified cells. Drawbacks include the complexity of isolation, culturing, correction, expansion and transplantation of the cells.
  Theoretically, all cell types could be genetically modified, but in most of the case neural/stem progenitor cells and mesenchymal stem cells are used for gene therapy. Another thing that must be ensured is that after the modification the cells are not reprogramming and differentiating before the transplantation, nor developing deleterious mutations.

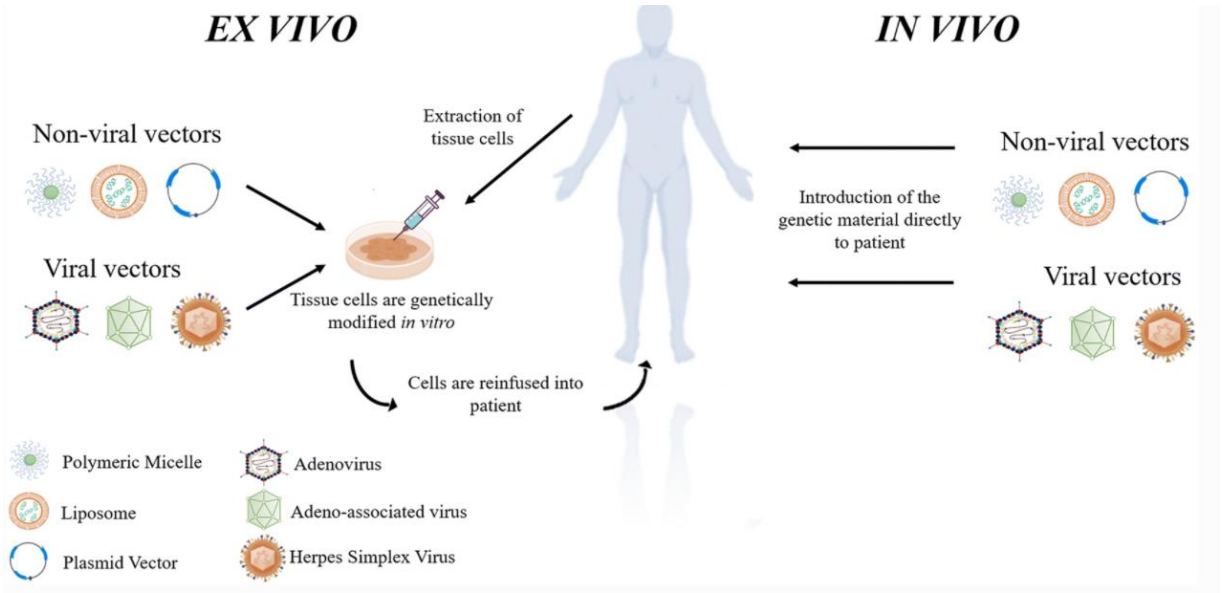

Figure 1) Gene therapy approaches. In the "in vivo" system the genetic material is directly transferred to the patient through specific chemical/physical or biological vectors. The "ex vivo" system consists in the collection and subsequent genetical modification of patient's cell and their transplantation back into the body. Both approaches can rely on viral or non-viral carriers. (Melim et al., 2020).

1.3.2 History of Gene Therapy

This branch of modern medicine has its roots in the 1970s, when a novel paper titled "*Gene therapy for human genetic disease?"* firstly outlined the immense potential of incorporating genetic material into patient's cells affected by genetic disorders (Friedmann & Roblin, 1972). At that time this new approach has been criticized because of the lack of information on gene regulation and genetic recombination in humans, as well as the possible short and long-term side effects of the gene therapy approaches.

Finally, after 18 years of research, the first approved gene therapy trial on humans has been launched. 1990 was an historically important day for gene therapy as a 4-year-old girl affected by a rare genetic disease termed severe combined immune deficiency (SCID) became the first human ever treated with gene therapy. Her pathology was caused by a lack of the enzyme adenosine deaminase (ADA), which left her immune system severely compromised. A functional copy of the ADA gene was delivered through a retrovirus into her T-cells, which were then infused back into her bloodstream. Surprisingly, her immune system managed to recover in the next weeks (Flanary, 2005).

This success strongly encouraged the launch of new trials during the 1990s: dozens of new gene therapy studies were approved and tested, until in 1999 a catastrophic event unfortunately happened. A 18 year-old boy affected by a genetic liver disease termed Ornithine Transcarbamoylase (OTC) deficiency and treated with a novel gene therapy trial based on the

infusion of corrective OTC gene died due to a massive immune reaction elicited by the adenovirus used as delivery vector (Sibbald, 2001). This event shook the scientific community and since then gene therapy came under an even higher level of scrutiny in order to guarantee the safety of the viral delivery systems, of the molecular events that were occurring in the organism after the gene expression and of the immune response to the treatment.

Still, the potential and the efficiency of this new approach was undeniable, and it took only a few years before all nations gradually started to invest into gene therapy and to launch new trials. China has been the first nation to approve a gene therapy for cancer in 2003, followed by Russia and Europe, in 2012 (D. Wang et al., 2020). The main reason of the great success of the recent gene therapy are to be found in the considerable advances in the viral vector technologies that are used to deliver the genetic material. Indeed, already in 2017 more than 3000 clinical trials were ongoing worldwide (Ginn et al., 2018), and 19 gene therapy products have been approved by the Food &Drugs Administration.

1.4 GENE DELIVERY SYSTEMS

One of the main challenged of gene therapy is to develop safe and effective delivery vectors. There are different strategies employed to achieve efficient genetic material delivery into cells, which can be generally divided into physical, chemical and biological methods.

Although the mechanisms are different, the common underlying principle of all gene delivery systems is that the genetic material need to overcome a great number of physical and biological barriers, and thereby requires an “external help”. This help can come from a physical force, a chemical compound or from a biological shuttle vector (viruses).

Generally, we refer to physical and chemical gene delivery methods as **non-viral** vector systems and to biological methods as **viral** vector systems (Nayerossadat et al., 2012). Viral vectors are usually the system of choice due to their ability to infect cells and to provide robust gene expression, although they can potentially provoke immune reaction or integrate into the host genome. Non-viral vector are safer alternatives which, on the other hand, are not as efficient as viral systems.

1.5 NON-VIRAL VECTORS

We refer to non-viral delivery systems when the genetic material is delivered to cells through its complexation with chemical molecules of any type or thanks to a physical or mechanical force.

Because of the significant safety concerns associated with viral vectors, new non-viral alternative methods have been studies in the past decades. Non-viral vectors offer the advantages of a lower induction of immune system and reduced immunotoxicity compared to the viral vectors, thereby resulting in a safer option (Liu et al., 1997). They are also easy to produce and much less expensive on a large scale. Moreover, they display no limitation in the size of the transgene, which allows the incorporation of regulatory elements to increase the transduction efficiency, the stability of the transgene and to confer specificity (Tolmachov, 2009). Indeed, the choice of enhancer-promoter combination has a great impact on both the level and the duration of transgene expression (Yin et al., 2014). High level of expression in mammal cells is, for example, ensured by the use of viral enhancer and promoters such as cytomegalovirus (CMV) or simian virus (SV40) (Pringle et al., 2009). A longer transgene expression can be obtained thanks to constitutive promoters such as the constitutive mammalian human ubiquitin C promoter. Finally, it is possible to obtain specificity by using a tissue-specific promoter such as the liver-specific alphafetoprotein enhancer–albumin promoter (Wooddell et al., 2008). Moreover, different cis-acting sequences, like polyadenylation sequences and introns can be used to further increase transgene stability and expression level (Miao et al., 2001). Although all the expression and regulation elements discussed above could be included in viral vectors as well, having no size restrictions represents an enormous advantage in the design of particularly efficient constructs, where different elements could be combined to achieve a better efficiency and safety profile.

However, at the moment, non-viral systems are not the first delivery choice for gene therapy, representing only around 20% of the total gene therapy clinical trials carried out until 2017 (john wiley & sons Ltd, 2017). This is due to their poor delivery efficiency compared to the viral vectors. Indeed, to achieve efficient gene expression, the genetic material must overcome multiple barriers to enter in the cells, and the non-viral vectors often are not able to provide enough support. The cellular and physical barriers that must be overcame by non-viral vectors are summarized in figure 2. The first step is to resist to degradation mediated by serum endonucleases present in physiological fluids and in extracellular spaces. Indeed, it has been proven that the half-life of plasmid DNA into mice bloodstream is about 10 minutes only (Kawabata et al., 1995). A second checkpoint is represented by macrophages and other immune system cells, which must be avoided by the non-viral vector. Moreover, carriers must avoid renal clearance from the blood and prevent nonspecific interaction, such as aggregation with erythrocytes and serum protein. Furthermore, vectors need to extravasate from blood vessels to reach specifically their target tissue, mediate cellular entry (usually through endocytosis) and eventually evade proteasome degradation. In the cytosol, the RNA can bind to his complementary machine (for example, mRNA must bind to translational complex), while DNA needs to reach the nucleus by passing the double nuclear membrane. This is usually achieved by using a nuclear localization signal (NLS), mostly a peptide, which can be attached to the surface of the carrier or fused to the transgene (Barraud et al., 2014)

Figure 2) Barriers to successful in vivo delivery using non-viral vectors. (Chen et al., 2017).

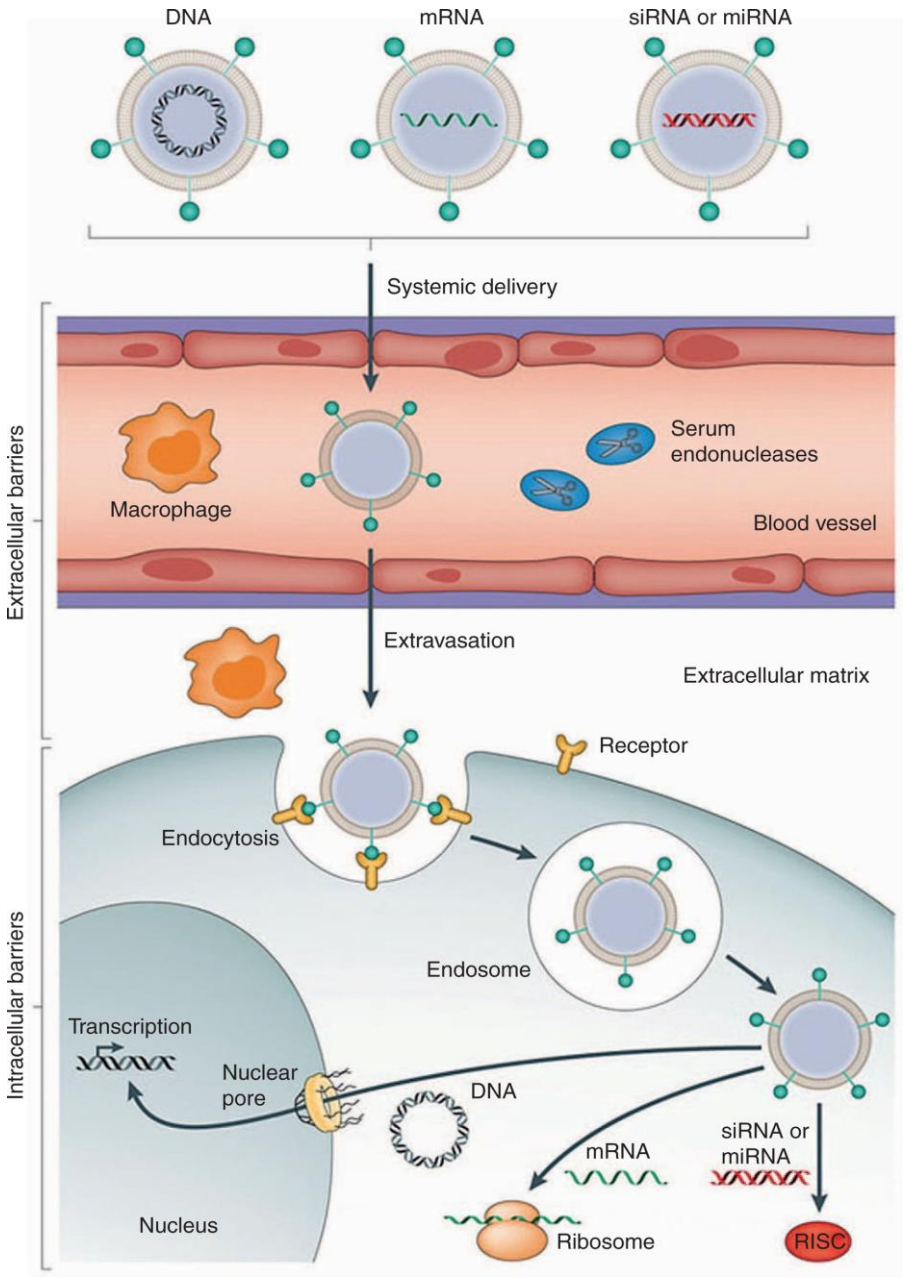

As previously discussed, one of the main reasons why non-viral vectors alternatives exist is their presumed safety. Nevertheless, a certain level of cytotoxicity, which depends on the specific vector used, still remains. Indeed, toxic effect of non-viral vectors are mainly caused by their cationic nature, since the interaction of cationic polymers of lipids with cell membranes may lead to an alteration of these membranes (Juliano, 2016). Another frequently occurring problem is the large molecular weight (MW) of the vector, combined with its chemical nature. For example, it has been shown that when the MW of PEI polymers is greater than 25 kDA, it could elicit a toxic effect on target cells (Helal et al., 2017).

As already mentioned above, the non-viral delivery systems can be divided into physical and chemical based methods. Furthermore, in the last years there have been tested also some non-viral biologically-responsive methods (Nayerossadat et al., 2012)

In the case of the physical delivery of genetic material, a physical or mechanical force is used to create pores into the cell membrane, allowing the passage of the DNA/RNA. Pores are then rapidly closed by cell's membrane repair systems. These systems are among the easier to perform, and they guarantee effective, specific and efficient transfection of the cells. They are also effective both in vitro and in vivo. However, the main drawback is their relatively high cytotoxicity caused by the physical damaged imparted to target cells.

The most used physical delivery system is the electroporation, which uses an electric field in the range of 10-20 Kv/cm to create pores in the cell membrane (Potter & Heller, 2018). Other systems include microinjection (direct injection into the nucleus), sonoporation (using sound waves) or gene gun (DNA coated metal particles are fired into the cells using a particular machine) (Mashel et al., 2020). Magnetofection is another physical method of great efficiency, given its very low cytotoxicity and high transfection rate. In this technique particles containing genetic material are delivered to cells using magnetic fields as driving force, allowing a rapid and almost saturating concentration of all the particles in target cells (Plank et al., 2003). However, all the systems here discussed are mainly used in vitro.

Chemical gene delivery systems rely on the cationic nature of particular chemical substances to create complexes with negatively charged target nucleic acids. Chemical carries can be divided in four groups: lipid-based vectors, polymer-based vectors, peptides and nanoparticles. In general, the roles of the carriers are to protect genetic material from degradation, conferring tissue specificity, enhancing carrier safety profile and sustaining transgene expression (Ramamoorth & Narvekar, 2015).

1.5.1 Lipid based carriers

Lipid-based vectors are divided into nanoplexes (cationic lipids complexed with DNA), liposomes (either complexed with DNA or with DNA encapsulated into liposomes) and lipid-based nano emulsions (Xue, 2015). Liposome are the most diffused non-viral carriers. They are self-assembling systems in which the lipidic molecules conceal their hydrophobic tails internally and expose their hydrophilic heads in the aqueous compartment. Negative charged DNA can easily interact with these structures to form lipoplexes. DNA can bind directly on the surface of the liposomes or can be internalized into the core of the complex. In case of encapsulated DNA, anionic, cationic, and non-ionic lipids can be used in the formulation of the liposomal structures. Finally, in the case of too high positive surface charge density, cationic liposomes can be conjugated with neutral liposomes, which has been demonstrated also to enhance endolysosomal escape (Balazs & Godbey, 2011).

The first monovalent cationic lipid that has been synthesized was DOTMA (Weiss et al., 1989), characterized by its ability to bind both RNA and DNA and its low toxicity. DOTMA has been modified during the years to improve its efficiency, even in combination with other molecules. Indeed, in 1993 a new derivate of DOTMA has been commercialized, which is still now one of the most

effective transfection reagents commonly used in every chemical biology laboratory: lipofectamine (FELGNER et al., 1995).

1.5.2 Polymer based carriers

Polymer-based carriers can be classified into natural based polymers, such as chitosan (Agnihotri et al., 2004) and synthetic, such as polyethylenimine (PEI) and poly-L-lysine (PLL). PLL is the simpler synthetic polymer, composed only by l-lysine repeated residues (Hartono et al., 2012). It is considered as the safer option for transfection, at the expense of its low efficiency. Indeed, the interaction with the DNA is quite unstable, and its safety profile limits its use in vivo. Anyway, to overcome PLL weak transfection efficiency, this polymer is usually modified with other molecules such as imidazole groups, polyhetylene glycol (PEG) or chitosan (Luo et al., 2011).

PEI is considered the efficiency gold standard for transfection. It has been characterized in 1995 (Boussif et al., 1995), and considered at the time the only non-viral alternative which was able to obtain a comparable level of efficiency to the viral options. It is composed by repeated units of amine groups separated by two carbon aliphatic spacers. It can be linear, composed only by secondary amines, or branched. The high positive charge content is responsible for its high efficiency, but, on the other hand, leads to a highly toxic profile, which is related to the MW of the compound. To improve the toxicity profile, PEI is often modified using biodegradable disulfate linkages and ester groups, coupled with PLL or PEGylated (Florea et al., 2002).

1.6 VIRAL VECTORS

Despite the advantages of the non-viral vectors, more than 70% of the total gene therapy trials carried out since 2018 were based on viral vectors (Ginn et al., 2018). This is due to the fact that viruses have evolved to deliver their genes to target cells: it is expectable that their efficiency is then higher compared to a synthetic vector. In general, to achieve successful gene delivery, viral vectors have to overcome the same barriers discussed for the non-viral vectors. However, the two main barriers for the non-viral vectors are represented by the plasmatic and nuclear membranes, while cell entry is it not a rate-limiting step of viral infection process. Moreover, viral vectors provide a better protection of the transgene against the extracellular endonuclease activity, since the transgene is encapsulated into the viral particle and is not only complexed with it.

On the other hand, even if viruses used in research are engineered into a replicative-deficient form, immune system activation following viral vector administration must be taken into consideration. Immune response can be innate, humoral or cell mediated and can be directed against both the vector and the transgene. The cell-mediated response again the vector/transgene can lead to the elimination of the interested cells, whereas an innate response can lead to local/systemic toxicity which can trigger a secondary antigen-mediated immune reaction. Humoral immunity can be directed against the transgene, something that is related to the amount of the gene product and

whether the target cell is a natural site for synthesis. For example, if the vector is taken by an antigen presenting cell, it is possible that an immune response will follow. A solution for this problem would be to design cell-specific vectors.

Moreover, since viral vectors used in clinic are recombinant version of wild type viruses, it is possible that the organism already has developed specific antibody during previous infections. For example, most humans have detectable level of neutralizing antibodies directed versus adenovirus serotype 5 or adeno-associated virus-2 (Rogers et al., 2011). The presence of already existing specific antibodies might significantly reduce the efficiency of the gene therapy treatment by neutralizing the recombinant viral particles before they can reach and transduce the cells of interest, something especially relevant in the case of cancer therapies in which multiple doses of vector are administrated.

Another problem concerns the persistence of the transgene, which can integrate into the host cell genome or persist as extrachromosomal entities, typically in the form of episomes. In the case of integrative viral vectors, the problem of insertional mutagenesis is a major issue, since it can lead to cellular/organ disfunctions and cancer. On the other hand, in case of non-integrative viruses, the expression of the transgene, which persists in an extrachromosomal form, is limited in time, decreasing at every cell division (Nayerossadat et al., 2012). Because of this, subsequent administrations are required in order to achieve the therapeutic effect (Mashel et al., 2020).Finally, the size of the transgene is a major limitation when viruses are used as vectors for gene delivery. In general, when a viral vector is reprogrammed for gene therapy purposes, the genome of the wild type virus is modified and all the genes required for the replication and the regulation are removed, leaving only those elements required for the viral assembly. The space that becomes available in the genome is used for the insertion of the transgene of interest. Depending on the class of viruses, the range of the transgene spaces from few kilobases (4.7Kb in the case of adeno associated viruses) to hundreds of Kb (150Kb in the case of herpes viruses), which is, however, less than the transgene capacity offered by synthetic solutions. (Nayerossadat et al., 2012)

At the moment there are around a dozen types of viruses used as delivery vectors both for research and clinic, which can be divided into the two families of integrative and non-integrative viruses, depending on their ability to integrate their genes into the host genome. Integrative viruses are represented by the retroviruses, and specifically by the lentivirus subclass. All the other viruses used in research and in clinic are typically non-integrative, and they include Adenoviruses (AV), Adeno-Associated viruses (AAVs), Sendai Virus, Herpes Virus, Poxvirus, Alphavirus and Epstein-Barr Virus.

Every class of virus exhibits typical characteristics, such as tropism, immunogenicity, efficiency and stability, thereby the choice of the appropriate viral vector must be taken in consideration of the final goal of the therapy or experiment. For example, the overwhelming majority of “in vivo” clinical trial utilize AAVs, while for the “ex vivo” approaches integrative viruses are the vectors of choice (figure 3). This is consistent with global data.

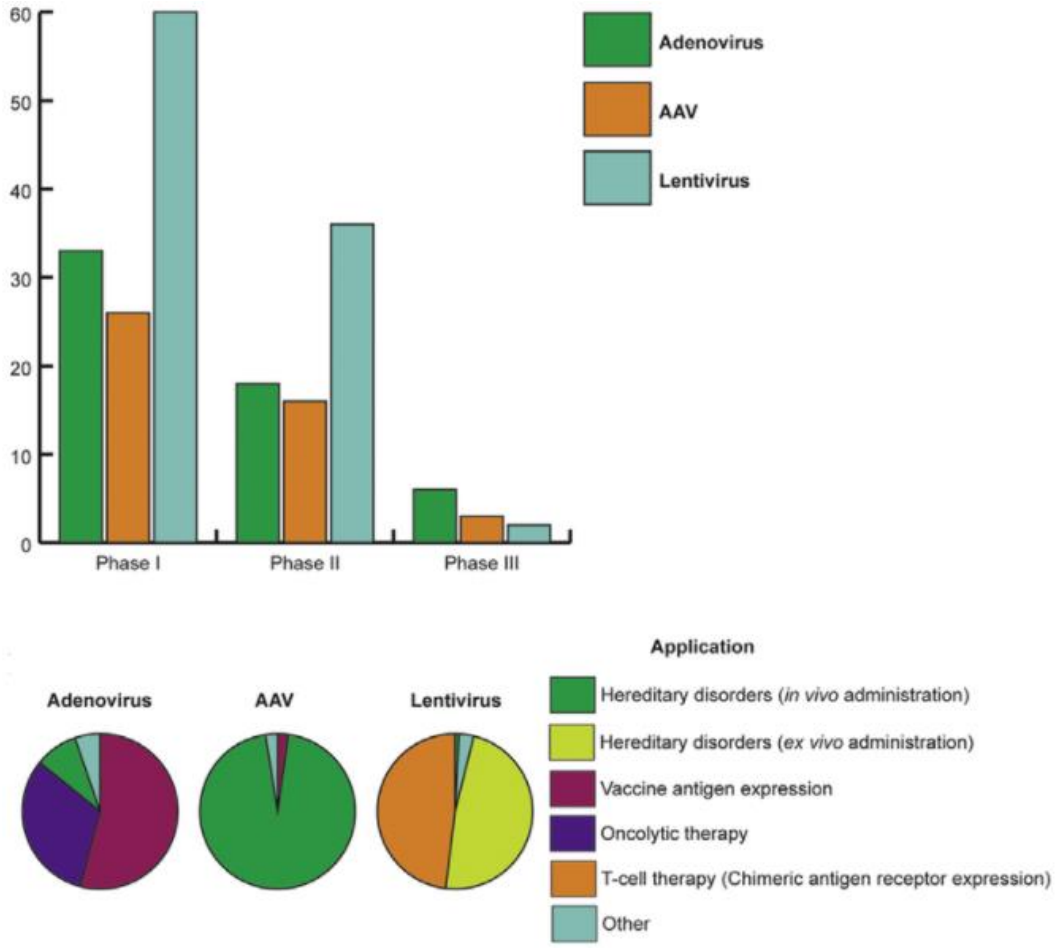

Figure 3) Distribution of viral vectors used for "in vivo" and "ex vivo" gene delivery. Different classes of virus are selected due to their proprieties for specific therapeutical approaches. (Sharon & Kamen, 2018).

1.6.1 RETROVIRUS

Retroviruses are one of the most efficient class of viruses in term of transduction efficiency, but their use raises safety concerns due to the fact that they integrate their genetic material into host cells genome, thus possibly leading to malicious mutations and oncogenesis (Anson, 2004).

The retrovirus family comprise six different genera which can be divided into simple retroviruses, also called oncoretroviruses, and complex retroviruses, which include the lentiviruses genera, widely used in clinic and research. Retroviruses are enveloped single-strand RNA (ssRNA) viruses whose genome is composed of the minimal essential genes *env*, *pol* and *gag*. The *env* gene codes for viral envelope glycoproteins, which form the core of the virus and interact with the two copies of the ssRNA genome, while *pol* and *gag* code respectively for reverse transcriptase, integrase, proteases and gag-derived structural proteins (Giacca, 2011). The viral genome is flanked by two long terminal repeats (LTR) sequences, which are the only "in cis" element required for viral production. Indeed, transgene capacity of oncoretroviruses is about 8Kb, while the one of lentiviruses reaches 9Kb, LTRs included.

The infection cycle is very similar for all the subclasses of retroviruses and it comprises cell attachment and entry, reverse transcription of the viral RNA into a complementary (c)DNA and integration into the genome. Cell entry can happen both for direct membrane fusion or receptor-mediated endocytosis, mediated by the interaction between capsid glycoproteins and their receptors on target cells. As soon as the mature virus enters into the cell it starts the uncoating process: structural and regulatory proteins dissociate from the viral core and complex with the viral RNA to form the reverse transcription complex (RTC). This RTC is actively transported into the nucleus, where the integration may occur (Bukrinsky et al., 1993). It ss during this migration that viral RNA is converted into proviral double-stranded DNA through reverse transcription, even if is still unclear if the reverse transcription is completed in the nucleus or in the cytosol. Here we can find the main difference between lentiviruses and general retroviruses: only lentiviruses RTC can cross the nuclear membrane through nuclear pores without relying on transitory membrane disruption. Indeed, retroviruses can only get access to the nucleus when the cell is under mitosis, the reason why they can only infect diving cells. In the nucleus, the proviral DNA can integrate into the host cell genome. This process is, for the majority of retroviruses, finely tuned. Indeed, gammaretroviruses prefer insertion near transcriptional start sites, while lentiviruses mainly integrate into transcriptional units (Milone & O'Doherty, 2018).

Despite their efficiency, safety of retroviruses has been object of discussion after the first oncoretroviral gene therapy launched in 2000. Indeed, 25% of treated patients of severe combined immune deficiency developed leukemia (Cavazzana-Calvo et al., 2000). To increase their safety profile, second-generation oncoretroviruses, called self-inactivating oncoretroviruses, has been developed in the following years. They harbor two modified LTR: the promoter region of the 5'LTR is replaced with a strong promotes (such as CMV promoter which provide a strong and sustained transgene expression) and a deletion is inserted in the 3'LTR. After viral infection, reverse transcription and second-strand DNA synthesis normally leads to the copy of the mutated region of the 3'LTR in the 5'LTR, thereby removing the custom promoter and resulting in the formation of a transcriptionally inactive 5'LTR (Shaw & Kohn, 2011).

1.6.2 LENTIVIRUS

Lentiviruses are a subclass of retroviruses characterized by their long incubation time ("lente" means "slow" in latin). The best know lentivirus is Human Immunodeficiency Virus (HIV), which usually requires years after the infection to cause serious damages to the organism. Lentiviruses exist in five serogroups (a serogroup is a variation within a species of bacteria/viruses that differ from the other due to the expression of specific antigens) which can infect specific taxonomic orders. Primate lentiviruses are characterized by their binding specificity toward the CD4 receptor (Agopian et al., 2006). The main difference between lentiviruses and retroviruses is that lentiviruses can infect both dividing and non-dividing cells, a reason why they are the integrative viral vector of choice at the moment (Cooray et al., 2012). The ability of the lentiviruses to infect also non-dividing cells and permanently modify the genome makes them the ideal vector for particular gene therapies which aim to target quiescent cells, such as hematopoietic stem cells (HSCs). Moreover, targeting non-dividing cells might reduce the oncogenic potential. As discussed, lentiviruses usually integrate into transcriptional units, and the chance to interfere with a transcriptional unit involved in cell

replication is higher when transducing highly dividing cell. A further step forward in term of safety is the use of self-inactivating lentiviruses, designed in the same way as self-inactivating oncoretroviruses (Modlich et al., 2009).

Currently, the mostly used lentiviruses are all derived from HIV, which is able to infect cells that are in both G0 and G1 phase (Tang et al., 1999). Lentiviral design and production is schematized in figure 4.

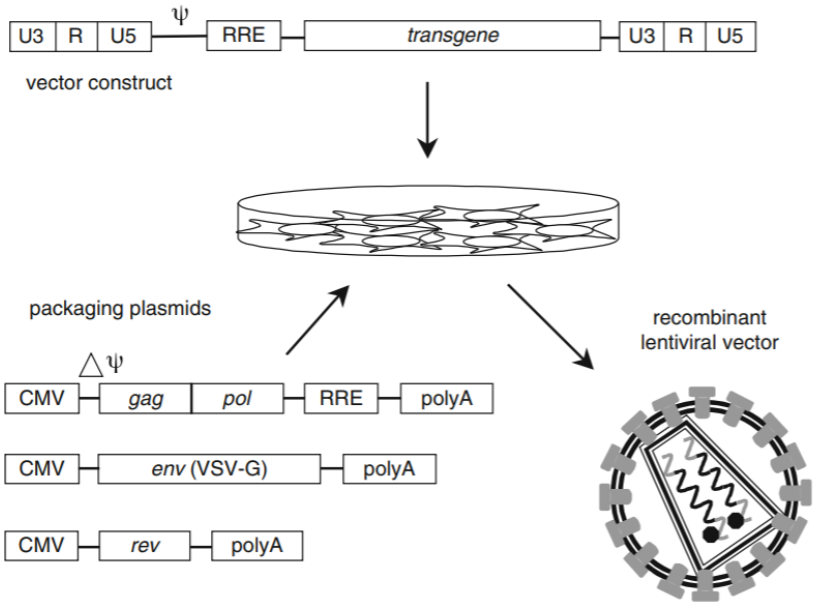

Figure 4) Third-generation Lentiviral vector design**.** Viral genes gag, pol, env are replaced by the transgene. Vector amplification and packaging are provided by the LTRs and rev responsive element (RRE), which interact with rev proteins. gag, pol and env are provided by separated packaging plasmids expressing a strong promoter (such as CMV) for enhanced expression. Furthermore, the accessory element rev is supplied in trans under a CMV promoter.

As anticipated in figure 3, lentiviruses are mainly used for "ex vivo" therapies, with main targets being HSCs and T-cells (Milone & O'Doherty, 2018). Lentivirus-mediated transfection of HSCs have been used to treat a broad list of genetic diseases, including X-linked adrenoleukodystrophy, metachromatic leukodystrophy and Wiskott-Aldrich Syndrome (Aiuti et al., 2013). Another good example is given by the work of Cavazzana-Calvo et al (Cavazzana-Calvo et al., 2010), in which a lentiviral vector has been successfully used to treat β-thalassaemia, a rare genetic blood disease which causes a major decrease of haemoglobin production.

Even if ex vivo gene transfer into HSCs has a lot of potential, more efforts have been carried out to study the possible application of modified T-cells in different medicine fields, including cancer immunotherapy. One of the most used approaches consist in infecting patient's T cells with a lentivirus carrying a specific receptor that aims to recognize tumor cells and subsequent infusion of the reprogrammed cytotoxic T cells back into the patient. Several phase 1 / 2 clinical trials have been carried out so far, in which tumor antigens have been expressed into T cells, including NY-ESO-1, MART-1, WT-1 (Liechtenstein et al., 2013). In a trial performed in 2009, lentiviral vectors have shown higher transgene expression efficiency of the Melan-A/MART-1 antigen compared to gammaretroviruses (Bobisse et al., 2009), and clinical responses have been obtained in 80% of patients with multiple myeloma treated with autologous T-cell modified to express a peptide that

recognizes myeloma cells (Milone & O'Doherty, 2018). Chimeric antigen receptors (CARs) are also a very powerful tool for immunotherapy. These custom receptors can be expressed into T-cell to target specific malignant cells, as in the case of patients with B-cells disfunctions. Notably, clinical trials using CD19-targeted CAR T cell therapy for B-cell acute lymphoblastic leukemia have demonstrated high efficacy (Maude et al., 2014) as well as trials on patients affected by non-Hodgkin lymphoma (Davila et al., 2015).

1.6.3 ADENOVIRUSES

Unlike retroviruses, DNA viruses contain single-or double-stranded DNA as the viral genome. Furthermore, as already mentioned, DNA viruses are typically non-integrating vectors. The main advantage that this brings with is about the safety profile. Indeed, non-integrating vectors specifically share reduced risk of genotoxicity, due to the lower chance of possible oncogenic integration into the host genome. On the other hand, unless they have been specifically genetically engineered for replication and segregation, non-integrating vectors will dilute progressively in proliferating cells. This means that in order to obtain a stable expression of the transgene, subsequent administrations are required.

Adenoviruses (AD) belong to the family adenoviridae, a name that derives from their first isolation from human adenoid tissue in 1953 (Rowe et al., 1953). They are double-stranded DNA noneveloped viruses with a diameter around 90/100nm and a weight of 150 MDa. The structure of the capsid is shown in figure 5. They can infect a broad range of species and more than 55 serotypes of AD have been discovered in humans, in which they are responsible of 5-10% of child acute respiratory diseases. The different serotypes are classified into 6 subgroups, from A to F, with the group C containing the AD2 and AD5 which are the most studied and used for gene therapy (Wold & Toth, 2014).

AD genome is linear, between 26 to 48 Kb, depending on the serotype. The genome contains five transcription units which are activated immediately after the infection (E1A, E1B, E2, E3 and E4), two intermediate transcription units (IX and Iva2) and a late transcription unit (major late, ML), which generates five populations of late mRNA (L1/L5). The entire genome is flanked by two ITR which act as DNA replication origins. The replication cycle is divided into two phases. The early phase happens in the first 5/6 hours after infection, and it includes the binding of the virus on target cell, internalization, endosomal escape, viral DNA nuclear translocation and expression of the early genes. During the DNA replication, the late transcription phase begins, characterized by the production of structural protein required for capsid formation and genome packaging (Giacca, 2011).

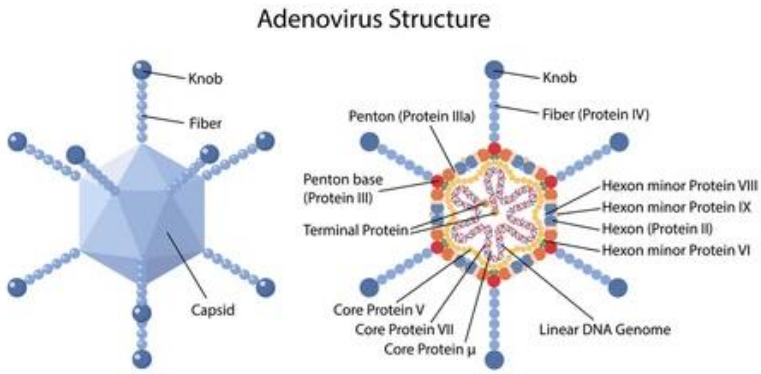

Figure 5) Adenovirus structure. AD capsid is made of 240 hexon protein complexes that form the sides of the icosahedron, while twelve penton bases cap the icosahedron's corners. Each hexon is composed by 3 copies of the protein II, associated with proteins VI, VII and IX. Each penton is connected to a variable length fiber composed by protein IV, which ends with a knob and interacts with the AD receptor. DNA is linear and is associated with core protein V, VII and mu. Source shutterstock.com

Due to their ability to infect both dividing and non-dividing cells without integrating into the host cell genome, AD are popular tools currently used in more than 400 gene therapy trials (Wold & Toth, 2014). Most of the AD vectors used in gene therapy are modified version of the adenovirus-5, and are mainly divided into two classes: replication-defective (RD) and replication-competent (RC). In the replication-defective AD, the early genes E1A and E1B are removed and replaced by the transgene, up to a maximum size of 35Kb. According to the need, different genome elements could be kept, as in the case of replication-competent AD in which the genes involved in viral replication are maintained. RD vectors are mainly used for vaccines due to their strong humoral and T cell response elicited on the transgene that they express. Indeed, many of the covid-19 vaccines are based on recombinant RD vectors, in which the goal is to express the covid-19 spike glycoprotein in order to develop specific immunity. For example, AstraZeneca vaccine is based on a chimpanzee adenovirus vector (ChAdOx1) (Folegatti et al., 2020), the Johnson & Johnson COVID-19 vaccine uses modified recombinant adenovirus type-26 (Logunov et al., 2021), and Convidecia's vaccine is based on AD5 (Zhu et al., 2020).

Both RD and RC AD are also used for cancer treatment. In the first case, RD vector express a transgene which is involved in the regulation of tumor cell cycle, immune system recognition or cell apoptosis. Gendicine has been the first cancer gene therapy ever approved for commercial use, available in China from 2003 for the treatment of head and neck squamous cell carcinoma (Tian et al., 2009). In contrast, RC vectors rely on their natural occurring lytic cycle to destroy infected cells, hence the name oncolytic vectors. Although there is evidence supporting the fact that cancer cells are generally more permissive for AD replication than quiescent or non-cancerous cells (Vaillancourt et al., 2005), essentially all oncolytic Ad vectors have genetic cell targeting features that permit efficient replication in cancer cells and that limit off target effects. ONYX-015 was the first oncolytic vector ever tested in clinical trials: it lacks a gene which is needed for viral replication but that is present in most of cancer cells, thereby allowing the vector to replicate only in tumor cells (O'Shea et al., 2004).

1.7 ADENO ASSOCIATED VIRUSES

Adeno-associated viruses (AAV) are small non-enveloped viruses which belong to the family Parvoviridae and genus Dependovirus. Their size is around 25nm, which classifies them as some of the smallest viruses known. As their genus suggest, they rely on other viruses help to complete their life cycle and replication.

They have been discovered in 1965 as a contaminant of adenoviral stocks, and one year after their discovery, Hoggan et al demonstrated their non-pathological nature (Hoggan et al., 1966). Their genome, that at the beginning was believed to be double strand, has been later identified to be single strand DNA (Rose et al., 1969).

The immense therapeutical potential of the AAVs was already clear at that point: a non-pathological and low immunogenic tool for the delivery of target DNA was definitely something that could have paved the way for new approaches to cure many genetic disorders. The first step in this direction was taken by Muzyczka in 1984, when the authors replaced the capsid genes of an AAV with the neomycin resistance gene and subsequently successfully transduced human and murine primary cells, thereby demonstrating for the first time the therapeutical potential of AAVs (Hermonat & Muzyczka, 1984) . Since then, various pre-clinical and clinical studies using AAV vectors have been carried out with the first approved human gene therapy product, Glybera, approved in Europe in 2012 (Gaudet et al., 2013). Even if Glybera has been withdrawn from the market only a few years after its approval due its high price and the low market request, it lay the foundation for a great number of constantly improving AAV based therapies.

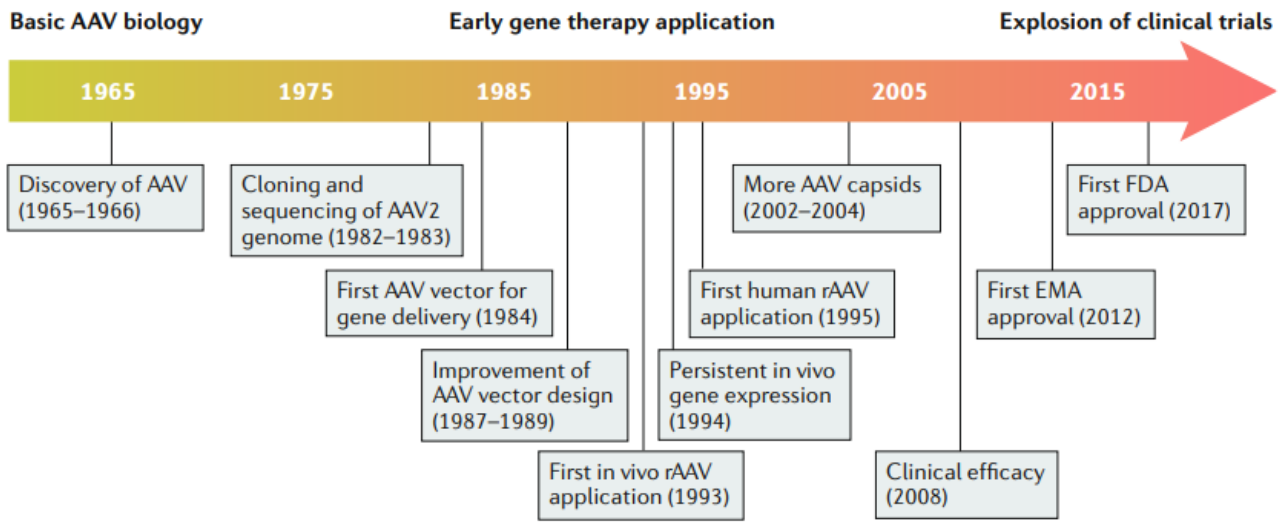

Figure 6) Milestones in AAV discovery and first applications. (Wang, 2019)

1.7.1 GENOME AND STRUCTURE

Currently, twelve human and non-human AAV serotypes have been characterized, which are divided in eight clades (A-F) according to sequence homology and antigen reactivity (Gao et al., 2004). The representative members of this groups are AAV1-AAV9, with AAV4 and AAV5 being the most different from each other and from the other members, but still sharing at least 60% of the genome.

Wild type AAV genome consists of a linear single stranded DNA which is ~4.7Kb in length (figure 7). It encompasses two open reading frames (ORF) flanked by an inverted terminal repeat (ITR) sequence that is 145bp in length (Bohenzky et al., 1988). Relying on different promoters and splicing mechanisms, the Rep gene codes for the replication proteins (Rep) 78/68/52/40, while the cap gene codes for the structural viral protein (VP) 1/2/3 and the assembly activating protein (AAP).

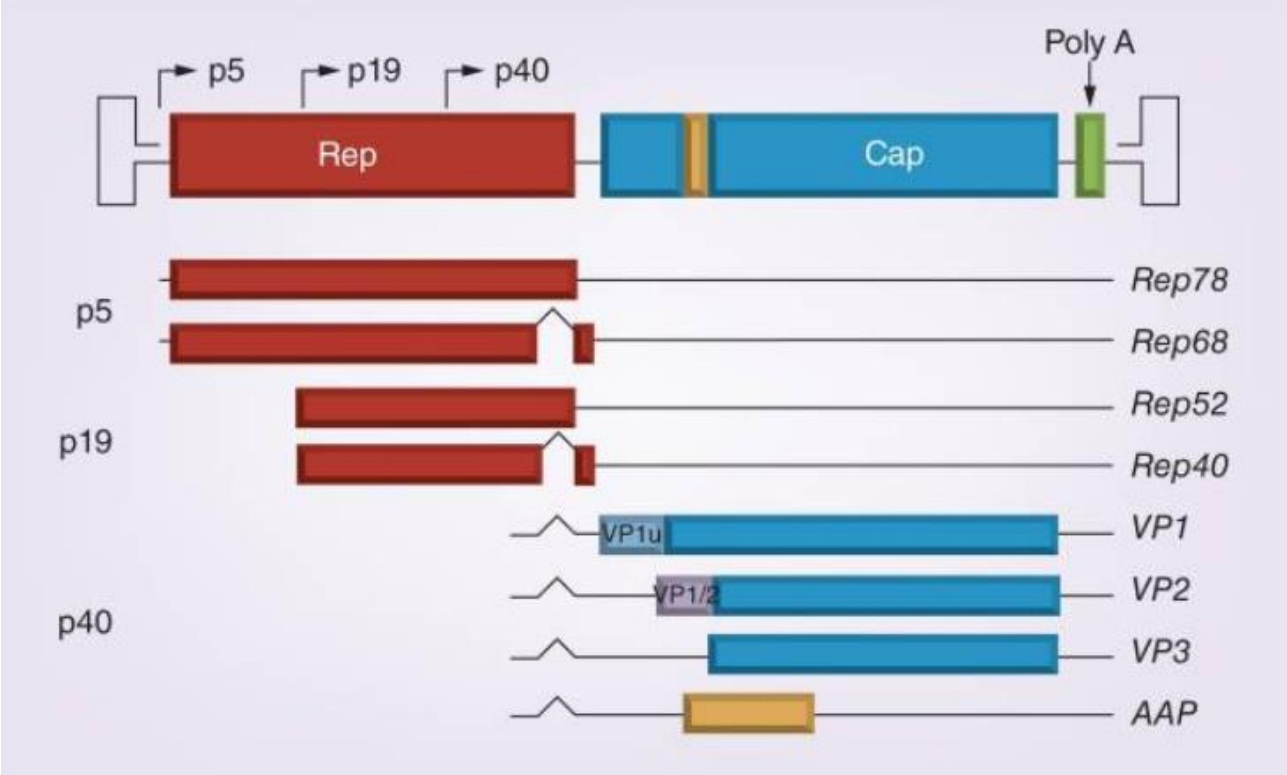

Figure 7) Wild-type AAV genome. (Wang & McKenna, 2013)

The main feature of the ITR, due to their symmetry, is the ability to form a hairpin structure which allows the typical "self-priming" mechanism that leads to a primase-independent replication of the second DNA strand. Indeed, the ITR is composed by a 125 base palindromic sequence that forms the T-shaped hairpin structure by complementary base pairing of three specific regions (AA' BB' CC'). The ITR can exist in two conformations named flip and flop, according to the orientation of the BB' CC' fragments (figure 8). The remaining 20 bases remain unpaired and are referred as the D-sequence, and they don't participate to the formation of the hairpin (Wilmott et al., 2019). However, D region is crucial for the encapsidation process due to the presence of a signal sequence that drives the 3' genomic transport into preassembled capsids (Myers & Carter, 1980)

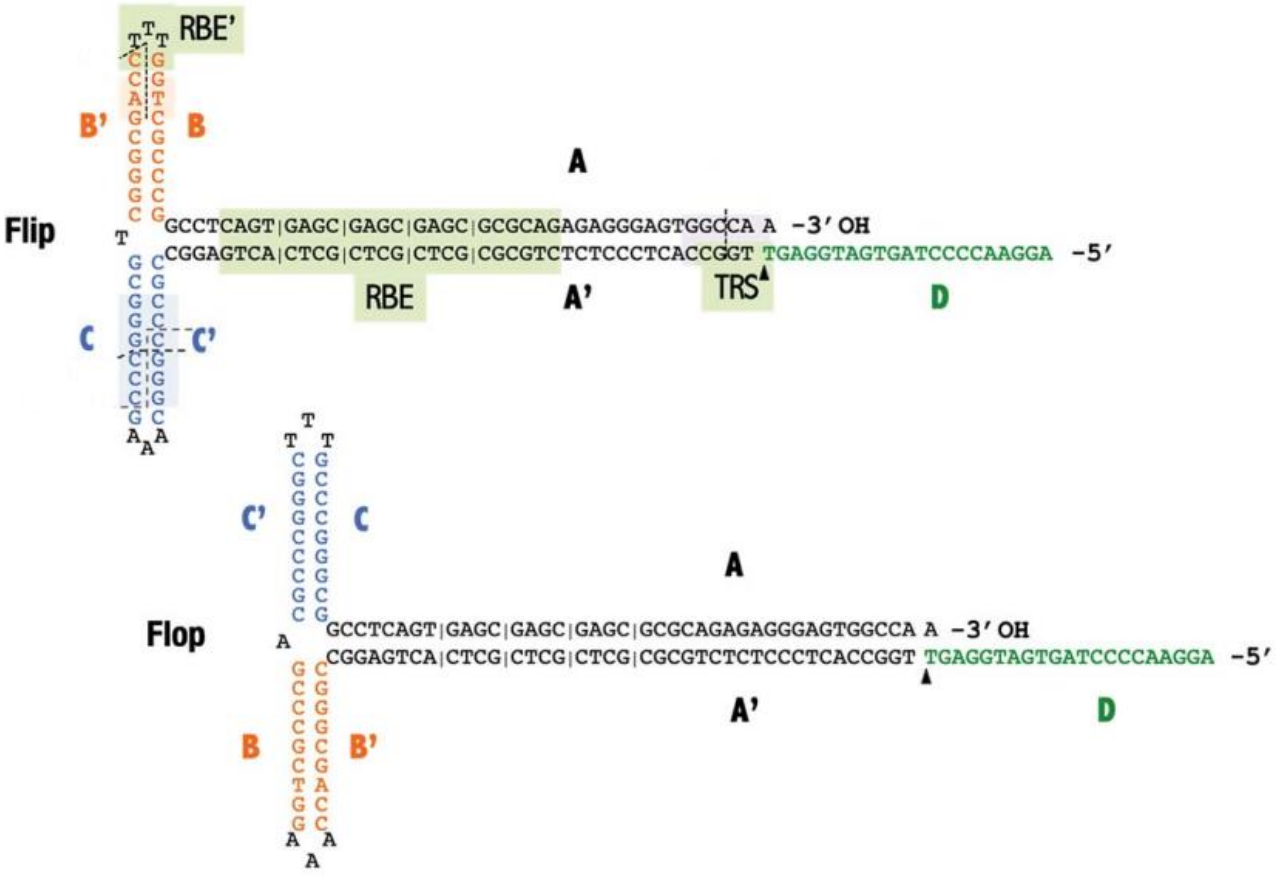

Figure 8) Secondary structure of AAV2 ITRs (Wilmott, 2019).

The tertiary structure of the ITR and recognition sequences are critical for the replication and encapsidation of the viral genome into empty capsids. In particular, the Rep-binding element (RBE), which is composed by five tetranucleotide repeat motifs containing the consensus sequence 5'-GAGY-3', plays a key role in the binding of the Rep 68/78 proteins coded by the rep ORF of the AAV (Ryan et al., 1996) . Once bound, Rep68/78 unwinds and nicks the terminal resolution site (TRS) in a sequence and strand-specific manner permitting both genome replication by host cell DNA polymerases and subsequent genome encapsidation (Brister & Muzyczka, 2000). Rep 68/78 can bind to the ITR of other AAVs serotypes, even if they are not always able to carry out terminal resolution, thereby not allowing the complete genome replication, as happens for example in the case of AAV2 rep 68/78 and AAV5 ITR.

AAV ITRs have been the target of different manipulations in order to obtain modified vectors with different proprieties. The self-complementary AAV (scAAV) consist in a virus with a modified ITR in which the TRS is removed. This prevents the Rep 68/78 nicking of the vector genome, thus resulting in duplicated vector genomes covalently joined by the internal TRS-deficient ITR (D. M. McCarty et al., 2003). Since the non-nicked genome self-anneal to form a double-strand DNA genome, there is

no need of the complementary strand synthesis or annealing of the positive and negative strand inside the target cell during the virus infection, resulting in a faster transgene expression. However, the main drawback of this system is that the packaging capacity of the vector is halved, making this option particularly useful only if the transgene to be expressed is shorter thank 2.2Kb. On the opposite hand, the split vector system is also used to deliver transgenes that exceed the 4.7Kb limit, thus being too large to be accommodated in a single AAV vector. This is possible due to ITR's ability to concatemerize in order to reconstitute full-length genomes. The transgene is divided into two halves: a splicing donor site is inserted at the 3' end of the first half, while a splicing acceptor signal is inserted at the 5' end of the second half. This allows splicing of the concatemerized ITR structure that forms in the middle of the therapeutic coding sequence following tail-to-head concatemerization of the two AAV genomes to obtain a single large mRNA molecule (Trapani, 2019). The major limitation of this platform, however, is that concatemerization can occur between any of the ITR of the two vectors, thus resulting in self-concatemerized vector, or vectors with wrong orientation. However, this problem could be addressed by using ITRs coming from different AAV serotypes, in order to promote specific head-to-tail junction and functional transgene formation (Yan et al., 2007).

In the WT AAV, the ITRs flank two open reading frames, called rep and cap. The rep ORF encodes four overlapping proteins: Rep78, Rep68, Rep52 and Rep40, fundamental for AAV replication and packaging. Expression of these four proteins is initiated from the p5 and p19 promoters, as shown in figure 7. P5 and p19 promoters initiate transcription of two different mRNAs, each containing an intron that can be either spiced out or not, forming the four rep proteins. DNA replication relies on the two larger proteins (Rep78 and Rep68), which have single-strand endonuclease, DNA helicase and ATPase activity, while the two smaller proteins (Rep52 and Rep40) are required for AAV packaging and only have helicase activity.

As previously discussed, ITRs form a hairpin structure that drives the AAV DNA replication. During infection, replication of the AAV genome is initiated by the host DNA polymerase using the 3'-hydroxyl primer of the hairpin ITR, which allows the replication of internal genes. However, in order to be able to replicate the ITRs, a site-specific, single-stranded nick into the ITR themselves and subsequent rep-dependent unwinding are required to generate a 3'-hydroxyl primer for repair synthesis of the ITR (Musatov et al., 2002). This nick is operated by Rep78 and Rep68 and it happens at the terminal resolution site of the ITR, but in order to be effectively operated it requires the previous binding of the Rep proteins on ITR's RBE and on a small palindrome sequence that comprises a single tip of an internal hairpin within the ITR, called RBE' (Brister & Muzyczka, 1999). The nicking process is divided in two steps: firstly, Rep DNA helicase activity unwinds the ITR, thereby extruding a stem-loop structure at the TRS, then, Rep endonucleases activity cleaves the TRS. At this point, a free 3'-hydroxyl is created and used as primer for the host DNA polymerase. Within the RBE, Rep proteins bind to a specific and conserved 22-bp sequence which includes the tetrameric GAGC repeat which is necessary for stable Rep binding to both linear and hairpinned TR substrates (Brister & Muzyczka, 1999). However, it has been proven that the position and the orientation of the Rep on the RBE is crucial for efficient cleavage of the TRS: modification of the space between the RBE and the TRS, the polarity of the RBE and changes in the RBE' sequence result in dramatic reduction of in vitro/in vivo replication of the AAV (J. Wu et al., 1999).

Rep78 and rep68 are not only involved in the AAV genome replication, but they also act as both a repressor and activator of AAV transcription during infection, and they are crucial for AAV targeted integration into host genome. AAV can not replicate without the presence of a helper virus such as adenovirus or herpesvirus. Indeed, in the absence of helper virus, the activity of the p5 promoter is silenced. This is mainly due to the activity of the cellular YY1 protein, a ubiquitously distributed transcriptional repressor protein (Laughlin et al., 1982). However, p5 activity is also heavily regulated by the p5 rep protein themselves. Indeed, the 22-bp sequence within the RBE is not only present in the ITR, but also in the p5 promoter. Thus, in presence of helper virus, rep78 and rep68 can bind and repress p5 transcription, while they transactivate the p19 and p40 promoters (Pereira et al., 1997). This leads to the production of the small rep proteins (rep52 and rep40) and of the structural capsid proteins required for the AAV expansion. The p19 rep proteins, that are now strongly expressed, can interact with rep78 and rep68 to form multicomplex, thereby eliminating the p5 repression. This creates a feedback loop that aims to control the level of expression of the different rep proteins. If the ratio of p19 to p5 transcripts increases, Rep52 and rep40 attenuates repression at p5 to raise the level of Rep78 and rep68. The net effect is a control loop which maintains a constant ratio of the p5 and p19 transcripts.

A 22-bp RBE sequence, composed by three CAGC repetitions, is also found in the large arm of the human chromosome 19, in the so-called AAVS1 site. Large rep proteins can simultaneously bind to this region and to the viral ITR, and due to their DNA helicase activity they can mediate site-specific integration of the viral genome into the human chromosome 19 (Deyle & Russell, 2009). However, large rep proteins are somewhat permissive in their binding specificity, and substitutions within the core sequence are tolerated. For example, the p5 RBE has only one CAGC repetition and one CAGT sequence, but rep78/68 are still able to bind. It has been estimated that in the human genome there may be 2×10^5 rep binding sites, but the AAVS1 site remains the main integration site. This is probably due to the presence of elements of chromosomal context such as nearby GpC sequences and transcription factor binding sites, which could explain why AAV integration into chromosome 19 has only been observed in higher primates (Douglas M. McCarty et al., 2004). In general, site-specific integration is not an efficient process, and only 0.1% of infecting wild type AAV genome integrates at AAVS1. Indeed, when AAV infect cells, the most common molecular state in which the genome can persist is in the form of double-strand molecular episomes. The episomes can be converted to high-molecular-weight concatamers that are observed as tandem repeats obtained by recombination of monomer genomes and they can provide stable and long-term gene expression, particularly on non-dividing cells (Rutledge & Russell, 1997).

The second ORF, called cap, encodes three capsid viral proteins, VP1, VP2 and VP3, which start from the same p40 promoter. VP3 is a 61-kDa protein that constitutes 90% of the capsid's protein content. The less abundant capsid proteins, VP1 (87 kDa) and VP2 (73 kDa), share the same C terminal amino acid sequence with VP3 but have additional N terminal sequences. VPs are assembled in a ratio of 1:1:10 for a total of 60 monomers that form a complete capsid with icosahedral symmetry (figure 9). VPs are translated from the same mRNA. After this mRNA is synthesized, it can be alternatively spliced to form two pools of mRNAs: a 2.3 kb- and a 2.6 kb-long mRNA pool. In the presence of adenovirus, the 2.3 kb mRNA form is mainly produced, which originates VP2 from an alternate start codon (ACG), and VP3 from a conventional downstream ATG.

VP1 is encoded by the 2.6 kb mRNA, which contains the entire cap ORF. VP1 contains a unique fragment at the N terminus, which possess a nuclear localization signal (NLS) and phospholipase A2 activity (PLA2), required for endosomal escape during the infection cycle (Girod et al., 2002). Moreover, cap gene encodes the assembly-activating protein (AAP) from the same p40 promoter, which has been shown to be crucial for capsid formation by interacting with the C terminus of VPs and facilitating their association into the final capsid structure (F. Sonntag et al., 2011). The topology of the structurally ordered common VP region (VP3) is highly conserved between the AAV serotypes and is made of a core of eight antiparallel beta-barrel motif (beta-B/beta-I) which forms the shell of the capsid plus an alpha-helix (alpha-A) and an extra beta-A strand at the N terminus of the VP3. Different beta-barrel strands are connected by insertional loop which form the majority of the VP3 and viral topology. These loops are named with the name of the strands they connect, for example loop GH between beta-G and beta-H encompasses 230 aa in AAV2 and forms most of its variable regions (Agbandje-McKenna & Kleinschmidt, 2011).

VP3 proteins interact to create the characteristic features of the AAV capsids, depressions at the twofold axes, protrusions surrounding a depression at the threefold axes, and cylindrical channels at the fivefold axes surrounded by a depression (figure 9). The twofold interactions are the least extensive between the VP monomers, being only one polypeptide chain thick, and are created by a conserved small loop at the C terminus (after beta-I) and alpha-A of the neighbor VP. Threefold protrusions are the biggest type of VP interaction and are formed by loop BC, EF and GH, while the depression at the fivefold axis of symmetry is made by HI loop and beta-BIDG sheet. Finally, the channel at the fivefold axis is formed by the DE loop, and due to the conformation of the capsid, it is close to the N terminus of the VP1, which can be exposed to elicit its PLA2 and nuclear signaling activity during the infection cycle (Bleker et al., 2005).

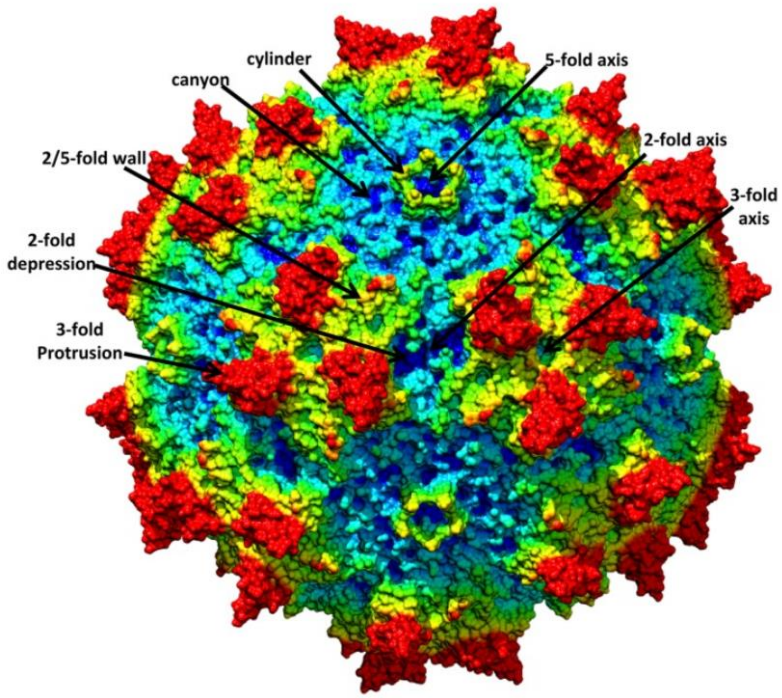

Figure 9. Radially-colored 3D structure of AAV2 capsid. Two, three and five-fold symmetry axis are shown along with the main surface features. (Tseng & McKenna, 2014).

The N-terminal residues, beta-A strand, and beta-BIDG sheet form the interior surface of the capsid, while the loops inserted between the beta-strands form the capsid surface. The AAV surface loop differences, formed by different amino acid, were designated I–IX based on the comparison of AAV2 and AAV4, and are responsible for the variability among the different serotypes, conferring different tropism, immunogenicity and infectivity to the vectors. One interesting feature of the surface loops is that according to their structure it is possible to divide AAV serotypes into two general topologies with respect to the protrusions that surround the icosahedral threefold axes: AAV1– AAV3b, AAV6–AAV8, AAV10 and AAV12 have pointed "finger-like" protrusions, while AAV4, AAV5, and AAV9 have "rounder" protrusions. However, the topology itself is not determinant for the viral tropism and infectivity, but is the amino acid composition of the variable region that confers the receptor binding activity, transduction efficiency and antigenic response (Drouin & Agbandje-Mckenna, 2013).

As already discussed, a new serotype, by definition, is a newly isolated virus that does not efficiently cross-react with neutralizing sera specific for all other existing and characterized serotypes. In other words, AAV whose epitopes are recognized by different types of antibodies are considered different serotypes. In general, the efficiency of a given AAV serotype is often unaffected by the presence of pre-existing neutralizing antibodies to another AAV serotype, but is not always the case, since a certain extent of cross-reactivity is sometimes present (W. Xiao et al., 1999). According to tissue specificity, specific serotypes are used for different therapeutic approaches. Tissue specificity of the main AAV serotypes is reported in table 1.

AAV serotype	Retina	CNS	Heart	Lung	Liver	Muscle
AAV1	X	X	X	X		X
AAV2	X	X			X	X
AAV3	X	X	X		X	
AAV4	X	X	X			
AAV5		X		X		
AAV6			X	X	X	X
AAV7	X	X			X	X
AAV8	X	X			X	X
AAV9	X	X	X	X	X	X
AAV-DJ	X	X	X	X	X	X

Table 1. Tissue specificity of the most commonly used AAV serotypes.

1.7.2 CELL CYCLE

Although AAV technologies are well advanced, our understanding of how the virus interacts with its host at the cellular level remains incomplete. Still, as summarized in figure 10, the main steps required by AAV for succesfull transduction are conserved through all serotypes.

The first step for an efficient cellular transduction sees the AAV capsid binding to glycans or glycoconjugates at the cell surface. This first interaction is crucial for the subsequent binding of the co-receptors for the stabilization of the binding and the internalization. As summarized in table 2, primary and secondary receptor are specific for the different serotypes, which further makes AAV an incredibly powerful tool to targer a broad range of diseases. AAV2, which has mainly been used for this thesis, binds to heparan sulfate proteoglycan (HSPG) as a primary receptor and uses integrins, laminin receptor and growth factor receptors as co-receptors for cell entry (Huang et al., 2014). Precisely, HSPG binding relies mainly on the electrostatic charge interaction between basic amino acids (R, H and K) and negatively charged sulfate residues (Hileman et al., 1998). A conserved cluster of basic residues at the threefold axis of symmetry is present in all the sulfate binding AAV serotypes, and particulary, R585 and R588 has been identified as the main residues involved in HSPG binding of wt AAV2. These arginines has been mutated into increasingly acid residues, and eventually the double mutant R585/588A has been proven to have approximately 2,000-fold-lower infectivety than wt AAV2 (Opie et al., 2003). Since the aim of this thesis project is to develop a tool for cell-type specific gene delivery based on chemical modifications of AAV capsids designed to change the normal AAV tropism, most of the AAV2 vectors I have been using carried the R585/588A mutations. However, this well characterized double mutant is not completely silent, since when used at high MOI, robust transduction of cells has been seen both in vitro and in vivo (Gorbatyuk et al., 2019).

Following the initial binding on the cell surface, some host factors responsible for post-attachment cell entry of AAV have been identified. KIAA0319L is a type I transmembrane protein, which has been recently indicated as an essential host factor required for internalization of most AAV serotypes, and thereby called universal AAV receptor (AAVR) (Pillay et al., 2016). It comprises five polycystic kidney domains (PKD1–5) on the ectodomain, which are short modules originally found in the extracellular segment of the glycoprotein polycystin-1 and involved in protein-protein/carbohydrate interactions. Only AAV5, the most divergent of the commonly studied serotypes, required PKD1 for transduction, while others interacted with PKD2, and among all serotypes, only AAV4-derived vectors seem not to require the AAVR for internalization (Dudek et al., 2018). AAV2 interaction with AAVR has been delineated by cryogenic electron microscopy at resolutions of 2.8 Å, and shown that PKD2 binds directly to the spike region of the AAV2 capsid adjacent to the icosahedral three-fold axis, precisely to the strands B, E and the BC loop (R. Zhang et al., 2019). A second recently identified host factor for AAV entry has been found as the G-protein coupled receptor GPR108 (Dudek et al., 2020). This protein acts independently from the AAVR, since AAV5 (but not AAV4) is the only serotype which seems not to rely on GPR108 for the cellular entry. As both KIAA0319L and GPR108 are mainly localized in the Trans-Golgi network (TGN) they are likely to be involved in the Golgi trafficking of AAV. The mechanism and the interaction between these two host factors is still to be investigated, but it has been proposed that AAVR binds the intact capsid

and traffics to the TGN, at which point endosomal acidification triggers a conformational change in capsid and extrusion of the VP1/2 unique region of capsid, then allowing engagement of GPR108 via the VP1 unique region (Dudek et al., 2020). Given the phospholipase activity of the VP1, is possible that GPR108 may facilitate endosomal escape, possibly by stabilizing the extruded VP1 unique domain or by generating a pore in the endosomal membrane.

Serotype	**Glycan Receptor**	**Co-receptor**
AAV1	2,3N/2,6N-Sialic Acid	Unknown
AAV2	HSPG	FGFR1, HGFR, LamR, Integrin
AAV3	HSPG	FGFR1, HGFR, LamR
AAV4	O-Sialic Acid	Unknown
AAV5	N-Sialic Acid	PDGFR
AAV6	N-Sialic Acid	EGFR
AAV7	Unknown	Unknown
AAV8	Unknown	LamR
AAV9	N-galactose	LamR

Table 2. Main AAV natural serotypes and their receptor and co-receptor(s). HSPG, heparan sulfate proteoglycan, EGFR, epidermal growth factor receptor, FGFR1, fibroblast growth factor receptor 1, HGFR, hepatocyte growth factor receptor, PDGFR, platelet derived growth factor receptor, LamR, laminin receptor, Integrin, Integrin a5b1/aVb5.

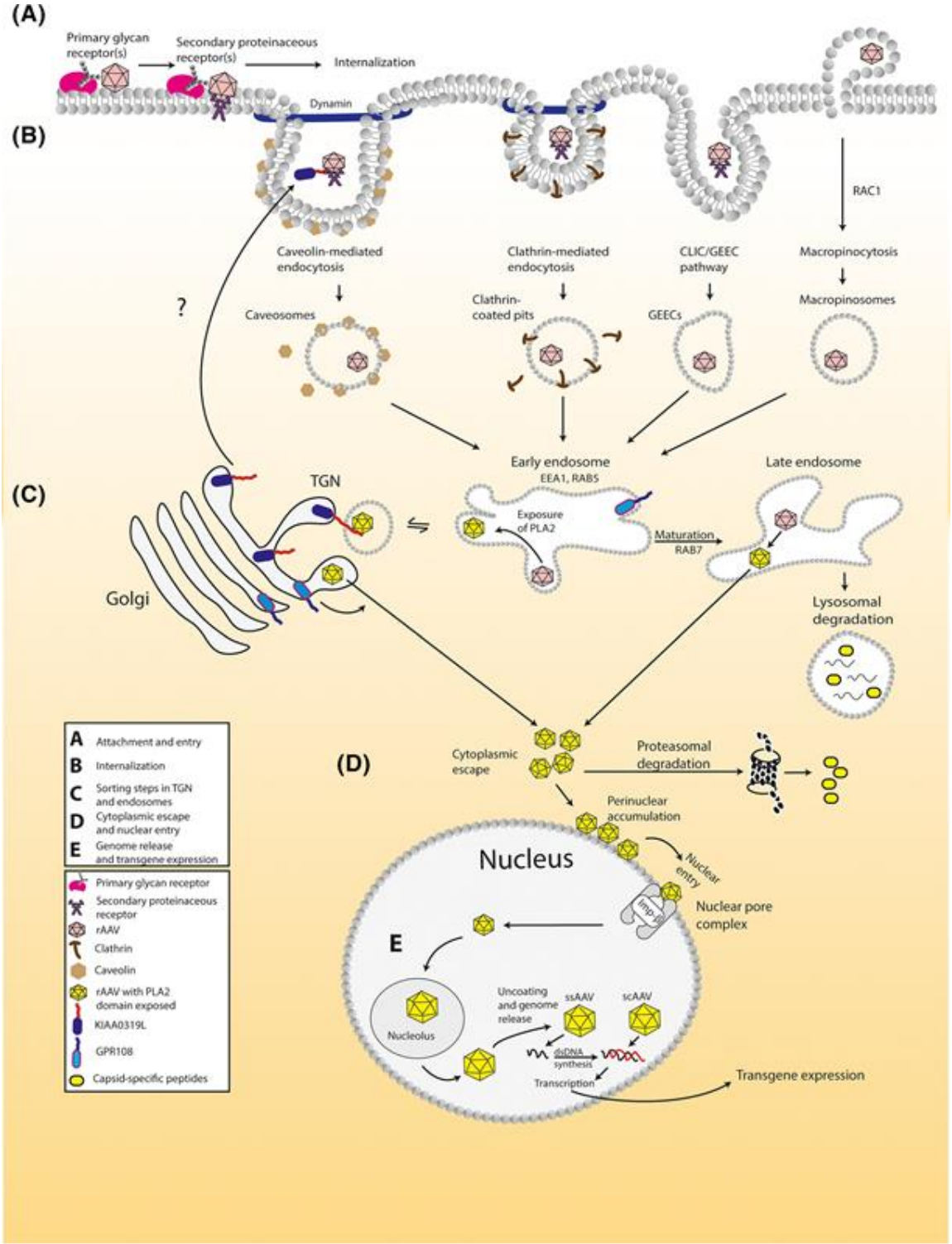

Figure 10. Overview of intracellular transport of AAV. A) Cell attachment is mediated by surface glycan proteins and stabilized by secondary receptors. B) Internalization can happen though different mechanisms, which include caveolin/clathrin coated vescicles, micropinocytosis and clathrin-independent endocytosis. C) Endosomal trafficking is required to expose VP1 PLA2 domain to escape endosomes and prime the viral vector for nuclear transport and DNA release. D) Intact viral particles are transported into the nucleus where DNA is released and transgene is expressed. (Dhungel, 2021).

Following cell attachment, AAV are internalized through different endocytosis mechanisms. Despite different pathways have different timing, the internalization process is very fast: it has been shown that after AAV2 infection of HeLa cells, 13% of the viral particles have already been internalized within 1.2 seconds, and that after 15 minutes, at least one VG has been detected in the nucleus of half of the cells (Seisenberger et al., 2001). Studies on Dynamin, a GTPase protein involved in the internalization of receptors and their ligands from the cellular membrane through clathrin-coated pits, indicated clathrin-dependent endocytosis as one of the main internalization mechanism taken by AAV2 (Duan et al., 1999). Similarly, caveolin-mediated endocytosis have been proposed to be an alternative and co-existing mechanism (B. P. Dhungel et al., 2021). Another study showed that the binding of AAV2 to the αVβ5 integrin and the activation of Rac1, a GTP binding protein not involved in clathrin/caveolin pathways, was necessary to initiate intracellular movement of AAV-2 to the nucleus via both microfilaments and microtubules through a mechanism called macropinocytosis (Sanlioglu et al., 2000). Finally, an alternative endocytosis mechanism has been proposed, in which AAV2 is transported directly to the Golgi via clathrin-independent carriers (CLICs) in glycosylphosphatidylinositol (GPI)-anchored protein-enriched endosomal compartments (GEECs) (Mathieu Nonnenmacher & Weber, 2011). Even if all the four endocytosis mechanisms have been reported, is still unclear which are the main routes taken by the different serotypes. Probably all the mechanisms coexist and contribute at different levels, depending on the cell type, the presence of receptors/co-receptors and the internal status of the cell. However, early internalization processes are crucial for efficient transduction, since direct injection of AAV2 in the cytosol or in the nucleus highly impairs transduction rates (Florian Sonntag et al., 2006). Indeed, cellular trafficking via early endosomes, late endosomes and Golgi are required for transduction. In this respect, Rab proteins, involved in many steps of membrane trafficking, play a central role in the sorting of viral particles after their internalization. Although the detailed molecular mechanism underlying the differential endosomal sorting processes remains unclear, studies have demonstrated that the distinct endosomal trafficking could be the result of viruses binding to different attachment receptors (Ding et al., 2006). Retrograde transport of AAV2 to Golgi has been observed, and in particular, AAV2 particles sorted toward late endosomes from early endosomes rely on a Rab9-facilitated pathway, while virions destined to perinuclear recycling endosomes are transported to the Golgi through a Rab11-dependent mechanism. It is believed that retrograde transport and accumulation in the Golgi induces profound changes in capsid conformation that are required for efficient transduction. Moreover, within the cytosol, only a small percentage of the viral particles can actually reach the nucleus: in the case of AAV2 infection, it is believed that 80% of the viral particles fail to escape the endosomes (Hansen et al., 2000). Indeed, degradation of AAV particles via ubiquitin-protease system results in unproductive transduction. First and second generation proteasome inhibitors have been used to enhance AAV infectivity, including MG132, a potent protease inhibitor, which has been shown to drastically increase AAV2 infectivity in vitro (Douar et al., 2001). Another strategy to avoid proteasome-dependent degradation is to mutate single or multiple surface-exposed tyrosine residues, which are involved in the ubiquitination. Epidermal growth factor receptor protein tyrosine kinase (EGFR-PTK) has been proved to phosphorylate exposed tyrosine residues on AAV2 capsids, which promotes ubiquitination and degradation of the vector. After exploring different mutant combinations, the triple mutant Y444+500+730F have been shown to be around 30-fold more efficient than wt AAV2 in mouse, and has also shown efficacy in phase I and II clinical trials of Leber hereditary optic neuropathy (Guy et al., 2017). However, since phosphorylation can also occur on serine and threonine residues, site-directed mutagenesis into valine of all these

residues have been explored, and different AAV2 variants with enhanced efficiency have been discovered (Aslanidi et al., 2013). Then, the most efficient Y, S, and T mutations were subsequently combined into one capsid, and the quadruple mutant (Y444+500+730F+T491V) AAV2 vector has been identified as the most efficient, with a 24-fold increased efficiency of transduction of murine hepatocytes both in vitro and in vivo (Aslanidi et al., 2013). Even if the exact molecular mechanism has still to be explored, modulation of the ubiquitin-protease system, autophagy, and endoplasmic reticulum-associated protein degradation pathways affects AAV transduction.

Prior to enter into the nucleus, AAV particles need to escape the endosomes, and for this step a conformational change induced by the endosomal trafficking is essential. The unique N-terminal domains of VP1, which is buried inside the capsid in intact virions and is not targetable by neutralizing antibodies, contains a phospholipase A2 (PLA2) domain that has been shown to be necessary for endosomal escape as well as three basic clusters (BC1, 2 and 3) that act as nuclear localization signals for the viral capsid (M. Nonnenmacher & Weber, 2012). As has been observed for other non-enveloped viruses, such as adenoviruses, the conformation change that happens within the endosomal compartment allows the externalization of the VP1 N-termini through the pore present at the five-fold axis of symmetry of the viral capsid, so that the PLA2 can elicit its function (K. Wang et al., 2000). Once in the cytosol, the basic residue clusters of VP1 would then mediate the nuclear import of full virions. What triggers the capsids conformation change within the endosomes is still to be fully understood, but endosomal acidification is required. Moreover, endosomal cathepsins B and L are required for transduction by “priming” the capsids by partial proteolysis, even if is not clear whether they act directly on the endosomal escape or on a later step of the transduction process (Akache et al., 2007). It is interesting to note however that different serotypes show different uncoating patterns and rely on different mechanisms: for example, AAV5 is not sensitive to cathepsin proteolysis, and AAV8 shows different kinetics (M. Nonnenmacher & Weber, 2012).

Following endosomal escape, AAV particles accumulate around the perinuclear space and are ready to be transported into the nucleus. Different evidence suggest that intact particles are translocated into the nucleus before DNA release, as it is possible to extract intact vectors from nuclei of infected cells, or intact particles could be directly detected by immunofluorescent microscopy (McGhee et al., 2016). Basic clusters BC1 and BC2, which are present in the VP1 and VP2 N-termini, form a bipartite nuclear localization signal which is required for the transport into the nucleus through the nuclear pore complex (NPC). Importin-β, a major constituent of the NPC, colocalizes and interacts with AAV, and knockdown of importin-β, as well as blockage of the NPC with wheat germ agglutinin (WGA), severely inhibits AAV2 nuclear entry and transduction (Nicolson & Samulski, 2014). When in the nucleus, intact viral particles are transported into the nucleolus, where AAV2 interacts directly with nucleolin and B23/nucleophosmin (M. Nonnenmacher & Weber, 2012). The exact role of this step in the transduction process is still unknown, and it actually seems to be detrimental, as nucleolin or nucleophosmin knock-down results in enhanced transduction (Johnson & Samulski, 2009). Probably, accumulation of intact viral particles into the nucleolus serves as a temporary storage for secondary transduction of the cell.

Genome release does not require a complete disassembly of the capsid, but the kinetics appear to be cell- and serotype-dependent. For example, although AAV2, 6 and 8 have similar uptake and

nuclear import rates during murine liver infection, AAV6 and 8 seems to release their genome earlier than AAV2 (Thomas et al., 2004).

Within the nucleoplasm, for transgene transcription to occur, the single-strand DNA molecule of AAV must be converted into double-strand. This is a time-limiting step for the transduction process that can be sped up by using self-complementary vectors, in which second-strand synthesis is not required at the expense of a reduced transgene capacity of the vector. Interestingly, the presence of some adenoviral genes can dramatically enhance this process. Expression of early region 1 and 4 (E1 and E4) genes of adenovirus seems to be directly proportional to the appearance of double-stranded replicative forms of the AAV genome (Fisher et al., 1996). In case of a normal AAV infection, double-strand DNA deposits have been observed into infected cells nuclei as soon as 3h post infection, associated with the MRE11-RAD50-NBS1 (MRN) complex. MRN, which is involved in DNA repair, seems to downregulate transgene expression: downregulation of MRN by RNA interference increases both the formation of dsDNA deposits and the level of AAV transduction (Cervelli et al., 2008). As already discussed, AAV genomes persist in postmitotic cells predominantly as episomes which could be converted into extrachromosomal concatemers, while only a small percentage of genomes (0.1%) integrate into host genome. Despite this, the issue of AAV-related genotoxicity is essential in the context of clinical gene therapy, with regards for liver-directed therapy, in which a higher insertional mutagenesis rate and tumorigenic potential have been observed in mouse models (Chandler et al., 2015). However, long-term studies on larger animal models, including non-human primates, raised no concerns over the genotoxicity risk of AAV vectors in liver, unless high doses of virus are delivered (Gil-Farina et al., 2016).

1.8 ENSTABLISHING CELL-TYPE SPECIFICITY WITH VECTOR ENGINEERING

In the last years, many efforts have been made to improve AAV technologies, in particular in terms of efficiency and specificity of the vectors. Indeed, for clinical applications, the minimal effective dose of virus delivered is always the best choice in order to avoid off-target effects and minimize the costs of the therapy. In this regard, capsid engineering aims to reach the full potential of AAV based gene therapies by acting on two main strategies: increasing the efficiency of transduction and conferring cell-type specificity to the vectors. Boosting the efficiency means to obtain the same level of transduction with a lower viral dose delivered, but still infecting cells that are not the target of the therapy. Despite a lower dose would be related to the reduction of off-target effects, the infection of unwanted cells would decrease the amount of virus available for the actual therapy and could lead to side effects such as hepatotoxicity, which is one of the main adverse effect of gene therapy. On the other hand, working on viral tropism in order to re-direct it toward the cell population of interest has an immense therapeutic potential. The main advantage of this strategy is the possibility to transduce directly the cells that carry genetical disfunctions and correct their functionality minimizing, at the same time, the loss of vector particles to irrelevant cells. It would then be possible to reduce off-targeting and side effect, thereby decreasing the amount of virus required to get the therapeutic effect as well.

To simplify, strategies employed to achieve cell-type specificity and increased transduction efficiency of AAV could be divided into two categories: genome engineering and capsid engineering.

AAV genome modifications are based on cell type-specific gene regulatory elements like enhancers/promoters for transcriptional targeting and cell/tissue-specific miRNAs for post-transcriptional targeting.

Capsid engineering strategies can be broadly divided into two main categories: directed evolution and rational design. Directed evolution consists in multiple rounds of infection of a target cell type with artificially created libraries of mutant capsids and the selection of the most efficient and/or tissue-specific. In the rational design strategy, target cell-specific proteins/peptides are included in different capsid sites that allow insertion without affecting packaging or transduction efficiency. Moreover, cell-type specificity is achieved by single/multiple amino acid mutagenesis or by the use of hybrid capsids.

1.9 AAV GENOME ENGINEERING

Transcriptional and post-transcriptional targeting strategies do not alter the biodistribution of a vector, but restrict the expression of the transgene product to the desired target cells. Tissue-specific promoters, which activation and regulation relies on different and specific regulatory elements and cellular factor present in the different cell populations, are often used to achieve specificity and avoid off-target effects. At the moment, many tissue-specific promoters are available, with proved efficacy in many clinical trials targeting different organs. In the case of hepatocellular carcinoma (HCC), for example, the Glypican 3 (GPC3) promoter has been used as a targeting strategy (B. Dhungel et al., 2018). Since GPC3 is expressed mainly in HCC and not in normal liver cells, vector carrying the GPC3 promoter succeeded in killing a significantly higher number of HCC cells than normal liver cells, suggesting that this targeting strategy could limit hepatotoxicity in case of liver-targeted gene therapy. Moreover, tissue-specific promoters are currently used to deliver AAV to the nervous system, with the possibility to discriminate between neuronal subtypes. For example, in the context of spinal cord injury, the mouse phosphoglycerate kinase (mPGK) promoter has been used to drive strong expression in cortical neurons and oligodendrocytes, while using the human synapsin (hSYN) promoter resulted in neuron-specific expression, including perineuronal net expressing interneurons (Nieuwenhuis et al., 2021).

In the same way, transcriptional regulatory elements such as enhancer can be inserted into vectors genome to modulate transgene expression. The human cytomegalovirus (CMV) immediate-early enhancer is one of the most commonly used regulatory elements to boost transduction levels. However, when combined with cell-specific promoters, CMV enhancer activity could lead to significant increase of transgene expression at the expenses of promoter leakiness and off-target infection (Gruh et al., 2008).

Finally, posttranscriptional targeting strategies that function at the mRNA level are also commonly used to restrict transgene expression only in cell types on interest, and could be used also in combination with specific promoters. This strategy exploits a class of physiologically expressed small noncoding RNAs (miRNAs), which bind to complementary RNA sequences in the 3´-UTR region of mRNAs, thereby either inducing their degradation or preventing their translation, according to the level of complementarity. These miRNAs could be expressed ubiquitously or just in particular stages

of development in specific cell types. The strategy relies on the insertion of miRNAs binding sites in the transgene of interest, thereby preventing transgene production in unwanted cells, which are the ones that express high levels of target miRNA. This technology has been used to prevent antigen-presenting cells to express transgene, thereby activating an immune system response, or to segregate transgene production between different cell types of the same tissue (Hacker & Büning, 2011).

To conclude, is worth to note that specific promoters are usually large in size, and the AAV packaging capacity is limited. For this reason, is often impossible to insert the desired transgene into one single vector, thereby requiring the use of alternative strategies such as split-system vectors, which are in general less efficient than normal recombinant AAVs. Moreover, as already discussed, using a specific promoter does not prevent the infection of non-desired cells, which means a loss of virus that will not contribute to the therapeutic effect, and an increased risk of genotoxicity and immune system activation.

1.10 AAV CAPSID ENGINEERING

As previously discussed, the first step for AAV infection is the attachment on the cell surface though AAV receptors and co-receptors. This process could be rationally engineered by mutating the contact residues on the AAV capsid and attaching targeting ligands to the capsid surface that display high affinity for a cell surface protein/receptor of choice. In this way, it is possible to selectively deliver genetic material to target-receptor positive cell types. Typically, these strategies require the disruption of the AAV main receptor, so that is possible to replace the vector binding ability by inserting the desired targeting ligand. In general, two main strategies for coupling targeting ligands to the AAV capsid can be distinguished. Genetic coupling consists in the expression of fusion proteins inserted in specific locations of the Cap ORF of the AAV, which will lead to the formation of a complex in which the ligand is directly fused to the viral vector. On the other hand, biochemical coupling strategies consist of the covalent conjugation of targeting ligands by biochemical reactions, typically exploiting natural occurring functional groups on the AAV capsid and/or on the target ligand. The main difference between these two strategies is that in the case of biochemical coupling, all the modification are performed post-translationally, which means the virus is already functional and there is no need of genetic modification of the vector or ne-novo production of new virus for every modification.

1.10.1 Genetic Modification

In the case of genetic coupling, the main challenge is to find the optimal place in which to insert the ligand, without affecting AAV packaging, binding ability or general functionality. Because of their exposed positions and their function in receptor binding, VRs forming loops of the protrusions are ideal positions for capsid modifications aiming to re-direct AAV tropism. Indeed, one of the first successful capsid modification for re-targeting of AAV2 has been performed at the insertion site I-587 (which is between the amino acid residue asparagine 587 and arginine 588) of the common VP3 region (Girod et al., 1999). The authors inserted a 14 amino acid long peptide which exhibited high affinity for the β1 integrin, whose expression is upregulated in some types of cancer cells. The resulting virus was able to transduce target cells, even in the presence of heparin, an analog of AAV2's main receptor, which indicated successful re-targeting of the vector. At the time, no crystal structure of AAV capsid was available, but in the next years it has been shown that insertion of peptides at I-587 changes the spacing between R585 and R588 and thereby destroys the AAV2 HSPG binding motif. Moreover, this region is known to be part of one of the most external loops at the 3-fold axis of symmetry (Xie et al., 2002). Subsequent studies confirmed the great potential of this insertion site (Büning & Srivastava, 2019). Indeed, the AAV2 I-587 insertion site allows insertions of small peptides (up to 34 amino acid) without interfering with capsid assembly or genome packaging, displays the foreign sequence in a position in which the peptides can interact with target cell surface receptors and eventually allows AAV2 re-targeting in a single step because the AAV2 primary receptor is destroyed upon insertion of the novel targeting ligand.

Exploiting the same principle, VR-IV, which forms the highest protrusion of the AAV2 capsid, have been the target for peptide insertion. The peptide RGD-4C, a high-affinity ligand of αvβ3 integrin, which is highly expressed in cancer cells and angiogenic vessels, has been inserted between glycine 453 and threonine 454 (I-453), together with arginine 585/588 to alanine substitution to destroy AAV2's natural HSPG binding ability. Successful surface cell targeting and transduction has been observed, even when simultaneous insertion of the same peptide in the position I-587 was performed, showing that AAV2 capsid could tolerate simultaneous peptide insertions (Boucas et al., 2009).

Rational design could be also combined with direct evolution in order to obtain cell-type specific vectors. As discussed, directed evolution involves the artificial generation of large mutant capsids libraries and high-throughput selection of vectors with enhanced proprieties after many rounds of infections of the desired cell-types. Typically, such approaches have been used to study the effects of random mutations of AAV capsids on gene delivery efficiency or vector's ability to evade antibodies neutralization (Maheshri et al., 2006). However, it is possible to apply the same principle to select for cell-type specific vectors after the insertion of random peptides libraries.

Indeed, positions I-587, I-588 and I-453 have been chosen as insertion sites to display library of peptides in order to identify possible ligands suited for targeted cellular transduction. Therefore, in order to be able to transduce desired cell types, not only an insertional strategy is required, but also the insert itself. In the first studies, new peptides have been classically identified through phage display technique, in which libraries of polypeptides are presented on the surface of lysogenic filamentous bacteriophages. These phage libraries can then be screened against other proteins, peptides or DNA sequences, in order to detect interaction between the displayed protein and those

other molecules, and therefore select binding phages and identify the targeting polypeptide (Ledsgaard et al., 2018). However efficient, this technique can't tell if the chosen peptide would still be functional after its coupling with the viral vector. Thereby, the AAV peptide display technique has been implemented. Using this technology is possible to directly select AAV variants with enhanced specificity or efficiency toward particular cell types, including cancer models (Michelfelder et al., 2011). In this case, oligonucleotides of random sequence are inserted into the CAP ORF typically at the insertions sites I-587, I-588, I-453, thereby generating a library plasmid pool that is subsequently used to produce the AAV peptide display library (Müller et al., 2003) (Perabo et al., 2003). The peptide library, in which all the vectors are identical except for the peptide displayed on the capsids, is used to transduce target cell population (usually AAV resistant, or in particularly stringent experimental conditions), typically in the presence of adenovirus to provide the helper functions required for the replication of the vectors that successfully infected target cells. Only infective AAV can thereby replicate, and multiple rounds of selections are made in order to eventually select the most efficient/specific variant of the library. An alternative to the use of adenovirus is the PCR-based amplification approach, in which infected cells are isolated, viral DNA extracted, amplified by PCR and cloned as a sublibrary plasmid pool. The new vectors produced with the selected DNA are then used for the subsequent rounds of amplification. One of the most famous application of this system lead to the identification of the AAV9 variant AAV-PHP.B, that exhibits enhanced transduction of mouse central nervous system by crossing the blood-brain-barrier (BBB) (Deverman et al., 2016). In this work, the authors devised a Cre recombination-dependent approach to selectively recover capsids that transduce predefined Cre expressing target cell populations. Since with standard PCR-based amplification approaches, it is impossible to discriminate between capsid variants that only enter into target cells and the ones that actually release their genome, a transgenic mice line expressing Cre recombinase specifically in astrocytes through the use of a cell-specific promoter has been used. In this way, by using specific PCR primer designed to amplify only the viral genome that underwent Cre-mediated recombination, it has been possible to select only infecting vectors. A library of AAV9 variants expressing random 7 amino acid-long (7-mer) peptides inserted at the I-588 position of VP1 have been systemically injected into Cre-mice, and the AAV-PHP.B variant, expressing the 7-mer TLAVPFK peptide, has been identified as able to successfully crossing the BBB and infect CNS with a 40-fold increased efficiency compared to wild type AAV9 (Deverman et al., 2016). Unfortunately, however, subsequent studies indicated that the enhanced CNS tropism of AAV-PHP.B is restricted only in the C57BL/6J mouse model, and not in other mice strains (such as BALB/cJ) or in non-human primates, due to the restricted expression pattern of the TLAVPFK peptide receptor L6YA (Hordeaux et al., 2018).

As we saw, even if capsid modification on the VP3 can be implemented, VP1 but mainly VP2 are mostly used as insertion sites, due to the fact that VP2 capsid protein is not essential for the assembly, packaging and functionality of AAV (Warrington et al., 2004). The first attempt to modify N-termini of VP2, and actually the first cell surface targeting approach for AAV in general, aimed to attach a single-chain antibody directed against human CD34, a cell surface marker on hematopoietic cells. Even if very low titre of virus was produced, the chimeric vectors were able to transduce a CD34 positive human cell line, thereby establishing the N-termini of VP2 as a valid position for

protein insertion (Q. Yang et al., 1998). Moreover, it is interesting to note that the N-termini of VP2 is buried inside the capsid in wt AAV2, but surface exposure on vector capsid following genetic modification is required for efficient binding on target cell. To address this gap, it has been actually shown that insertion of target sequences interferes with the natural folding and thus prevents masking of the N termini of VP1 and VP2 within the capsid, which can however retain its functionality (P. Wu et al., 2000).

Successive studies shown that genetic insertion of small peptides one or two residues after N-terminal methionine of the VP2 start codon were also tolerated (P. Wu et al., 2000). However, since VP1 is an N-terminal extension of VP2, insertions are not only displayed at the N -termini of VP2, but also at the amino acid position 138 or 139 of VP1. For this reason, since VP1 is important for capsid assembly, the presence of large foreign inserts could prevent AAV formation. Indeed, only peptides up to 32 amino acids have been successfully inserted in this position so far, without providing additional VP *in trans* during vector production to compensate the dysfunctional VP1 (P. Wu et al., 2000). As proof of concept, the authors have shown that insertion of the serpin receptor ligand in the N-terminal regions of VP1 or VP2 can re-target AAV tropism. However, insertion of larger proteins in the same I-138 position results in a reduced production of VP3, which inhibits capsid assembly. To overcome this issue, expression of one capsid protein is isolated and combined with the remaining two capsid proteins expressed separately. Typically, VP2 fused with insertional protein is expressed via a non-AAV promoter from a different plasmid, and genome-containing capsid are formed regardless of which capsid proteins were supplied separately. Using this strategy, different proteinaceous ligands have been fused at the I-138 position, but viral functionality has been maintained only when exclusively VP2 and not VP1 was modified (Warrington et al., 2004).

An interesting application of the technology discussed above is to fuse fluorescent protein to AAV's VP2 in order to quantify dynamics of viral vector uptake in cells. Current strategies for visualizing infectious pathways of viruses rely on fluorescent labelling of capsid proteins, such as luciferase enzyme or GFP. By fusing the gene coding for the luciferase enzyme on the N-termini of VP2 and simultaneously providing wt VP1 and VP3 in trans, chimeric AAVs have been obtained and have been used for studying cellular uptake kinetics of serotype 1, 2 and 8 (Asokan et al., 2008).

Moreover, the possibility to accomodate big inserts in the VP2 have been exploited to develop AAV-based single-shot prime-boost vaccines (Rybniker et al., 2012). Specifically, this approach is based on antigen-VP2 fusion proteins that are incorporated into the AAV capsid to prime the antigen-specific humoral immune response, which can be coupled with the insertion of the same antigen into the vector genome to boost the immunogenic effect. For example, a modified version of Ag85A, a well-described target antigen of *Mycobacterium tuberculosis* vaccines, have been inserted into AAV2 VP2, and the immunogenic potential of the resulting vector has been tested in mice (Rybniker et al., 2012). Results showed a faster onset of antigen-specific antibodies, which exhibited a significantly higher avidity compared with the ones originated by the injection of AAV2 coding for the same Ag85A, but without any capsid modification. Moreover, a single injection of the modified vector was sufficient to induce a memory recall response.

Another interesting application of the insertion of a large protein on AAV surface is the development of switchable AAV vectors, which are modified vectors whose infectivity can be controlled by small chemical molecules. The first work aimed to re-target AAV2 in order to specifically infect epidermal growth factor receptor (EGFR) positive cells required the insertion of the FK-binding protein (FKBP)

as targeting ligand and the presence of an adapter protein composed by a modified FKBP-rapamycin binding domain (FRB) connected to a fluorescent protein and to a EGFR-specific DARPin (Hörner et al., 2014). Upon addition of the rapamycin analog AP21967, binding of FKBP to FRB is induced leading to recruitment of the AAV-2 particle to the EGFR-positive cells and subsequent infection. Likewise, without any addition of AP21967, modified AAV2 were not infective.

In the attempt of exploiting the great viability and specificity of single-chain antibodies to re-direct AAV tropism, efforts have been made to fuse this class of protein to the VP2, but in all the cases the vectors obtained were not functional, probably due to the conditions in the cell nucleus that interfere with correct folding due to inhibition of cysteine bridge formation (Büning & Srivastava, 2019). Designed ankyrin repeat proteins (DARPin) offer a powerful alternative to antibodies: they are small antibodies-mimic proteins with high affinity and specificity, and they do not contain cysteine bridges in their structure, thereby being easier to produce by cells. In one of the main studies in which DARPins have been used to modify AAV tropism, the authors demonstrated that AAV2 made specific for Her2/neu, EpCAM or CD4-positive cells through the use of specific DARPins fused to the VP2 N-termini were able to selectively infect only the cells of interest, with no detectable off-targeting, both in vitro and in rodents models (Münch et al., 2015).

1.10.2 Chemical Modification

Beside genetic manipulations, ligand coupling on AAV capsids can also be achieved by chemical modifications. The principle remains the same: exploiting the specificity of the chosen ligand to direct the modified vector on the cell types to which the coupled ligand binds. In this case, macromolecules of different nature are coupled to the virus though chemical reactions which rely on chemically active groups present of both the components of the system. These reactive groups can be naturally present or can be artificially inserted.

As previously discussed, the main advantage of this approach is that since the chemical modifications are made directly on a virus which is fully formed there is no need to produce new vectors for every single modification protocol. By skipping the production part, it follows that the modifications can be done in a time and money-saving manner. In general, chemical modification protocols are thereby more versatile than the respective genetic modification, since they are easier to be done and they usually do not require particular equipment or material. Moreover, since no genetic manipulation is performed, there is no risk of affecting viral assembly or packaging by inserting a ligand. On the other hand, it is possible however that during the modification both the insert and the vector could lose their functionality. For example, if the insert is modified on a site crucial for its binding ability, after the conjugation with the vector it will not be able to bind to target cells anymore. In the same way, by coating too much the vector with the ligands one could prevent the virus interacting with the cellular structures required for its internalization, thereby neutralizing the infectivity. Keeping this in mind, it is expected however that chemical coupling could allow for the insertion of bigger ligands compared to genetic modifications. Indeed, by chemically coupling a ligand on the vector, it will remain attached directly on the capsid surface, and not *into* it. This means that the viral structure itself will not be impacted by the size of the ligand, that is instead one of the problems of genetic insertion of proteins.

Moreover, if the aim is to re-direct viral tropism, natural binding site of the original AAV must be destroyed beforehand. In the case of AAV2 manipulation, for example, it means that chemical modification must be performed on vectors which carry the R585/588A substitution to destroy the HSPG binding domain. This is not relevant in the case of tropism expansion experiments (in which the aim is to confer a broader tropism to the vector) or efficiency boosting approaches (by coupling a ligand with the same cellular specificity of the chosen AAV serotype).

As discussed, chemical modifications rely on specific reactive groups that can be naturally present in the molecule structure or directly inserted. In the case of artificial insertion, one of the most popular strategy relies on unnatural amino acids (UAAs). In this case, genetic modification of the capsid is paired with a subsequent chemical modification. One of the best example of this strategy consist in the insertion of an azide moiety into the AAV2 capsid by mutating the VP3 (C. Zhang et al., 2016). Specifically, an amber codon (TAG) has been inserted in different position of the VP3 (including I-588 to disrupt natural HSPG binding ability), following incorporation of the UAA Nϵ-2-azidoethyloxycarbonyl-l-lysine (NAEK) via co-expression of the NAEK-specific orthogonal tRNA/aminoacyl-tRNA synthetase pair. This led to the creation of modified AAV2 particles carrying an exposed azide moiety directly on the protrusions of the capsid. A modified version of the RGD motif has been chosen as the guiding ligand, consisting in the RGD peptide directly connected with a dibenzocyclooctyne (DBCO) molecule, which specifically reacts with the azide group. The RGD motif is well known to be highly specific for a subset of integrin αvβ3 molecules that are highly expressed in a wide variety of tumors. When tested on U87 cells, which expressed high levels of integrins, the modified vectors shown an enhanced tropism and transduction compared to unmodified AAV2, thereby indicating successful re-targeting of the vectors(C. Zhang et al., 2016). However efficient, this approach still implies a genetic modification step, thereby remaining very demanding because it requires optimization of each step of production and modification, followed by functional and structural characterization of the vectors.

On the other hand, an easier approach to chemically attach ligands on the AAV surface is by exploiting reactive groups that are naturally present in the amino acid sequence that composes the capsid. In chemical bioconjugation protocols, the most relevant amino acid that are modified are the lysins residues. Lysine residues present a primary amine group (-NH2) on their side chain, the so-called ε-amine (which is the amine functional group directly connected to the fifth carbon atom of the lysine backbone). These primary amines are positively charged groups and therefore they tend to take place on the outside surfaces of proteins where they are readily accessible to conjugation reagents.

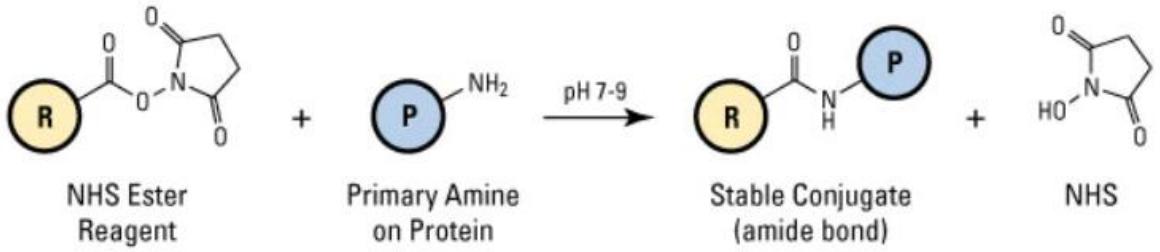

Figure 11. NHS-ester reaction scheme. R represent a general compound, while P represent a protein carrying a primary amine. Source, Thermo Scientific -Crosslinking Technical Handbook, 2012.

Furthermore, primary amines are especially nucleophilic, which makes them suitable for reaction with a wide range of synthetic chemical groups, including isocyanates, n-hydroxysuccinimide (NHS) esters, sulfonyl chlorides, aldehydes, glyoxals, epoxides, oxiranes, carbonates, aryl halides, imidoesters and carbodiimides (Thermo Scientific -Crosslinking Technical Handbook, 2012). For example, the reaction of -NH2 with an aldehyde is used in the fixation of biological tissues, though the reaction with formaldehyde and glutaraldehyde. However, NHS esters and imidoesters are the most popular amine-specific functional groups that are used for bioconjugation with primary amines. NHS is an organic compound used as a reagent for the preparation of active esters, which are functional groups that, being highly susceptible toward nucleophilic attack, present a strong reactivity towards primary amines to give amides. Specifically, NHS esters are made by carbodiimide-activation of carboxylate molecules. The most common carbodiimide compound, 1-Ethyl-3-(3-dimethylaminopropy) (EDC) reacts and activate carboxyl groups by forming an active O-acylisourea intermediate which reacts with primary amines through an amide bond. However, EDC is mainly used for NHS activation: EDC couples NHS to carboxyls, forming an NHS ester that is considerably more stable than the O-acylisourea intermediate, thereby making NHS-esters a more attractive option for amine coupling rather than just using EDC to activate carboxyl groups. NHS-ester-activated crosslinkers react with primary amines to form stable amine bonds, releasing NHS, as shown in figure 11. Even if NHS esters are more stable than O-acylsourea intermediates in aqueous solutions, hydrolysis of the NHS ester competes with the primary amine reaction. Indeed, the rate of hydrolysis increases with buffer pH and contributes to less-efficient conjugation with amine-containing ligands. The half-life of hydrolysis for NHS-ester compounds is 4 hours at pH 7.0 and 0°C, decreasing to 10 mins at pH 8.6 and 4°C, the reason why is important to use fresh-prepared NHS ester solutions prior of every conjugation process. Phosphate, carbonate-bicarbonate, HEPES or borate buffers can be used for the conjugation reaction, while amine-containing buffers such as Tris (TBS) should be avoided because they compete for reaction (Thermo Scientific -Crosslinking Technical Handbook, 2012).

According to the AAV2 sequence, every VP3 contains 34 lysine residues, 10 of which are exposed on the capsid external surface. This means that there are around 550 lysine residues potentially accessible for chemical coupling.

One of the first attempt to chemically modify AAV2 capsid by acting on lysine residues aimed to conjugate polyethylene glycol (PEG) molecules to the virus in order to cover the antibodies binding sites and help the virus avoid the immune system (Lee et al., 2005). Indeed, since most of the population present pre-existing immunity against AAV vectors, dramatic inhibition of AAV vector gene delivery by neutralizing antibodies highly impairs the effects of vectors, even in immune privileged organs (Sanftner et al., 2005). One strategy to overcome this problem is to prevent antibody binding and subsequent neutralization by masking the antigenic regions of the vector. This can be achieved by coating the capsid with biologically inactive polymers, such as PEG, in a process called PEGylation, which has been proved to highly enhance circulatory half-life of many therapeutic proteins like IFN and TNFa (Edwards et al., 2003). Different PEG-NHS chains with increasing sizes have been tested, to see whether an excessive level of coating would impair viral infectivity. Results shown that in a certain range of PEGylation, which is dependent of PEG chain length, antibody neutralization is inhibited to a greater extent than transduction efficiency, thus conferring enhanced infectivity to the modified vectors (Lee et al., 2005).

Lysine residues have also been the target of chemical modifications aimed to conjugate chemotherapeutic drugs to AAV. This is the case of Taxol, a drug used to treat many types of cancer, including ovarian, breast and lung tumors. A Taxol-NHS ester derivate have been conjugated to AAV2 capsid, with the idea to exploit the viral delivery platform to increase the solubility and biodistribution of the drug. Despite successful conjugation having been achieved and viral infectivity preserved, the complex did not succeed in decreasing cancer cell viability in vitro, probably due to a limited delivery of drug, below the LD50 of taxol (Wei et al., 2012).

At the moment, not many attempts to chemically conjugate ligands to AAV's capsid in order to re-target the vectors have been carried out, while more effort has been put on genetic modification strategies. However, some promising studies have been published in the last years. In the context of liver-targeted therapies, for example, chemically modified hepatocyte-targeting vectors have been developed (Mével et al., 2020). Since hepatocytes are known to express high levels of the asialoglycoprotein receptor (ASGP-R), the strategy consisted in using *N*-acetylgalactosamine (GalNAc) as a targeted ligand for the chemical modification of the vectors. Different GalNAc derivated ligands have been produced, carrying a terminal isothiocyanate functional group, which would form a covalent thiourea bond with the amino groups of the lysine on the AAV surface. Modified vectors shown receptor mediated transduction of primary mouse hepatocytes with significantly higher efficiency and specificity compared to wild type AAV2. Interestingly, by measuring total and neutralizing antibodies against AAV2 in the serum of mice injected systemically, a drastic inhibition of antibody formation has been observed in animals injected with GalNAc-modified vectors compared to the ones treated with wt AAV2. This effect could be explained by the fact that the chemical modifications can actually coat the capsid and elicit an epitope shielding effect. Indeed, differently from genetic modification approaches, in which a ligand is inserted only in few specific positions of the capsid, in chemical conjugation approaches the viral particles become mostly coated with the ligand, which thereby can physically cover neutralizing antibodies binding sites on the vector. This is actually similar to what happens in the case of PEGylation of the virus, and thereby could be considered an ulterior advantage of re-targeting strategies based on chemical modifications.

1.11 AIM OF THE PROJECT: A NOVEL WAY TO RE-TARGET VIRAL TROPISM THROUGH POST-PRODUCTIONAL CHEMICAL MODIFICATIONS

The aim of this project is to develop a technology that would allow for easy, fast, reproducible and tunable chemical modification of AAV vectors in order to obtain a reliable cell-type specific gene delivery system. As previously discussed, such a technology would provide many advantages for AAV applications. In the context of gene therapy, being able to selectively target the cell population of interest would lead to the reduction of the amount of virus needed to obtain a desired therapeutic effect, thereby reducing the dose of vector required. In turn, a lower dose would be beneficial on different aspects, including the mitigation of the side effects of the therapy, the risk of insertional mutagenesis and immune system activation, and eventually the cost of the therapy. Moreover, obtaining specificity by chemically modifying AAV capsids would mean that genomic modifications such as insertion of cell type specific promoters or regulatory elements would not be needed. It is true that AAVs with specific promoters can express their transgene only in the cell types of interest, but with this strategy the virus still infects non-specifically different cell populations, thereby increasing the risk of side effects and subtracting therapeutic potential.

As discussed, at the moment there are not many established approaches for AAV re-targeting, despite the huge need for more specificity in AAV based applications. The most reliable systems rely on genetic modifications, although these approaches are often time consuming and difficult to implement. In the case of rational insertion of a ligand as a fusion protein into the cap ORF, there are no guarantees that the insertion will not prevent capsid assembly or vector infectivity, and unfortunately the only way to ensure this is to test the recombinant AAV, thereby requiring many steps of manufacture, including plasmids manipulations, production and purification. Moreover, this system is not customizable, unless all the procedure is repeated from the beginning, even for small modifications of the strategy. On the other hand, using AAV display libraries and directed evolution is often possible to obtain modified AAV with enhanced proprieties, including accurate specificity for the cell type on which the vectors have been amplified in. However, this system requires advanced technical skills and a long time to be implemented.

The strategy that I have developed would allow for AAV re-targeting in an extremely versatile and easy way, without requiring expensive reagents or skill intensive procedures. Moreover, the chemical modification itself can be performed in only two days of work, thereby being very fast and easy to reproduce or optimize according to the needs. Moreover, even if the work has been carried out on the AAV2 serotype, the protocol is theoretically applicable on all AAV serotypes, and possibly on different classes of virus, since is based on lysine residues modification which are present on all viral capsids.

The strategy consists of chemically coupling a ligand to the AAV2 capsid by using heterobifunctional crosslinker molecules. The general structure of the crosslinker is preserved and consists of two different chemically reactive groups separated by a variable spacer chain composed by polyethylene

glycol (PEG) polymers. A schematic representation of the strategy is outlined at the end of this paragraph.

Since we want to modify lysine residues on AAV capsid, one of the two functional groups of the crosslinker is always an NHS ester group. Reactivity and properties of NHS ester have been already discussed. The reason why we decided to select NHS ester as amine-reactive group is because the reaction itself is very fast and easy to perform, it does not require particular buffers or conditions, nor the presence of specific catalysts or chemical carriers. It is also simple and stable to store and can be readily prepared in solution prior to the use. Moreover, there is a vast choice of NHS containing crosslinker molecules already in the market, and many studies supporting their functionality and reliability.

In order to connect and distance the NHS ester molecule to the second reactive group of the crosslinker we used PEG chains of different length composed of repeating ethylene glycol units. PEGs are synthesized using a ring-opening polymerization of ethylene oxide to produce a broad range of geometries (linear, branched, Y-shaped, or multi-arm) and molecular weights, as shown in figure 12. What makes PEGs really useful in bioconjugation is that they can be activated by the replacement of the terminal hydroxyl end group with a broad range of reactive functional terminal groups enabling crosslinking and conjugation chemistries. PEG chains are mostly available as mixtures of different oligomer sizes, obtained by polymerization of single PEG units, which range from an average molecular weight of 40 g/mol for each single PEG. Otherwise, dPEG (discrete PEG) crosslinkers are also available, in which all the PEG units have the exact same molecular weight and length, to provide a more accurate and less variable composition of the crosslinker. Due to their hydrophilic nature, attachment to proteins and other biomolecules decreases aggregation and increases their water solubility. Finally, PEGylation of therapeutic molecules have been proven to reduce renal clearance and enhance biodistribution and half-life of the molecule (Benincasa et al., 2015). Moreover, PEGs are biocompatible, non-toxic and poorly immunogenic; indeed, as we discussed, PEGylation has been used as a strategy to shield viral (and other molecules) epitopes and prevent immune system activation in vivo. However, recent studies shown the presence of anti-PEG antibodies in patients treated with PEGylated drugs and even in subjects who have consumed PEG containing products. The presence of anti-PEG antibodies has been related to an increased clearance of PEGylated drugs and thereby a minor therapeutic effect caused by subsequent administrations, along with potential side effects elicited by the immune system activation (Thi et al., 2020). However, despite this drawback, currently no valid alternatives to PEG have been proposed in order to improve blood circulation time and drug efficiency, thus making PEG the gold standard for drug delivery.

In the context of bioconjugation, choosing the right molecular weight and polymer architecture of the crosslinker is important. For bioconjugation procedures and crosslinks, linear PEGs are usually used, but also Y-shaped polymers could be considered, since the branched structure can support two functional groups and it might improve stability in vivo. Moreover, in order to prevent steric hindrance in bioconjugates which could impair the functionality of the molecules, different chain lengths and weights must be tested for each protocol. For this reason, in this thesis we have been using various crosslinkers with the same reactive end groups but different length PEGs spacers, according to the particular experiment.

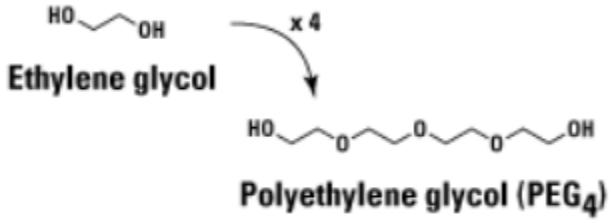

Figure 12. Synthesis of PEG4

The choice of the other functional group of the heterobifunctional crosslinkers relied on the particular chemistry or coupling mechanism used to covalently bind ligands to the viral capsid.

Particularly, the first experiments have been done using the self-labelling protein SNAP-tag. This technology has been implemented in 2003, and is currently one of the most used methods for covalent labelling of fusion proteins (Keppler et al., 2003). The SNAP-tag is a modified version of the human DNA repair protein O6-alkylguanine-DNA alkyltransferase (hAGT), a small enzyme (19.4 kDa) which role is to transfer the alkyl group from O6-alkylguanine-DNA to one of its cysteine residues. However, this enzyme is not totally specific toward its substrate, but it reacts also with the nucleobase O6-benzylguanine (BG). For this reason, substrates containing derivatives of O6-benzylguanosine with substituted benzyl rings can also be accepted as substrates of hAGT, therefore becoming covalently attached to the hAGT though the reaction between the -SH group of a cysteine residue of the enzyme and the benzyl ring of the substrate, as shown in figure 13. Guanine is released during the process and can be removed from the reaction. In order to increase the affinity of hAGT for BG-labelled substates, a mutated version of the enzyme, carrying the G160W substitution, has been developed with the name of SNAP-tag (Keppler et al., 2003).

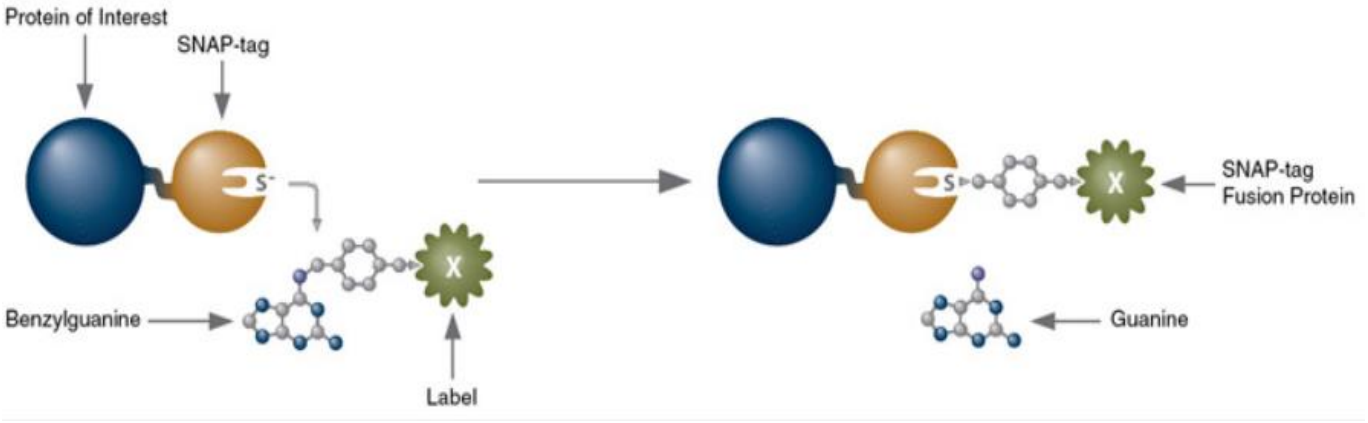

Figure 13. SNAP-tag reaction mechanism. Source, NEB.com

This technology offers many advantages for selective covalent labelling of proteins. In particular, SNAP-tag substrates are chemically inert towards other proteins, thus ensuring accuracy and

specificity. Moreover, the reaction itself is independent on the nature of the substrates, and finally, many BG-substrates are cell permeable, thus allowing intracellular labelling of proteins of interest.

The use of SNAP-tag is very simple, and it requires only some basic knowledge of molecular biology for the synthesis of the SNAP-tagged ligand. Usually the SNAP-tag coding sequence is cloned in specific sites of the protein of interest, which is then expressed as a SNAP-tag fusion. The SNAP-tag should be inserted in a position which would not affect the functionality of the original protein, which is usually the trickiest step of the procedure. The SNAP-tagged fusion protein can then be reacted with a broad range of commercially available BG-substrates, including fluorophores, dyes, biotin, or beads, and custom-made BG-substrates can be synthetized according to the needs as well.

The reaction itself can be performed in PBS, at room temperature for a few hours or over-night at 4°C, and it does not require any particular reagent or catalyst to be performed, while particular conditions could improve the reaction. For example, since stability of the SNAP-tag is improved in the presence of reducing agents, addition of 1mM dithiothreitol (DTT) is suggested. pH can range from 5.0 to 10.0, and salt concentration from 150mM to 1M, but direct testing of different conditions is suggested to optimize the reaction. Free guanine and excess of BG-substrates can be removed from the reaction with different methods, typically by dialysis or filtration, and since labelled protein is linked to the SNAP-tag label by a covalent bond, it remains stable for several months (New England BioLabs Inc. Technical protocols).

The second functional group I have been using for this project is dibenzocyclooctyne (DBCO) alkyne, a reactive group involved in some particular reactions which are generally denoted under the name of “click chemistry” reactions. The term click chemistry was introduced by K. B. Sharpless in 2001, to describe those reactions that must be “*modular, wide in scope*, give *very high yields*, generate only *inoffensive byproducts* that can be removed by nonchromatographic methods, and be *stereospecific”* (Kolb et al., 2001). In other words, click chemistry reactions are easy to perform, occur in one pot, are not disturbed by water or oxygen, and are characterized by a high thermodynamic driving force that drives it quickly and irreversibly to high yield of a single reaction product. There are several reactions that are included in the click chemistry term, but the main example, which is actually the original version of the reaction I have used in this project, is the 1,3-dipolar cycloaddition, sometimes referred as Huisgen cycloaddition, from the chemist who firstly described this reaction in 1963 (Huisgen, 1963). In general, the 1,3-dipolar cycloaddition is a chemical reaction between a 1,3-dipole (which is a dipolar compound carrying a separation of charge over three atoms – good examples are azides molecules RN_3) and a dipolarophile (any compound that reacts with 1,3-dipoles) to form a five-membered ring. Huisgen cycloaddition is an example of this kind of reaction in which an azide reacts with an alkyne to generate a 1,2,3-triazole (chemical compounds which contain a five-membered ring of three nitrogen atoms in position 1,2,3 and two carbon atoms in position 4 and 5). Historically, the copper-catalyzed azide-alkyne cycloaddition have been widely used due to its fast kinetics, but the cytotoxic effects of copper in living systems largely impaired its use in biology. Indeed, both metal or high temperature are required to overcome the activation barrier of deforming the alkyne’s bond angle to form the triazole. However, in the last 15 years, a subclass of click reactions termed biorthogonal click reactions have allowed scientists to couple azide-tagged ligands in a biocompatible way without relying on high temperature or on the presence of any metal to catalyze the reaction. These reactions are based on a class of molecules called cyclooctyne, cyclic analog of alkynes with an eight-

carbon ring, whose bond angle of carbons, which is ~160°, is distorted toward the transition state of the cycloaddition reaction, resulting in a drastic rate acceleration. By using cyclooctyne molecules is possible to selectively couple azide-labelled protein with alkyne-decorated ligands via copper free azide-alkyne cycloaddition. One of the most broadly used cyclooctynes is dibenzocyclooctyne (DBCO), firstly used to label azide-modified sugars on living cells in 2008 (Ning et al., 2008).

A schematic representation of a copper free azide-alkyne cycloaddition between DBCO and the azide group is reported in figure 14a.

DBCO and azides are not present in biological systems, thus they efficiently react with each other while remaining inert to naturally occurring functional groups, ensuring an efficient, selective and specific conjugation. Specifically, DBCO possess a good stability in aqueous buffers, and within physiological temperature and pH ranges it does not react with other groups such as amines and sulfhydryls. Moreover, DBCO reagents possess an embedded chromophore that can be used for spectroscopic analysis, that can be useful to evaluate the yield of the reaction. The reaction itself is easy to perform, is compatible with phosphate buffers in a broad pH range and can be completed in 2 hours at room temperature or over-night at 4°C.

The structure of NHS-peg4-DBCO heterobifunctional crosslinker used for this project is shown in figure 14b. The NHS group is used to attach the linker to -NH2 groups present on exposed lysine residues of the viral capsid, while DBCO reacts with azide-labelled ligands.

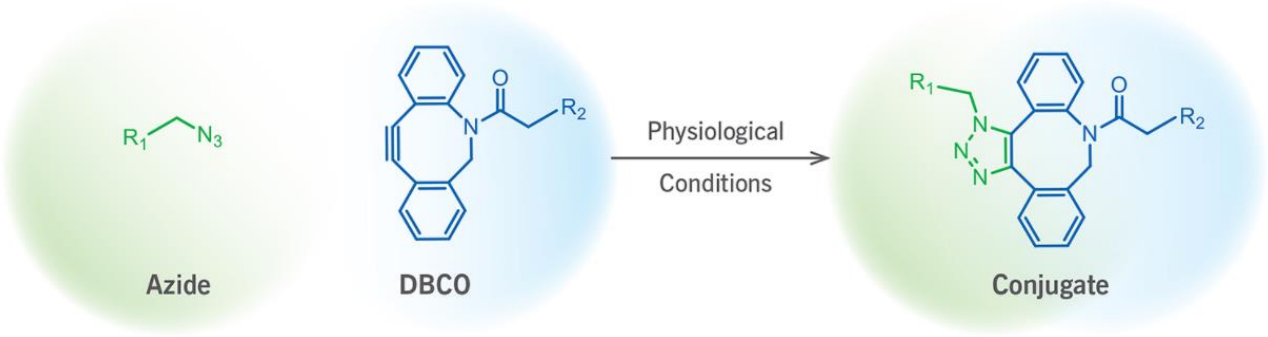

a)

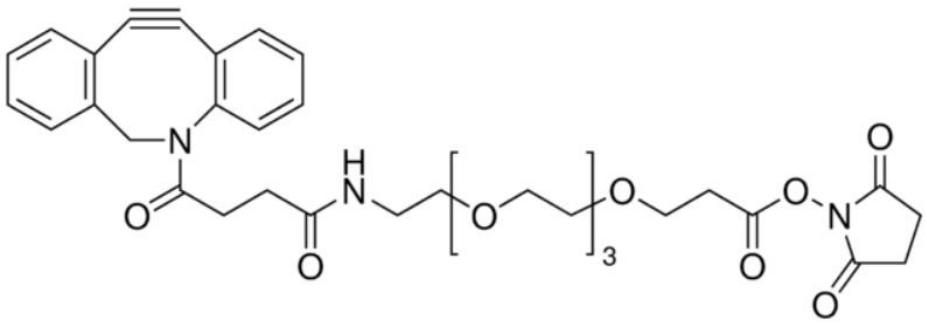

b)

Figure 14. a) Cu-free azide-alkyne cycloaddition reaction scheme. b) DBCO-peg4-NHS linker structure. Source, clickchemistrytools.com

Another reactive group that has been used in this project as an alternative to the NHS is the maleimide, a chemical compound with the formula $H_2C_2(CO)_2NH$. This compound is particularly popular in bioconjugation thanks to its reactivity toward sulfhydryl groups (-SH), which can be naturally found on the side chains of cysteine residues. The maleimide group reacts specifically with sulfhydryl groups when the pH of the reaction mixture is between pH 6.5 and 7.5, resulting in the formation of a stable and non-reversible thioether linkage. In more alkaline conditions (pH >8.5), the reaction favors primary amines and also increases the rate of hydrolysis of the maleimide group to a non-reactive maleamic acid. Another thing to be considered is the state of the -SH group before the reaction with the maleimide. Indeed, in biological systems cysteines are often joined together between their side chains via disulfide bonds, which therefore must be reduced to free thiol before the reaction. Common reducing agents such as dithiothreitol (DTT) and betamercaptoethanol (BME), however, must be removed before the maleimide reaction because they contain thiols which would compete with the reaction. An efficient alternative is the thiol-free reducing agent TCEP (tris (2-carboxyethyl) phosphine). Maleimide are often used together with NHS esters to form heterobifunctional crosslinkers employed in the preparation of targeted therapeutics (mainly antibodies-drug complexes due to the high presence of Cys residues in the Ab structure), protein conjugates, protein-based microarrays, or proteins immobilization essays (Thermo Scientific - Crosslinking Technical Handbook, 2012).

As proof of concept to test our conjugation system we firstly decided to use lectins as potential ligands, in particular the *Wheat Germ Agglutinin* (WGA) and the *Griffonia Simplicifolia Lectin I isolectin B4* (IB4). Lectins are small oligomeric carbohydrate-binding proteins characterized by the presence of a carbohydrate recognition domain that is highly specific for sugar moieties, in a way that is comparable to the binding of antigen to an antibody. In general, a protein, to be classified as a lectin must possess the ability to weakly and reversibly bind to glycans with high specificity, must have nonimmune origin (immunoglobulins are not lectins) and should not change the structure of the glycan it binds to. They are ubiquitous and can be classified in five different specificity groups according to the sugar they bind to: mannose, galactose/N-acetylgalactosamine, N-acetylglucosamine, fucose and N-acetylneuraminic acid. It is important to note, however, that lectins bind not only to oligosaccharides on cells, but also to free-floating glycans, even if in a weaker way (Gajbhiye & Gong, 2013).

Lectins play a role in many different biological functions, including regulation of cell adhesion, agglutination or precipitation of polysaccharides, regulation of solubility and blood protein levels, glycoprotein synthesis and many more. Their function is mainly dependent on their locations: lectins that are located intracellularly are involved in trafficking, sorting, and targeting of glycoprotein to various pathways, while lectins secreted or expressed on cell surface are involved in cellular adhesions and recognition. In particular, surface lectins offer an attractive opportunity for many clinical applications, including drug delivery, gene delivery, vaccine delivery, imaging and anti-

microbial actions(Gajbhiye & Gong, 2013). Indeed, specificity of lectins toward glycans has been exploited in nanobiotechnologies to create lectin functionalized nanoparticles able to target drugs to various tissues with minimized systemic side effects (Devi & Basil-Rose, 2018). When coupled with a lectin, the complex of interest can bind to specific glycans on target cells and can be internalized through lectin-mediated endocytosis, thereby leading to an efficient cellular uptake of the ligand. In the context of gene delivery for example, nucleic acid complexed with liposomes and functionalized with liver-specific lectins successfully increased plasmid delivery rate in vitro (Letrou-Bonneval et al., 2008).

WGA is a lectin composed by two identical subunits of 18 kDa and 171 amino acids which dissociate into monomers at acid pH. Each protomeric unit of WGA consists of four structurally homologous domains, called A, B, C and D, connected by disulfide bonds, for a total of eight sugar binding sites of the WGA dimer, which are all simultaneously functional. In particular, affinity studies shown that WGA affinity to oligosaccharides is higher than affinity to monosaccharides, and that A, B and C domains bind to GLcNAc while D domain interacts with glycosides (Balčiūnaitė-Murzienė & Dzikaras, 2021). WGA carbohydrate-binding modules, called CBM18, recognize N-acetyl-D-glucosamine (GLcNAc) and sialic acid residues, which are commonly present in many glycoproteins expressed on membranes of different cell types, including neurons (Goldstein et al., 1997). Moreover, since most cancer cell lines express high levels of sialic acid, WGA is an attractive candidate for selective targeting strategies and cancer therapy, as in the case of pancreatic carcinoma, wherein WGA shows a marked cytotoxic effect (Schwarz et al., 1999).

WGA has been widely used as a neuronal circuit tracer molecule to study cellular connections and neuronal projections. One of the first studies has been carried out in 1988 (Broadwell et al., 1988), where the authors shown how WGA could enable delivery of macromolecules through the blood-brain-barrier (BBB). WGA has been conjugated with the enzymatic tracer horseradish peroxidase (HRP) and injected intravenously in mice. After only five minutes, the entire cerebrovascular tree from the luminal side was labelled. Pericytes, located on the abluminal surface of cerebral endothelia were positive after six hours, and signal was detected in the pituitary lobe and hypophysis within one day. It has been shown that WGA binds to cell surfaces and is internalized by adsorptive endocytosis. Adsorptive endocytosis is a type of pinocytosis, an internalization mechanism that requires a ligand-cell surface interaction and is triggered by an electrostatic interaction between the positively charged proteins and negatively charged plasma membrane surface (G. Xiao & Gan, 2013). WGA-HRP has been shown to be uptaken by adsorptive endocytosis by cerebral nonfenestrated endothelia and conveyed to the Golgi complex where is processed for eventual exocytosis from the cerebral endothelium to the abluminal surface. Moreover, when HRP is uptaken by bulk-phase endocytosis, no signal is detected in the abluminal side, thereby demonstrating that adsorptive endocytosis is required for transcytosis through the blood-brain barrier without compromising the integrity of the BBB (Broadwell et al., 1988).

WGA, alone or conjugated with markers including fluorophores, has not only been used to trace neuronal circuits in the brain, but also in the spinal cord and in the peripheral nervous system, exploiting the fact that it can be transported in both in the anterograde and retrograde directions (Van Der Want et al., 1997). Interestingly, after being taken up by neurons, it seems that WGA can even jump transganglionically (in peripheral circuits) or transsynaptically (in central circuits) (Schwab et al., 1978) (Sillitoe, 2016). Transsynaptic transport can also be bidirectional, as it has been

reported in many different works, supporting the originally assumed adsorptive endocytosis-dependent mechanism (Yoshihara, 2010).

However, WGA has also therapeutic potential. Indeed, WGA ability to cross the BBB has been exploited to transport different drugs to the CNS. For example, intranasal administration of WGA functionalized nanoparticles loaded with miR132 micro-RNA, which is involved in neuronal survival, significantly improved learning and memory function of a murine model of Alzheimer's disease (Su et al., 2020). Moreover, WGA-incorporated nanoparticles have been used to target drugs to different types of cancer, including ovarian carcinoma (Plattner et al., 2008).

The widespread tropism of this lectin and the fact that multiple binding sites are present are the reason why we have decided to use WGA as testing ligand to validate our AAV chemical conjugation system. Indeed, sialic acid and GLcNAc are generally expressed on cell membrane of different cell types, including most of the tumor-derived cell lines commonly used for in vitro testing, thus making WGA a very versatile tool to test and refine our conjugation protocol. Moreover, the high stability and the particular conformation of WGA is a point in favor in the choice of this ligand. WGA has been functionalized by adding an azide group directly on its lysine residues, using an NHS-peg4-Azide crosslinker. However, since we could not predict exactly how this would affect the structure and functionality of the lectin, having multiple binding sites which are independent from each other could increase the chance that WGA would remain functional after the azide insertion.

The second lectin used in this project is *Griffonia Simplicifolia* Lectin I (GSL I) isolectin B4. Lectins from *Griffonia simplicifolia* are made by two different subunits (A and B), and, according to their composition it is possible to distinguish five tetrameric isolectins: BSI-B_4 (IB4), BSI-AB_3, BSI-A_2B_2, BSI-A_3B and BSI-A_4. The A subunit recognizes N-acetyl-α-D-galactosaminyl residues, while the B subunit is specific for α-D-galactosyl residues. Thereby, IB4, which only contains four B subunits, can only bind to α-D-galactosyl residues. Historically, GLS I have been used to study blood groups, since subunit A and B respectively agglutinates human blood group A and B cells.

More relevant for this project, IB4 has been shown to mark endothelial cells and neovascular structures, also in the context of cancer therapy (Niethammer et al., 2002). Since surface glycoconjugate expression pattern seems to be similar in different endothelial tissues, IB4 can be effectively used to study endothelial plasticity during development, chronic inflammation and tumor neovascularization in different models (Benton et al., 2008).

Concerning specifically the nervous system, IB4 can be used as a marker for glia and activated microglia during inflammation and pathologic conditions (Morioka et al., 1993). Moreover, IB4 is commonly used to distinguish peptidergic and non-peptidergic nociceptors, since IB4 binds to non-peptidergic unmyelinated primary afferent neurons (Von Banchet & Schaible, 1999). Indeed nociceptors can be broadly divided in two categories, peptidergic nociceptors contain different neuropeptides, including substance P and Calcitonin Gene Related Peptide (CGRP), and their regulation relies on Nerve Grown Factor (NGF) signaling, while non-peptidergic nociceptors express the ATP-gated ion channel $P2X_3$, they bind to IB4 and they are regulated by Glial cell-derived neurotrophic factor (GDNF) signaling (Zylka, 2005). The peptidergic population terminates almost exclusively in the outer laminae of the superficial dorsal horn (laminae I and outer II), where they

make contact with neurons projecting to the CNS, while non-peptidergic nociceptors mainly project into the inner part of lamina II, contacting local interneurons (Malmberg et al., 1997).

As for WGA, IB4 has been functionalized with an azide group by modifying it with an NHS-peg4-Azide crosslinker, thus attaching the -N3 group directly on its lysine residues. This modified version of IB4 has been used as a ligand to re-direct AAV2 tropism. Again, the stability and the presence of four binding domains on IB4 contributed to the efficient modification of the lectin without interfering with its functionality.

Since the interest of our group in pain and nociception, the third ligand we have used is the well-known protein Nerve Growth Factor (NGF), which would allow us to re-direct AAV2 tropism toward nociceptors and potentially propose new strategies for chronic pain therapies. NGF has been discovered nearly 60 years ago as a protein which induces nerves growth (Liuzzi et al., 1965). Initially, it is a complex of three proteins (alpha/beta/gamma NGF) termed proNGF, but after gamma-NGF mediated cleavage, the beta subunit is activated into functional NGF, a 26 kDa protein which forms biologically active homodimers (Wiesmann & De Vos, 2001). NGF binds with high affinity to the tropomyosin receptor kinase A (TrkA) and with lower affinity to the p75 neurotrophin receptor (p75NTR) (Hutton et al., 1992). Three specificity sites are involved in receptor binding. The N-termini NGF residues 6–9 form a helix which participates in the hydrophobic interaction with TrkA, residues protruding from the two central sheets of both subunits of the NGF homodimer (including W21, I31, F54, and F86) form the second binding site, while two connecting loops located on the opposite side of the -N and -C termini act as third binding site (McDonald et al., 1991). The NGF main receptor, TrkA, is expressed in many tissues, including immune cells, digestive tract, uterus, skin, kidney, CNS and PNS, where it is a marker of peptidergic nociceptors. TrkA exists in an inactive form, but binding to NGF promotes TrkA dimerization and trans-autophosphorylation of tyrosine residues 676/680/681 of the contralateral monomer, which leads to the phosphorylation of other proteins (including PI3K/Akt and Ras/Raf/MEK1/2/ ERK1/2 Map kinases) and the activation of different signaling cascade. NGF also binds to the p75 receptor, which has been shown to directly interact with TrkA and to facilitate high affinity binding of NGF and activation of cell survival pathways, while when only p75 is involved it activates cell death pathways, particularly relevant in some nervous system pathologies such as Alzheimer's Disease (Kumar et al., 2020).

NGF signaling regulates the survival and activity of neurons both in embryonal and adult life. It Is involved in axon growth and synapse formation, influences neurotransmitter and neuropeptide synthesis and the expression of ion channels, as well as neuronal plasticity in pathological conditions. Beside this main function, NGF is involved in many different pathways, including ovulation and proliferation of pancreatic cells. Moreover, NGF contributes to regulate immune system: during inflammation NGF is released by different immune cells and promotes axonal growth in nearby nociceptors and maturation of T-cells (Lambiase et al., 1997). Finally, NGF plays a crucial role in pain signaling. In fact, NGF levels are high in a variety of acute and chronic pain states, and local NGF administration causes persistent hypersensitivity, allodynia and hyperalgesia (McKelvey et al., 2013). By binding to its TrkA receptor on nociceptors, NGF directly facilitates the activation of these neurons, while by binding to immune cells, including mast cells, it induces the release of pain mediators such as histamine, prostaglandins and NGF itself (McKelvey et al., 2013). Given NGF's role in pain, many different strategies to treat chronic pain have been developed based on modulation

of NGF signaling, including genetic modification of NGF/TrkA genes (Sarasola et al., 2011), blocking antibodies (Ugolini et al., 2007) or antagonist drugs (Abdiche et al., 2008). However, most of the therapies for chronic pain currently available have serious downsides, including side effects, difficulty of administration and poor long-term efficiency, mainly due to the insurgence of tolerance and dependence.

For this reason, we think that being able to re-direct an AAV vector specifically to nociceptors would have an immense therapeutic potential in the context of chronic pain treatment. For example, one could use the delivery system to selectively deliver gene editing tools such as CRISPR/cas effectors, ionic channels, different class of drugs or effector proteins to modulate neuronal activity.

In this case, NGF has not been functionalized with an azide group, but rather we have decided to use a previously characterized NGF-SNAP fusion protein already used in our lab (Nocchi et al., 2019). This protein is based on a mutated version of NGF, carrying the point substitution R121W, which leads to the formation of a protein which still binds to TrkA/p75 but it loses its phosphorylation activity, thus preventing the activation of pain cascade signaling. This painless version of NGF, named NGF^{R121W}, has been then fused to a SNAP-tag, and produced as a fusion protein. NGF^{R121W}-SNAP has been then conjugated to AAV2 by using two different crosslinkers (termed long linker and short linker), both carrying an NHS and a BG functional group on the ends, separated by a spacer structure of two different lengths. Since the relatively large size of NGF, this has been done to test whether steric hindrance would have been a major impairment for the functionality of the system.

Finally, as a last ligand, we have decided to use a synthetic peptide that acts as full agonist for a member of the protease-activated receptor (PAR), named PAR1. PAR1 is the prototypical representative of a set of protease-activated G-protein coupled receptors (CGRP), a group of seven-transmembrane domain receptors that rely on the activation of G-protein to trigger specific transduction pathways. PAR1 receptor is highly expressed in endothelial cells and platelets, as well as in astrocytes and in different neuronal populations (Vance et al., 2015). When PAR1 is recognized by its natural ligand, the serine protease thrombin, it cleaves the LDPR/SFLL site in the N-terminal exodomain of PAR1, generating a new N-terminus which acts as a tethered peptide agonist and binds to the extracellular loop 2 of PAR1, triggering a conformation switch and the activation of G-protein cascade, followed by the internalization and degradation of the activated receptor. However, many different classes of protease can bind and activate PAR1, including matrix metalloproteases (MMP1/2/9/13), cathepsin C and activated protein C (Flaumenhaft & De Ceunynck, 2017). Moreover, many synthetic agonists can be used to mimic the tethered N-termini of PAR1, including the well characterized small peptide SFLLRN (Q. Zhang et al., 2018). All these different ligands activate PAR1 in specific ways, which leads to entirely different and even opposing cellular responses. For example, in platelets, thrombin-dependent activation of PAR1 results in aggregation and activation of adhesion proteins, while in neurons it triggers cytoprotective signaling and regulates neuronal functionality. Moreover, it has been shown that in endothelium PAR1 activation stimulates exocytosis, expression of adhesion proteins, loss of barrier function, transcriptional activation and angiogenesis (Flaumenhaft & De Ceunynck, 2017). Different studies demonstrated how thrombin activation of PAR1 increases permeability in various vascular beds such as pulmonary microvascular endothelial cells (Arce et al., 2008). In this context, particularly interesting is the involvement of PAR1 in brain microvascular endothelial cells (BMECs), pericyte

regulation and BBB dysfunction. It has been shown that upon thrombin stimulation, BMECs and pericytes, which are the main component of the BBB, can release high levels of the matrix metalloprotease 9 (MMP9), which leads to BBB dysfunctions and increased brain endothelial permeability by inducing temporary barrier breakdown (Machida et al., 2017). In a separate study, authors demonstrated that after thrombin activation of PAR1, BMECs highly increase the release of nitric oxide and different reactive oxygen species, which contributes to the disruption of the tight junctions and to the permeabilization of the BBB, indicating multiple mechanisms by which PAR1 activation leads to BBB disfunctions (Brailoiu et al., 2017). Finally, a recent study showed how PAR1 is required for lymphocyte transmigration across MBECs through the activation of specific signaling pathways, including cascade events that lead to the modulation of vascular-endothelial cadherins, a group of adhesion molecule located at junctions between endothelial cells and crucial for transendothelial migration (Dragoni et al., 2020).

It is interesting to note that depending on the specific PAR1 activator ligand, subsequent cellular signaling can lead to different cellular responses. For example, as stated above, thrombin activation of PAR1 leads to BBB dysfunction, but if the same PAR1 receptor is activated by the activate protein C, the result would be the trigger of barrier protective signaling (Feistritzer & Riewald, 2005). However, since SFLLRN-dependent PAR1 activation mimics thrombin-dependent activation, we can expect that the effects of thrombin on BBB functionality (increased permeability) will be similar to the ones elicited by our SFLLRN-AAV2 complex. According to this, it is possible that our SFLLRN-N_3 could promote AAV transendothelial migration trough the BBB, thus allowing efficient infection of the nervous system.

The most widespread route of gene delivery to the CNS is cerebrospinal fluid (CSF) administration, which is typically achieved through injection into the cisterna magna or with intrathecal injection. Pia mater, the innermost layer of the meninges, is a highly vascular layer that directly invests the brain and spinal cord, and is separated from the overlying arachnoid by the subarachnoid space. CSF fills the subarachnoid space and ventricular system around the brain and spinal cord, and due to the close contact with the CNS it represents a valid way for CNS targeting. Moreover, by delivering viral vectors directly into the CSF is possible to overcome the challenges presented by the BBB and to avoid circulating neutralizing antibodies, thus increasing transduction of CNS (Taghian et al., 2020). Lumbar intrathecal injection is commonly used to delivery AAVs to the spinal cord, but transduction of the spinal cord in mice is mostly limited to the lower thoracic and lumbar areas, together with only minimal brain transduction, probably due to the distance to intracranial structures (Gray et al., 2013). Considering the anatomy of pia mater, composed by a one- to two-cell-thick layer of leptomeningeal cells (or meningeal fibroblasts), which is richly vascularized, it is possible to speculate that PAR1 agonist SFLLRN-N_3 could facilitate AAV transmigration directly into CNS parenchyma by binding to vascular cells or directly to meningeal fibroblasts and mediating transmigration. If this is the case, strong transduction of the whole spinal cord could be achieved following intrathecal injection, with possible infection of the brain as well.

1.12 SCHEMATIC REPRESENTATION OF THE COUPLING STRATEGY

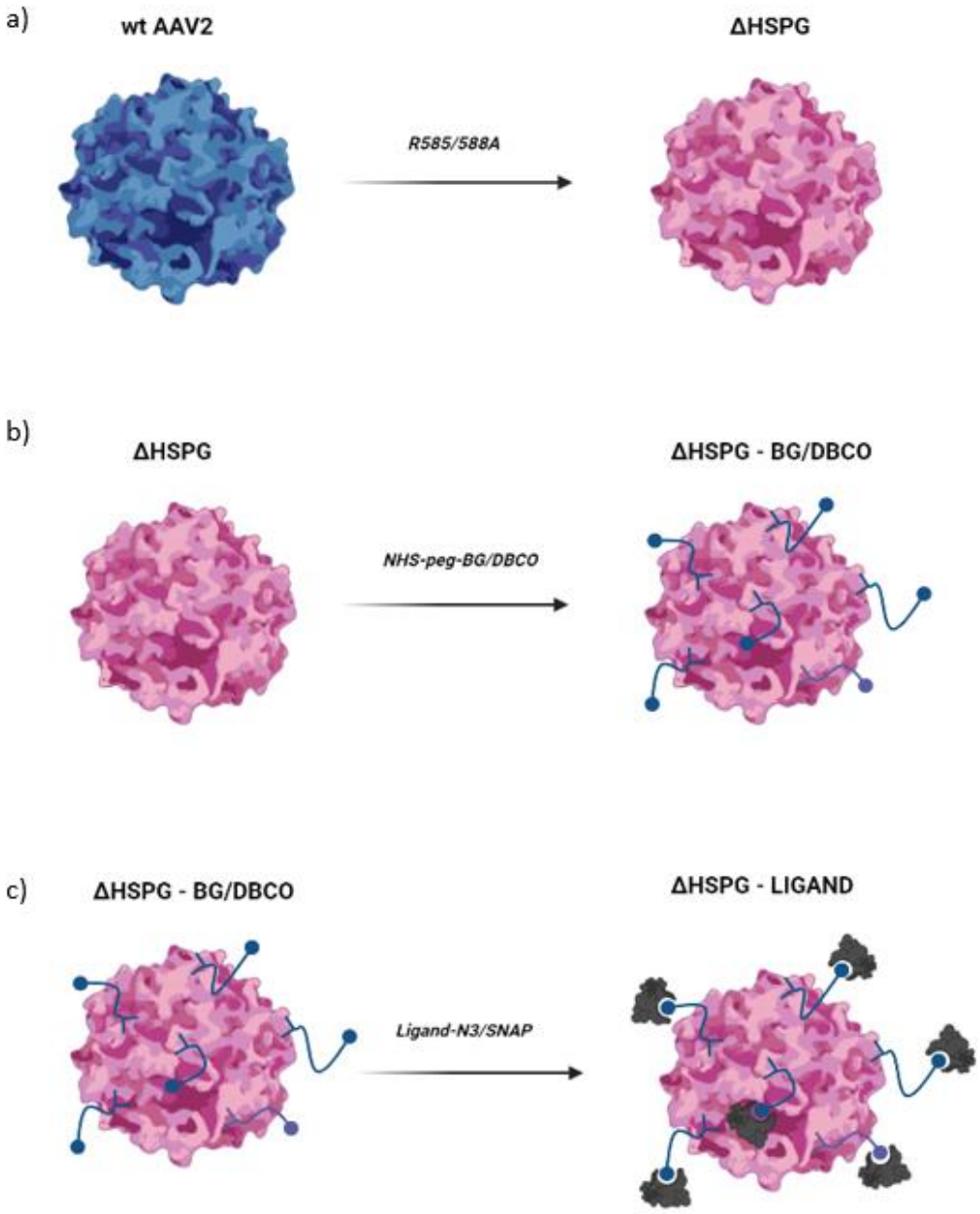

Schematic representation of the chemical modification strategy. a) wild type AAV2 is genetically modified to disrupt HSPG binding site by arginine585/588-to-alanine substitutions. b) ΔHSPG vectors obtained are functionalized with different heterobifunctional crosslinkers carrying an NHS molecule on one end and a specific reactive group on the other (BG/DBCO). c) Primed ΔHSPG are then reacted with appropriately modified ligands carrying a SNAP/N3 tag in order to obtain stable ΔHSPG-ligand conjugates.

2 RESULTS

2.1 BEST MODIFICATION RATIO

As discussed above, most of the experiments have been carried out using a mutant rAAV2 carrying specific point mutations to either disrupt HSPG binding site or to enhance transduction efficiency. Firstly, I have inserted the well-known R585/588A substitutions in the VP3 coding region to generate vectors (ΔHSPG vector) not able to bind to HSPG residues, thus being a good model to ensure the efficiency of our modification strategy to re-direct viral tropism in a specific and background-free manner. Next, Y444+500+730F+T491V substitutions have been added to the already modified ΔHSPG VP3 coding region. These modifications aim to replace some key residues which are phosphorylated following viral infection, and prime subsequent ubiquitination and proteasome – mediated degradation of the vectors. This has been suggested to significantly enhance AAV2 infectivity both in vitro and in vivo, thus permitting to reduce the amount of virus used for the experiments while still obtaining high levels of transduction.

Plasmid coding for the modified AAV2 capsid has been used to produce vectors carrying the tdTomato fluorescent protein gene driven by the synthetic CAG promoter, followed by the Woodchuck Hepatitis Virus Posttranscriptional Regulatory Element (WPRE) and the Simian Virus 40 Poly-adenylation (SV40 Poly-a) sequence (figure 15a). The strong and bright red fluorescent signal of tdTomato (emission wavelength = 581 nm), as well as its photostability make it an excellent fluorophore for in vivo studies. The choice of a strong mammalian promoter and of regulatory elements to enhance mRNA stability aim to obtain high level of protein expression, displayed as a bright red fluorescent signal in infected cells.

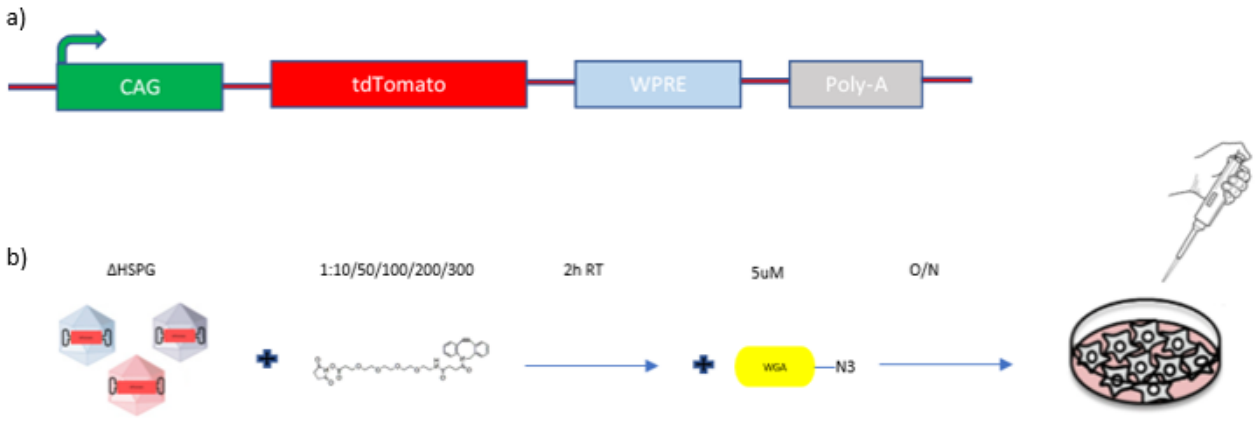

Figure 15. a) Schematic representation of ΔHSPG vector expression cassette. b) Workflow of the procedure to find the optimal viral titre::moles of linker ratio. ΔHSPG vectors are modified with increasing amount of linker, then WGA-N_3 is added. Fluorescence is analyzed on freshly prepared DRG cultures 3/5 days post-infection.

Despite different vectors, ligands and linkers having been used throughout this project, the first step of all modification processes relied on the functionalization of viral capsids with a reactive group that could be used to further attach the ligand to the complex. As previously discussed, this has been achieved by using different types of heterobifunctional crosslinker molecules, which all share a common NHS-ester group. The NHS-ester group has been exploited to modify the capsid's lysine residues, but since an AAV2 capsid carries around 550 lysine residues, we firstly sought which was the best viral titre::moles of linker ratio (or in other words, the best number of lysine to modify in each viral particle) to obtain the optimal modification yield. Obviously, being volume the same, a more concentrated viral batch requires higher amount of linker to be used to maintain the best molar ratio. Despite all viral batches produced during this project having a yield of around $3x10^{12}$ VG/ml, the ratio of empty:full capsids may vary within different preps as well as other changeable factors (glycosylation, prep purity, …). For this reason, for every new batch of virus produced, the best viral titre::moles of linker ratio has always been evaluated separately. ΔHSPG vectors are modified with increasing virus::linker ratios and then the functionalized viruses are coupled with the proper ligand. Modified vectors are then tested on different cell lines (Hek293, PC12) or primary dorsal root ganglia (DRG) cultures, and fluorescence intensity is evaluated 3 to 5 days post-infection. The workflow to find the best viral titre::moles of linker ratio is schematized in figure 15b.

To find the optimal viral titre::moles of linker ratio for every new batch of ΔHSPG produced, $3x10^9$ VG for each condition are reacted with increasing concentrations of NHS-peg4-DBCO linker (0,17/0,85/1,7/3,4/5,1 picomoles (pmol)) in PBS for 2 hours. Unmodified ΔHSPG vectors (no linker) were used as control. 5uM WGA-N_3 is then added to the reaction, which continues over night. All conditions plus the negative control (unmodified ΔHSPG) are then applied on freshly prepared DRG cultures obtained from C57BL/6J wild-type mice. Red fluorescence is evaluated 3-5 days post infection by fluorescence microscopy. Results can be seen in figure 16.

The first clear thing we can see is that unmodified ΔHSPG still retains some of its ability to infect cells, even if at a much lower level compared to wt AAV2, as we will discussed later. On the other hand, the addition of WGA is effectively able to restore viral infectivity by reinstating initial binding of the vectors to GLcNAc and sialic acid residues, highly expressed on neuronal membranes, and facilitating subsequent internalization. However, as we speculated, the number of lysines actually modified make a difference in the efficiency of the system. Including data from different experiments it was clear that if a certain threshold is exceeded, the virus starts losing infectivity, probably because an excess of lysine modification results in the overcoating of the vectors which than fail to enter the cell after the initial attachment. On the contrary, if not enough linker is used, then a lower percentage of lysines will be modified, resulting in vectors which are infective but not up to their maximum potential. This is particularly evident in figure 16c, where the strongest signal is registered in the 0,85 pmol condition. Despite in all conditions the signal is much stronger compared to the negative control, proving that our modification system can actually restore and re-direct viral tropism, it is possible to see that the fluorescence starts at 0,17 pmol of linker used, reaches its maximum at 0,85pmol and then begins to decrease to the minimum level at 5,1 pmol (fig 16g). Continuing this experiment to even higher ratios would eventually bring to a total impairment of viral infectivity.

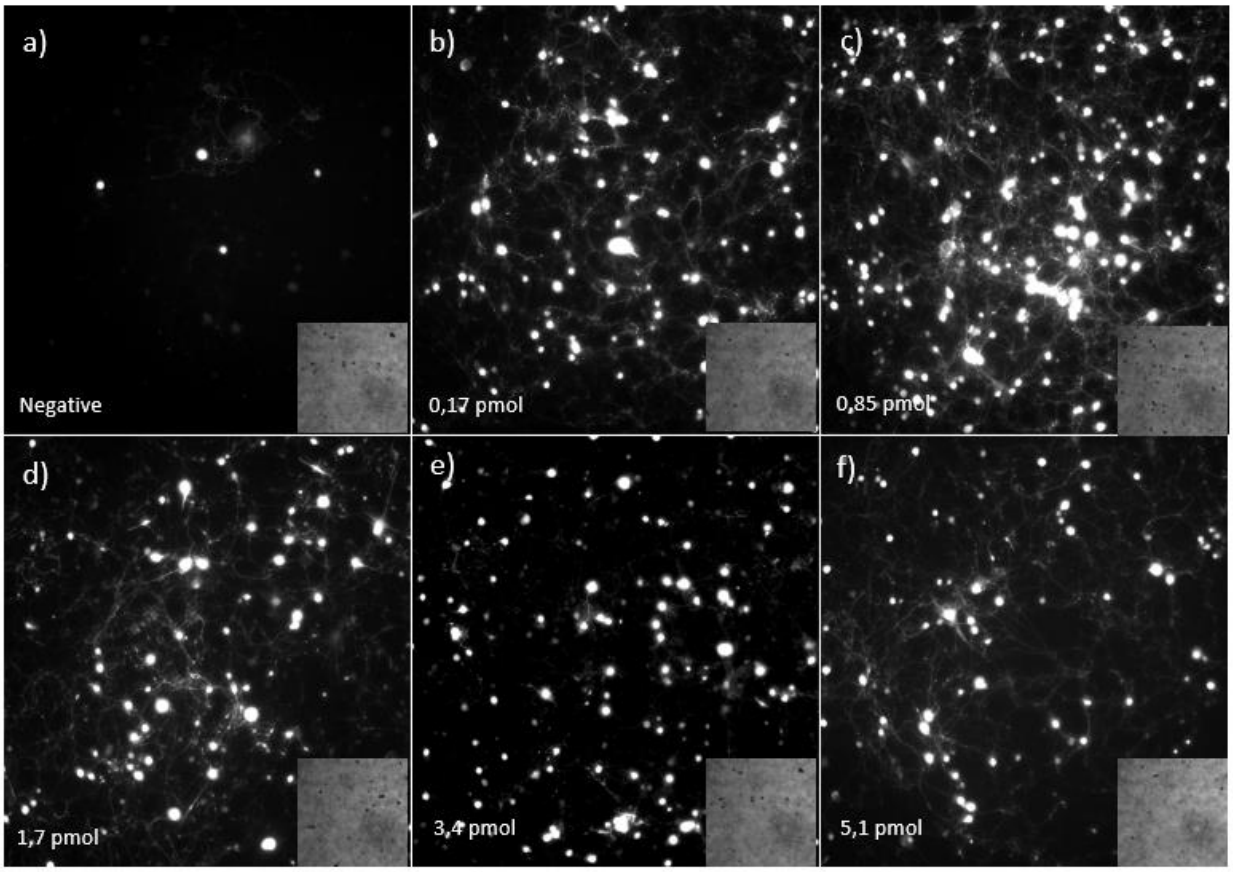

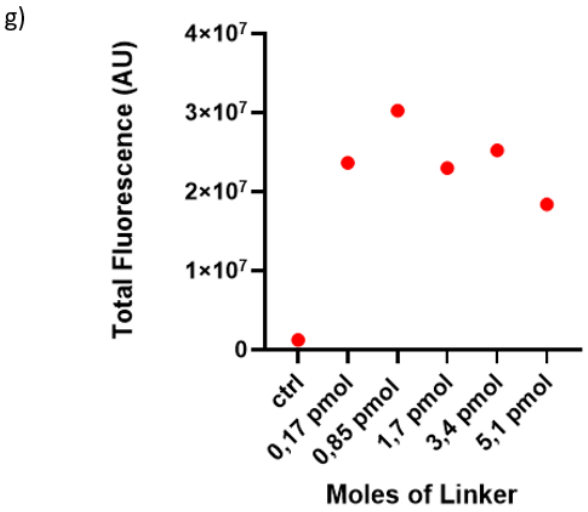

Fig 16. Finding the optimal concentration of linker using NHS-peg4-DBCO + WGA-N_3. The strongest signal is evident in the 0,85 pmol group (c), despite it being drastically higher than the control in all the conditions tested (g).

2.2 BEST LIGAND CONCENTRATION

The next step was to investigate whether the concentration of the ligand used to actually replace viral binding ability could influence its efficiency. Indeed, we thought that an excess of ligand attached to the viral surface could resemble the effect of the overcoating obtained when too much linker was added to the reaction. In a similar way, it is reasonable to think that if the viral particle is completely covered by proteins, steric hindrance problems could arise, which could lead to impairments in the functionality of the protein itself or in viral ability to enter the cells after attachment. This is largely depending of the nature of the ligand, particularly from its biochemical proprieties, size, amino acid composition, structure and interaction patterns. For example, smaller or particularly stable ligands should be impacted to a lesser extent by steric hindrance constrains, but given the difficulty to predict the final outcome, the best strategy it is to directly test the effect of different concentrations of ligands on our chemical modification protocol. To test the best ligand concentration to use in order to obtain the maximum efficiency of our modified vectors, $3x10^9$ VG of ΔHSPG-tdTomato per condition have been modified at their respective optimal linker concentration, previously found with other experiments as shown above. NHS-PEG4-DBCO linker has been used. After 2 hours of incubation, IB4-N_3 and WGA-N_3 have been added at the concentrations of 1, 2, 5 and 10 uM. Modified ΔHSPG vectors have been tested directly on PC12 cells, plated at 70% density in a 96well culture dish. Fluorescence has been monitored 3 days post infection by fluorescence microscopy. Workflow and results can be viewed in figure 17.

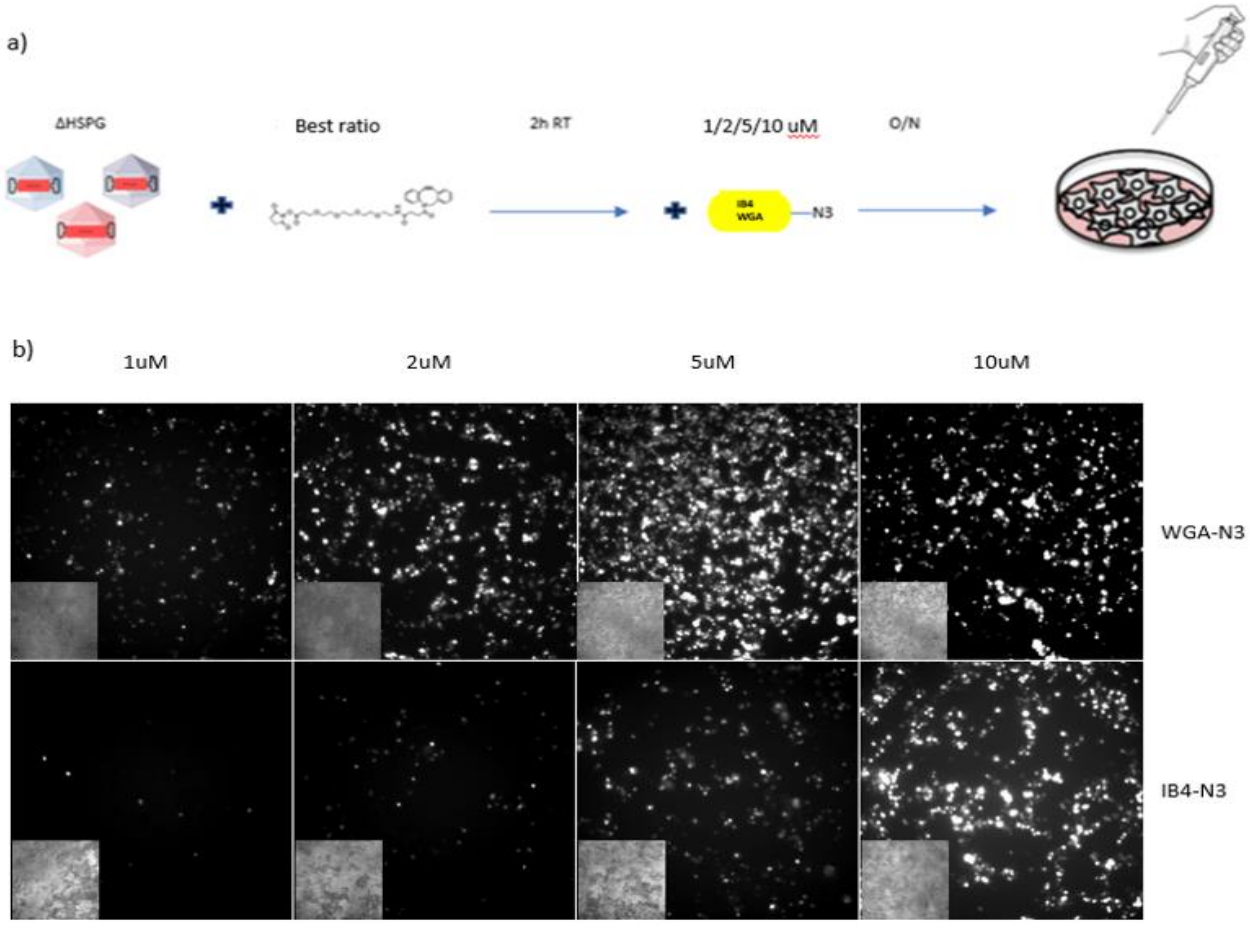

c)

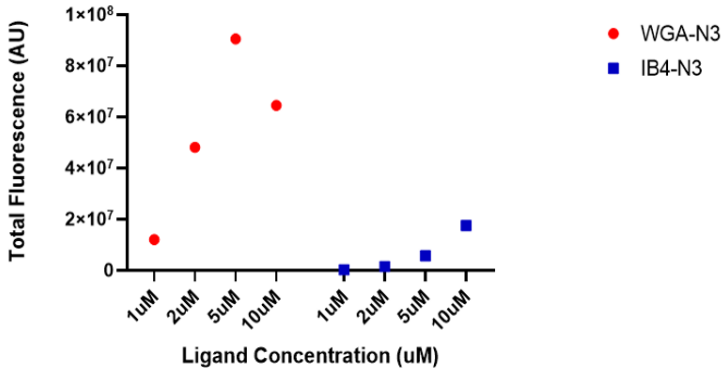

Figure 17. a) Schematic representation of the workflow to find the optimal ligand concentration. tdTomato expressing ΔHSPG vectors are modified at their best virus::linker molar ratio with NHS-peg4-DBCO, then 1, 2, 5 and 10uM of WGA-N_3 or IB4-N_3 are added. Modified vectors are used to infect PC12 cells. b) best ligand concentration depends on the ligand itself. With WGA, the highest fluorescence is registered when a concentration of 5uM is used, while for IB4 it increases to 10uM. c) Quantification of total fluorescence of positive cells in each condition.

In the case of WGA, signal starts at 1uM and reaches its maximum peak at 5uM, decaying at higher concentration (10uM). On the other hand, IB4-modified ΔHSPG show best efficiency at 10uM. Based on this result, it seems that ligand concentration can affect the functionality of the modified vectors. Efficiency has been evaluated by calculating the total fluorescence of all the positive cells in each condition (figure 17c).

However, it is interesting to note that there is not an absolute optimal ligand concentration that could be used, since it seems to rely on the biological and biochemical proprieties of the specific ligand. For example, in the case shown in figure 17b, IB4 needs to be used at double concentration compared to WGA to reach its best efficiency. However, it is important to note that since we directly produce our IB4/WGA-azide tagged molecules, the yield and the purity of the reaction may vary, thus it is hard to give an accurate and absolute value for the best ligand concentration. However, what seems to be clear is that for all ligands used in this project a concentration of 5uM has been always related to a good fluorescent signal both in vitro and in vivo. For this reason we have decided to adopt 5uM as our reference condition for further experiments.

2.3 BEST CHEMICAL REACTION: SNAP-TAG VS AZIDE

Another variable that could affect the functionality of the technology is the choice of the chemical reaction used to covalently attach ligands on viral capsid. Two different strategies have been used in this project, both having advantages and disadvantages, which rely on the SNAP-TAG or on the azide-DBCO reaction.

The SNAP-TAG is a self-labelling enzyme that can be inserted as a fusion protein directly into well-defined regions of a target ligand, thus ensuring great spatial control of the modification site, and 1:1 molar labelling. Of course, given its size of 19.4 kDA, it is possible that the insertion would negatively influence the functionality of the modified ligand in different ways, including protein structure, stability or binding ability. For these reasons it is necessary to carefully plan the synthesis of a SNAP-tagged ligand considering that the insertion must be well tolerated.

On the other hand, an azide (N_3^-) is a chemical group composed by only 3 atoms of nitrogen, thus its size should not represent an issue when the azide is inserted into a ligand because it would not cause any steric hindrance issue or mask any functional site of the modified protein. An azide motif can be inserted in a ligand in different ways, both pre and post translationally. One of the most commonly used pre-translational system relies on unnatural amino acids carrying an azide group which can be inserted in a specific site of the gene coding target ligand. By contrast, azide insertion by post translational modification can be achieved using specific crosslinker molecules, such as NHS-peg_x-Azide. While this way is considerably easier and faster than pre translational modifications, it is hard to predict exactly how many and where the azide motifs would bind on target ligand, thus conferring much more variability at the system.

To explore how the choice of the chemical reaction used to covalently bind target ligand on ΔHSPG capsid would influence the efficiency of the system, I have compared the transduction levels of ΔHSPG vectors modified respectively with WGA-SNAP or WGA-N_3.

WGA-SNAP has been synthetized as SNAP-tag fusion protein by the Protein Core Facility, EMBL, Heidelberg. WGA-azide has been produced in our laboratory by modifying the lectin with a NHS-peg4-Azide linker, as discussed in the Material & Methods section.

Increasing amount of ΔHSPG vectors ($7{,}5x10^8$, $1{,}5x10^9$ and $3x10^9$ VG) were modified with NHS-peg4-DBCO or NHS-peg13-BG linkers at their optimal linker concentrations. 5uM WGA- N_3 or WGA-SNAP were added on vectors respectively modified with DBCO or BG linker. Modified vectors were then applied on freshly prepared wild type DRG cultures. Fluorescence has been monitored 3 days post infection by fluorescence microscopy. Workflow and results can be viewed in figure 18.

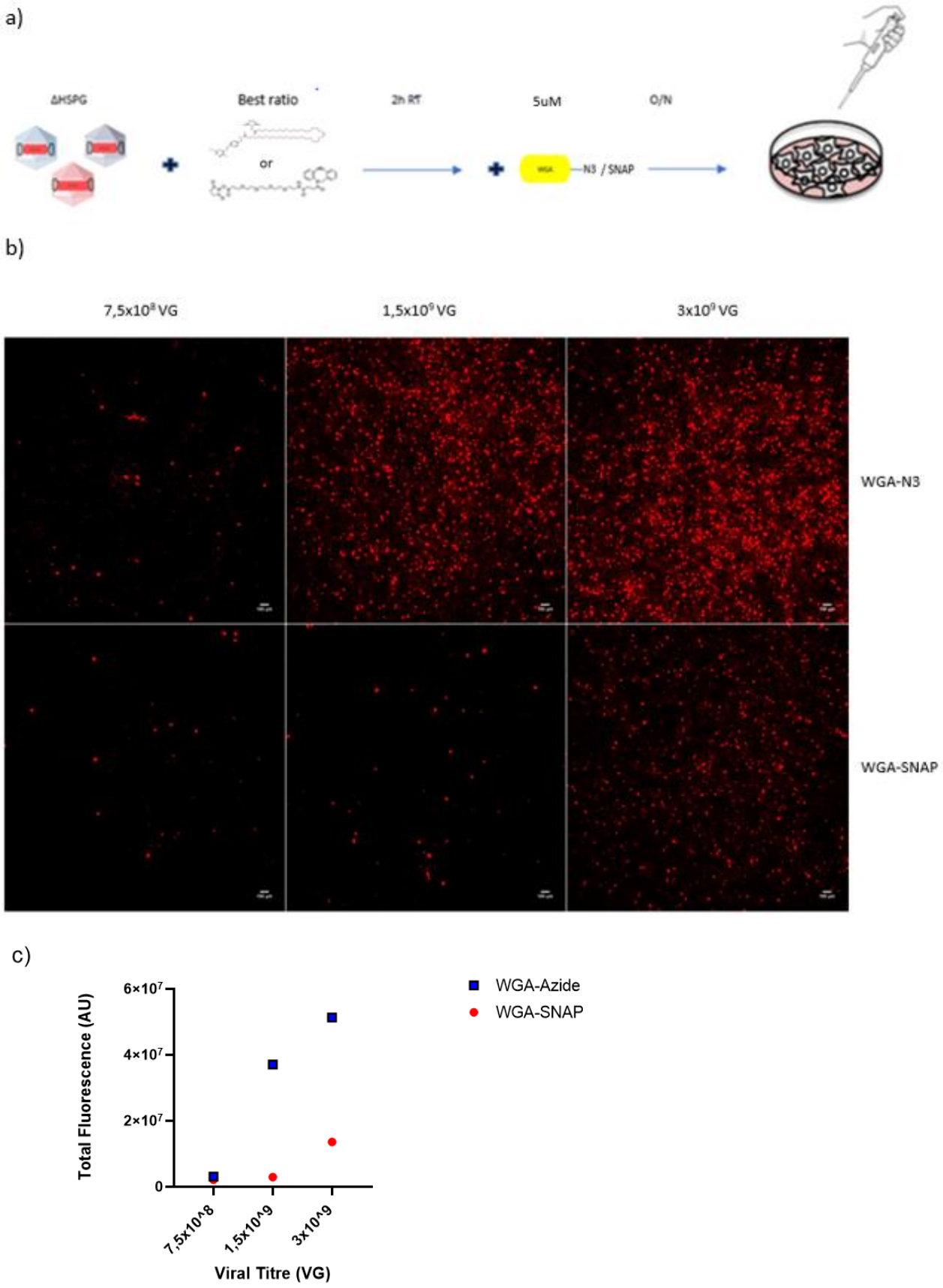

Figure 18. a) Schematic representation of the workflow to find the best chemical modification strategy. tdTomato expressing ΔHSPG vectors are modified at their optimal linker concentration with NHS-peg4-DBCO or NHS-peg13-BG,

then 5uM of WGA-N_3 or WGA-SNAP are respectively added. b) Different doses of modified vectors are used to infect DRG cultures. c) Quantification of total fluorescence shows that transduction efficiency, along with being dose dependent, relies on the particular chemistry used.

Red fluorescent signal, as indicator of viral transduction, is evident in all conditions, and regardless of the chemistry used, it is dependent on viral dose. When the azide-based reaction is chosen, ΔHSPG-WGA displays high level of fluorescence already at $1{,}5x10^9$ VG dose, reaching its maximum level of transduction at $3x10^9$ VG. On the other hand, when WGA-SNAP is used, the overall efficiency of ΔHSPG-WGA is drastically reduced. Only a few cells are infected at $7{,}5x10^8$ and $1{,}5x10^9$ VG doses, increasing when the higher $3x10^9$ VG dose is used, but still being markedly lower than its corresponding condition with WGA- N_3. Total fluorescence of positive cells in each conditions have been measured as an indicator of viral efficiency (figure 18c).

This experiment proves that WGA can be effectively conjugated to viral capsid using both SNAP-TAG or azide-based chemical reactions in order to efficiently re-target viral tropism. However, WGA-N_3 exhibit drastically higher efficiency when compared with WGA-SNAP. Presumably, in terms of efficiency, the choice of the optimal chemical reaction to covalently bind ligands to viral capsid depends on different factors, including the particular system used to introduce functional groups required for the specific chemistry, proprieties of the ligand itself and reaction conditions. Since it is difficult to predict the exact functionality of a particular ligand after a specific chemical modification, the most efficient strategy is to empirically find which are the best condition for each ligand used, including the choice of the chemical reaction to be used.

2.4 POTENTIAL INTERNALIZATION MECHANISM

AAV2's cell cycle begins with its access into target cell. The mechanism of internalization consists of two steps, the first of which is cell attachment. This first interaction sees the recognition of HSPG residues on cell membrane by a cluster of basic amino acid present on the virus that act as primary receptor, followed by the stabilization of the linkage due to the engagement of co-receptors such as integrins, laminin receptor and growth factor receptors. When the virus is firmly attached to the cell, the internalization occurs. The exact internalization mechanisms adopted by AAVs to effectively enter in the cells are still a matter of discussion, but what is known is that after attachment, AAVs interact with the so-called universal AAV receptor (AAVR), which has been proved to be crucial for internalization of AAV2 (Pillay et al., 2016). AAVR is a type I transmembrane protein which directly interacts with AAV2 and is responsible for subsequent endocytosis from the plasma membrane and trafficking to the trans-Golgi network. As previously discussed, it has been shown that anti-AAVR antibodies efficiently block AAV2 infection, and that in vivo gene delivery is highly impaired in Aavr(-/-) transgenic mice (Pillay et al., 2016).

Since our modification system consists in replacing the ability of AAV2 to bind to target cells, we are actually modifying the first step of cell entry, which is the cell attachment, theoretically without interferring with the latter internalization. However, it is also possible that the conjugation of a ligand on the viral capsid could somehow modify the normal pathway that leads to cell entry. For this reason, I have decided to check whether the AAVR was still needed by the virus to get internalized, or if the foreign ligand would impair the interaction between AAV2 and AAVR and/or possibly mediate an alternative internalization pathway.

To test this possibility, I generated a transgenic cell line by using CRISPR/Cas9 in combination with the piggyBac™ transposon system to knock-out the AAVR gene, KIAA0319L, from a Hek 293-T cell line. The resulting AAVR-KO HEK 283-T cell line has been used to test the infectivity of our modified AAV2s. PiggyBac™ transposon system is a technology commonly used in genetic enegineering that facilitates the integration of specific DNA sequences (transposons) into the genome of target cells. The system is composed by two effectors: a transposon, in which the cargo of interest is inserted between two piggyBac™ ITRs, and a transposase, wich facilitates direct integration of the donor-transposon into random 'TTAA' sites throughout the genome. It is possible to combine piggyBac™ system with gene editing tools such as CRISPR/Cas9 to generate stable transgenic cell lines. In our case, piggyBac™ transposon has been used to insert *Streptococcus pyogenes* Cas9 (spyCAas9) and gRNA plasmids, carrying a selection marker, into Hek 293-T genome in order to obtain stable and precise knockout of the KIAA0319L gene (enconding for AAVR). Succesfully transfected cells have been selected with specific antibiotics, and correctly edited clones have been screened by using wt AAV2 carrying tdTomato as cargo. Indeed, cells which underwent correct knockout of AAVR should be resistant to wt AAV2, while non edited cells should be permissive and thereby becoming fluorescent after viral infection. Four rounds of fluorescence-activated cell sorting (FACS) analysis combined with antibiotic screening allowed for an accurate selection of correctly edited cells.

To investigate whether AAVRKO Hek cell line is resistant to AAV2 infection, unmodified wtAAV2 have been directly applied to AAVRKO cells and normal Hek 293-T cells (as positive control) at a MOI = 1000 GC/cell. Cells were fixed four days post infection and a DAPI nuclear staining have been performed to facilitate subsequent quantification of fluorescence. Data are shown in figure 18a/e.

Strong signal has been recorded just one day post infection in normal Hek 293-T cells, reaching its maximum peak after 3 days. On the other hand, just weak fluorescence has been recorded 3 days post infection in AAVRKO cells, thus indicating successful knockout of AAVR and its crucial role in AAV2 internalization mechanisms. To further validate the knockout cell line, and to ensure at which extent the ΔHSPG mutation can actually impair AAV2 transduction, unmodified ΔHSPG vectors have been then applied at the same conditions to both the cell lines (figure 18c/g). Notably, data clearly confirm that the R585/588A substitutions are not completely silent, as high level of fluorescence is evident when ΔHSPG vectors are applied on wt Hek 293-T cells (fig. 18c). However, the absence of AAVR drastically reduced transduction efficiency, as confirmed by the almost total absence of signal in AAVRKO Hek 293-T cells (fig. 18g).

Having demonstrated the reliability of the AAVRKO model, modified vectors have been used to investigate if the presence of WGA on viral capsid would interfere with subsequent internalization and infection. ΔHSPG and wt AAV2 vectors have been modified, as previously shown, with NHS-peg4-DBCO linker and WGA-N_3, and subsequently used to infect normal Hek 293-T cells and AAVRKO Hek 293-T cells at a MOI = 1000 GC/cell (figure 18 b/d/f/h). As expected, both wt AAV2 and ΔHSPG vectors modified with WGA exhibited high level of transduction of wt Hek 293-T cells, in line with what previously found. However, when same vectors have been applied on AAVRKO Hek, only few cells were infected, thus further confirming the crucial role of AAVR in viral internalization and infection. Nevertheless, when applied on the AAVRKO Hek cell line, WGA-modified vectors exhibited substantially greater efficiency if compared to their respective unmodified version, an effect which was not evident in the wt Hek cell line.

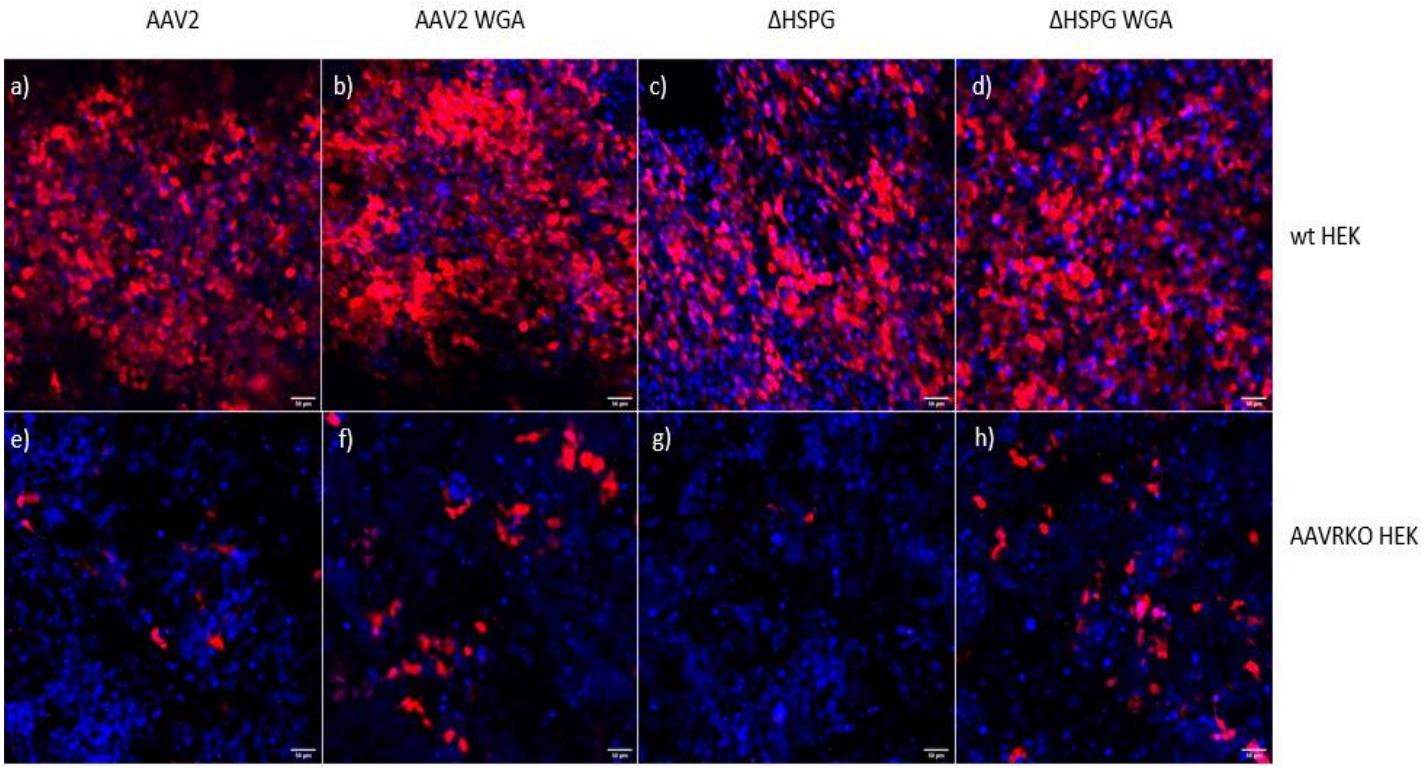

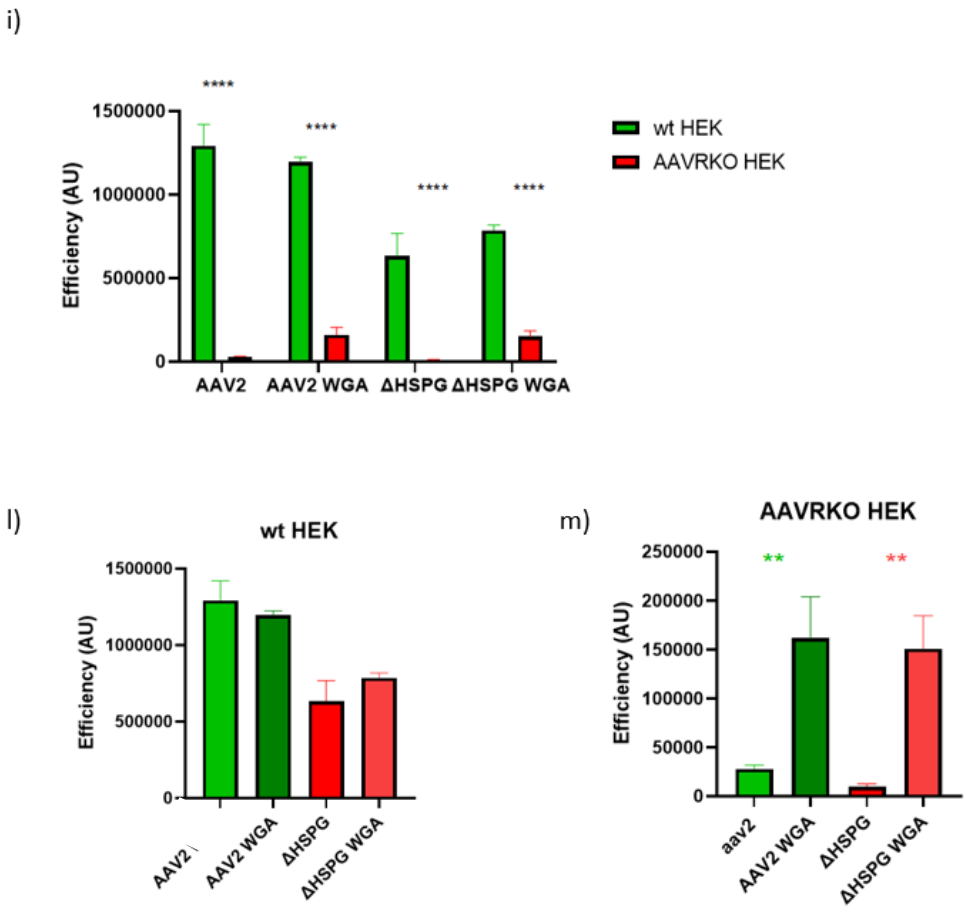

Figure 18. wt AAV2, wt AAV2-WGA, unmodified ΔHSPG and ΔHSPG-WGA applied respectively on Hek 293-T cells (a,b,c,d) and AAVRKO Hek 293-T cells (e, f, g, h). DAPI staining is evident in blue. Viral efficiency expressed as mean fluorescence of all treated cells of each condition (i), in wt Hek (l) and AAVRKO Hek (m) have been analyzed using a two-way Anova test (p**<0.01, p****<0.0001). Ensured the requirement of AAVR for AAV2's cellular entry, data suggest the presence of a WGA-dependent internalization mechanism.

In order to better study the effects of WGA and AAVR on AAV infectivity, transduction efficiency has been measured as the mean value of fluorescence intensity of all the treated cells for each condition (fig. 18 i/l/m). As shown in figure 18i, a statistically significative difference in viral efficiency is evident when the same virus is applied either on wt Hek or AAVRKO Hek, thus confirming the role of AAVR in AAV infectivity, in accordance with previously published literature. Moreover, considering the experiments carried out on wt Hek, the presence of WGA does not statistically affect viral efficiency, probably due to the high background level caused by the great intrinsic permeability for AAVs of wt Hek 293-T cells (fig. 18l). However, when the same vectors are applied on the knockout model, a statistically significative difference in viral efficiency is evident (fig. 18m). As discussed, when the AAVR is eliminated, AAV infectivity decreases, thus generating the conditions to better appreciate potential differences in viral efficiency caused by the presence of WGA. In this context, while it appears that AAVR is still required for efficient transduction even in our modified ΔHSPG vectors, WGA could trigger other pathways for viral entry. In this respect, we can assume that, rather than negatively influencing AAVR-dependent viral internalization, our modification

system could confer novel proprieties to facilitate the internalization of viral particles, which are, however, derived by the specific ligand used for the modification.

2.5 BOOSTING VIRAL EFFICIENCY WITH CHEMICALLY MODIFIED ΔHSPG

Beside the main aim of this project, which is to develop a strategy to selectively deliver genetic material in a cell-type specific way using AAV vectors, we further explored other different applications of our technology. Indeed, by acting on the very first step of viral infection, which is the cell attachment, it could be possible to increase the total amount of viral particles that are actually able to enter into target cell and, therefore, express their transgene. This is basically a direct consequence of the modification technology that arises when a particularly efficient ligand is used to modify the vectors. Moreover, by using a ligand whose receptor is widely expressed in different cells types at high levels, it would be possible to effectively increase the overall efficiency of the vectors. In this respect, lectins are ideal ligand candidates. Indeed, as discussed, their tropism is exceptionally broad, they are particularly stable and they present multiple and independent binding sites. Moreover, they shown great efficiency when coupled with ΔHSPG vectors in our preliminary experiments, and their conjugation protocols have been already optimized.

To specifically asses and quantify this lectin-mediated "boosting effect" on viral delivery efficiency, I firstly produced a wild type (wt) AAV2 designed to express a GFP reported under the control of CMV promoter. Unmodified wt-AAV2 has been applied to PC12 cells at increasing concentrations, to asses an efficiency baseline (figure 19a-f). The same wt-AAV2 has been modified with NHS-peg4-DBCO and IB4-N_3, and applied to PC12 cells at the same concentrations tested for unmodified AAV2 (figure 19g-l). Cells were fixed four days post infection and a DAPI nuclear staining have been performed to facilitate subsequent quantification of the green fluorescent signal, expressed as the average brightness of all cells for each condition, and collected data have been compared (figure 19m).

GFP fluorescence has not been detected at any tested concentration with unmodified wt-AAV2, while strong signal was evident at all doses above $5x10^8$ VG with AAV2-IB4. Viral efficiency, expressed as average brightness of cells, was dependent on the viral dose used, and at the maximum concentration of $5x10^9$ VG, modified AAV2-IB4 shown drastically increased efficiency compared to the unmodified wt-AAV2.

Thus the presence of IB4 on the AAV2 capsid can effectively boost efficiency and even rescue the functionality of a poorly infective virus. Indeed, even if no signal has been detected for wt-AAV2 at all concentrations tested, when the same virus is modified with IB4 it recovers its infectivity. This offers the opportunity to simply use the modification system to increase the overall efficiency of an AAV vector. Indeed, a general strategy to increase the efficiency of viral transduction could be to directly act on the ability of the virus to attach on the surface of target cells. Simply put, the more viral particles are actually able to firmly bind to target cells, the highest gene transfer rate could be achieved. In this case, an AAV2 has been used, but it is expectable that any AAV serotype could be adapted to our approach. In this way, it could be possible to dramatically reduce the viral amount required to achieve any particular experimental goal, just by optimizing the efficiency of the chosen vector.

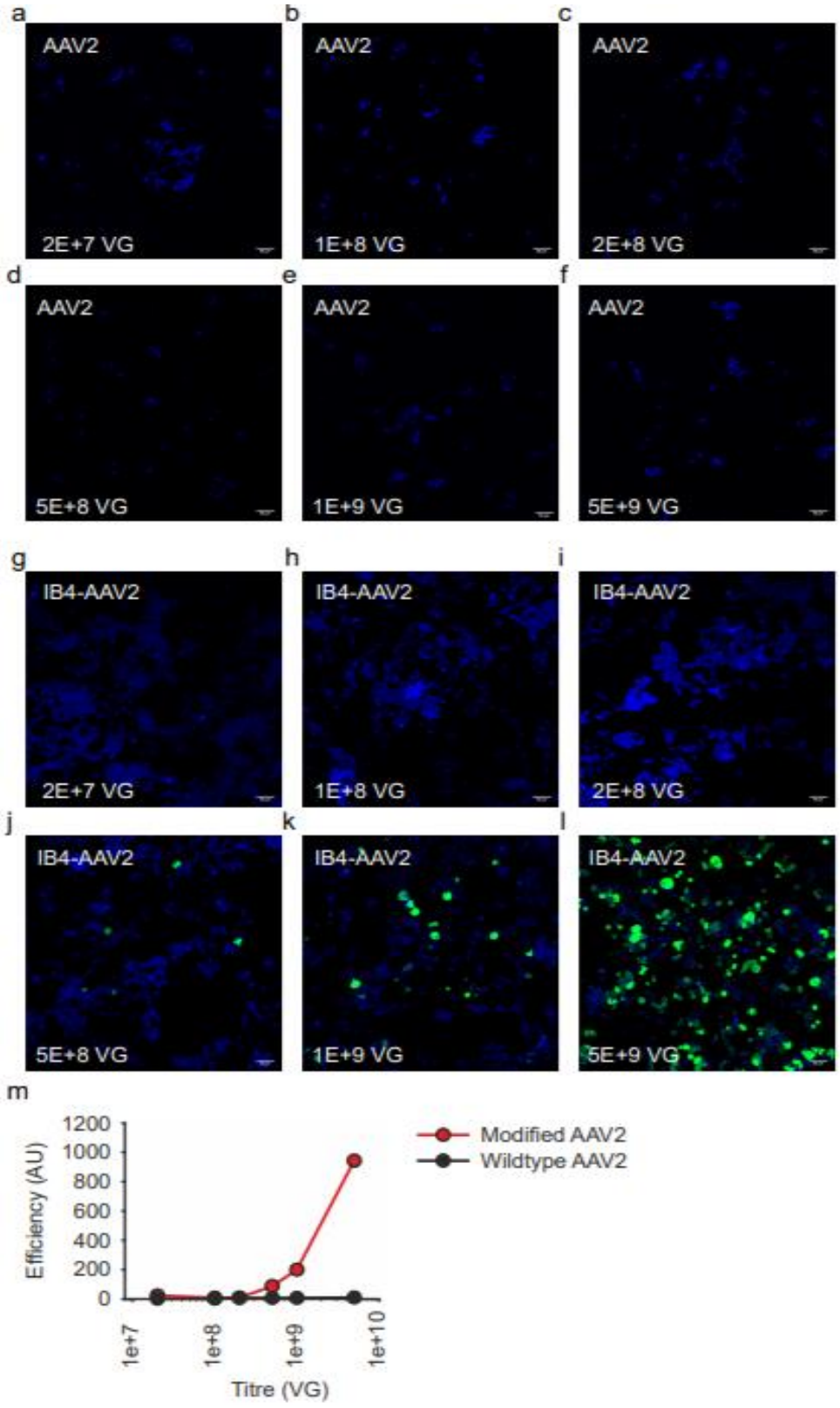

Figure 19. Increasing concentrations of unmodified wt-AAV2 (a-f) and AAV2-IB4 (g-l) on pc12 cells. GFP green fluorescence is evident only at the highest concentrations of AAV2-IB4 applied (j-l). DAPI (blue) has been used to quantify average brightness as transduction efficiency indicator (m).

However, it is important to keep in mind that in the previous experiment, by adding IB4, the tropism of wt-AAV2 has been modified, and vectors gained specificity for galactosyl residues as well as for its own natural receptor HSPG residues. In this way, the virus gained new proprieties, and its tropism has been extended. If on one side this resulted in a significant boost of efficiency, the specificity change could lead to different problems when the vector is used in an in vivo model. Indeed, if a specific AAV serotype is chosen for its own tropism to optimize the effect on a specific tissue, modifying its tropism could not be the best option, mainly if the virus is delivered systemically. It is true that the efficiency could be boosted, but high levels of unspecific targeting could be present, due to the broad tropism of the ligand used. In this respect, the best way to boost a specific AAV serotype efficiency without acting on its natural tropism would be to use a ligand with the same specificity of the serotype chosen. In other words, the idea is to use our technology to modify a specific AAV with a ligand having the same cellular specificity as the chosen AAV serotype in order to boost its efficiency without re-direct its tropism.

In order to test viral efficiency boosting without modifying the natural tropism of the vectors, we have selected the AAV9 serotype, which shares the same tropism of IB4 toward N-linked galactose (Shen et al., 2011). The same experiment shown previously for wt-AAV2 has been repeated using a wild type AAV9 vector carrying the same GFP reported gene under the control of CMV promoter. Increasing concentrations of unmodified AAV9 (figure 20a-f) and AAV9-IB4 (figure 20g-l), modified following the same protocol used for wt-AAV2, have been applied on PC12 cells. Again, four days post infection, cells have been stained with DAPI, imaged and signal has been analyzed (figure 20m).

Similarly to wt-AAV2, signal from unmodified AAV9 was not evident at most concentrations, but became visible at the highest dose of $5x10^9$ VG (fig. 20f). However, when the same AAV9 has been modified with IB4, GFP fluorescence has been registered at $1x10^9$ and $5x10^9$ VG (fig. 20k-l). Once again, viral efficiency, expressed as average brightness of cells, was dependent on the viral dose used, and at the maximum concentration of $5x10^9$ VG, modified AAV9-IB4 showed drastically increased efficiency compared to the unmodified wt-AAV9, which had barely visible signal.

By comparing the average fluorescence of cells in each condition it is clear that the presence of IB4 is effectively able to enhance viral efficiency. Starting from a virus in which efficiency was barely detectable, it has been possible to obtain a more functional vector while retaining its own original tropism. In this way it is expectable that AAV9-IB4 would still bind to the same cells when delivered in vivo but with higher efficacy, resulting in more efficient gene delivery.

Figure 20. Increasing concentrations of unmodified wt-AAV9 (a-f) and AAV9-IB4 (g-l) on pc12 cells. While GFP green fluorescence is barely present only in the $5x10^9$ VG condition for the unmodified wt-AAV9 (f), strong signal is registered in both $1x10^9$ and $5x10^9$ VG when AAV9-IB4 is used (k-l). DAPI (blue) has been used to quantify average brightness as transduction efficiency indicator (m).

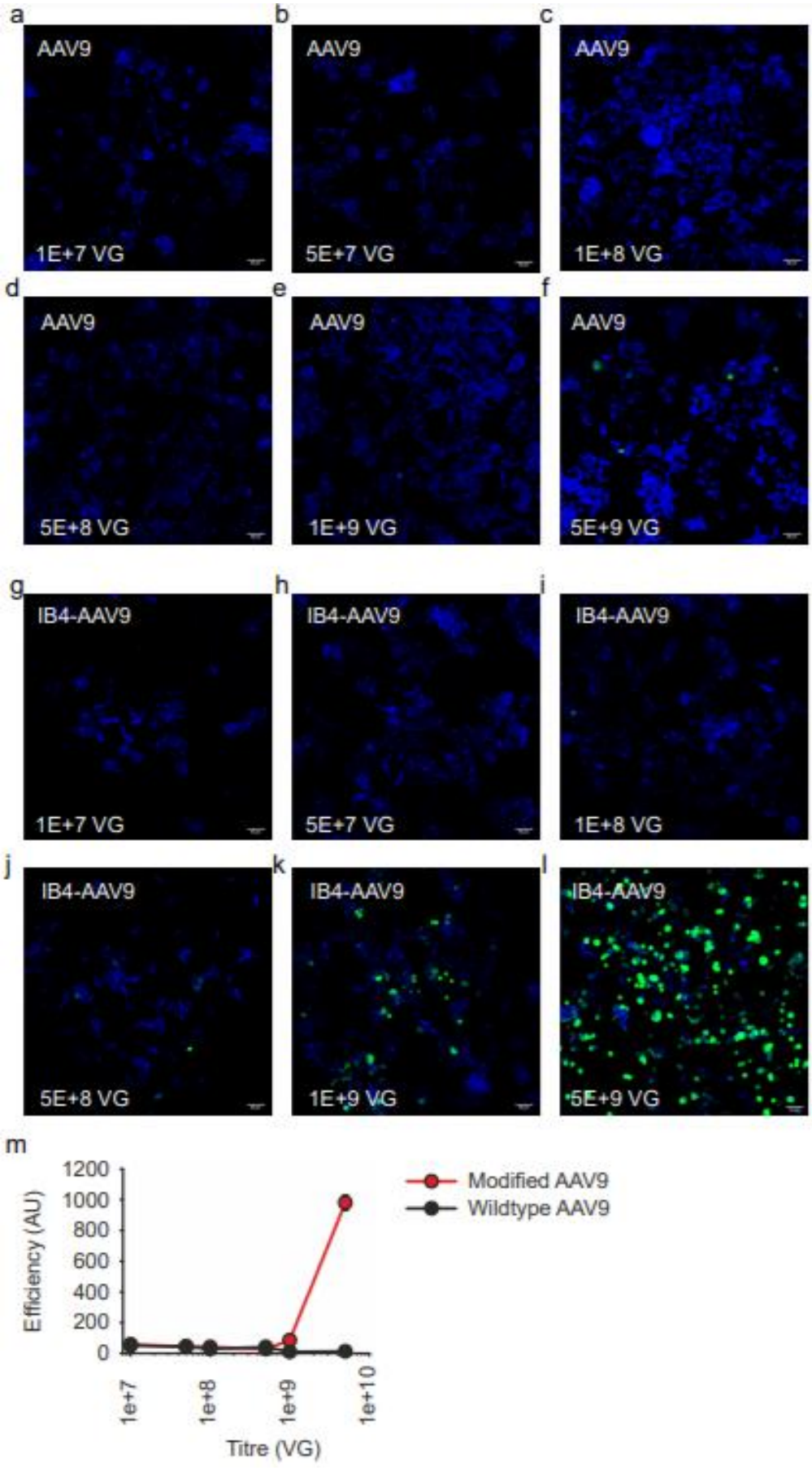
a
AAV9
1E+7 VG
b
AAV9
5E+7 VG
c
AAV9
1E+8 VG
d
AAV9
5E+8 VG
e
AAV9
1E+9 VG
f
AAV9
5E+9 VG
g
IB4-AAV9
1E+7 VG
h
IB4-AAV9
5E+7 VG
i
IB4-AAV9
1E+8 VG
j
IB4-AAV9
5E+8 VG
k
IB4-AAV9
1E+9 VG
l
IB4-AAV9
5E+9 VG
m
Efficiency (AU)
1200
1000
800
600
400
200
0
1e+7
1e+8
1e+9
1e+10
Titre (VG)
Modified AAV9
Wildtype AAV9

2.6 IN VIVO - ΔHSPG-IB4

Given the functionality of the modification system in vitro, we next sought to determine whether the same modified vectors were also able to retain their enhanced efficiency in vivo. It is important to mention the fact that in the in vivo model there are a number of obstacles that viral particles have to overcome to efficiently infect their targets. As previously discussed, the immune system plays a crucial role in the neutralization of viral particles, thus limiting the effectiveness of gene delivery. Immune response could be elicited specifically by capsid proteins, the vector DNA expression cassette or by the product of these genes, and despite many strategies having been developed to overcome these issues, in vitro models are still more permissive. Moreover, given the huge variety of cellular types present in vivo, it is expectable to observe some grade of off-targeting, which results in a loss of potentially functional virus through infection of unwanted cells. This is particularly true when a serotype with broad tropism is used, or, in our case, when a ligand which can bind to many different tissues is used to expand or re-direct viral tropism.

In an attempt to reduce as much as possible off-targeting, all in vivo experiments have been performed using the ΔHSPG vectors, modified with different classes of ligands. In this way, viral tropism can be restricted just to the cells expressing the receptor of the ligand used, thus avoiding detrimental waste of virus and undesirable possible side effects on the animal.

The first ligand that I have been testing in vivo was IB4. Previous experiments have been already performed in order to optimize ΔHSPG-IB4 modification protocol, and furthermore shown the efficiency of the system in vitro.

Different injection routes have been chosen, based on the particular selectivity of IB4. Since IB4 is commonly used as a marker for nonpeptidergic nociceptors, I firstly checked whether its natural tropism for neurons was also maintained in vivo after conjugation with ΔHSPG capsid. Intra sciatic nerve injection is a technique for intraneural targeting, applicable to mouse peripheral nerves, with low impact on the nerves and which reduces the variability of label recovery by limiting delivery specifically to lumbar #3, #4, #5 DRG homolateral to injection site (Heape et al., 1986).

ΔHSPG AAV2 vectors were modified with NHS-peg4-DBCO linker at the best virus::linker ratio previously found for the batch used in vitro, then 10uM IB4-N_3 was added. Since a small volume is required for intra sciatic nerve injection (3ul), modified virus was concentrated with 100kDA molecular weight cut-off column. As negative control, ΔHSPG coming from the same batch as the one conjugated with IB4 were concentrated to a final volume of 3ul with the same 100kDA columns, and no chemical modifications were performed.

C57BL/6J wild-type mice were injected with $9x10^9$ VG for each condition in either right or left sciatic nerve following nerve identification and exposure. Animal's health condition and mobility were monitored after the injection, and tissues were collected 4 weeks post injection.

Mice were sacrificed, lumbar #3, #4, #5 DRG and spinal cords were collected and promptly fixed for 2 hours in PFA 4%. Samples were then washed three times with PBS, embedded in 2% agarose blocks and cut with a vibratome to obtain 50uM thick sections. This procedure was used for the preparation of the histological sections of all the tissues collected in each in vivo experiment.

To ensure selective targeting of nonpeptidergic nociceptors, green fluorescent Alexa Fluor® 488 isolectin GS-IB_4 conjugate was used for specific cellular staining. Samples were finally mounted and imaged at confocal microscope. Results are shown in figure 21 and 22.

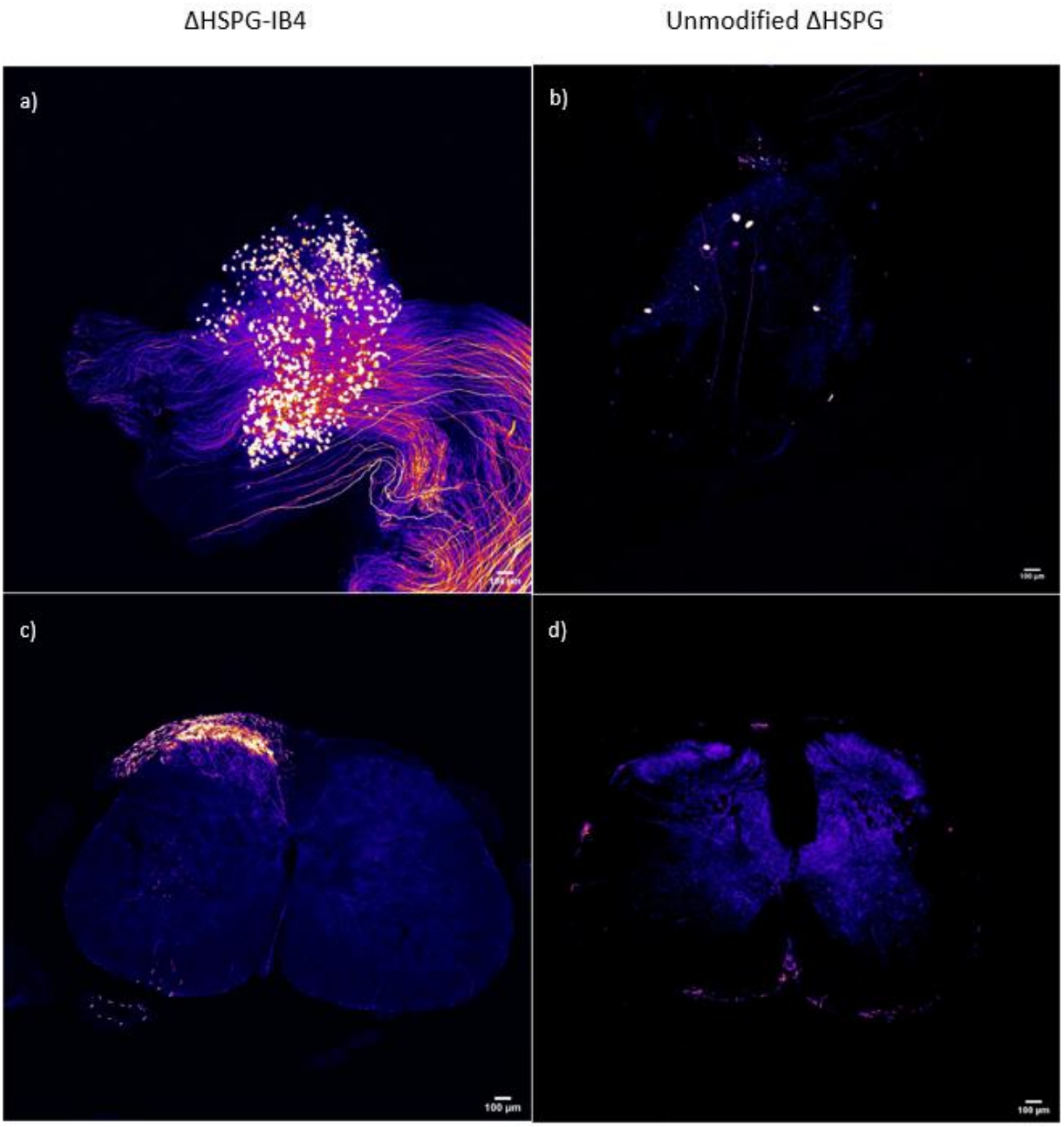

Figure 21. Fluorescence detected in lumbar #3 DRG and spinal cord from wild type mice injected respectively with ΔHSPG-IB4 (a,c) and unmodified ΔHSPG (b,d) carrying tdTomato fluorescent reporter.

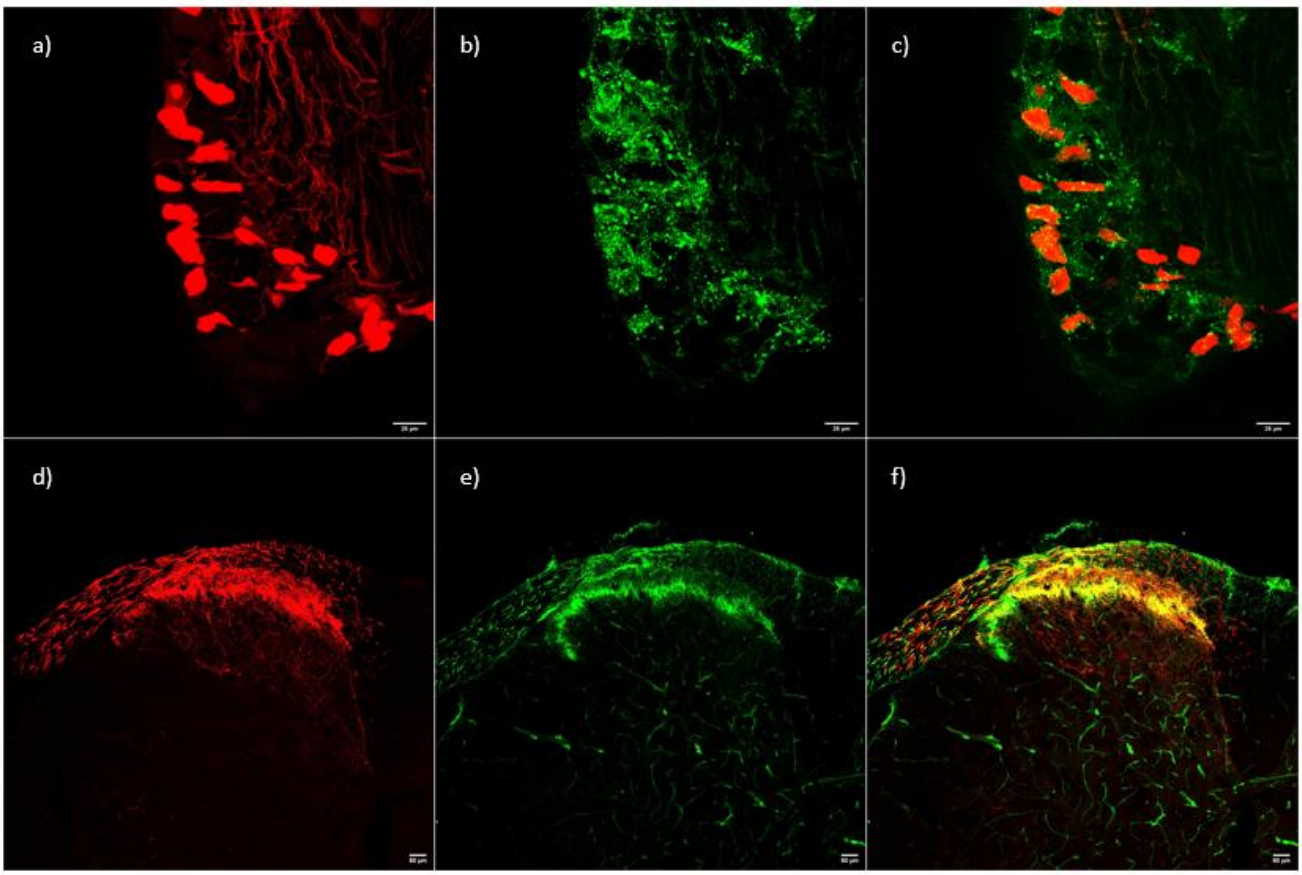

Figure 22. DRG and spinal cord sections from wild type mouse injected intra sciatic nerve with HSPG-IB4 vector expressing fluorescent tdTomato reporter. #3 lumbar DRG and spinal cord showing strong red fluorescence (a,d) are stained with green fluorescent Alexa Fluor® 488 isolectin GS-IB_4 (b,e). Merged channels are shown (c,f).

Fluorescent signal has been found in #3, #4, #5 lumbar DRG in mice injected either with ΔHSPG-IB4 and unmodified ΔHSPG, with the higher peak in #3 lumbar DRG (figure 21 a,b). However, DRG from mice injected with modified vectors shown substantially stronger signal when compared with the control group. To note, some signal in the control animals is perfectly expectable and in line with previous studies showing that ΔHSPG AAV2 still maintain some of its activity, especially when high doses of virus are used.

On the other hand, while strong red fluorescence can be detected in the dorsal horn of the spinal cord ipsilaterally to the injection site in experimental mice (figure 21c), no signal at all is detected in the control animals (figure 21d).

The localization of the signal within the spinal cord matches the expectations, given the connection of lumbar #3, #4, #5 DRG projection to the second lamina of dorsal horns, where nonpeptidergic nociceptors are located. Moreover, the absence of signal in control mouse spinal cords indicates a weaker level of transduction of DRG, due to the limited efficiency of unmodified ΔHSPG vectors.

In order to assess accurately cell type specificity, samples have been stained with fluorescent Alexa Fluor® 488 isolectin GS-IB_4 (figure 22b, d). A shown in figure 22c,f, substantial colocalization of red

signal (virus) and green signal (dye) is detected. In DRG the efficiency, calculated as percentage of infected cells among the total of IB4-positive cells, reaches the 69 ± 4,9 %. Red fluorescence in the spinal cord appears to be localized selectively in the second lamina of the dorsal horn on the side of injection (figure 22d), the termination site of nonpeptidergic nociceptors. IB4-488 staining confirms correct targeting of modified vectors (figure 22f).

I next investigated whether ΔHSPG-IB4 was able to target another cellular population which is known to express high levels of α-galactose residues: vascular cells. Given the high affinity of IB4 for vascular cells, I performed subcutaneous injections in the paw of wild type C57BL/6 mice, with the aim to target both neuronal projections and vascular networks beneath the skin.

ΔHSPG vectors were modified with IB4-N_3 as for intra sciatic nerve injections, and $1{,}5x10^{10}$ VG were injected subcutaneously along with unmodified vectors as control. Skin of the paw was taken 4 weeks post injection, fixed and imaged (figure 23).

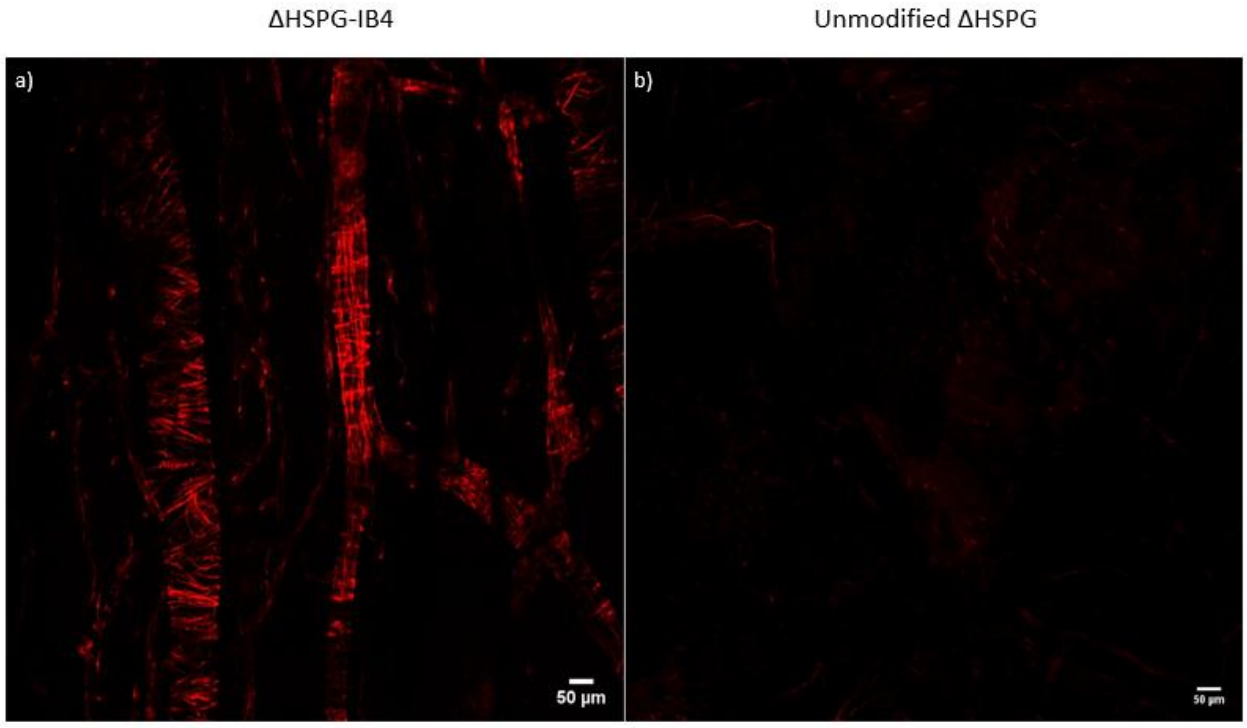

Figure 23. Fluorescence detected in the skin of the paw from wild type mice injected respectively with ΔHSPG-IB4 (a) and unmodified ΔHSPG (b). While no vasculature is evident in the control animals, modified ΔHSPG-IB4 successfully mark endothelial cells and vascular smooth-muscle cells.

As shown in figure 23a, blood vessels but no nerves are easily detectable in the whole sample, while vasculature is not evident in control mice (figure 23b). According to the morphology, ΔHSPG-IB4 seems to target specifically endothelial cells and vascular smooth muscle cells which surround blood vessels. The strong fluorescent signal demonstrates that IB4 is able to mark vascular

elements even if not delivered directly into the blood stream, as it is usually done for this purpose, and, moreover, is able to selectively drive the conjugated virus to its target enabling specific infection.

2.7 IN VIVO - ΔHSPG-NGF

We next investigated the conjugation of another ligand, the neurotrophic factor NGF. This ligand has been selected for multiple reasons. First, being a protein, it represents a different class of ligands that we have never tried to conjugate to a viral vector capsid in vitro, therefore it was important for us for to further probe the versatility of the technology. Second, our group has an interest in pain and nociception, and NGF signaling and proprieties were already familiar to us. Indeed, our lab have previously worked with a mutated form on NGF, named NGF^{R121W}, which retains its ability to bind to its receptor but does not activate the signaling cascade which leads to pain transmission. Finally, and most important, NGF tropism for peptidergic nociceptor could have therapeutic potential. Being able to obtain AAV vectors which can selectively target nociceptors could be a huge boost for the development of therapies to treat chronic pain.

In contrasts to the experiments with IB4, in this case the ligand was modified with a SNAP-tag and not with an azide motif. Indeed, the NGF^{R121W}-SNAP complex has been previously characterized and its efficiency and functionality validated directly in our lab (Nocchi et al., 2019), thereby we decided to test it directly in conjugation with the ΔHSPG vectors.

Because of the relatively large size of the NGF^{R121W}-SNAP complex, we firstly investigated whether steric hindrance issues could arise when NGF is coupled to the viral capsid. In order to provide a certain level of mobility of the protein after the conjugation, two distinct linkers with different length have been tested. The rational here is that a more flexible linker could allow the ligand to move with more freedom and to facilitate the binding to its receptor, as well as enabling the exploration of a wider surface on the target cell surface.

The first administration route chosen was the retro orbital injection, a technique commonly used to administrate different compounds directly into the retro-orbital sinus of mice as an alternative of tail vein injection (Yardeni et al., 2011).

For this experiment, I have been using ΔHSPG vectors carrying the Cre recombinase gene under the control of the strong mammalian CMV promoter, and vectors have been injected in transgenic Rosa-CAG-LSL-tdTomato mice (Ai14 RCL-tdT-D). The transgenic mice line is designed to have a *loxP*-flanked STOP cassette preventing transcription of a CAG promoter-driven red fluorescent protein variant (tdTomato) which can be reverted upon Cre-mediated recombination. In this way, cells infected by ΔHSPG-Cre can express robust tdTomato fluorescence following Cre expression and deletion of the STOP cassette.

ΔHSPG vectors were modified with either the short linker (BG-GLA-NHS) or long linker (BG-peg13-NHS) at their best virus::linker molar ratio, and excess of unconjugated linker were filtered through a 100kDA column. 5uM NGF^{R121W}-SNAP was then added, following subsequent concentration with

100kDA columns to the volume required for the injection. Injections were performed in either the right or left eye of each animal.

Mice were injected retro orbitally with $9x10^9$ VG per animal, and tissues were collected 3 weeks post injection. Red fluorescent signal was analyzed at the level of the trigeminal ganglion, thoracic DRG and lumbar DRG, and fluorescence was compared between the two different length linkers to ensure the most efficient system, as shown in figure 24.

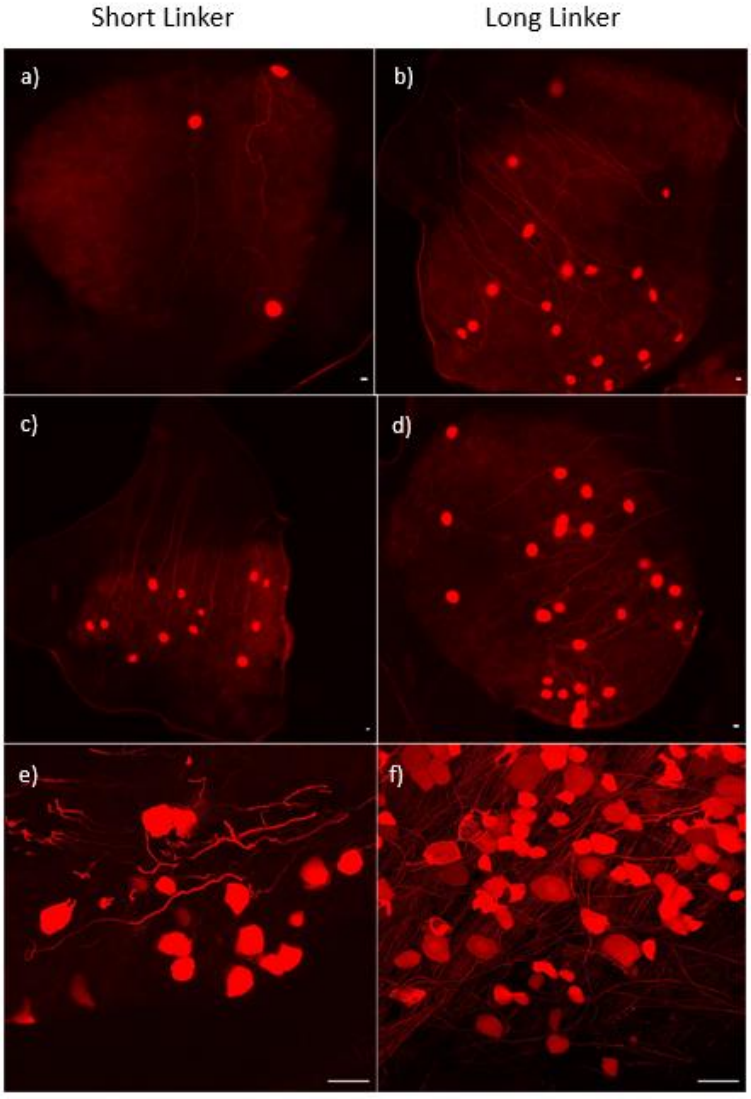

Figure 24. Retro orbital injections. Thoracic (a,b), lumbar (c,d) DRG and trigeminal ganglion (e,f) sections from mice injected respectively with ΔHSPG modified with NHS-GLA-BG (short linker) and NHS-peg13-BG (long linker) and NGF^{R121W}-SNAP. Red fluorescent signal is correlated to the level of viral transduction. Scale bar, 25um.

Regardless of the type of linker used, ΔHSPG-NGF vectors efficiently infect and express their transgene in neurons following retro orbital injection. Strong fluorescence has been detected in trigeminal ganglion, with a maximum level in the one ipsilateral to the injection site (figure 24e,f), and in DRG located at different levels of the spinal cord, including thoracic and lumbar area (figure

24a-d). Nevertheless, virus modified with long linker shown overall greater efficiency when compared to the short linker one, as can be seen by the highest number of positive cells in all samples analyzed.

To ensure accurate and specific transduction of only TrkA expressing neurons (the expected target of ΔHSPG-NGF), immunostaining with an anti-TrkA was performed. Fixed sections of trigeminal ganglion from mouse injected with NGF long linker were permeabilized and incubated with primary anti-TrkA antibody and subsequently with proper secondary antibody carrying an Alexa-488 fluorophore (figure 25).

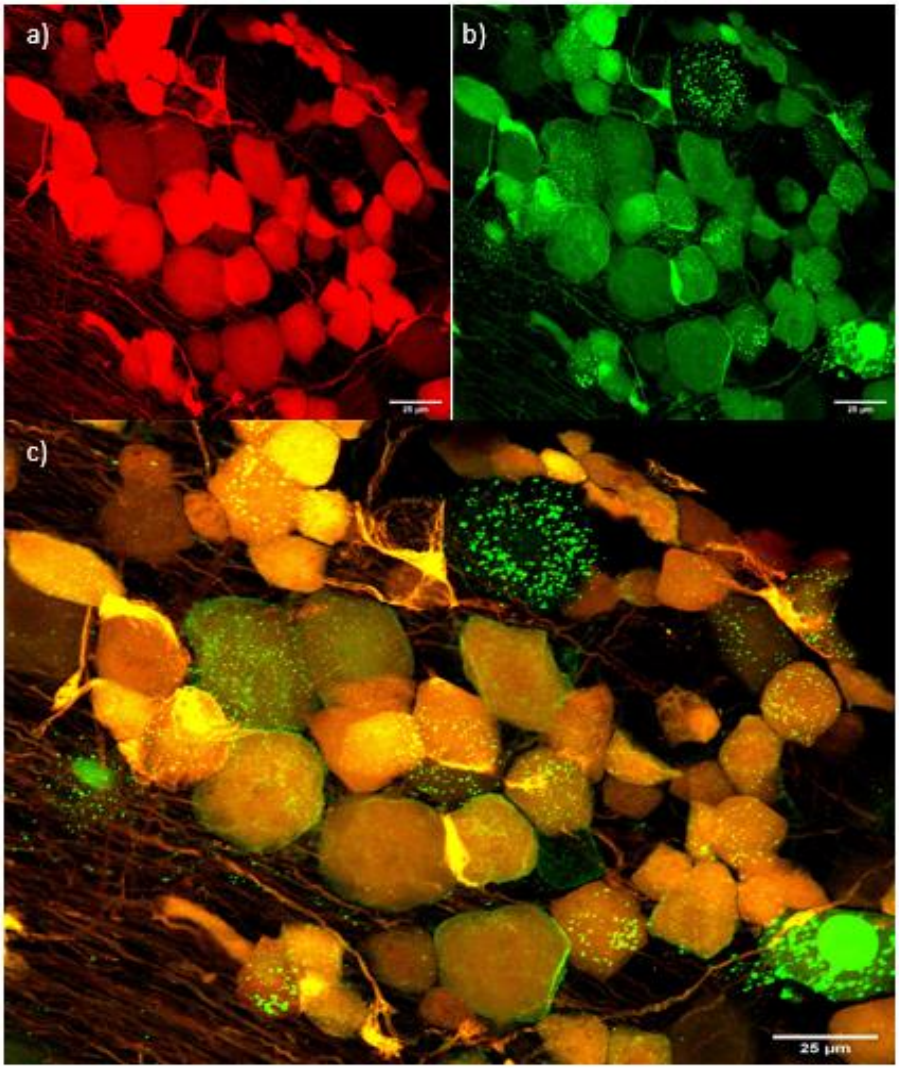

Figure 25. Trigeminal ganglion sections from mouse injected retro orbitally with ΔHSPG-NGF (long linker) (a) immunostained with an anti-TrkA antibody (in green) (b). Merged channels are shown (c).

Anti-TrkA staining shows almost showed a high degree of colocalization of red (indicator of viral transduction) and green fluorescence (TrkA staining). ΔHSPG-NGF (long linker) infects most of the TrkA expressing cells, with an efficiency of 83 ± 3,5 %, expressed as the ratio between infected cells

and total of $TrkA^+$ population. This experiment shows that our ΔHSPG-NGF vectors can effectively and selectively target $TrkA^+$ cells in vivo with high specific activity.

Next, I investigated if the same ΔHSPG-NGF vectors could retain their infectivity if administrated systemically. Intraperitoneal injection (IP) is a commonly used technique for systemic delivery of drugs in rodents which allows quick reabsorption of large volumes of substances which are delivered in the peritoneal cavity (Baek et al., 2015). However, since administrated substances are absorbed by surrounding tissues and subsequently carried away by capillary blood or lymph, metabolized by tissue enzymes or bound to tissue proteins, is hard to predict how much virus can effectively reach target tissues. Nevertheless, it is a non-invasive and very easy to perform technique, which could be done without any particular skill or equipment.

Again, for this experiment, Ai14 RCL-tdT-D transgenic mice (Jackson Laboratories, Strain #007914) have been injected with ΔHSPG vectors carrying the Cre recombinase gene.

Since ΔHSPG-NGF modified with the long linker exhibited greater efficiency than the short linker version, mice were injected IP with ΔHSPG-NGF (long linker) which was prepared in the same way as for the retro orbital injection. $3x10^{10}$ VG per animal were administrated for both experimental and control mice (injected with unmodified ΔHSPG). Trigeminal ganglion, spinal cord and DRG were collected 3 weeks post injection, sectioned and spinal cord from ΔHSPG-NGF injected animal was stained with Alexa Fluor® 647 isolectin GS-IB4.

As shown in figure 26, while unmodified ΔHSPG displayed just some weak activity in DRG (fig. 26d), ΔHSPG-NGF efficiently transduced neurons in different tissues, including trigeminal ganglion (fig. 26a), DRG (fig. 26c) and DRG neuronal terminals in spinal cord. Specifically, focusing on the dorsal horn of spinal cord, it is clear that the virus specifically infects only cells situated in the first lamina, where peptidergic nociceptor are located. This can be seen *indirectly* by performing an anti-IB4 staining to specifically mark the second lamina: red fluorescence is present above the blue marked layer (fig. 26e), which constitutes the second lamina of dorsal horns of spinal cord where $IB4^+$ nonpeptidergic nociceptors are located.

In general, ΔHSPG-NGF retains its functionality also when delivered intraperitoneally, and is able to infect neurons in a broad range of tissues. Again, modification of the ΔHSPG vectors seems to be necessary to restore viral infectivity, and NGF conjugation can effectively drive specific re-targeting viral tropism with low background activity.

Figure 26. Intraperitoneal injections. Trigeminal ganglia (a,b), thoracic DRG (c,d) and spinal cord sections (e,f) from mice injected respectively with ΔHSPG-NGF (long linker) and unmodified ΔHSPG. Anti-IB4 staining is shown in blue (e). Red fluorescent signal is correlated to the level of viral transduction. Scale bar, 50um.

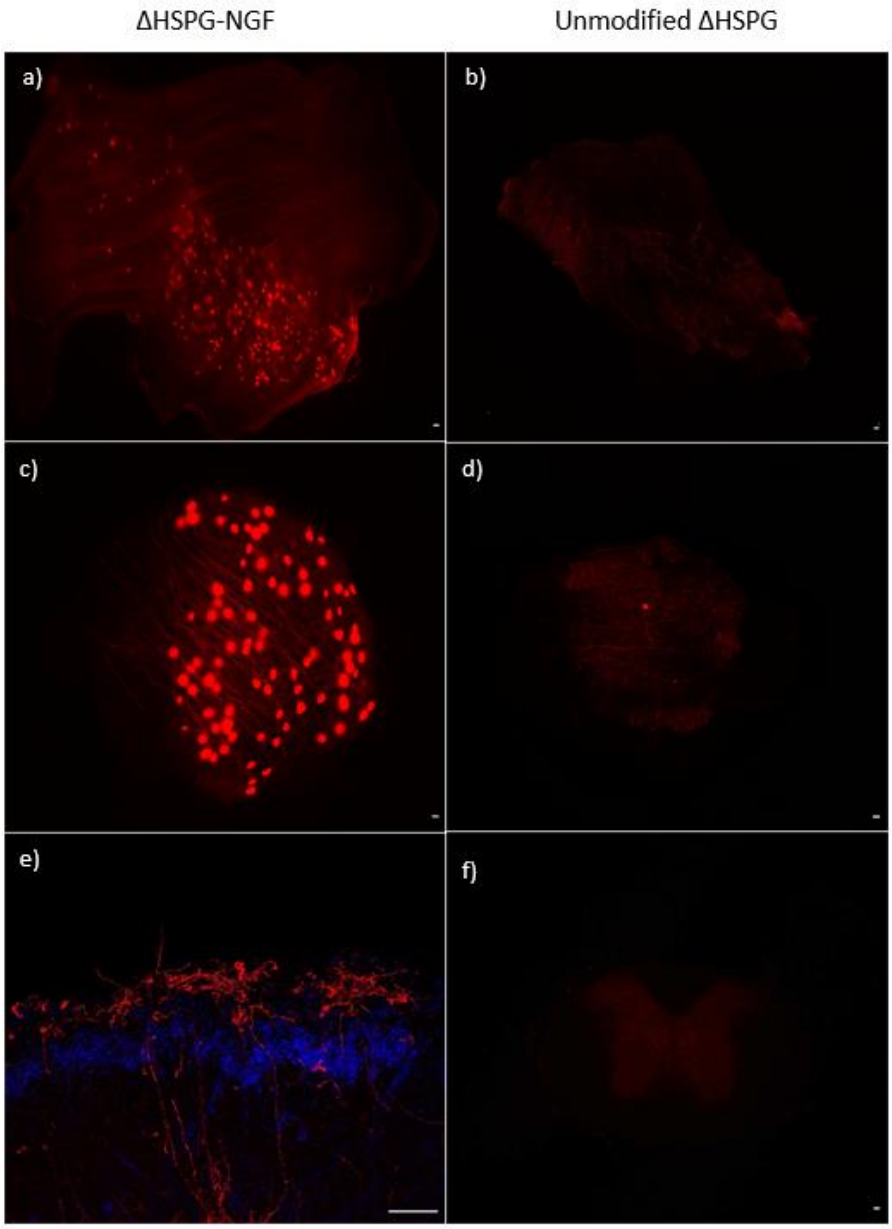

To further confirm the specificity of the modified ΔHSPG-NGF vectors for TrkA expressing neurons and to test another administration route, modified vectors were delivered with intra sciatic nerve injections. Indeed, this administration route proved to be very selective in terms of accuracy, because of the lack of variability in the distribution of the vectors, which, following correct injection into the nerve, can only track the connections of the nerve itself, thereby avoiding off target effects in non-neuronal tissues.

Moreover, as discussed in the introduction, it has been shown how the same AAV vector, if administrated in different ways could lead to diverse levels and patterns of transduction. In this respect, delivering ΔHSPG-NGF with intra sciatic nerve injection could further confirm its efficiency regardless of the administration route.

ΔHSPG-NGF (long linker) carrying a tdTomato reporter was modified as discussed above for retro orbital injections and concentrated with a 100kDA MWCO filter. C57BL/6J wild-type mice were

injected into either the right or left sciatic nerve with $9x10^9$ VG per animal. Control mice were injected with the same amount of unmodified ΔHSPG. 3 weeks post injection the animals were sacrificed and lumbar #3, #4, #5 DRG, spinal cord and the skin of the paw from the same side of the injection were collected (figure 27). Skin was taken to examine the peripheral terminal endings of the sciatic nerve which innervate the paw.

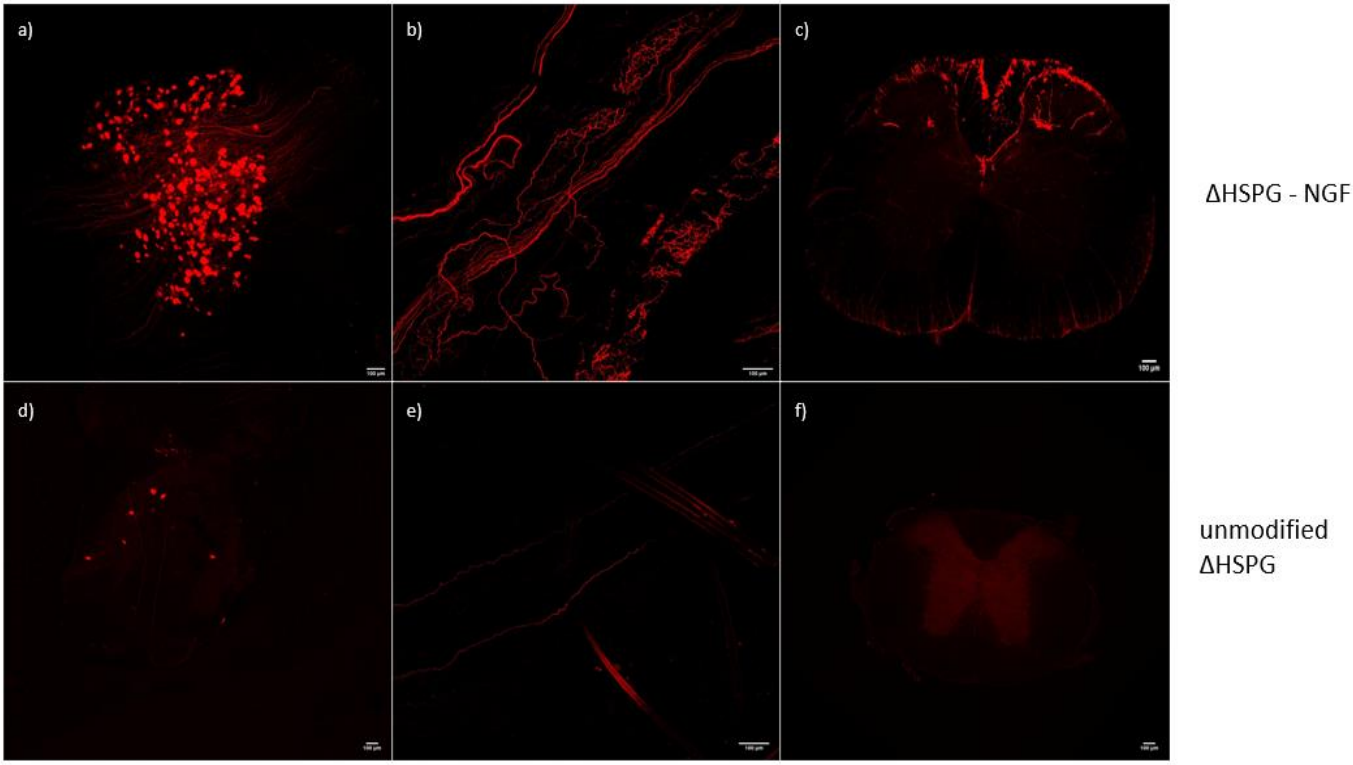

Figure 27. Intra sciatic nerve injections. #3 lumbar DRG sections, (a,d), paw skin (b,e) and spinal cord sections (c,f) from mice injected respectively with ΔHSPG-NGF (long linker) and unmodified ΔHSPG. Red fluorescent signal is correlated to the level of viral transduction.

Mice injected with unmodified ΔHSPG show presence of signal in #3 lumbar DRG located at the same side of the injection, consistent with data found with intra sciatic nerve injection of IB4 modified ΔHSPG (fig. 27d). Moreover, it is possible to see some positive fibres in the skin of the paw (fig. 27e) but no signal at all in spinal cord sections (fig. 27f). This further confirms the weak background activity in unmodified ΔHSPG as a normal feature of this AAV2 mutant.

On the other hand, when ΔHSPG-NGF is injected, red fluorescence is detected at much stronger level in all the tissues examined. In particular, the signal in the lumbar spinal cord sections innervated by the sciatic nerve is particularly clean and is limited to the top lamina of the dorsal horn ipsilateral to the injection site (fig 27c). In the skin of the paw, many nerves are visible, presumably the terminal endings of nociceptors from the injected sciatic nerve (fig 27b). All #3, #4 and #5 lumbar DRG exhibit strong fluorescence localized in multiple neuronal bodies, with the brightest being #3 ipsilateral to injection site (fig 27a).

This experiment further confirms that while unmodified ΔHSPG is only able to infect a reduced number of cells, when NGF is coupled to ΔHSPG the modified vectors gain enhanced tropism and infectivity, which is maintained in vivo.

In order to ensure cellular specificity, DRG and spinal cord from mice injected with ΔHSPG-NGF were immunostained with an antri-TrkA antibody, again to investiage whether modified vector tropism can be re-targeted in a clean and effective way (figure 29).

In both DRG and spinal cord samples a clear co-localization of signals is present. In DRG, ΔHSPG-NGF infects around 80 ± 5,1% of TrkA positive neurons (fig. 29e). Some unspecific labelling is also observed, but it could be explained by the fact that, as discussed, the R585/588A substitution does not completely prevent AAV2 from binding to HSPG residues, thus driving the modified vectors also to cell which do not express the TrkA receptor.

The signal in the spinal cord appears to be specifically localized in the first lamina of dorsal hornsipsilateral to injection site. Anti-TrkA staining confirms the specificity of ΔHSPG-NGF for peptidergic nociceptors.

This experiment further supports the reliability of the ΔHSPG-NGF as a tool for selective targeting of peptidergic nociceptors when delivered in vivo.

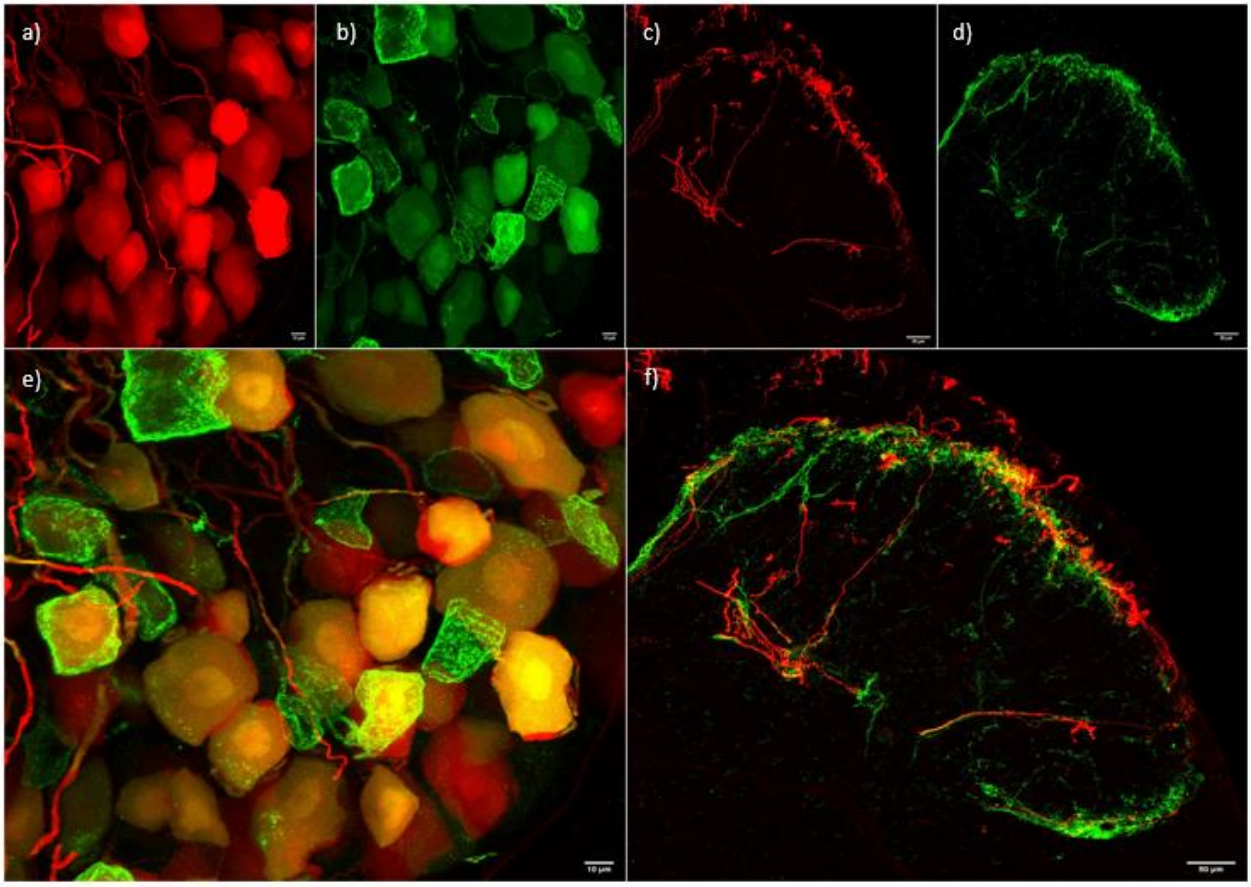

Figure 29. #3 lumbar DRG and spinal cord sections from mouse injected intra sciatic nerve with ΔHSPG-NGF (long linker) (a,c) immunostained with anti-TrkA antibody (in green) (b,d). Merged channels are shown (e,f).

2.8 IN VIVO - ΔHSPG-PAR1 AGONIST

To expand the range of different classes of ligand that could be used for the technology, we wished to include peptides as potential candidates. Peptides are short chains of amino acid, typically comprising 2 to 50 residues. Their functions are countless as well as their receptors distribution, thus potentially enabling selective targeting of a high number of tissues.

The synthetic oligopeptide SFLLRN is a selective agonist of the PAR1 receptor. It corresponds to the tethered ligand sequence unmasked by thrombin cleavage of the PAR1 extracellular N-terminus and it can activate the receptor independently of proteolysis. As discussed, PAR1 is involved in various signaling pathways that regulate different processes including wound healing, clotting, immune system regulation but also endothelial transmigration and barrier dysfunctions. The latter are of particular interest in terms of applications of our system. Indeed, one of the major concerns for gene therapy and in general for AAV based delivery is the ability of the vectors to cross barriers, particularly when targeting the CNS. For this reason, obtaining a vector with enhanced permeability for BBB and meninges could have a massive impact on currently used strategies to efficiently infect brain and spinal cord following different administration routes.

Since SFLLRN is used in its amidated form (-C terminus is modified with an amine group: SFLLRN-NH_2) to obtain maximum activation of PAR1, the addition of an azide tag using NHS-peg-N_3 linker would likely be detrimental for the peptide functionality, because both -N and amidated -C terminus would be modified. To test this assumption I firstly modified SFLLRN (100uM) with a NHS-peg4-N_3 linker at increasing peptide::linker molar ratios (1:1, 1:5, 1:10). Resulting azide-tagged peptides were coupled (5uM) to $3x10^9$ VG per condition of ΔHSPG vectors previously modified with NHS-peg4-DBCO, as described above, and used to infect freshly prepared DRG cultures, along with unmodified vectors as negative control. 5 days post infections DRG were imaged. Results are shown in figure 30.

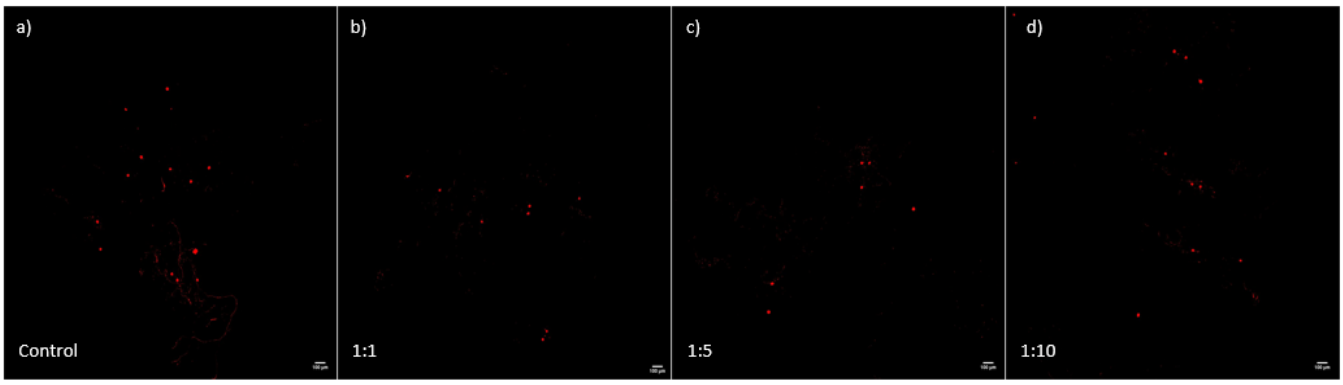

Figure 30. DRG cultures infected with unmodified ΔHSPG (a) and ΔHSPG-SFLLRN. SFLLRN was functionalized with an azide group through the reaction with NHS-peg4-N_3 linker used at 1:1, 1:5, 1:10 peptide::linker molar ratios, respectively (b,c,d).

No differences in viral efficiency can be seen between the control and the experimental groups, thus indicating that SFLLRN is not able to restore viral infectivity if modified with NHS-peg4-N_3 linker, probably due to an excessive alteration of SFLLRN structure, as discussed above.

In order to minimize the impact of the modification on SFLLRN, I decide to use an altered version of the peptide carrying an extra cysteine residue at the -C terminus. The resulting peptide, SFLLRNC, was then reacted with Maleimide-peg4-N_3. Exploiting the specific reaction between the -SH group of the extra cysteine with the maleimide functional group, the azide motif was incorporated without altering the terminal ends of the peptide.

To firstly ensure that the modified PAR1 agonist SFLLRNC-N_3 retained its functionality after the modification, it was tested in vitro as a ligand for ΔHSPG vectors. In the same experiment I also wanted to see whether the small size of the ligand would also reduce the effects of steric hindrance on vectors functionality independently of the length of the linker used. ΔHSPG vectors have been modified with various NHS-peg-DBCO linkers in which the two functional groups were separated by an increasing number of peg monomers (0/4/8/24). DBCO groups, attached on the viral capsid and spaced by increasing lengths proportional to the number of peg contained in the particular linker used, were reacted with SFLLRNC-N_3. Unmodified ΔHSPG were used as negative control. Vectors were used to infect DRG cultures ($3x10^9$ VG per condition). Red fluorescence was evaluated 5 days post infection (figure 31).

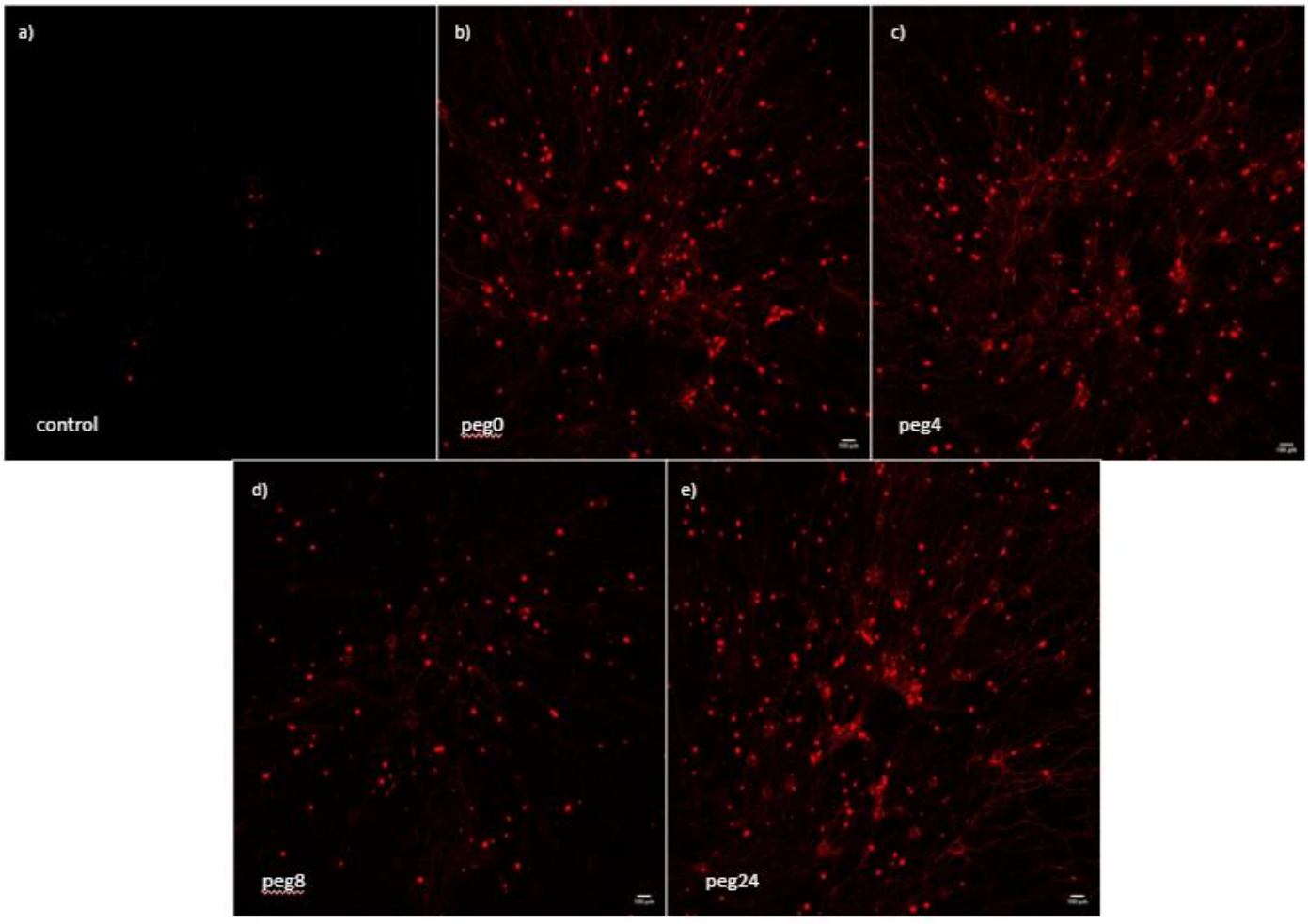

f)

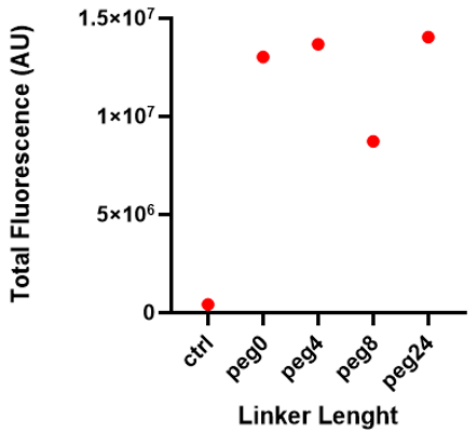

Figure 31. DRG cultures infected with unmodified ΔHSPG (a) and ΔHSPG-SFLLRNC respectively modified with NHS-DBCO (b), NHS-peg4-DBCO (c), NHS-peg8-DBCO (d) and NHS-peg24-DBCO (e). Transduction efficiency was calculated as total fluorescence of positive cells in each condition (f).

Regardless of linker used, all conditions showed strong signal in different DRG neurons (fig 31 b-e), while control experiment only displayed a few bright cells (fig 31a), thus showing that SFLLRNC-N_3 retains its binding ability even after the insertion of the azide motif on the extra cysteine, and is able to restore viral infectivity. Transduction efficiency was calculated as total fluorescence of all positive cells in each condition, as shown in figure 31f.

Next, different doses of ΔHSPG- SFLLRNC were injected intrathecally. Considering the involvement of PAR1 in transcytosis, delivering the modified vector directly into the CSF could demonstrate whether SFLLRNC could facilitate crossing of the pia mater and efficient infection of the parenchyma of the spinal cord.

ΔHSPG vectors were modified with NHS-peg4-DBCO linker and SFLLRNC-N_3 as previously described using the NHS-peg4-DBCO linker and subsequent concentration with a 100kDa MWCO filter to reach a suitable volume for intrathecal injection (10ul). Three different doses ($3x10^9$, $1,5x10^{10}$ and $3x10^{10}$ VG/mouse) of ΔHSPG- SFLLRNC vectors were administrated via lumbar intrathecal injection in wild type C57BL/6J mice. The higher dose ($3x10^{10}$ VG) of unmodified ΔHSPG was used as a negative control. 3 weeks post injection mice were sacrificed and spinal cord and brain collected. Spinal cords and brain were then sections and imaged with confocal microscopy (figure 32).

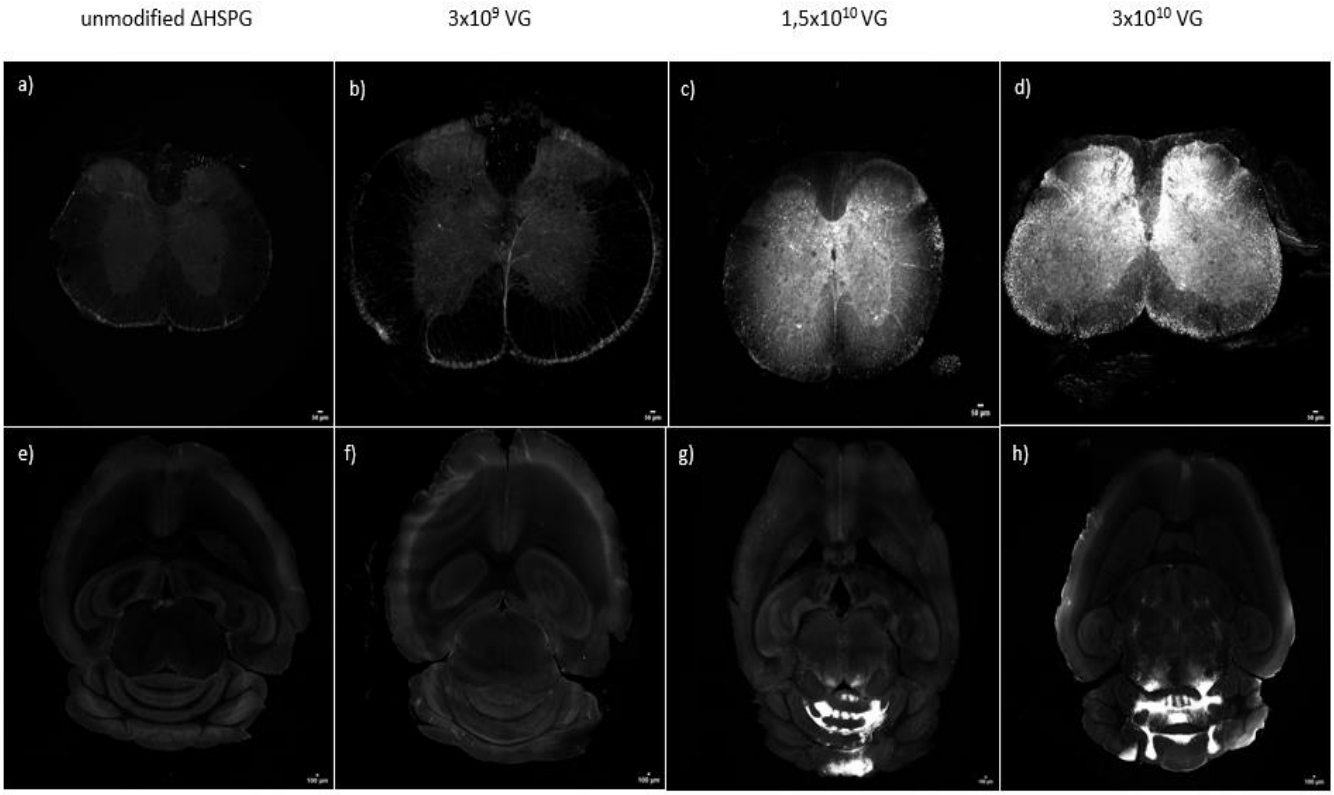

Figure 32. Spinal cord and brain sections from mice injected intrathecally with increasing doses of ΔHSPG- SFLLRNC. While no fluorescence is detected in the negative control and low dose animals (a,b,e,f), strong signal is present in spinal cords (c,d) and brains (g,h) of middle and high dose animals.

No signal was detected in the spinal cord parenchyma of mice injected with lower dose (fig 32 b,f) nor in the negative control (fig 32 a,e), while strong fluorescence is present in the other conditions in both spinal cord and brain sections. In middle and high dose animals, spinal cords showed fluorescence mainly localized in the deeper grey matter (fig 32 c,d). The signal was maintained throughout the whole spinal cord, being at its peak close to the injection site in the lumbar area, and the higher dose of $3x10^{10}$ VG was selected as the most efficient. Sections of spinal cord from high dose animals, collected from the lumbar, thoracic and cervical areas, were stained with an anti-NeuN antibody, a selective nuclear marker of neuronal bodies, to further examine the pattern of viral transduction (figure 33). Ascending toward the brain, fluorescence seems to be mainly localized in the internal part of the spinal cord, following the route of the main ascending tracts, and, eventually, conveying into the brain.

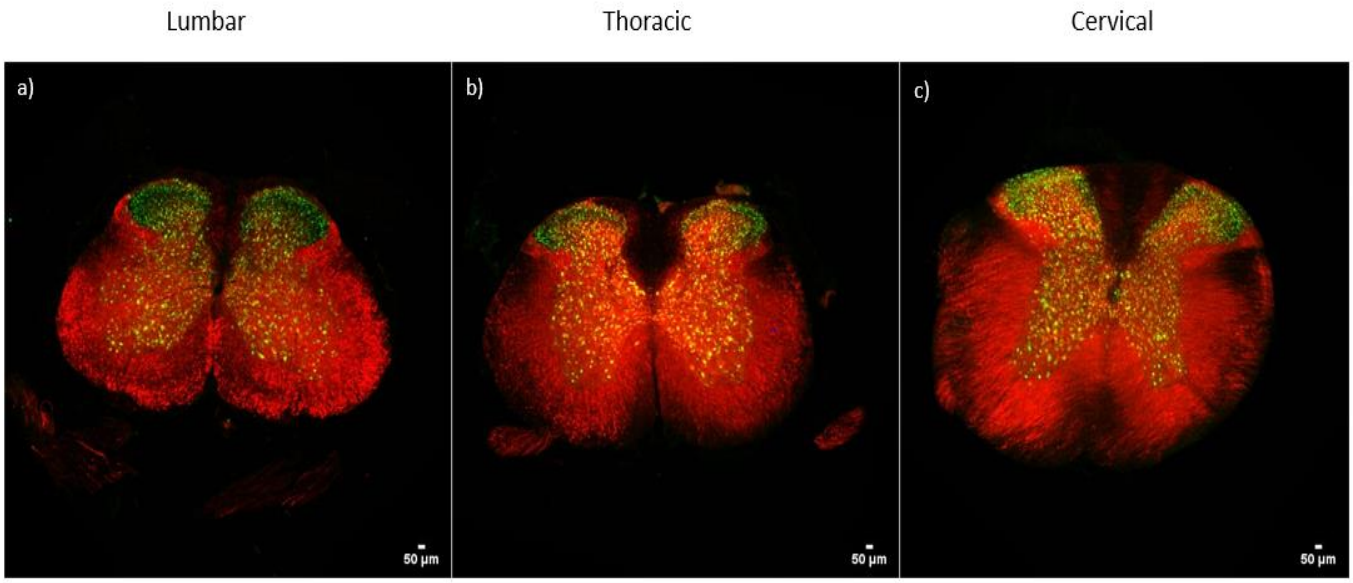

Figure 33. Spinal cord sections from mouse injected intrathecally with $3x10^{10}$ VG of ΔHSPG- SFLLRNC (red) and stained with an anti-NeuN antibody (green). Lumbar section (a), thoracic section (b), cervical section (c).

Spinocerebellar tracts, spinothalamic tracts, spinoolivary tract and spinotectal tracts were successfully targeted by the virus. Fasciculus of Lissauer is also evident. In order to reach their destination, all ascending tracts pass from pons and midbrain, which are the regions of the brain, together with cerebellum, which exhibit the strongest level of fluorescence. Horizontal sections of the brain of animals injected with $3x10^{10}$ VG of ΔHSPG- SFLLRNC were stained with an anti-NeuN antibody, and presence of the signal was evaluated in different areas, as shown in figure 34. A dense network of fibres is evident at the level of the midbrain and the cerebellum (fig. 34a), as well as neuronal bodies in various cortical sites (fig. 34b), cerebellum (fig. 34c) and midbrain structures (fig. 34d).

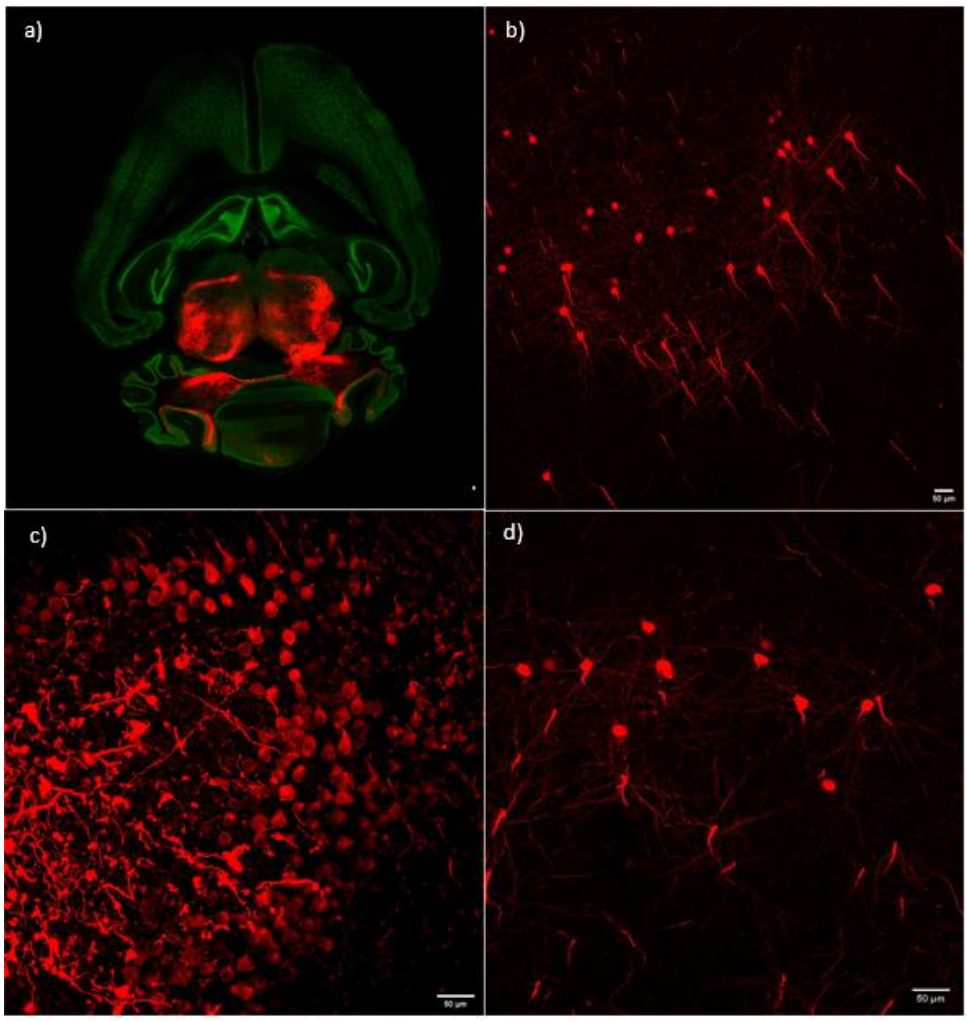

Figure 34. a) Brain horizontal section from mouse injected intrathecally with $3x10^{10}$ VG of ΔHSPG- SFLLRNC (red) and stained with an anti-NeuN antibody (green). The high fluorescence intensity of the fibres masks the signal present in other regions of the brain, which is nevertheless evident when higher magnifications are used. Neurons are visible in the cortex (b), cerebellum (c) and medial colliculus (c).

Next, with the aim to prove the specificity of ΔHSPG- SFLLRNC vectors, both L3 DRG of the high dose animal were sectioned and stained with an anti-Par1 antibody, as shown in figure 35. Unfortunately, despite many attempts have been done in order to optimize the staining protocol, I was not able to effectively mark the Par1-positive population. Indeed, only few cells seemed to be labeled by the anti-Par1 antibody (green) (fig.35a,b), and transduced cells (red) did not colocalize with the stained ones (fig. 35c,d). However, taking into account the dysfunctionality of the anti-Par1 antibody used, this experiment cannot be considered a reliable way to validate the cell-type specificity of ΔHSPG-SFLLRNC vectors.

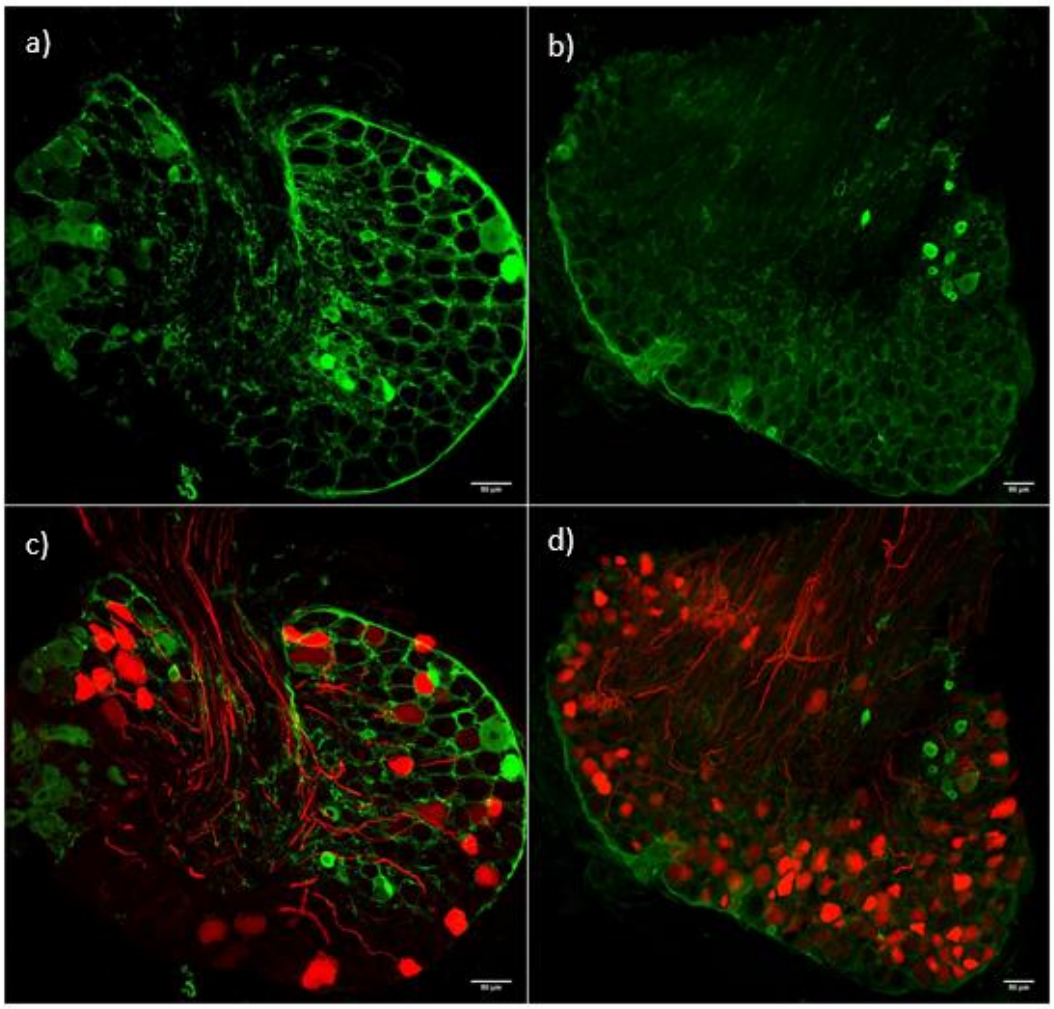

Figure 35. L3 DRG sections from mouse injected intrathecally with $3x10^{10}$ VG of ΔHSPG- SFLLRNC (red) and stained with an anti-Par1 antibody (green). The anti-Par1 antibody only marks few DRG cells (a,b), which do not colocalize with infected cells (c,d).

However, despite the failure of the immunostaining experiments, an effect of SFLLRNC on ΔHSPG infectivity, presumably induced by an increased permeability for the pia mater, was clearly evident. In this context, to further probe the ability of SFLLRNC to promote barriers transmigration, ΔHSPG-SFLLRNC vectors were injected intravenously (IV) at the dose of $9x10^{10}$ VG/animal. With this administration route the virus is directly injected in the bloodstream, thus allowing us to evaluate its ability to permeate the BBB. Animals were sacrificed 3 weeks post injection and presence of signal was evaluated in brain and spinal cord, as shown in figure 36. While no viral transduction is visible in the spinal cords of both the control and the experimental mice, various positive neuronal cells are present in different regions of the brain of the mice injected with ΔHSPG-SFLLRNC, including cerebellum, midbrain structures, basal ganglia and different cortical regions.

With this administration route, the viral pattern of transduction appears to be completely different from the one obtained with IT injections. Indeed, if the virus is delivered through the bloodstream, its distribution will not be localized in a specific region, but will be uniform throughout the nervous system. In this respect, the presence of positive neurons in different regions of the brain of the mice

injected with ΔHSPG-SFLLRNC could indicate the effective ability of the Par1 agonist SFLLRNC to confer enhanced BBB permeability to the ΔHSPG vectors.

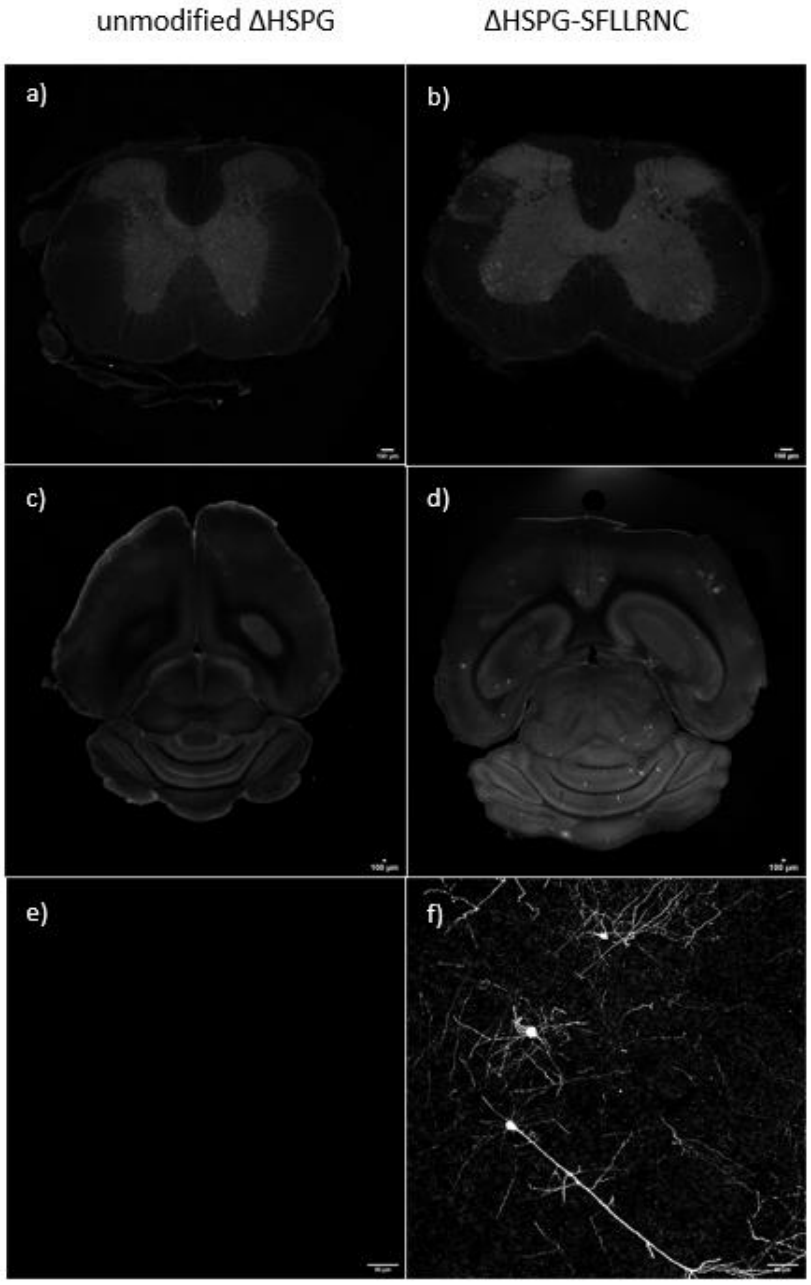

Figure 36. Spinal cord and horizontal brain sections of mice injected IV with $9x10^{10}$ VG/animal of unmodified ΔHSPG and ΔHSPG-SFLLRNC, respectively (a,c) (b,d). 20x magnification on the cortex reveals presence of positive cells in the experimental condition (f) but not in the control (e).

At this point, the question to be investigated was whether SFLLRNC alone was sufficient to confer to the vectors their enhanced permeability. Indeed, if the role of SFLLRNC was to activate the Par1 signaling pathway on barrier cells, thus increasing their permeability, SFLLRNC could have exerted its effects regardless of being linked to the ΔHSPG vectors. In this way, by delivering intrathecally unmodified ΔHSPG vectors together with unbound SFLLRNC agonist, the unmodified virus should

display higher transduction efficiency of the spinal cord due to SFLLRNC-mediated permeabilization of the meningeal barrier when compared to unmodified ΔHSPG injected alone.

To test this theory, wild type mice were injected intrathecally either with $3x10^{10}$ VG/animal of unmodified ΔHSPG, ΔHSPG-SFLLRNC or unmodified ΔHSPG together with 5uM of non-conjugated SFLLRNC. 3 weeks post injection the animals were sacrificed and presence of signal was evaluated in spinal cord and brain sections (figures 36 and 37, respectively). The infection pattern was markedly different among the different conditions. Indeed, in the lumbar area of the spinal cord, close to the injection site, strong fluorescence was noticed in the ΔHSPG-SFLLRNC and not in the control animals, in accordance with previous results (fig. 36a,b). However, in the mice injected with ΔHSPG + unconjugated SFLLRNC, positive fibres were localized only in specific sites of the spinal cord, mainly in the medial lemniscus tract and at different levels of the outermost portion of the white matter (fig. 36c).

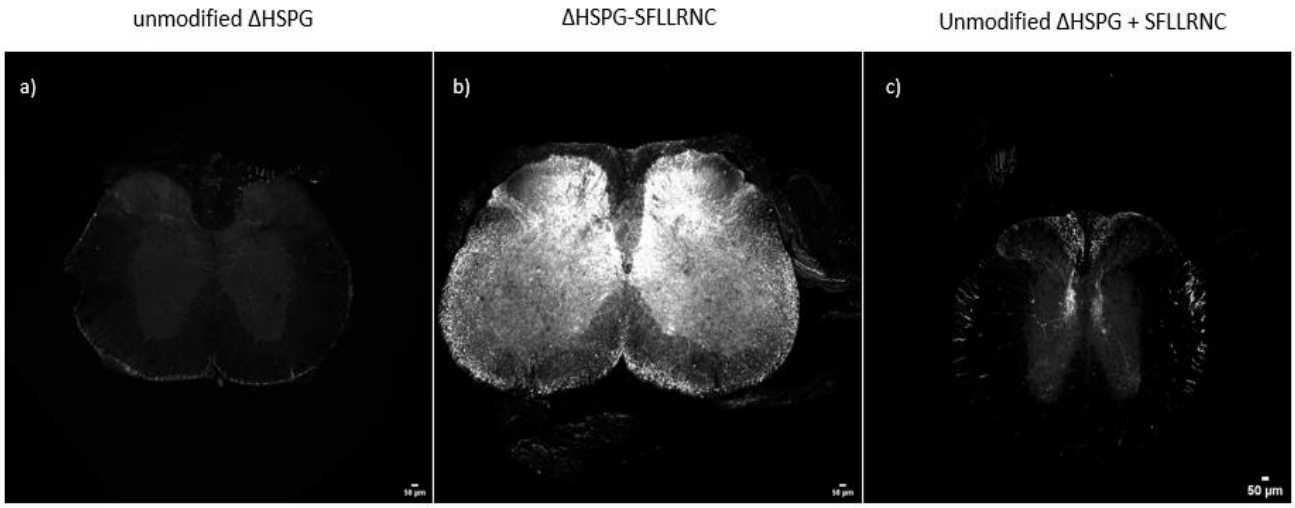

Figure 36. Spinal cord sections from mice injected intrathecally with $3x10^{10}$ VG of unmodified ΔHSPG (a), ΔHSPG-SFLLRNC (b) and unmodified ΔHSPG + 5uM unconjugated SFLLRNC (c).

Proceeding towards the brain and focusing on the pons and midbrain, positive fibres were detected only in the ΔHSPG- SFLLRNC condition (fig 37c). However, the number of positive neurons in different regions of the brain varied among the conditions. Indeed, focusing on the cortex, only a few cells are evident in the unmodified ΔHSPG group while their number increases in both ΔHSPG-SFLLRNC and unmodified ΔHSPG + 5uM unconjugated SFLLRNC conditions. In particular, when unmodified ΔHSPG are delivered together with unconjugated SFLLRNC, the number of positive neurons in the cortex reaches its maximum (fig 37f). Therefore, this experiment suggests that the presence of the Par1 agonist SFLLRNC alone is sufficient to increase the level of viral transduction of CNS, possibly due to the permeabilization of the pia mater which separates the CNS from the CSF. In this respect, the different infection pattern seen with unconjugated and conjugated SFLLRNC could be caused by a different diffusion profile of the vectors, which, when conjugated with SFLLRNC, their distribution would likely be restricted mainly in the injection area.

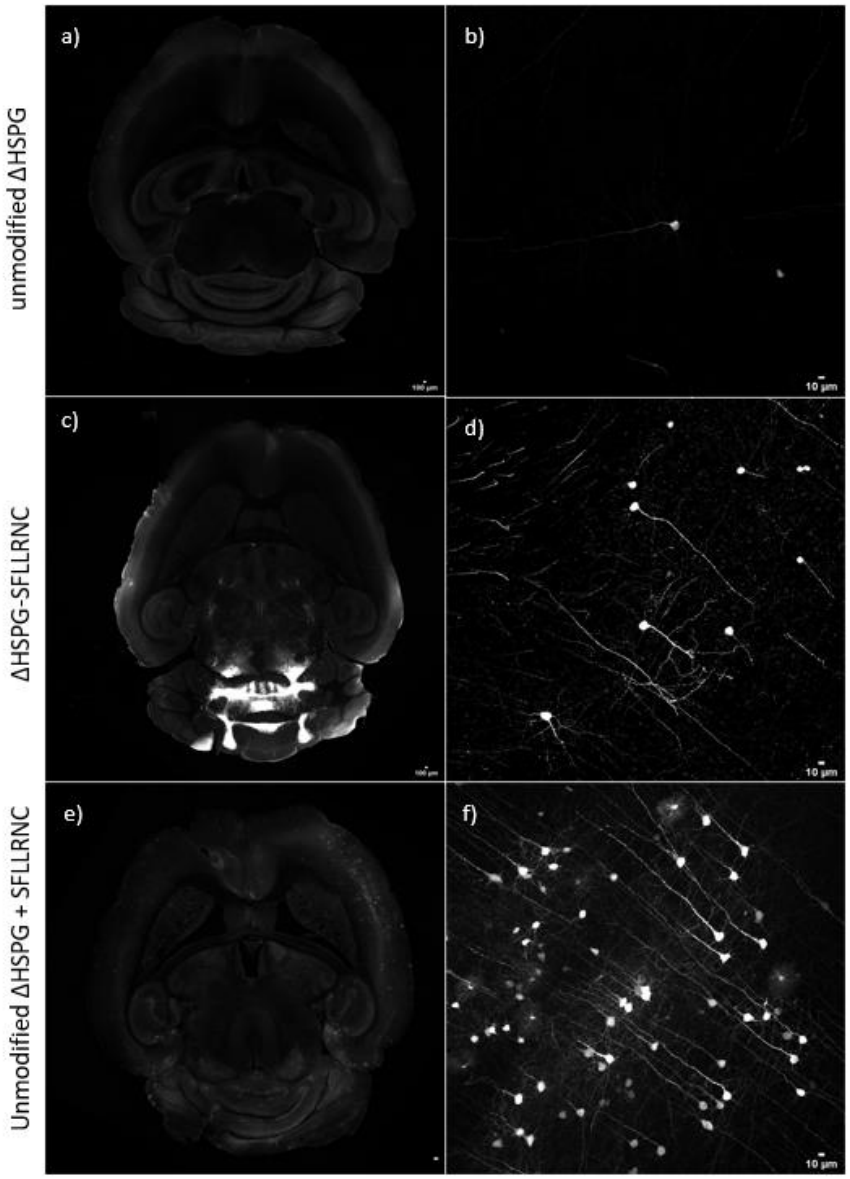

Figure 37. Horizontal brain sections from mice injected intrathecally with $3x10^{10}$ VG of unmodified ΔHSPG (a), ΔHSPG-SFLLRNC (c) and unmodified ΔHSPG + 5uM unconjugated SFLLRNC (e). 20x magnification on the cortex reveals presence of positive cells in all conditions (b,d,f), with the maximum level in the unmodified ΔHSPG + 5uM unconjugated SFLLRNC group (f).

3 DISCUSSION

In the last years the use of AAV vectors as carriers for gene delivery has became increasingly popular for both research and clinical applications. AAVs are considered the vector of choice because of their non-pathogenic nature and their low integration rate, which reduces the chance of DNA damage and unpredictable consequences. Moreover, the presence of at least 12 natural occurring serotypes and many more variants give a lot of flexibility in terms of applications due to the particular proprieties of each different vector. Indeed, serotypes exhibit specific tropism for various tissues, are recognized and neutralized by different antibodies and possess multiple particular features, such as the enhanced permeability for BBB of AAV9 (Hordeaux et al., 2018). However, despite their versatility, several challenges remain that still impede their mainstream use in the clinic. In general, two main aspects of AAV based therapy are currently being improved, which are the safety and the efficiency of the system. Concerning the efficiency, it can be seen as both boosting delivery and expression of the transgene or conferring selective targeting of specific tissues or cells. In both cases, the final goal would be to decrease as much as possible the dose of virus used to obtain the desired therapeutic effect. As a result, administration of a limited amount of virus would improve the safety profile by reducing off target effects, immune response, integration frequency and cytotoxicity.

At the moment, many different strategies are employed to improve both viral specificity and transduction efficiency. In general, optimization can be achieved by modifying either the transgene or the capsid. For example, it is possible to enhance transgene expression by using modified ITRs (scAAV), engineering the promoter to increase transcription, optimizing the codons in the transgene to augment mRNA production and translation and improving the delivery of large transgenes (Li & Samulski, 2020). Expansion or re-direction of AAV tropism can be achieved by modifying AAV genome using cell type-specific gene regulatory elements such as enhancers/promoters for transcriptional targeting and cell/tissue-specific miRNAs for post-transcriptional targeting (B. Dhungel et al., 2018).

Moreover, enhanced tropism and efficiency can be obtained by modifying the capsid through different methods, including rational engineering, direct evolution or computationally designed capsid (Li & Samulski, 2020).

With the aim to develop a tool to achieve selective targeting of specific cellular population using AAV vectors, we designed a system to chemically modify AAV capsid in order to re-direct viral tropism.

The effectiveness of AAV is in large part determined by the molecular interactions between the capsid and target cell surface receptors and subsequent downstream events following particle internalization. Given the importance of initial cellular binding, we acted on the capsid structure to alter the original viral binding ability by replacing the main viral receptor with a custom designed ligand. Modified AAVs, displaying a targeting ligand on their capsids, would then acquire specificity for the cellular population expressing the surface receptor of the particular ligand used. In this way we expect modified vectors to selectively transduce only cells/tissues of interest, thus limiting background activity and off-target effects when delivered in vivo.

Different studies based on the use of ligands to modify viral tropism have already been published, but the greatest majority of them rely on genetic modifications of the capsid (C. Zhang et al., 2016). In these cases, the ligand is expressed as a fusion protein inserted in specific sites of AAV's cap ORF. While conferring improved expression and spatial control of the insertion, genetic modifications are often poorly tolerated by the vectors, thus careful design, characterization and validation steps are required. Moreover, insertion of large ligands is usually difficult (Girod et al., 1999). In general, although their efficiency and versatility, insertion of ligands through genetic modifications require time, highly specialized skills, specific equipment and obviously the production of new vectors each time a new modification is implemented.

On the other hand, insertion of ligands through chemical modifications are based on the covalent linkage of a particular ligand with specific viral capsid residues by exploiting natural or artificial functional groups present on both parts (Mével et al., 2020). Even if they only represent a small part of all ligand insertion technologies developed so far, chemical coupling strategies offer unique advantages. Firstly, chemical reactions are performed directly on the assembled viral capsid, thus there is no risk to affect the correct assembly and packaging of neo-formed vectors, since all the modifications are performed post production. This is particularly relevant when larger ligands are inserted. Indeed, genetic insertions of large proteins are much less tolerated than small insertion, thus chemical coupling could allow conjugation of molecules that could not be genetically inserted. Second, after establishing a conjugation protocol, chemical modifications can often be performed without any particular equipment or advanced skills requirement, thus reducing timings and costs. Finally, they offer high versatility due to the ease of the conduction, thereby allowing direct optimization of each step in a limited timeframe. On the other side, chemical modifications are often less efficient compared to genetic modifications, and the resulting engineered vectors not always exhibit expected infectivity, mainly due the loss of functionality of the ligand after chemical conjugation or an excessive overcoating of the vector (Wei et al., 2012).

Our approach relies on the selective modification of exposed lysine residues that constitute the viral capsid. Amino groups ($-NH_2$), which are present on the side chain of lysines, are reacted with an N-hydroxysuccinimide-ester (NHS-ester) functional group placed on one end of a heterobifunctional crosslinker molecule. The other end of the linker consists in another chemically active group that can be reacted with a functional group inserted directly into target ligand. Ligands used have been functionalized with either a SNAP-TAG or an azide motif. In the case where azide-tagged ligands are chemically conjugated with AAV vectors, the second functional group of the linker was a dibenzocyclooctyne (DBCO) molecule. Instead, linkers carrying a O^6-benzylguanine derivate were used for the reaction with SNAP-tagged ligands.

Most of the experiments have been conducted with AAV2 vectors. This serotype has been chosen mainly because it is one of the most studied and characterized serotypes, whose safety and efficiency is supported by several approved clinical trials. Moreover, a wide set of capsid mutations have been discovered in the years, enabling implementation of particular features, such as enhanced transduction efficiency, conferred ability to evade immune system or ameliorating endosomal escape (Aslanidi et al., 2013; P. Wu et al., 2000).

In this respect, I have inserted into AAV2 VP3 coding region the Y444+500+730F+T491V substitutions. Indeed, threonine and tyrosine residues are common targets for phosphorylation and subsequent ubiquitination, which leads to proteasome-mediated degradation of internalized

vectors, thus reducing overall transduction rate. Replacing of these key residues has been correlated with enhanced transduction of mouse tissues (Büning & Srivastava, 2019), and since the mutations would not affect our chemical modification strategy, I have decided to include them.

Moreover, in order to achieve accurate re-targeting of AAV2 with reduced background activity, the first step is to prevent the unmodified vectors to infecting cells, thus setting a starting point from which viral tropism can be restored in a customized way. AAV2 enters target cells following initial attaching on cell surface exposed HSPG residues through the interaction with a specific region of the capsid situated close to the three-fold protrusions. The HSPG binding region is composed by several residues, including arginine 585/588 on viral VP3s. These residues play a crucial role in early interactions with target cells, thus is possible to drastically reduce viral binding ability, and infectivity as a consequence, by replacing R585/588 with more acid residues, typically alanine (Opie et al., 2003). This well characterized mutation creates vectors, called ΔHSPG, which are virtually functional but due to their inability to bind on target cells they lose most of their infectivity. Despite AAV2 also relying on various co receptors for stabilizing the initial binding, mutations on the main receptor are sufficient to greatly impair infectivity. Nevertheless, note that infectivity is not totally eliminated, thus, when high doses of ΔHSPG are used a certain level of background activity is expected (Opie et al., 2003). However, it is possible to get rid of this inconvenience by tuning the amount of virus used for each experiment.

R585/588A substitutions along with Y444+500+730F+T491V mutations have been inserted into AAV2's VP3 coding regions, and the resulting capsids have been packaged with a single-strand transgene coding for the fluorescent protein tdTomato under the control of the strong CAG promoter. Wild-type AAV2 ITRs have been used, and transgene expression was regulated by a WPRE and SV40-polyA sequences. The resulting vectors, with enhanced transduction efficiency but lacking their natural tropism for HSPG residues were used as a model to evaluate whether our chemical modification technology was actually able to restore viral tropism in a selective way.

Each AAV2 particle contains 34 lysine residues in each VP3, of which 10 are surface-exposed (Xie et al., 2002). This means around 550 exposed lysines and as many amino groups on each of their side chains, which can serve as potential modification sites for our chemical modification strategy. The first variable that we decide to optimize was the quantity of lysines that we can actually modify with NHS-peg-linkers without overriding viral infectivity. Indeed, it has been shown that PEGylation operated on lysine residues of AAV2 capsids affects viral infectivity proportionally to PEG chain length and the molar ratio of lysine residues to linker molecules used for the conjugation reaction (Lee et al., 2005). It is believed that viral infectivity is increasingly compromised due to inhibition of vectors binding to cell surface receptors or subsequent steps in cell entry by masking viral receptors and co-receptors. For this reason, the first validation experiment consisted in the evaluation of viral infectivity following chemical modification with increasing virus::linker molar ratios.

Since the quantity of available -NH_2 groups is proportional to viral concentration in the same volume condition, we directly correlated the amount of virus used with different molar concentrations of linker. For these preliminary experiments we have employed our prototypical ligand, WGA. Due to the high stability of the lectin and the presence of multiple and independent binding sites in its structure, we believed that this ligand could easily tolerate various modifications without losing its functionality. WGA has been functionalized with an azide group, and reacted with vectors previously modified with different virus::linker ratios of NHS-peg4-DBCO. We found that the virus::linker ratio

is actually crucial for our technology, since there is an intermediate range in which viral infectivity reaches its maximum peak. This can be explained by the fact that when no linker is used, the vectors cannot bind to WGA, thus remaining non infective due to their HSPG binding region mutation. When some linker is added, lysine residues begin to be modified and to bind to WGA, which partially restore viral infectivity by conferring the vectors the ability to bind to N-acetylglucosamine. The more lysines are modified the more WGA can be recruited, up to a certain threshold in which the excessive presence of linker or WGA is more detrimental then beneficial. Too much linker attached to the viral capsid could itself impair the correct binding of WGA, or steric hindrance issues caused by the excessive presence of WGA could arise. Moreover, if the virus gets completely coated, other crucial sites of the capsid would then be masked, thus impairing downstream events following internalization, first and foremost the correct binding to AAVR on target cells. For all these reasons is important to obtain the best virus::linker ratio before doing other experiments. Since the ratio of a specific linker is dependent on the concentration of both the vectors and the linker, one could theoretically calculate it as a function of these two variables, but we found that the best way to go is just to empirically obtain the optimal modification ratio of the specific linker for each new batch of virus produced, thereby taking into account the variability of the production process (purity, presence of empty capsids,..).

The second parameter that must be considered for our chemical modification strategy is the concentration of the ligand used to saturate functional groups present on the end of the linker not involved in the reaction with lysine residues. To see whether the concentration of the ligand used was affecting the functionality of the vectors, I firstly tested increasing concentrations of WGA-N3 and IB4-N3 on ΔHSPG vectors previously modified with NHS-peg4-DBCO. Similarly to what was found when calculating the best virus::linker ratio, it was evident that after a certain threshold of ligand used viral infectivity was reduced. On the other hand, if not enough ligand was added then the modified vectors were still able to infect cells but not up to their maximum potential. The main thing that should be noticed is that is important to use a ligand concentration high enough to completely saturate all free DBCO functional groups present on the capsids. However, an excess of unbound ligand would compete with modified vectors for the binding on its specific receptors when delivered to target cells, thus impairing overall transduction level. This is particularly important if no washes are performed after the chemical modification procedure. Indeed, the original modification process included several clean up steps to firstly remove the excess of unbound linker and later the excess of ligands not attached to the virus by using filtering columns featuring appropriate molecular weight cut off membranes. This step was also used to concentrate the virus to the small volume required for some particular injections (intrathecal, intra sciatic nerve, retro-orbital,…). However, we have noticed that multiple filtration and passage through plastic instruments, including columns, resulted in a loss of viral vectors, which is in line with what already found by other groups (Fischer et al., 2016). Despite pre-treatment of plastic equipment with the surfactant Pluronic-F68, a solution of polyoxyethylene-polyoxypropylene block copolymer that serves to prevent AAV attachment to plastic, a certain level of vectors loss during the process is expected (Sanmiguel et al., 2019). In this situation, is important to evaluate if the loss of virus during the clean-up is more beneficial than the presence of an excess of ligand that would compete with receptor binding on target cells. Again, this largely depends on the nature of the particular ligand and its receptor.

For example, in DRG cultures, the saturating concentration of NGF for TrkA/p75 receptors is in the order of few nanomolar (Hory-Lee et al., 1993). If 5uM NGF is used in the reaction and no clean-up

of the excess is performed when ΔHSPG-NGF is applied on DRG cultures, it is expected that most cellular receptors would be saturated by free NGF, thus impairing viral binding and infection. Moreover, if excess of linker is not eliminated prior to NGF addition, some NGF will be captured by unreacted linker, thereby chelating it away from the virus. For these reasons when working with NGF the filtering steps are required and are more beneficial in terms of infectivity of the resulting modified vectors than the loss of virus due to the contact with plastic during the clean ups. On the other side, when vectors are modified with lectins they can tolerate much more the excess of unbound linker or ligand. The first reason is the presence of multiple binding sites on the lectins, which means that even if some linker molecules react with free lectins, they will not lose their functionality as easy as a molecule with only one binding site. The second reason is because lectins saturate surface glycoproteins at concentrations in the order of micromoles, thus the possible presence of an excess of unbound lectins together with modified vectors will not saturate completely all the glycoproteins present on target cells, despite it will still compete with the reaction (Shinohara et al., 1997). This means that when ΔHSPG vectors are modified with lectins it is possible to avoid cleaning the excess of linker and ligand, unless vectors need to be injected in small volumes, circumstance in which the filtration through 100kDA MWCO columns is required mainly to concentrate the virus.

With the aim to further improve our technology, I have decided to directly compared the two coupling mechanisms used in this project to assess which was the most functional, the SNAP-TAG or the azide-based click chemistry. Indeed, these systems both have pros and cons. The SNAP-TAG is a protein, a self-labeling enzyme of 19.4kDA. Being an enzyme, it has an intrinsic catalytic ability and a certain level of activity, which is dependent, among other factors, by interaction with other co-factors, pH, temperature and buffering conditions. Moreover, it could be subject to inactivation following interaction with different effectors. Considering its size, is also more likely that the insertion of a SNAP-TAG could negatively affect the functionality of a ligand. Finally, to insert the SNAP-TAG is necessary to carefully choose a specific site in the coding gene of target ligand, clone the insert and finally produce the recombinant protein. Despite this process not being particularly complicated, it still requires time and some level of skill, followed by the functional validation of the recombinant ligand. However, being able to directly select the insertion site, it is possible to have a complete spatial control of the modifications on the ligand, deciding where the SNAP-TAG is placed, considering multiple insertions and carefully tuning the ligand according to specific needs. This is particularly relevant in terms of clinical application, where an absolute control of each variable is required.

On the other hand, an azide motif is just a small chemical group composed by three atoms of nitrogen, thus it does not possess any intrinsic proprieties or activity, and unless it reacts with other chemical species it remains functional and stable in biological systems. Obviously, the reaction can be optimized using different buffering conditions, tuning reagent concentrations and reaction timings/pH, but not having an intrinsic activity offers a great advantage as compared with enzymes. It is possible to insert an azide functional group in different ways, that could be both genetic or chemical. One example of genetic insertion of an azide motif into a protein is the use of unnatural amino acids (Huber et al., 2013). With this system is possible to insert a modified amino acid carrying the azide group directly into the coding region of target ligand, thereby obtaining a modified ligand

with the functional group exactly in the chosen site, as for the SNAP-TAG insertion. Again, this is not a straight-forward process, but it offers the greatest level of precision. Another way to insert azide motifs relies on chemical reactions exploiting specific functional groups naturally present on target ligands. In the same way we use to conjugate a DBCO or BG group on viral capsids with heterobifunctional crosslinkers, it is possible to employ other types of linkers carrying an azide group on one end. This is the system we have used to functionalize ligands used in this project with an azide motif. By using an NHS-peg4-N_3 linker is possible to modify lysine residues normally present on target ligand in a fast and convenient way. However, with this system it is impossible to control the exact number of modified lysine residues and/or azide motifs inserted into the ligand, which can in turn lose functionality. By tuning the molar ratio of ligand to linker it is possible to roughly steer the number of lysines modified, but in general the product would be a heterogenous population of ligand molecules each carrying presumably a different number of azide groups at different positions, some of which would be non-functional. However, this does not represent such a big issue for our technology, since we only need to saturate the linker molecules attached to the virus by adding the functionalized ligand. In this way, non-functional and unbound ligand would just be washed away.

To directly compare the two chemistries, ΔHSPG vectors have been modified with either WGA-SNAP or WGA-N_3. Despite both systems being functional in vitro, WGA coupled thought click chemistry exhibited enhanced efficiency compared to WGA-SNAP. Presumably this is due, as discussed early, by the fact that the SNAP is effectively an enzyme, whose reaction rate could not reach the level of efficiency of a chemical reaction between two organic groups. Moreover, it is also possible that the insertion of the larger SNAP-TAG into WGA is less tolerated than the presence of the smaller -N_3 group. In general, considering the overall greater efficiency of click chemistry and the ease of the modification protocol, we have decided to mainly rely on the azide specific reaction for subsequent experiments. The only exception being NGF. Indeed, in our laboratory we already had experience with a functional mutated form of recombinant NGF fused to a SNAP-TAG, and considering the possible clinical application of this ligand we decided to maintain the more controlled and validated SNAP-tagged version of NGF.

After the evaluation of the main variabilities of our technology, I next focused on the mechanism underlying internalization of resulting modified vectors. In particular, the question was whether the presence of a particular ligand on the viral capsid would affect the internalization mechanism. Indeed, it is well established that cellular infection begins with the capsid binding to glycans or glycoconjugates at the cell surface. This first interaction relies on specific binding regions on viral capsids that are variable among all serotypes and confer the typical broad tropism of AAV vectors. In particular, the capsid of AAV2 binds to heparan sulfate proteoglycan (HSPG) as a primary receptor and uses integrins and growth factor receptors as co-receptors for entry into the cell (B. P. Dhungel et al., 2021). What we do when we mutate AAV2 capsid to obtain ΔHSPG vectors is to create viruses that are not able to bind to cells and thus they will not be internalized. The addition of a ligand on the capsid restores binding ability and confers altered tropism for different cell populations. However, mechanisms involved in the succeeding internalization should not be affected by our modification system, which means that engineered ΔHSPG should theoretically be internalized in the same way as wt AAV2. Indeed, it is now known that most serotypes, including AAV2, rely on the AAVR receptor for efficient translocation into target cells (Pillay et al., 2016). In an attempt to see

whether vector internalization was still dependent on the interaction between the modified capsid and the AAVR on target cells, I have generated a transgenic cell line featuring the knock-out of the AAVR gene by using CRISPR-CAS9 technology. The resulting stable HEK 293-T AAVRKO cell line has been firstly tested to see whether wild type AAV2 infection was impaired, and subsequently ΔHSPG-WGA have been applied on either unmodified HEK 293-T or mutated HEK 293-T AAVRKO cells. A reduction of infectivity was evident when wt AAV2 or ΔHSPG-WGA were used on the AAVRKO line compared to wt HEK cells. This means that AAVR is still needed for efficient infection for both unmodified and modified vectors, thus confirming that the modification process does not disturb downstream processes following cellular internalization. However, comparing data from AAVRKO HEK infected with unmodified ΔHSPG and ΔHSPG-WGA there was a difference in the level of transduction. Indeed, while ΔHSPG was completely silent in the AAVRKO model, ΔHSPG-WGA exhibited some level of signal. WGA is a widely used neuronal tracer that can be transported both anterogradely and retrogradely and can jump transsynaptically from neurons, as well as being implicated in the activation of transmigration and active transport mechanisms of particles across cellular barriers (Makhlof et al., 2011; Yoshihara, 2010). In this respect, we believe that WGA firstly mediates initial attachment of the virus on target cells surface, and subsequently promotes active transport mechanisms that results in the internalization of the vectors. Therefore, WGA not only restores viral infectivity by replacing canonical binding of the vectors, but also implements a new alternative mechanism that does not rely on AAVR for internalization. However, this cannot be generalized as an intrinsic characteristic of our modification process, but depends on the particular ligand used. Theoretically, if ligands able to trigger translocation mechanisms across membranes are conjugated to ΔHSPG vectors, the resulting virus would gain enhanced permeability for specific cellular types as an additional feature beside targeted tropism. This could be exploited, for example, to obtain vectors with enhanced permeability to physiological barriers such as BBB or meninges, thus improving delivery of AAV vectors in the nervous system.

During the validation and the optimization of the chemical modification protocol developed in our group, it was increasingly clear how lectin modified vectors in particular exhibited high efficiency. For this reason, beside the main aim of this project, we explored another possible application of lectin modified vectors. In particular, the rational was that by attaching a high number of lectins on a single capsid, each having strong avidity for glycoproteins, it would be possible to boost the normal binding rate of the vectors. In other words, having multiple possible receptors on the capsid, the possibility to obtain successful attachment of the virus on target cell would increase. Indeed, considering that in the wild type AAV2 capsid there is only one HSPG binding site for each VP3 but as many as 10 exposed lysin residues, the total potential number of functional receptors that could be implemented would dramatically increase, taking also into account the particularly high avidity of lectins for their receptors. Moreover, since downstream processes following internalization are not altered, the presence of the ligand would not affect normal viral processing and transgene expression when in the cytosol.

Taking IB4 as an example, the presence of multiple lectins on AAV2 capsid, each having strong affinity for galactosyl residues, would cooperate with HSPG binding region for cellular binding. To show this application of the system, I have directly compared the efficiency of different doses of unmodified wild type AAV2 and wt AAV2-IB4 in vitro. The results showed that the presence of IB4

was effectively able to drastically boost efficiency, even at concentrations in which the unmodified wt AAV2 was totally silent.

Nevertheless, is important to note that in this case the natural tropism of the virus would be altered, thus conferring the vectors an infection pattern that does not resemble the natural one. Translated into a more complex system, such as any animal model, it is expectable that different tissues would be targeted, thus requiring a careful assessment of the viral distribution following the administration. This could mainly be a problem if a specific serotype is chosen for its particular tissue preference because of modified virus expanded tropism.

However, is also possible to boost efficiency without altering natural viral tropism. This is for example the case on serotype AAV9. Indeed, both IB4 and wt AAV9 recognize galactosyl residues on target cells, thus is possible to modify wt AAV9 with IB4 to basically increase the number of potential receptors that recognize the same target. Again, unmodified wt AAV9 and wt AAV9-IB4 were compared in vitro, and similarly to what was found for wt AAV2, lectin-modified AAV9 showed drastic enhanced efficiency.

This other feature of our technology could have useful applications in many fields. For example, having a batch of virus which is not particularly infective could be overcame by increasing vectors binding rate and thereby boosting overall transduction level. Moreover, using a particularly efficient modified virus would reduce the dose of vectors required to obtain an expected therapeutic effect, thus reducing the costs, side and off-target effects, integration rate and immune system activation.

After a careful in vitro validation of the chemical conjugation strategy, I next investigated the efficiency of modified vectors in vivo, using the mouse as an animal model. Having a virus that works in vitro does not necessarily mean that the same functionality is expected in vivo, particularly when seeking for accurate tissue specificity. Indeed, two main concerns arise when the virus is delivered into an animal, which are the presence of a spectrum of potential receptors in different cell population and the activation of the immune system. The host immune response to vector-mediated gene transfer could be elicited by both capsid proteins or transgene, and leads to the neutralization of AAV and subsequent loss of transgene expression. The first thing that should be noticed is that since capsids of recombinant AAV are usually very similar to the capsids of wild type virus, which are naturally present in the environment, it is expected that the host immune responses triggered by vector administration will be similar to those associated with a natural infection with AAV. This means that pre-existing neutralizing antibodies against capsid protein could negatively affect AAV based gene transfer, as it has previously been observed (Manno et al., 2006). Another aspect that should be considered is the $CD8^+$ T cell-mediated cytotoxic immune response toward viral particles and transduced cells presenting AAV capsid antigens. Moreover, AAV DNA genome and capsid structure can be sensed by Toll-like receptor (TLR) 9 and TLR2, respectively, therefore working as adjuvants for the elicitation of immune responses. This effect arises in a dose-dependent fashion, and further contributes to the loss of vectors availability (Colella et al., 2018). Finally, neutralizing antibodies towards the transgene product can be generated, even if this is a problem that mainly happens when repeated administration of the same transgene are performed. However, T-cell immune response can be elicited also toward infected cells that express the transgene of interest. In general, immune system activation is probably the main issue of AAV-mediated in vivo

gene transfer technologies, and a careful evaluation of the balance between viral dose and effective transgene expression, taking into account the dose-dependent activation of the immune system that impairs overall gene expression, must be considered.

Furthermore, in any animal model, the variety of potential targets of the administrated virus drastically increases if compared to an in vitro experiment. Concerning wild type AAV2, HSPG residues are ubiquitously expressed on cell surfaces and in the extracellular matrix of most animal tissues, thus most of the cells represent possible target for AAV2 (Kreuger & Kjellén, 2012). The preferential tropism of AAV2 for liver, kidney, and retina depends on the higher expression of HSPG residues in these tissues, but it is not exclusive. When we use ΔHSPG vectors, we drastically reduce overall infectivity. However, when a ligand is conjugated on the capsid, new specificity for a different receptor is obtained. Again, if the selected receptor is expressed in different cell types, it is expected to obtain a certain level of variability in terms of transgene expression. This depends on many factors, including the level of expression of the receptor in different cell types, the route of administration, the affinity of the ligand toward its receptor and the dose of virus used. It is expected that cells having the highest expression of target receptor would be mainly infected, unless particular injection routes are selected. For example, if ΔHSPG-IB4, which exhibits high affinity for both vascular cells and non-peptidergic nociceptors, is administrated directly into the CNS, transgene expression will be mainly limited to neurons. However, if the same vector is injected systemically intravenously, probably most of it would be captured by vascular cells and no infection of CNS would be observed. Another aspect to be considered is the viral dose administrated. Indeed, if too much virus is present and total saturation of receptors is reached, it is predictable that the excess of unbound virus would bind to other possible receptors which still have some level of affinity for the ligand used for the modification. This is particularly relevant in the case of local injections in which the vectors are administrated into a small area, as it happens with intrathecal or intra sciatic nerve injections. In this case it is important to work with a viral dose that will not completely saturate all main receptors on target cells, because otherwise the risk to get unspecific transduction will increase.

The first modified virus that I have injected in vivo was ΔHSPG-IB4. As previously discussed, IB4 binds to α-D-galactosyl residues, and it is a commonly used marker for endothelial and vascular cells (Benton et al., 2008), microglia and different types of neurons (Zylka, 2005). Considering that injection route can affect the distribution and subsequent infection of different tissues, I firstly evaluated if it was possible to exploit ΔHSPG-IB4 to achieve selective transduction of non-peptidergic nociceptors. ΔHSPG-IB4 was injected intra sciatic nerve, thereby bypassing the blood system and concentrating the virus directly into the peripheral nervous system. The sciatic nerve innervates upper lumbar DRG and peripheral terminal endings effecting the paw of the animal. In turn, non-peptidergic nociceptors project to the second lamina of the dorsal horns of the spinal cord. All these tissues were successfully transduced by ΔHSPG-IB4, and subsequent staining experiments validated the specificity of the infection. Signal in the spinal cord matched with the staining, and it was located in the second lamina of the spinal cord, with no background. Lumbar DRG and various nerves in the paw were infected at a ratio higher than control mice, which exhibited just some fluorescence in DRG. To assess whether ΔHSPG-IB4 could also be used to efficiently mark vasculature, modified vectors were injected subcutaneously. As discussed, IB4 has been widely used to study new blood vessel formation, vascular sprout migration and plasticity in different pathological and traumatic conditions (Wälchli et al., 2015). In this way I wanted to ensure that

changing the administration route would actually allow for preferential targeting of different cellular populations. Following subcutaneous administration of ΔHSPG-IB4, the blood vessel network under the injection site was clearly visible, with perivascular and endothelial cells exhibiting strong fluorescence. This further proves the efficiency of modified vectors and shows how the administration route can actually influence viral targeting. To date, this is the first time that an AAV is conjugated with a lectin to obtain a highly specific carrier for targeted gene delivery. Considering the incredibly broad tropism of lectins, this could unlock a wide range of applications to target different tissues.

As second ligand to be tested in vivo we selected NGF. The main reason behind this decision was the therapeutic potential that this technology could have. Indeed, after the validation of the chemically modified vectors with IB4 in vivo, we investigated the functionality of a more complex ligand. Beside its neurotrophic proprieties during development, NGF plays a key role in pain signaling in the adult by binding to TrkA and p75 receptors, which are expressed on the peripheral terminals of A-delta and unmyelinated C fibres. TrkA/NGF complex is then internalized and transported to cell bodies in DRG where it modulates the expression of different effectors involved in pain signaling (Denk et al., 2017). NGF levels are upregulated during pain states, which leads to peripheral and central sensitization of nociceptors, and local administration of NGF causes long-lasting pain sensitivity and hyperalgesia (Woolf et al., 1994).

We employed a modified version of NGF, carrying a point mutation that results in the loss of NGF ability to trigger pain associated pathways following TrkA/p75 binding, together with a SNAP-TAG protein inserted in its -C terminus. To firstly assess whether the length of the linker used could affect functionality due to steric hindrance between NGF molecules attached to the capsid, two different linkers, here referred as short and long linker, have been used. Firstly, ΔHSPG vectors modified with NGF^{R121W}-SNAP together with either short or long linker were injected retro-orbitally, to assess which version worked the best. Surprisingly, fluorescence was registered in trigeminal ganglions and DRG for both conditions, with the long linker group showing higher numbers of positive neurons compared to the short linker. Considering the greater efficiency of vectors modified with the longer linker, I further analyzed samples to confirm cellular specificity. Indeed, using an anti TrkA antibody it was possible to ensure that ΔHSPG-NGF specifically targeted $TrkA^+$ peptidergic nociceptors. Moreover, the high efficiency of the system was striking: more than 80% of $TrkA^+$ neurons were efficiently infected by our modified vectors, with almost no background activity. The fact that some fluorescence has been detected also in lower lumbar DRG further confirms the great efficacy of the vectors, along with their selective tropism.

Other administration routes have been explored, again to ensure the validity and reliability of the system. With an intraperitoneal injection it is possible to obtain systemic administration of vectors in a simple and easily reproducible way. However, the poor spatial control which derives from this administration route does not guarantee the same level of transduction in a particular organ as the one elicited by a local injection. Considering that the vectors are taken up by the bloodstream, the possibility of viral loss before reaching neuronal population increases. However, signal has been registered in trigeminal ganglia, DRG and spinal cord. Mice injected with unmodified vectors did not show any fluorescence in examined tissues. Exploiting an alternative to TrkA antibodies to investigate specificity, sections of spinal cord were stained with Alexa Fluor® 647 isolectin GS-IB_4 to

mark the second lamina of the dorsal horn of spinal cord, which liesbeneath the first lamina, in which $TrkA^+$ peptidergic nociceptors are located. tdTomato-derived fluorescence was found to be mark the region of spinal cord above the $IB4^+$ layer, thus indirectly confirming the specificity of ΔHSPG-NGF.

Finally, previously obtained data were further validated by analyzing tissues from mice injected intra sciatic nerve. Also in this case, selective transduction of lumbar DRG neurons, spinal cord and fibres innervating the skin of the paw close to the injection site was registered. Anti TrkA antibody confirmed specificity in both DRG are spinal cord, with an efficiency rate in DRG very similar to the one obtained with the retro orbital injection. In this case some unspecific labelling was noticed. Indeed, less than 10% of infected cells were not positive to the anti TrkA staining. This could be explained in different ways. Firstly, immunohistochemistry techniques are rarely totally efficient, and some level of unstained cells is expectable. Secondly, despite TrkA being the main receptor for NGF, the protein also binds with lower affinity to the neurotrophin receptor p75, whose main function is to enhance nerve growth factor signaling by interacting with TrkA and promoting TrkA tyrosine autophosphorylation. However, it was shown that p75 can also interact with TrkB receptor, thus becoming a suitable target for NGF, even if at a lower rate (Vesa et al., 2000). According to this, is possible that unstained cells which were infected by ΔHSPG-NGF were actually $TrkB^+$. In any case, this background activity could be reduced and probably totally eliminated by tuning the dose of vectors administrated. As discussed, if the quantity of virus is high enough to saturate all main receptors of the ligand used for the chemical modification, the virus would recognize other possible binding sites that exhibit lower affinity, thus generating unspecific labelling of unwanted cells.

Having a system able to specifically target NGF^+ peptidergic nociceptors using modified AAV vectors could have utility in the development of therapeutic strategies to treat chronic pain. Indeed, at the moment there is a huge need for therapeutics for treatment of chronic pain, because currently adopted strategies mainly rely on nonsteroidal anti-inflammatory drugs or opioids which are usually associated with dependence and tolerability issues along with overall safety concerns (Bélanger et al., 2018). Given the involvement of NGF in pain signaling, different therapeutic approaches have been proposed. One strategy consists of the blockage of NGF signaling using antibodies directed against either NGF or TrkA receptor. Tanezumab is a humanized monoclonal antibody with high selectivity and specificity for NGF, which is able to prevent the interaction between NGF and TrkA, thus silencing NGF-dependent pain sensitivity (Abdiche et al., 2008). However efficient in patients, this drug has not been approved by FDA due to serious adverse effects. Despite different NGF antagonist and various blocking antibodies having been proposed so far, a safe and long-lasting effective strategy to treat chronic pain still needs to be found.

In this context, cellular modulators could play a crucial role, and could be combined with our delivery system to achieve selective regulation of neurons directly involved in pain signaling. Applications are countless. For example, paroxysmal extreme pain disorder is a genetic diseases caused by point mutations in SCN9A gene, which codes for a sodium channel that regulates neuronal activity, highly expressed in peptidergic nociceptor (Sexton et al., 2018). A possible strategy to treat this disease could be to exploit our ΔHSPG-NGF to selectively deliver CRISPR/cas effectors and directly correct the mutation by homologous direct repair, thus addressing not only the symptoms but also the cause of the disease. This approach could be also applied in patients suffering from familiar episodic pain syndrome and many more genetic diseases in which mutations cause anomalous nociceptor

activity (Sisignano et al., 2019). Another possible application could be to selectively deliver with our modified vectors regulatory siRNAs to modulate excitability and activity of nociceptors. Disregulation of different channels and receptors are often associated with neuropathic pain, and it has been shown that RNA interference could ameliorate symptoms in patients (Kress et al., 2013). As an example, considering that TrkA activation leads to increased pain hypersensitivity due to enhanced activity of TRPV1 and voltage-gated sodium channels in nociceptors, a downregulation of these channels could be considered as a possible strategy to treat chronic pain (Khan & Smith, 2015). Moreover, different molecules derived from plants or animals that show analgesic proprieties have been used to treat pain states. For example, Na(v)1.7-inhibiting peptides isolated from the venom of the centipede Scolopendra subspinipes mutilans shows strong analgesic effects in animals, and could be a valid candidate for AAV-based delivery into nociceptors (S. Yang et al., 2013). Botulin toxin has been used for years to treat different conditions including chronic pain. It inhibits the release of pain mediators from peripheral nerves endings, DRG and spinal cord neurons, reduces inflammation and deactivates sodium channel reducing neuronal excitability (Park & Park, 2017). However efficient, currently there are no clinical guidelines for administration of botulin toxin for neuropathic pain, and all delivery routes used still face the same concerns about low tissues permeability. Our system could offer an effective and highly specific way to bypass surrounding tissues and deliver the toxin directly into neurons. Indeed, delivering therapeutic molecules or activity modulators in the form of DNA directly into nociceptors offers the advantage to instruct neurons to continuously produce these effectors without the need of genome integration given the non-dividing nature of neurons, thus providing long-term beneficial effects without requiring continuous administration of therapeutic agents. These are just some examples of possible applications of our ΔHSPG-NGF vectors in the context of chronic pain treatment, but many more uses could be done in basic research as well. Having a tool that allows for specific manipulation of peptidergic nociceptors could be of great help in the study of the functionality and modulation of these neurons and their relationship with other systems.

To further explore new possible applications of our chemical modification technology in order to obtain AAV vectors with enhanced proprieties, I next studied how the conjugation of a small synthetic peptide that selectively activates the PAR1 receptor on ΔHSPG capsid could be exploited to obtain vectors with increased permeability to cellular barriers. Indeed, PAR1 is involved in many different functions including disruption of endothelial barriers in different tissues upon thrombin stimulation (Dragoni et al., 2020). PAR1 signaling is complicated and the exact mechanisms leading to barrier dysfunction are diverse and not fully understood. Moreover, it is important to note that different activation modalities of PAR1 signaling lead to potentially opposite effects. For example, PAR1 activation by activated protein C (APC) has been demonstrated to have potent anti-inflammatory proprieties and barrier protective effects (Feistritzer & Riewald, 2005). Similar endothelial cytoprotective effects can be obtained upon treatment with different PAR1 agonists (De Ceunynck et al., 2018).

In general, thrombin induces endothelial barrier dysfunction via two major independent pathways. One of them is calcium dependent: thrombin stimulation leads to cellular influx of extracellular Ca^{2+} and subsequent phosphorylation of regulatory myosin light chains (MLC) by Ca2+/calmodulin-dependent myosin light chain kinase (MLCK). MLC phosphorylation induces cellular shape changes

which lead to contraction and intercellular gap formation, which results in the loss of barrier functionality (Garcia et al., 1995). The second mechanism is calcium independent and relies on the Rho-associated protein kinase (ROCK). It has been shown that endothelial barrier permeability is influenced by increased F-actin stress fiber-related contractile tension which is regulated by the activation of RhoA/ROCK pathway (Carbajal et al., 2000). PAR1 mediates RhoA activation (Loberg et al., 2007) and subsequent positive modulation of ROCK, which in turn enhances MLC phosphorylation that leads to cellular contraction and disruption of tight junctions (Carbajal et al., 2000). Despite the main mechanisms underlying PAR1-dependent barrier dysfunctions having been widely studied, different studies propose alternative and coexisting pathways which are involved in PAR1 functional regulation of barriers integrity.

In one study authors have underlined the importance of the thrombin-matrix metalloproteinase (MMP)-9 axis in BBB increased permeability. Thrombin activation of PAR1 seems to induce the release of MMP-9 from pericytes with the BBB, via activation of both Akt and ERK1/2 pathways, which leads to transient permeabilization of the barrier (Machida et al., 2017). Moreover, brain microvascular endothelial cells (BMECs) have been shown to increase nitric oxide synthesis and mitochondrial/cytosolic reactive oxygen species production via PAR1-dependent pathways, leading to BBB dysfunction (Brailoiu et al., 2017), suggesting the presence of different mechanisms that regulates PAR1 induced barrier functionality.

PAR1 activation can be achieved not only after thrombin or other protease cleavage of PAR1 N-terminus, but also by different synthetic peptides that mimic the unmasked tethered ligand portion of the receptor. In particular, the direct tethered ligand sequence, SFLLRN, has been extensively used as a full agonist of PAR1 and partial agonist of PAR2 in different studies (McLaughlin et al., 2005). However, even if SFLLRN peptide mimics thrombin activation of PAR1, there is an emerging body of evidence which suggests that agonist peptides do not activate PAR-1 in the same manner as does thrombin (Hollenberg et al., 2014). Both thrombin and synthetic peptide activation of PAR1 lead to a fast intracellular Ca^{2+} increase, but mechanisms, kinetics and cellular effects are different. While at saturating concentrations of ligand this variability seems to be masked, when dose-response curves are considered, thrombin and SFLLRN activation of PAR1 lead to different activation of both Gαq and Gα12/13 pathways, while only Gα12/13-mediated Rho kinase activity can induce actin stress fibres formation and increased barrier permeability in human endothelial monolayers (McLaughlin et al., 2005). However, in another study, calcium influx and Gαq modulation seems to contribute to increased endothelial permeability, thus suggesting that different responses depends on the particular cell type considered (Bogatcheva et al., 2002). Whichever pathway is preferentially activated, myosin light chain (MLC) phosphorylation is the final commitment step in induced endothelial cell contraction. MLC kinase (MLCK) activation is calcium-dependent, while MLC phosphatases are regulated by Rho kinase, which downregulates MLC phosphatases thus favouring the phosphorylated state of MLC (McLaughlin et al., 2005). However, despite both thrombin or SFLLRN activation of PAR1 being related to an intracellular Ca^{2+} increase, this does not always leads to increased endothelial permeability, and seems to depend on the structural and functional proprieties of involved cells. For example, stimulation of Ca^{2+} influx is sufficient to induce pulmonary macrovascular but not microvascular endothelial barrier dysfunctions, thus further underlining the variability in the effects elicited by PAR1 activation (Kelly et al., 1998).

When viral vectors are delivered in vivo, the virus needs to overcome eventual barriers protecting target tissues from efficient infection. This is particularly relevant in the context of CNS targeting, where the three meninges envelop the brain and where the BBB separates it from the cerebral microvasculature. If complex and invasive direct brain injections want to be avoided (not easily feasible in humans), systemic targeting of CNS could be obtained following direct administration of vectors directly into the bloodstream or in the cerebrospinal fluid (CSF). In the case of intrathecal injection, vectors are administrated into the subarachnoid cavity and are thereby separated from the spinal cord just by the pia mater, the innermost of the meninges. The pia mater is a highly vascular membrane composed by a one- to two-cell-thick layer of leptomeningeal fibroblasts that directly enfolds the brain and spinal cord (Adler, 2010). In the spine, the pia mater can be divided into two parts, the intimal and the epipial layers. The epipial layer consists of a network of collagenous fibers and meningeal fibroblasts while the intimal layer is composed of reticular and elastic fibers which lie directly on the glia limitans, the outermost layer of neural tissue. Blood vessels meander into the epipial layer and eventually reach the parenchyma of the spinal cord through the intimal layer (Adeeb et al., 2013). Although a possible role of PAR1 in the regulation of pia mater permeability has not been investigated so far, some evidence suggests that PAR1 activation could lead to barrier dysfunction also in this tissue. Despite being less studied, PAR1 is also expressed on fibroblasts, where its activation has been related to the modulation of Gαq and Gα12/13 pathways, involved, as discussed above, in barrier dysfunction via regulation of Ca^{2+} influx and Rho kinase activity, respectively (Deng et al., 2008). Moreover, PAR1 activation has been shown to stimulate fibroblast-mediated contraction of three-dimensional collagen matrices, thus further underlying its role as a mediator of tissue remodelling (Fang et al., 2004). In this respect, since pia mater is mainly composed by fibroblasts which respond to PAR1 activation in a similar way of endothelial cells, it can be expected that PAR1 could elicit the same barrier-disrupting effects induced in other tissues. Moreover, due to the high vascular nature of the pia mater, PAR1 could promote AAV migration into the parenchyma of the spinal cord directly through microcapillaries by inducing endothelial barrier dysfunction. In this way, vectors which are administrated into the subarachnoid cavity could directly cross capillary endothelial layer and enter into the parenchyma of the spine through the local vascular microcircuits. According to this prospect, vectors could infect neuronal tissues without interfering with the integrity of the pia mater, although it is more likely that both discussed migration mechanisms could coexist. However, whichever route is pursued is eventually advisable that by chemically linking the selective PAR1 agonist SFLLRN on ΔHSPG capsid it would be possible to obtain vectors with enhanced permeability toward different cellular barriers, including the pia mater.

In order to test this hypothesis, I have worked with a modified version of the well characterized Par1 agonist SFLLRN, in which an extra cysteine (C) residue was included at its amidated C-termini. The resulting peptide, SFLLRNC, was subsequently modified with maleimide linkers in order to accept an azide motif directly linked to its extra C residue. Different linker and reaction conditions have been tested to eventually select the most efficient conjugation protocol. ΔHSPG- SFLLRNC vectors successfully infected DRG cultures with all the linkers tested, with their length minimally effecting transduction efficiency, demonstrating that SFLLRNC conjugation can effectively restore ΔHSPG infectivity. At this point, ΔHSPG- SFLLRNC has been injected intrathecally at different doses, with the aim of assessing whether the modified vectors could overcome the pia mater and infect underlying spinal cord. ΔHSPG-SFLLRNC successfully infected spinal tissues in a dose-dependent

manner, while unmodified ΔHSPG only displayed low background activity in the control animals. Distribution of fluorescence has been analysed and signal was present throughout the entire spinal cord, with its maximum peak being in the lumbar region, close to the injection site. Moreover, positive fibres successfully conveyed the signal to different areas of the brain. This is by itself a notable result, considering that intrathecal administration of many rAAV serotypes, including AAV2, fails to provide sustained transgene expression in spinal cord and, even more, in the brain (Gray et al., 2013). Different studies have been carried out in which authors tried to infect spinal cord of rodents by delivering rAAV2 in the subarachnoidal cavity with different methods, but only poor and short-lasting transgene expression was achieved, thus indicating how the intrathecal space is resistant to efficient gene transfer (Beutler et al., 2005). However, capsid structure plays a crucial role in this. For example, AAV9 is widely known for its BBB crossing proprieties and its ability to transduce neurons and glia throughout the central nervous system following different administration routes, including intravenous and intrathecal injections (Schuster et al., 2014). This indicates that despite CSF delivery of rAAV being particularly challenging, effective CNS transduction could be achieved by using vectors with specific proprieties.

Different factors could contribute to the successful ΔHSPG- SFLLRNC transduction of CNS. As discussed above, SFLLRN activation of the Par1 signaling cascade is involved in barrier disruption in different tissues, including endothelial cells, BBB and fibroblast. It is possible that upon SFLLRN binding to meningeal fibroblasts that compose the pia mater, and subsequent Par1 signaling cascade activation, an impairment of barrier integrity would lead to an increased trafficking of viral vectors directly into spinal cord parenchyma. According to this possibility, the reason for the increased viral transduction would be found in a physical disruption of pia mater integrity, and the creations of gaps from which the virus could access to the underlying nervous tissues. In order to confirm this theory and to assess whether the Par1 agonist SFLLRNC alone was enough to induce pia mater permeabilization, animals have been injected intrathecally with unmodified ΔHSPG together with unconjugated SFLLRNC peptide. Surprisingly, the pattern of infection found was completely different from the one obtained in animals injected with modified ΔHSPG-SFLLRNC. Indeed, while only few positive cells were observed in the lumbar spinal cord (injection site), a high number of positive neurons was evident in different sites of the cortex, mainly located in the outermost regions. This is very different from that found in ΔHSPG-SFLLRNC injected animals, in which the signal is concentrated in the lumbar spinal cord and is maintained throughout the whole structure to eventually convey into the pons, cerebellum and midbrain. However, the number of positive neurons in the cortex of mice injected with ΔHSPG + unconjugated SFLLRNC is higher than in both ΔHSPG-SFLLRNC and control groups. One possible explanation could be that, following intrathecal injection in the lumbar subarachnoidal cavity, the Par1 agonist is transported in the CSF and therefore can spread and permeabilize the whole pia mater which surrounds the entire spinal cord and the brain. At this point, ΔHSPG vectors, which are not linked to anything that can confer them any binding proprieties, can loosely be transported by the CSF and eventually reach all the regions of the CNS. Since the pia mater integrity is disrupted, the unmodified vectors could directly contact and infect neuronal tissues. Indeed, despite the R585/588A mutation, ΔHSPG vectors still retain some level of affinity for HSPG residues, and are not completely silent, as we have previously discussed. In this respect, considering the high dose of virus used for these experiments, it is reasonable to expect some level of infection when ΔHSPG vectors are used. This possibility is supported by the fact that infected cells were only present in the outermost region of the cortex of

the animals injected with unconjugated SFLLRNC. This indicates the possibility that the virus could preferentially infect those cells that it contacts first, which are the closest to the pia mater. However, despite the high number of positive cells in the brain, the spinal cord was poorly transduced, if compared to the ΔHSPG-SFLLRNC group. A possible explanation could be found in the anatomy of the pia mater itself. Indeed, while in the spinal cord the pia mater is composed by a two cell-thick layer of leptomeningeal cells, in the brain it becomes thinner and is formed only by the intimal layer, on which cerebral blood vessels lie directly (Adeeb et al., 2013). In this respect, is possible that the greater thickness of the pia mater in the spinal cord represents a major obstacle for efficient viral infection if compared to the anatomy of the same barrier in the brain. However, whichever is the mechanism involved, is clear that SFLLRNC plays a crucial role in the acquired enhanced viral infectivity. Indeed, if unmodified ΔHSPG vectors are injected alone at the same dose used for the experimental groups, the number of positive cells in both spinal cord and brain is drastically lower. On the other hand, when modified ΔHSPG-SFLLRNC are injected, the infection pattern appears to be different. In this context, the main difference can be found in the fact that when ΔHSPG-SFLLRNC are injected, all the viral particles are modified with the Par1 agonist and thereby they will localize mainly in the injection site by binding on their target cells. In this way, it is reasonable that the highest level of infection would be detected in the lumbar region of the spinal cord, because most of the virus injected will be able to spread only locally. As a consequence, less viral particles would be free to be transported by the CSF to the brain, and thereby it is expected to see a lower number of positive cells in the cortex.

Another possible way in which the modified ΔHSPG-SFLLRNC vectors could access and infect CNS could rely on the effect of Par1 signaling in endothelial barriers and BBB integrity. The pia mater is a particularly vascular tissue, where blood vessels course before entering into the brain and spinal cord parenchyma. We have largely discussed about the mechanisms in which Par1 activation leads to increased endothelial and BBB permeability, and in this respect, it is possible that our vectors could reach the CNS directly from the bloodstream following intrathecal administration. According to this possibility, we cannot exclude that some modified viral particles could bind to the endothelial cells and, after the internalization into the blood vessels, be transported by the bloodstream directly to the parenchyma of the CNS. To test this possibility, and in general to ensure whether ΔHSPG-SFLLRNC could be effectively transported by the bloodstream to different regions of the CNS, modified vectors were delivered systemically with intravenous injection (IV). Brains and spinal cords were analysed and, surprisingly, a difference in the transduction pattern between the two groups was evident. Indeed, while few positive cells were found in the spinal cords of the experimental group but not in the control, different scattered groups of positive cells were detected in the brain of ΔHSPG-SFLLRNC injected animals, with a distribution pattern different from those found in IT injected animals. In this case, positive cells were homogeneously distributed in different regions of the brain, and where not localized just in the outermost part of the cortex (as for unconjugated SFLLRNC + unmodified ΔHSPG IT) or in the pons/midbrain (as for ΔHSPG-SFLLRNC IT). This seems to be logical considering that the vascularization of the brain is extended to all the different regions of this organ, and indicates that ΔHSPG-SFLLRNC are effectively able to transmigrate across the endothelial barrier and even cross the BBB. However, despite the high dose used, the number of positive cells in the brains was not particularly high, and besides, only a few scattered cells were detected in the spinal cords of ΔHSPG-SFLLRNC injected animals. One possibility could be that, since the IV injections were performed in the mice tail veins, most of the modified vectors transmigrated

across the endothelium before arriving to the CNS. In this respect, is possible that part of the vectors injected were dispersed throughout the whole organism following the normal vascularization of the animal and thereby infected other tissues, thus decreasing the total amount of available vectors able to reach and transduce the CNS. The reason why a large number of positive cells were found in the brain but not in the spinal cord could be simply the fact that the brain is a bigger and most vascular tissue if compared to the spine. However, considering the differences with the control groups, there is evidence suggesting that the Par1 agonist SFLLRNC could effectively affect barriers integrity and, as a consequence, facilitate viral infection of the CNS.

To conclude, the experiments carried out outlined a possible involvement of SFLLRNC-mediated Par1 signaling activation on the regulation of the integrity of different cellular barriers, including pia mater, endothelium and BBB, in accordance with published literature. Moreover, when the Par1 agonist is conjugated to binding-deficient ΔHSPG vectors, is able to restore viral infectivity both in vitro and in vivo. The enhanced viral tropism and barrier permeability proprieties conferred by the SFLLRNC peptide could be of great utility for many different purposed. Indeed, being able to boost viral efficiency in vivo would reduce the amount of vector required to obtain a given effect, when vectors are delivered IV or IT. Moreover, considering all the different Par1 expressing cells, SFLLRNC modified vectors could show increased infectivity in a broad range of different tissues in which Par1 signaling has been already involved in barrier dysfunctions, including gastrointestinal tract, lungs and bladder (Arce et al., 2008; Pontarollo et al., 2020). Despite the presence of the Par1 receptor on platelets prevents the use of SFLLRNC modified vectors in humans, the technology could be of particular interest for research in rodents models (Arachiche et al., 2014).

4 CONCLUSIONS

With the aim of improving currently adopted methods for AAV based gene delivery, we have developed a tool that could enable cell-type specific reprogramming of viral tropism. Despite most of my research being based on AAV2, the technology could be applied to virtually any known serotype of AAV. During the first part of the project, we have developed and optimized a chemical coupling strategy that would allow for the post-translational insertion of a specific ligand on the viral capsid. In this way, the conjugated ligand could direct the modified vectors directly to the cell population expressing the membrane receptor of the ligand used. After the systematic evaluation of all the different conditions implied in the modification strategy and their subsequent optimization, I have validated our system directly in vivo. Results obtained demonstrated the functionality and specificity of the modified vectors using two different classes of ligands, represented by the protein NGF and the lectin IB4. In both cases, modified vectors showed correct tropism re-targeting toward the cell population of interest. Next, we have evaluated other possible applications of our technology. Indeed, conjugating a ligand implied in the regulation of different cellular mechanisms could confer particular proprieties to the modified virus. In this respect, we have successfully decorated AAV2 capsid with a small peptide known to be a selective activator of Par1 signaling and thereby involved in the regulation of barriers integrity. When tested in vivo, the modified vector displayed enhanced transduction efficiency for the CNS, presumably due to an increased permeability for meningeal barriers and BBB.

Notably, our system offers a valid alternative to the most popular genetic modifications of vectors suited to establish altered tropism and tissue specificity. Being able to post-translationally modifying viral tropism offers several advantages if compared to genetic engineering approaches. Chemical coupling strategies can be easily tested without the need to produce a new vector for every modification of viral genome, thus allowing the exploration and optimization of different experimental options in a less time/money-consuming manner. Moreover, the risk of interfering with viral packaging is considerably lower, which mitigates the insert size limitations that usually restrict the applicability of genetic modification approaches. Thanks to its versatility, the tool we have developed can be easily adapted to specific needs. Indeed, virtually any class of ligand could be included in the modification strategy, thus allowing the selective targeting of different cell types and tissues. Despite specificity being the main goal of the technology, the versatility of the system is evident also in terms of possible applications. For example, attaching a ligand with broad tropism and high affinity for its receptor(s) will lead to the formation of a vector characterized by a superior efficiency. Another example could be, as already discussed, the conjugation of a ligand characterized by specific proprieties, such as increased barrier permeability. The efficiency boosting effect could be exploited to reduce the viral dose of a particular virus required to obtain an expected response, thereby reducing off-target effects and potential immune reaction, if used in vivo. On the other hand, acquired specificity could be employed to regulate specific cellular responses through the expression of appropriate transgenes. In this context, the tool could be leveraged for targeted therapy (immunotherapy, cancer therapy, gene therapy,..) or targeted regulation of neuronal and non-neuronal activity (optogenetics, chemogenetics, epigenetic modifications, gene expression control,..).

In conclusion, the tool developed within this project shows that post-translational chemical modifications of AAV are a valid alternative to genetic manipulation of vectors aimed to re-direct viral tropism and provide a potent new platform for selective targeting of different cellular population both in vitro and in vivo.

5 MATERIALS & METHODS

5.1 CELL CULTURE

5.1.1 HEK293T, PC12 and Sf21 cell lines

HEK293T (ATCC, CRL-3216™) and PC12 (ATCC, CRL-1721™) cells were maintained in DMEM, high glucose, GlutaMAX™ Supplement (Gibco, 10566016) media supplemented with 1% Penicillin-Streptomycin Solution (10,000 U/mL) (Gibco, 15140122) and, respectively, 10% Fetal Bovine Serum (euroclone, ECS0180L) or 5% Fetal Bovine Serum plus 5% Horse Serum (ThermoFisher, 16050130), and kept at 37°C in humidity-saturated 5% CO_2 atmosphere. Cells were passed upon reaching 90-100% confluence.

Insect Sf21 cell line was kindly provided by EMBL Protein Expression and Purification Core Facility, Heidelberg. Cells were maintained in Sf-900™ III serum-free media (ThermoFisher, 12658019) supplemented with 1% Penicillin-Streptomycin (10,000 U/mL) (Gibco, 15140122) and kept in suspension (shaking at 130rpm) at 27°C in standard atmosphere conditions. Cells were maintained at a concentration between 10^6-10^7cells/ml and were monitored on a daily base.

5.1.2 Primary DRG Culture

Adult C57BL/6J mice were anesthetized with 3% isoflurane administration and sacrificed using CO_2. Immediately, all DRG were collected and kept in PBS during the collection. DRG were subsequently treated with a 0,01% Collagenase (Sigma, C7657-100MG) in PBS solution for 30 minutes at 37°C on a shaker. DRG were then centrifuged at 1000RPM for 3 minutes at room-temperature (RT) and digested with trypsin 0,05% EDTA (Gibco, 25300-054) for 12 minutes, mixed, and digested for further 12 minutes at 37°C on a shaker. Trypsin was inactivated by adding fresh HEK293T complete media and digested DRG were passed through a 0,22um cutoff filter (Millex, SLGP033RS) to remove debris. Lysate was centrifuged at 1000RPM for 3 minutes at RT, cell pellet was resuspended in fresh HEK293T complete media and DRG neurons were plated in 35mm plastic dishes. DRG were kept at 37°C in humidity-saturated 5% CO_2 atmosphere and media were replaced the day after the collection and subsequently as needed.

5.2 GENERATION OF HEK293T AAVR KNOCK-OUT CELL LINE

To generate the AAVR knock-out HEK293T transgenic stable cell line, a CRISPR/Cas9 based strategy combined with the PiggyBac Transposon system has been used. The three plasmid components of the system (PiggyBac Transposase, p133_pPB_mU6-gRNA-StemLoop_Ef1a-Puro-2A-BFP and p065_pPB_CAG_Cas9_IRES_Hygro) were kindly provided by J. Hackett group, Epigenetic and

Neurobiology Unit, EMBL Rome. A single-guide (ATAGGTGTAACTACGTCACT) targeting the human KIAA0319L gene has been cloned in the enhanced gRNA-scaffold vector (p133) at BlpI/BstXI sites. Briefly, oligoes with BstXI-BlpI overhangs (5' TTGATAGGTGTAACTACGTCACTGTTTAAGAGC and 5' TTAGCTCTTAAACAGTGACGTAGTTACACCTATCAACAAG) were annealed at 95°C for 3 minutes and cooled at room-temperature for 30'. Double-stranded oligos have been inserted into p133 plasmid previously cut with BstXI and BlpI using T4 DNA ligase (Thermofisher, EL0011) following manufacturer's guidelines. Resulting plasmid has been sequenced (Eurofins, mix2seq kit, custom DNA sequencing service) with a standard U6 primer (5' CTTAATGTGCGATAAAAGAC) and used to transform Stbl3 chemically competent E. coli (Invitrogen, C737303). HEK293T cells were plated into 75cm^2 plastic flask and when 80% confluent they were transfected with PiggyBac Transposase, p065 and edited p133 plasmids (1:1:1 molar ratio for a total of 10ug DNA) using 0,33mg/ml linear-PEI 25k (Polysciences, PEI 25k, 23966-100 – 1:11 DNA to PEI molar ratio). Complete HEK293T media supplemented with puromycin (1ug/ml) and hygromycin (200ug/ml) was changed every 3 days for a total of 9 days to select positively transfected cells. The selection of correctly edited cells was done following an empirical strategy. Cells were exposed to a wild type AAV2-GFP (see wt AAV2-GFP production) at a MOI = 1000 GC/cell, and GFP$^+$ cells were eliminated using a BioRad S3 cell sorter (BioRad). Briefly, the control cell population was identified based on physical parameters (FSC and SSC) and a threshold was set using the 488 laser and the green fluorophores filter set. Then the samples were run and the cells that expressed the fluorescent protein (fluorescence values above the threshold) were separated from those that did not express it. Non-fluorescent cells were re-plated in 48-well cell culture dish and exposed to viral selection and sorting for further three cycles. Finally, cells which passed all the four selection rounds were considered AAVR deficient and used for subsequent experiments.

5.3 AAV PRODUCTION

5.3.1 Wild Type AAV9-GFP

Wild type AAV9-GFP was produced by AddGene, viral prep #37825-AAV9

5.3.2 ΔHSPG AAV2-tdTomato and ΔHSPG AAV2-CRE

The production of ΔHSPG AAV2 carrying a tdTomato fluoresce reporter or the Cre recombinase gene was done following the standard triple-transfection method as previously described (McClure et al., 2011). Briefly, HEK293T cells were transfected with the three plasmids necessary for rAAV production: Helper pFdelta6 (Agilent), pAAV-CAG-tdTomato (codon diversified) (AddGene, Plasmid #59462) or pAAV-CMV-Cre (kindly provided by J. Sawitzke, Head of Genetic & Viral Engineering Facility (GAVEF), EMBL Rome) and a modified version of the AAV2 capsid plasmid pAAV2-Rep/Cap-ΔHSPG (kindly provided by J. Sawitzke, Head of Genetic & Viral Engineering Facility (GAVEF), EMBL Rome). The Rep/Cap plasmid, which already displayed the ΔHSPG R585/588A substitution in the VP3, was further modified to include Y444/500/730F and T491V VP3 substitutions. A DNA insert with the specific aminoacidic substitutions was cloned in SsP1 and Sma1 site of pAAV2-Rep/Cap

ΔHSPG plasmid (ThermoFisher,5’ atttgtattTcttgagcagaacaaacactccaagtggtaccaccacgcagagtcgacttcagttttctcaggccggagcgagtgacattcggg accagtctaggaactggcttcctggaccctgttaccgccagcagcgagtatcaaagGTatctgcggataacaacaacagtgaatTctcgtgg actggagctaccaagtaccacctcaatggcagagactctctggtgaatccgggcccggccatggcaagccacaaggacgatgaagaaaagt tttttcctcagagcggggttctcatctttgggaagcaaggctcagagaaaacaaatgtggacattgaaaaggtcatgattacagacgaagag gaaatcaggacaaccaatcccgtggctacggagcagtatggatccgtatctaccaacctccaggctggcaacgcccaagcagctacagctg atgtcaacacacaaggcgttcttccaggcatggtctggcaggacagagatgtgtaccttcaggggcccatctgggcaaagattccacacacg gacggacattttcacccctctcccctcatgggtggattcggacttaaacaccctcctccacagattctcatcaagaacaccccggtacctgcga atccttcgaccaccttcagtgcggcaaagtttgcttccttcatcacacagtactccacgggacaggtcagcgtggagatcgagtgggagctcc agaaggaaaacagcaaacgctggaatcccgaaattcagtacacttccaactacaacaagtctgttaatgtggactttactgtggacactaat ggcgtgtattcagagcctcgccccattggcaccagatTcctgactcgtaatctgtaattgcttgttaatcaataaaccgtttaattcgtttcagtt gaactttggtctctgcgtatttctttcttatctagtttccatggctacgtagataagtagcatggcgggttaatcattaactacagccc) using traditional Gibson Assembly Cloning Kit (NEB, E5510S, 10 reactions), following manufacture’s instruction. SsP1 and Sma1 sticky-ends induced compatible homology arms were designed and included at 5’ and 3’ ends of the insert, respectively (5’ cgtctcatgaatcctctcatcgaccaat, 5’ gggcgtttaaacagcgggcggagggg). Correct cloning of the insert in pAAV2-Rep/Cap ΔHSPG plasmid was confirmed by sequencing (Eurofins, mix2seq kit, custom DNA sequencing service) using custom primers targeting a region immediately 5’ of VP3 position 444 (5’ ggagtactttccttctcagatg) or VP3 position 730 (5’ ggacaggtcagcgtggagatc).

HEK293T cells were plated in ten 150mm cell culture plastic dishes and upon reaching 80% of confluence they were triple transfected with plasmids described above (in a 1:1:2 molar ratio, with the latter being pFdelta6, for a total of 600ug of DNA) using linear PEI 25k (1:11 DNA to PEI molar ratio). Fresh HEK293T media was changed the day after transfection and cells/media were collected 3 days after. Rnase-A (sigma, R4875-100mg) and triton-x100 (Sigma, X100-500ml) were added to collected cells/media to a final concentration of 5ug/ml and 0.5%, respectively, and incubated at 37°C for 2 hours on a shaker. Mixture was then centrifuged at 3700g, 30’ at RT to remove debris and supernatant was further filtered through stericup quick release filter 0,22um (Millipore, S2GPU02RE). Next, clean supernatant was concentrated using a peristaltic pump (Sartorius, VivaFlow, 11532084) equipped with filtering cartridge 100kDa (Sigma, Z615390), and excess of media was discarded. Viral particles were purified through iodixanol gradient (Optiprep, 1114542) by ultracentrifugation (Beckmann, optima XE-90 ultracentrifuge) at 44400g for 2 hours at 18 °C. In order to further concentrate the virus and to remove iodixanol excess, collected supernatant was filtered with Amicon Ultra-15 centrifugal filter units 100kDa (Sigma-Aldrich, UFC910024) at 4000g, 4°C until a final volume of 200ul was reached. Amicon filters were pre-treated with a pluronic acid (Gibco, 24040-032) gradient prior use to prevent viral loss due to its interaction with plastic material. Finally, purified vectors underwent snap freeze in liquid nitrogen and were stored in low binding plastic tubes (Sarstedt, 72706600) at -80°C.

5.3.3 Wild type AAV2-GFP

Wild type AAV2-GFP was produced following an optimized baculovirus expression vector (BEV)-mediated rAAV production system, as previously described (Y. Wu et al., 2019). A dual-functional BEV/Cap-(ITR-GOI) that carries the cap gene and the ITR-GOI suitable for AAV2 production, together

with a modified DH10EBacY E. *coli* packaging cell line were kindly provided by EMBL Protein Expression and Purification Core Facility, Heidelberg. The baculovirus expression vector, pFD.cap2.ITR-GFP.Rep2, was designed to express EGFP under the control of a CMV promoter. rAAV production was performed following baculovirus expression system protocol provided by the Eukaryotic Expression Facility, EMBL Grenoble. Briefly, pFD.cap2.ITR-GFP.Rep2 expression vector was transposed into DH10EBacY baculoviral genome and correctly edited colonies were selected through specific antibiotics and blue-white screening. The modified baculoviral genome harboring the correct insertion of AAV2-GFP expressing vector was isolated and used to transfect adherent sf21 cells using X-tremeGENE HP DNA Transfection Reagent (Roche, 6366244001). YFP (contained into the baculoviral genome) expression was monitored as an indicator of successful viral infection of sf21 insect cells, and 3 days post transfection the media, containing secreted functional baculovirus, was collected and used for further expansion of the vectors. Serial expansions were carried on until at least 75% of 200ml of 10^6sf21 cells/ml exhibited YFP signal. Next, cells and media were collected and rAAV particles purified through iodixanol gradient as described above for ΔHSPG-AAV2 production.

5.4 CHEMICAL MODIFICATIONS OF rAAVs

5.4.1 Ligand modification protocol

WGA Lectin from *Triticum vulgaris* (Sigma, L9640-10MG) and IB4 Lectin from *Bandeiraea simplicifolia* (Sigma, L3019) were functionalized with an azide group through chemical reaction with the heterobifunctional crosslinker NHS-peg4-azide (Thermofisher, 26130). 1-10mg/ml of lectin were modified with ~ 20 fold excess of linker::protein molar ratio in PBS on a shaker for 3 hours at RT. Next, modified protein was concentrated and excess of unbound linker was cleaned-up through Amicon Ultra-0.5 Centrifugal Filter Unit 10kDa MWCO (Sigma, UFC501008). Columns were pre-treated with a pluronic acid gradient prior use. Briefly, columns were filled with 0,1% pluronic acid in PBS for 10 minutes at RT, then the solution was removed by centrifugation. Columns were further washed with 0,01% pluronic acid in PBS for 1 minute and subsequently with 0,001% + 200mM NaCl solution for 1 minute. The concentration of modified lectins was measured using a nanodrop microvolume spectrophotometer.

WGA-SNAP was synthetized as SNAP-Tag fusion protein by EMBL Protein Expression and Purification Core Facility, Heidelberg.

NGF^{R121W} -SNAP was previously synthetized in our laboratory and used by authors for other purposes (Nocchi et al., 2019).

PAR1 agonist (SFLLRNC) was synthetized by GeneScript, and functionalized with an azide group in our laboratory. The azide group was added following a two-step maleimide reaction. Azide-peg3-maleimide crosslinker was prepared immediately before use following manufacture's guidelines (Jena Bioscience, CLK-AZ107-25). 100uM of PAR1 agonist were modified with 10 fold molar excess of linker and 10 fold molar excess of TCEP (Sigma-Aldrich, 646547) in PBS for 2 hours at RT on a shaker.

5.4.2 Virus modification protocol

Viral vectors to be modified were thawed immediately prior use, and reacted with the optimal virus::linker molar ratio previously found for each viral prep produced. The choice of the linker was made according to the presence of an azide motif or a SNAP-tag on the ligand used. NHS-DBCO (Sigma-Aldrich, 761524) NHS-peg4-DBCO (Sigma-Aldrich, 764019), NHS-peg8-DBCO (BroadPharm, BP-24019), NHS-peg24-DBCO (BroadPharm, BP-25726), BG-gla-NHS (NEB, S9151S), BG-peg13-NHS (synthesized by EMBL Chemical Biology Core Facility, Heidelberg) were diluted in DMSO 99,8% to a stock concentration of 20mM and conserved at -20°. In order to find the optimal virus::linker molar ratio for each new batch of virus produced, the linker of choice was thawed immediately prior to use and diluted in PBS to a concentration of 20uM. Next, $3x10^9$ VG were reacted with increasing linker concentrations for 2 hours at RT on a shaker. Excess of unbound linker was removed using Amicon Ultra-0.5 100kDa Centrifugal Filter Units. Filtering columns were pre-treated with a pluronic acid gradient as described above. WGA-azide or NGF-snap were used as reference ligands to ensure modified vector efficiency. 5uM of ligand were reacted with primed vectors for 1 hour at RT on a shaker and further over night at 4°. Prior to administration, excess of unbound ligand was washed using pre-treated Amicon Ultra-0.5 100kDa Centrifugal Filter Units as described above. Modified vectors were tested on PC12 cells or freshly prepared DRG primary cultures and red fluorescence, as an indicator of viral infection rate, was monitored 3 to 5 days post infection with a fluorescence microscope. Control experiments using unmodified vectors were always run in parallel. The selection of the optimal virus::linker molar ratio was done by empirically assessing the maximal presence of fluorescent signal among all the conditions tested.

The modification of viral vectors to be used for other experiments was done similarly to the protocol described above for the selection of the optimal virus::linker molar ratio. Briefly, viral vectors were modified with their respective optimal virus::linker molar ratio, taking into account the starting amount of virus to be modified. Excess of linker was removed and 5uM of ligand was added. Before administration, excess of unbound ligand was removed and final volume was adjusted according to the specific experiment. Indeed, for particular applications, such as intra-sciatic nerve or intrathecal injections, for which a volume of 3ul or 10ul respectively was required, further filtering was performed following the same procedure. Modified vectors were applied to cells or injected within the same day of preparation.

5.5 ANIMALS

Adult mice (8-32 weeks old) belonging to C57BL/6J strain or Rosa-CAG-LSL-tdTomato (Ai14(RCL-tdT)-D, The Jackson Laboratory, 007914) were used in this project. C57BL/6J wild-type mice were bred and maintained at the SISSA Scuola Internazionale Superiore di Studi Avanzati, Trieste, in accordance with Italian legislation (Art. 9, 27. Jan 1992, no. 116) under license from the Italian Ministry of Health. Rosa-CAG-LSL-tdTomato were breed and maintained at EMBL Rome in accordance with Italian legislation (Art. 9, 27. Jan 1992, no. 116) under license from the Italian

Ministry of Health. Experimental protocols were approved by the EMBL and SISSA Ethics Committee and the Italian Ministry of Health.

5.6 INJECTIONS

Young adult (8-16 weeks old) C57BL/6J mice of both sexes were housed with food and water ad libitum, under a 12 hours light/dark cycle and kept at a maximum of 6 animals per cage. Anaesthesia was induced with 4% isoflurane delivered with 2% O2 and room air in a closed chamber, until loss of reflexes was reached. During the injection procedure, isoflurane was lowered to 2-3% (according to the type of injection) and delivered through a funnel-shaped nose cone connected to a non-rebreathing apparatus. A charcoal scavenging device was used to manage waste anaesthetic gases and decrease exposure time of personnel.

Intraperitoneal injections were performed without anaesthesia using plastic 27,5 gauge (or smaller) 0,5ml insulin syringes. The animals were manually immobilised in the head-down position and vectors were injected into the lower right quadrant of the abdomen in order to avoid damage of abdominal organs. Needle was positioned with bevel facing up at an angle of approximately 40° to horizontal, until the entire bevel was inside the abdominal cavity, and substances were slowly injected.

Retro orbital injections were performed entering into the retro-bulbar sinus by approximately 5 mm using plastic 27,5 gauge (or smaller) 0,5ml insulin syringes. Eyeballs were partially protruded by applying gentle pressure to the skin dorsal and ventral to the target eye, and needle was inserted, bavel down, at an angle of approximately 30° into the medial canthus. Needle was hold in place for 30 second before being slowly withdrawn.

For intra sciatic nerve delivery of vectors, the lower back of anaesthetized animals was disinfected with 70% ethanol and a small incision was made at the level of the mid-thigh region. Next, muscles overlying sciatic nerves were gently separated using forceps and sciatic nerve was exposed and maintained in place with concave tweezers. Injections were performed using a Hamilton glass syringe equipped with a 30-gauge needle by inserting the needle, bevel down, directly into the sciatic nerve towards the medial axis of the animals. 3 ul of total volume were slowly injected and carefully monitoring of the procedure was conducted under a binocular microscope. After the injection, sciatic nerve was positioned back to its site and skin was sutured with Michel suture clips.

Intrathecal injections were performed using plastic 27,5 gauge (or smaller) 0,5ml insulin syringes. Firstly, the lower back of anaesthetized animals was disinfected with 70% ethanol and a small incision was made to expose the lumbar region of the backbone. Injections were performed typically in the intrathecal space separating L3 to L4, according to the visibility of the spinal column. On larger animals (12+ weeks old) injections were performed at a higher level of the lumbar region. A total volume of 15ul maximum was slowly administrated keeping the syringe at an angle of 90° to horizontal and needle was hold in place for 30 seconds before being withdrawn to prevent backflow. Skin was then sutured using Michel suture clips.

After injections, animals were left to recover on a heating pad to prevent postoperative hypothermia and were monitored for eventual complications until full motor activity was recovered and overall good health was ensured.

5.7 TISSUES PROCESSING AND IMMUNOSTAINING

3 to 5 weeks post injection, animals were sacrificed by CO_2 administration (100% CO_2 was introduced in the chamber until lack of respiration was observed) and relevant tissues were collected and immediately fixed in 4% PFA (Sigma-Aldrich, 158127) in PBS. DRG and trigeminal ganglion were fixed for 2 hours at RT while brain, spinal cord and skin were fixed overnight. Next, tissues were washed 3x with PBS and, if necessary, embedded in 2% agarose (Sigma-Aldrich, A9539) in PBS and cut in 50µm-thick sections using a vibratome (Leica, VT1000S). Sections of whole DRG/trigeminal ganglions were then mounted on glass slides with ProLong Diamond Antifade Mountant (Thermo, P36970) and eventually imaged using a Nikon A1R confocal microscope.

In order to perform immunostaining techniques, tissues sections were firstly permeabilized using Tween-20 (Sigma-Aldrich, 9005-645) 0,3% in PBS for 10min at room temperature for 2 times, washed in PBS and incubated with blocking solution (5% normal goat serum, ThermoFisher 31873, in PBS) for 1 hour at room temperature on gently shaking. If an anti TrkA primary antibody was required, normal donkey serum (Sigma-Aldrich, D9663-10ml) was used in the blocking solution. Sections were incubated with primary antibodies (concentrations below) in blocking solution overnight at 4° on gently shaking. Next, samples were washed for 2 times in PBS and secondary antibodies in blocking solution were added and the sections were incubated for 1 hour and 30 minutes in the dark at room temperature on gently shaking. After further two washes with PBS, slides were mounted with ProLong Diamond Antifade Mountant and imaged using a Nikon A1R confocal microscope.

Anti trkA antibody (R&D Systems AF1056) (1:200)

Isolectin GS-IB_4 From *Griffonia simplicifolia*, Alexa Fluor™ 488 Conjugate (Invitrogen, I21411) (1:500)

Isolectin GS-IB_4 From *Griffonia simplicifolia*, Alexa Fluor™ 647 Conjugate (Invitrogen, I32450) (1:500)

Anti-NeuN antibody (Invitrogen, 78639) (1:500)

Anti-Thrombin R Antibody (ATAP2) – (Par1) (Santa Cruz Biotechnology, sc-13503) 1:200

All secondary antibodies were Alexa-conjugated and were used at a concentration of 1:1000.

Dapi 0,5mg/ml (Merck-Sigma, 32670) was used to counterstain nuclei. Samples were incubated for 30 minutes with 1:1000 DAPI in PBS and washed for 2 times with PBS.

5.8 IMAGE PROCESSING

Confocal images were analysed with imageJ software. Quantification of the boosting effect of IB4-modified AAV2 and AAV9 on PC12 cells and quantification of the efficiency of wt AAV2, wt AAV2-WGA, ΔHSPG and ΔHSPG-WGA on wt or knockout HEK 293-T cells lines were performed by dividing total fluorescence by the total number of cells, identified via DAPI staining, to obtain the average fluorescence of cells for each condition. Quantification of all other *in vitro* experiments was performed by measuring the total fluorescence of all positive cells for each condition. Statistical analysis were performed using GraphPad Prism software.

Abdiche, Y. N., Malashock, D. S., & Pons, J. (2008). Probing the binding mechanism and affinity of tanezumab, a recombinant humanized anti-NGF monoclonal antibody, using a repertoire of biosensors. *Protein Science*, *17*(8). https://doi.org/10.1110/ps.035402.108

Adeeb, N., Mortazavi, M. M., Deep, A., Griessenauer, C. J., Watanabe, K., Shoja, M. M., Loukas, M., & Tubbs, R. S. (2013). The pia mater: A comprehensive review of literature. In *Child's Nervous System* (Vol. 29, Issue 10). https://doi.org/10.1007/s00381-013-2044-5

Adler, J. T. (2010). Gray's Anatomy: The Anatomical Basis of Clinical Practice, 40th Edition. *Journal of Surgical Research*, *158*(1). https://doi.org/10.1016/j.jss.2009.01.035

Agbandje-McKenna, M., & Kleinschmidt, J. (2011). AAV capsid structure and cell interactions. In *Methods in Molecular Biology* (Vol. 807). https://doi.org/10.1007/978-1-61779-370-7_3

Agnihotri, S. A., Mallikarjuna, N. N., & Aminabhavi, T. M. (2004). Recent advances on chitosan-based micro- and nanoparticles in drug delivery. In *Journal of Controlled Release* (Vol. 100, Issue 1). https://doi.org/10.1016/j.jconrel.2004.08.010

Agopian, K., Wei, B. L., Garcia, J. V., & Gabuzda, D. (2006). A Hydrophobic Binding Surface on the Human Immunodeficiency Virus Type 1 Nef Core Is Critical for Association with p21-Activated Kinase 2. *Journal of Virology*, *80*(6). https://doi.org/10.1128/jvi.80.6.3050-3061.2006

Aiuti, A., Biasco, L., Scaramuzza, S., Ferrua, F., Cicalese, M. P., Baricordi, C., Dionisio, F., Calabria, A., Giannelli, S., Castiello, M. C., Bosticardo, M., Evangelio, C., Assanelli, A., Casiraghi, M., Di Nunzio, S., Callegaro, L., Benati, C., Rizzardi, P., Pellin, D., … Naldini, L. (2013). Lentiviral hematopoietic stem cell gene therapy in patients with wiskott-aldrich syndrome. *Science*, *341*(6148). https://doi.org/10.1126/science.1233151

Akache, B., Grimm, D., Shen, X., Fuess, S., Yant, S. R., Glazer, D. S., Park, J., & Kay, M. A. (2007). A two-hybrid screen identifies cathepsins B and L as uncoating factors for adeno-associated virus 2 and 8. *Molecular Therapy*, *15*(2). https://doi.org/10.1038/sj.mt.6300053

Anson, D. S. (2004). The use of retroviral vectors for gene therapy-what are the risks? A review of retroviral pathogenesis and its relevance to retroviral vector-mediated gene delivery. In *Genetic Vaccines and Therapy* (Vol. 2). https://doi.org/10.1186/1479-0556-2-9

Arachiche, A., De La Fuente, M., & Nieman, M. T. (2014). Platelet specific promoters are insufficient to express protease activated receptor 1 (PAR1) transgene in mouse platelets. *PLoS ONE*, *9*(5). https://doi.org/10.1371/journal.pone.0097724

Arce, F. T., Whitlock, J. L., Birukova, A. A., Birukov, K. G., Arnsdorf, M. F., Lal, R., Garcia, J. G. N., & Dudek, S. M. (2008). Regulation of the micromechanical properties of pulmonary endothelium by S1P and thrombin: Role of cortactin. *Biophysical Journal*, *95*(2). https://doi.org/10.1529/biophysj.107.127167

Aslanidi, G. V., Rivers, A. E., Ortiz, L., Song, L., Ling, C., Govindasamy, L., van Vliet, K., Tan, M., Agbandje-McKenna, M., & Srivastava, A. (2013). Optimization of the Capsid of Recombinant Adeno-Associated Virus 2 (AAV2) Vectors: The Final Threshold? *PLoS ONE*, *8*(3). https://doi.org/10.1371/journal.pone.0059142

Asokan, A., Johnson, J. S., Li, C., & Samulski, R. J. (2008). Bioluminescent virion shells: New tools for quantitation of AAV vector dynamics in cells and live animals. *Gene Therapy*, *15*(24). https://doi.org/10.1038/gt.2008.127

Baek, J. M., Kwak, S. C., Kim, J. Y., Ahn, S. J., Jun, H. Y., Yoon, K. H., Lee, M. S., & Oh, J. (2015). Evaluation of a novel technique for intraperitoneal injections in mice. *Lab Animal*, *44*(11). https://doi.org/10.1038/laban.880

Balazs, D. A., & Godbey, W. (2011). Liposomes for Use in Gene Delivery. *Journal of Drug Delivery*, *2011*. https://doi.org/10.1155/2011/326497

Balčiūnaitė-Murzienė, G., & Dzikaras, M. (2021). Wheat germ agglutinin—from toxicity to biomedical applications. In *Applied Sciences (Switzerland)* (Vol. 11, Issue 2). https://doi.org/10.3390/app11020884

Barraud, P., Banerjee, S., Mohamed, W. I., Jantsch, M. F., & Allain, F. H. T. (2014). A bimodular nuclear localization signal assembled via an extended double-stranded RNA-binding domain acts as an RNA-sensing signal for transportin 1. *Proceedings of the National Academy of Sciences of the United States of America*, *111*(18). https://doi.org/10.1073/pnas.1323698111

Bélanger, P., West, C. R., & Brown, M. T. (2018). Development of pain therapies targeting nerve growth factor signal transduction and the strategies used to resolve safety issues. In *Journal of Toxicological Sciences* (Vol. 43, Issue 1). https://doi.org/10.2131/jts.43.1

Benincasa, M., Zahariev, S., Pelillo, C., Milan, A., Gennaro, R., & Scocchi, M. (2015). PEGylation of the peptide Bac7(1-35) reduces renal clearance while retaining antibacterial activity and bacterial cell penetration capacity. *European Journal of Medicinal Chemistry*, *95*. https://doi.org/10.1016/j.ejmech.2015.03.028

Benton, R. L., Maddie, M. A., Minnillo, D. R., Hagg, T., & Whittemore, S. R. (2008). Griffonia simplicifolia isolectin B4 identifies a specific subpopulation of angiogenic blood vessels following contusive spinal cord injury in the adult mouse. *Journal of Comparative Neurology*, *507*(1). https://doi.org/10.1002/cne.21570

Beutler, A. S., Banck, M. S., Walsh, C. E., & Milligan, E. D. (2005). Intrathecal gene transfer by adeno-associated virus for pain. In *Current Opinion in Molecular Therapeutics* (Vol. 7, Issue 5).

Bleker, S., Sonntag, F., & Kleinschmidt, J. A. (2005). Mutational Analysis of Narrow Pores at the Fivefold Symmetry Axes of Adeno-Associated Virus Type 2 Capsids Reveals a Dual Role in Genome Packaging and Activation of Phospholipase A2 Activity. *Journal of Virology*, *79*(4). https://doi.org/10.1128/jvi.79.4.2528-2540.2005

Bobisse, S., Rondina, M., Merlo, A., Tisato, V., Mandruzzato, S., Amendola, M., Naldini, L., Willemsen, R. A., Debets, R., Zanovello, P., & Rosato, A. (2009). Reprogramming T lymphocytes for melanoma adoptive immunotherapy by T-cell receptor gene transfer with lentiviral vectors. *Cancer Research*, *69*(24). https://doi.org/10.1158/0008-5472.CAN-09-0494

Bogatcheva, N. V., Garcia, J. G., & Verin, A. D. (2002). Molecular mechanisms of thrombin-induced endothelial cell permeability. In *Biochemistry. Biokhimiia* (Vol. 67, Issue 1). https://doi.org/10.1023/A:1013904231324

Bohenzky, R. A., Lefebvre, R. B., & Berns, K. I. (1988). Sequence and symmetry requirements within the internal palindromic sequences of the adeno-associated virus terminal repeat. *Virology*, *166*(2). https://doi.org/10.1016/0042-6822(88)90502-8

Boucas, J., Lux, K., Huber, A., Schievenbusch, S., Von Freyend, M. J., Perabo, L., Quadt-Humme, S., Odenthal, M., Hallek, M., & Büning, H. (2009). Engineering adeno-associated virus serotype 2-based targeting vectors using a new insertion site-position 453-and single point mutations. *Journal of Gene Medicine*, *11*(12). https://doi.org/10.1002/jgm.1392

Boussif, O., LezoualC'H, F., Zanta, M. A., Mergny, M. D., Scherman, D., Demeneix, B., & Behr, J. P. (1995). A versatile vector for gene and oligonucleotide transfer into cells in culture and in vivo: Polyethylenimine. *Proceedings of the National Academy of Sciences of the United States of America*, *92*(16). https://doi.org/10.1073/pnas.92.16.7297

Boyle, J. (2008). Molecular biology of the cell, 5th edition by B. Alberts, A. Johnson, J. Lewis, M. Raff, K. Roberts, and P. Walter. *Biochemistry and Molecular Biology Education*, *36*(4). https://doi.org/10.1002/bmb.20192

Brailoiu, E., Shipsky, M. M., Yan, G., Abood, M. E., & Brailoiu, G. C. (2017). Mechanisms of modulation of brain microvascular endothelial cells function by thrombin. *Brain Research*, *1657*. https://doi.org/10.1016/j.brainres.2016.12.011

Brister, J. R., & Muzyczka, N. (1999). Rep-Mediated Nicking of the Adeno-Associated Virus Origin Requires Two Biochemical Activities, DNA Helicase Activity and Transesterification. *Journal of Virology*, *73*(11). https://doi.org/10.1128/jvi.73.11.9325-9336.1999

Brister, J. R., & Muzyczka, N. (2000). Mechanism of Rep-Mediated Adeno-Associated Virus Origin Nicking. *Journal of Virology*, *74*(17). https://doi.org/10.1128/jvi.74.17.7762-7771.2000

Broadwell, R. D., Balin, B. J., & Salcman, M. (1988). Transcytotic pathway for blood-borne protein through the blood-brain barrier. *Proceedings of the National Academy of Sciences of the United States of America*, *85*(2). https://doi.org/10.1073/pnas.85.2.632

Bukrinsky, M. I., Sharova, N., Mcdonald, T. L., Pushkarskaya, T., Tarpley, W. G., & Stevenson, M. (1993). Association of integrase, matrix, and reverse transcriptase antigens of human immunodeficiency virus type 1 with viral nucleic acids following acute infection. *Proceedings of the National Academy of Sciences of the United States of America*, *90*(13). https://doi.org/10.1073/pnas.90.13.6125

Büning, H., & Srivastava, A. (2019). Capsid Modifications for Targeting and Improving the Efficacy of AAV Vectors. In *Molecular Therapy - Methods and Clinical Development* (Vol. 12). https://doi.org/10.1016/j.omtm.2019.01.008

Carbajal, J. M., Gratrix, M. L., Yu, C. H., & Schaeffer, J. (2000). ROCK mediates thrombin's endothelial barrier dysfunction. *American Journal of Physiology - Cell Physiology*, *279*(1 48-1). https://doi.org/10.1152/ajpcell.2000.279.1.c195

Cavazzana-Calvo, M., Hacein-Bey, S., De Saint Basile, G., Gross, F., Yvon, E., Nusbaum, P., Selz, F., Hue, C., Certain, S., Casanova, J. L., Bousso, P., Le Deist, F., & Fischer, A. (2000). Gene therapy of human severe combined immunodeficiency (SCID)-X1 disease. *Science*, *288*(5466). https://doi.org/10.1126/science.288.5466.669

Cavazzana-Calvo, M., Payen, E., Negre, O., Wang, G., Hehir, K., Fusil, F., Down, J., Denaro, M., Brady, T., Westerman, K., Cavallesco, R., Gillet-Legrand, B., Caccavelli, L., Sgarra, R., Maouche-Chrétien, L., Bernaudin, F., Girot, R., Dorazio, R., Mulder, G. J., … Leboulch, P. (2010). Transfusion independence and HMGA2 activation after gene therapy of human β-thalassaemia. *Nature*, *467*(7313). https://doi.org/10.1038/nature09328

Cervelli, T., Palacios, J. A., Zentilin, L., Mano, M., Schwartz, R. A., Weitzman, M. D., & Giacca, M. (2008). Processing of recombinant AAV genomes occurs in specific nuclear structures that overlap with foci of DNA-damage-response proteins. *Journal of Cell Science*, *121*(3). https://doi.org/10.1242/jcs.003632

Chandler, R. J., La Fave, M. C., Varshney, G. K., Trivedi, N. S., Carrillo-Carrasco, N., Senac, J. S., Wu, W., Hoffmann, V., Elkahloun, A. G., Burgess, S. M., & Venditti, C. P. (2015). Vector design influences hepatic genotoxicity after adeno-associated virus gene therapy. *Journal of Clinical Investigation*, *125*(2). https://doi.org/10.1172/JCI79213

Chen, J., Guan, X., Hu, Y., Tian, H., & Chen, X. (2017). Peptide-Based and Polypeptide-Based Gene Delivery Systems. In *Topics in Current Chemistry* (Vol. 375, Issue 2). https://doi.org/10.1007/s41061-017-0115-x

Colella, P., Ronzitti, G., & Mingozzi, F. (2018). Emerging Issues in AAV-Mediated In Vivo Gene Therapy. In *Molecular Therapy - Methods and Clinical Development* (Vol. 8). https://doi.org/10.1016/j.omtm.2017.11.007

Cooray, S., Howe, S. J., & Thrasher, A. J. (2012). Retrovirus and lentivirus vector design and methods of cell conditioning. In *Methods in Enzymology* (Vol. 507). https://doi.org/10.1016/B978-0-12-386509-0.00003-X

Davila, M. L., Sauter, C., & Brentjens, R. (2015). CD19-targeted t cells for hematologic malignancies clinical experience to date. In *Cancer Journal (United States)* (Vol. 21, Issue 6). https://doi.org/10.1097/PPO.0000000000000153

De Ceunynck, K., Peters, C. G., Jain, A., Higgins, S. J., Aisiku, O., Fitch-Tewfik, J. L., Chaudhry, S. A., Dockendorff, C., Parikh, S. M., Ingber, D. E., & Flaumenhaft, R. (2018). PAR1 agonists stimulate APC-like endothelial cytoprotection and confer resistance to thromboinflammatory injury. *Proceedings of the National Academy of Sciences of the United States of America*, *115*(5). https://doi.org/10.1073/pnas.1718600115

Deng, X., Mercer, P. F., Scotton, C. J., Gilchrist, A., & Chambers, R. C. (2008). Thrombin induces fibroblast CCL2/JE production and release via coupling of PAR1 to Gαq and cooperation between ERK1/2 and Rho kinase signaling pathways. *Molecular Biology of the Cell*, *19*(6). https://doi.org/10.1091/mbc.E07-07-0720

Denk, F., Bennett, D. L., & McMahon, S. B. (2017). Nerve Growth Factor and Pain Mechanisms. *Annual Review of Neuroscience*, *40*. https://doi.org/10.1146/annurev-neuro-072116-031121

Deverman, B. E., Pravdo, P. L., Simpson, B. P., Kumar, S. R., Chan, K. Y., Banerjee, A., Wu, W. L., Yang, B., Huber, N., Pasca, S. P., & Gradinaru, V. (2016). Cre-dependent selection yields AAV variants for widespread gene transfer to the adult brain. *Nature Biotechnology*, *34*(2). https://doi.org/10.1038/nbt.3440

Devi, R. V., & Basil-Rose, M. R. (2018). Lectins as ligands for directing nanostructured systems. *Current Drug Delivery*, *15*. https://doi.org/10.2174/1567201815666180108101246

Deyle, D. R., & Russell, D. W. (2009). Adeno-associated virus vector integration. In *Current Opinion in Molecular Therapeutics* (Vol. 11, Issue 4).

Dhungel, B., Andrzejewski, S., Jayachandran, A., Shrestha, R., Ramlogan-Steel, C. A., Layton, C. J., & Steel, J. C. (2018). Evaluation of the Glypican 3 promoter for transcriptional targeting of hepatocellular carcinoma. *Gene Therapy*, *25*(2). https://doi.org/10.1038/s41434-018-0002-2

Dhungel, B. P., Bailey, C. G., & Rasko, J. E. J. (2021). Journey to the Center of the Cell: Tracing the Path of AAV Transduction. In *Trends in Molecular Medicine* (Vol. 27, Issue 2). https://doi.org/10.1016/j.molmed.2020.09.010

Ding, W., Zhang, L. N., Yeaman, C., & Engelhardt, J. F. (2006). rAAV2 traffics through both the late and the recycling endosomes in a dose-dependent fashion. *Molecular Therapy*, *13*(4). https://doi.org/10.1016/j.ymthe.2005.12.002

Douar, A.-M., Poulard, K., Stockholm, D., & Danos, O. (2001). Intracellular Trafficking of Adeno-Associated Virus Vectors: Routing to the Late Endosomal Compartment and Proteasome Degradation. *Journal of Virology*, *75*(4). https://doi.org/10.1128/jvi.75.4.1824-1833.2001

Dragoni, S., Papageorgiou, A., Araiz, C., Greenwood, J., & Turowski, P. (2020). Endothelial Protease Activated Receptor 1 (PAR1) Signalling Is Required for Lymphocyte Transmigration across Brain Microvascular Endothelial Cells. *Cells*, *9*(12). https://doi.org/10.3390/cells9122723

Drouin, L. M., & Agbandje-Mckenna, M. (2013). Adeno-associated virus structural biology as a tool in vector development. In *Future Virology* (Vol. 8, Issue 12). https://doi.org/10.2217/fvl.13.112

Duan, D., Li, Q., Kao, A. W., Yue, Y., Pessin, J. E., & Engelhardt, J. F. (1999). Dynamin Is Required for Recombinant Adeno-Associated Virus Type 2 Infection. *Journal of Virology*, *73*(12). https://doi.org/10.1128/jvi.73.12.10371-10376.1999

Dudek, A. M., Pillay, S., Puschnik, A. S., Nagamine, C. M., Cheng, F., Qiu, J., Carette, J. E., & Vandenberghe, L. H. (2018). An Alternate Route for Adeno-associated Virus (AAV) Entry Independent of AAV Receptor. *Journal of Virology*, *92*(7). https://doi.org/10.1128/jvi.02213-17

Dudek, A. M., Zabaleta, N., Zinn, E., Pillay, S., Zengel, J., Porter, C., Franceschini, J. S., Estelien, R., Carette, J. E., Zhou, G. L., & Vandenberghe, L. H. (2020). GPR108 Is a Highly Conserved AAV Entry Factor. *Molecular Therapy*, *28*(2). https://doi.org/10.1016/j.ymthe.2019.11.005

Edwards, C. K., Martin, S. W., Seely, J., Kinstler, O., Buckel, S., Bendele, A. M., Cosenza, M. E., Feige, U., & Kohno, T. (2003). Design of PEGylated soluble tumor necrosis factor receptor type I (PEG sTNF-RI) for chronic inflammatory diseases. *Advanced Drug Delivery Reviews*, *55*(10). https://doi.org/10.1016/S0169-409X(03)00112-1

Fang, Q., Liu, X., Abe, S., Kobayashi, T., Wang, X. Q., Kohyama, T., Hashimoto, M., Wyatt, T., & Rennard, S. I. (2004). Thrombin induces collagen gel contraction partially through PAR1 activation and PKC-E. *European Respiratory Journal*, *24*(6). https://doi.org/10.1183/09031936.04.00005704

Feistritzer, C., & Riewald, M. (2005). Endothelial barrier protection by activated protein C through PAR1-dependent sphingosine 1-phosphate receptor-1 crossactivation. *Blood*, *105*(8). https://doi.org/10.1182/blood-2004-10-3985

FELGNER, P. L., TSAI, Y. J., SUKHU, L., WHEELER, C. J., MANTHORPE, M., MARSHALL, J., & CHENG, S. H. (1995). Improved Cationic Lipid Formulations for In Vivo Gene Therapy. *Annals of the New York Academy of Sciences*, *772*(1). https://doi.org/10.1111/j.1749-6632.1995.tb44738.x

Fischer, M. D., Hickey, D. G., Singh, M. S., & MacLaren, R. E. (2016). Evaluation of an Optimized Injection System for Retinal Gene Therapy in Human Patients. *Human Gene Therapy Methods*, *27*(4). https://doi.org/10.1089/hgtb.2016.086

Fisher, K. J., Gao, G. P., Weitzman, M. D., DeMatteo, R., Burda, J. F., & Wilson, J. M. (1996). Transduction with recombinant adeno-associated virus for gene therapy is limited by leading-strand synthesis. *Journal of Virology*, *70*(1). https://doi.org/10.1128/jvi.70.1.520-532.1996

Flanary, B. (2005). More than Human: Embracing the Promise of Biological EnhancementMore Than Human: Embracing the Promise of Biological Enhancement. By Ramez Naam . Broadway Press, Louisville, KY, 2005, 247 pages, ISBN 0767918436, $24.95. *Rejuvenation Research*, *8*(1). https://doi.org/10.1089/rej.2005.8.61

Flaumenhaft, R., & De Ceunynck, K. (2017). Targeting PAR1: Now What? In *Trends in Pharmacological Sciences* (Vol. 38, Issue 8). https://doi.org/10.1016/j.tips.2017.05.001

Florea, B. I., Meaney, C., Junginger, H. E., & Borchard, G. (2002). Transfection efficiency and toxicity of polyethylenimine in differentiated Calu-3 and nondifferentiated COS-1 cell cultures. *AAPS PharmSci*, *4*(3). https://doi.org/10.1208/ps040312

Folegatti, P. M., Ewer, K. J., Aley, P. K., Angus, B., Becker, S., Belij-Rammerstorfer, S., Bellamy, D., Bibi, S., Bittaye, M., Clutterbuck, E. A., Dold, C., Faust, S. N., Finn, A., Flaxman, A. L., Hallis, B., Heath, P., Jenkin, D., Lazarus, R., Makinson, R., … Yau, Y. (2020). Safety and immunogenicity of the ChAdOx1 nCoV-19 vaccine against SARS-CoV-2: a preliminary report of a phase 1/2, single-blind, randomised controlled trial. *The Lancet*, *396*(10249). https://doi.org/10.1016/S0140-6736(20)31604-4

Friedmann, T., & Roblin, R. (1972). Gene therapy for human genetic disease? *Science*, *175*(4025). https://doi.org/10.1126/science.175.4025.949

Gajbhiye, V., & Gong, S. (2013). Lectin functionalized nanocarriers for gene delivery. In *Biotechnology Advances* (Vol. 31, Issue 5). https://doi.org/10.1016/j.biotechadv.2013.01.005

Gao, G., Vandenberghe, L. H., Alvira, M. R., Lu, Y., Calcedo, R., Zhou, X., & Wilson, J. M. (2004). Clades of Adeno-Associated Viruses Are Widely Disseminated in Human Tissues. *Journal of Virology*, *78*(12). https://doi.org/10.1128/jvi.78.12.6381-6388.2004

Garcia, J. G. N., Davis, H. W., & Patterson, C. E. (1995). Regulation of endothelial cell gap formation and barrier dysfunction: Role of myosin light chain phosphorylation. *Journal of Cellular Physiology*, *163*(3). https://doi.org/10.1002/jcp.1041630311

Gaudet, D., Méthot, J., Déry, S., Brisson, D., Essiembre, C., Tremblay, G., Tremblay, K., De Wal, J., Twisk, J., Van Den Bulk, N., Sier-Ferreira, V., & Van Deventer, S. (2013). Efficacy and long-term safety of alipogene tiparvovec (AAV1-LPL S447X) gene therapy for lipoprotein lipase deficiency: An open-label trial. *Gene Therapy*, *20*(4). https://doi.org/10.1038/gt.2012.43

Giacca, M. (2011). Introduzione alla terapia genica. In *Terapia Genica*. https://doi.org/10.1007/978-88-470-1989-8_1

Gil-Farina, I., Fronza, R., Kaeppel, C., Lopez-Franco, E., Ferreira, V., D'Avola, D., Benito, A., Prieto, J., Petry, H., Gonzalez-Aseguinolaza, G., & Schmidt, M. (2016). Recombinant AAV Integration Is Not Associated with Hepatic Genotoxicity in Nonhuman Primates and Patients. *Molecular Therapy*, *24*(6). https://doi.org/10.1038/mt.2016.52

Ginn, S. L., Amaya, A. K., Alexander, I. E., Edelstein, M., & Abedi, M. R. (2018). Gene therapy clinical trials worldwide to 2017: An update. In *Journal of Gene Medicine* (Vol. 20, Issue 5). https://doi.org/10.1002/jgm.3015

Girod, A., Ried, M., Wobus, C., Lahm, H., Leike, K., Kleinschmidt, J., Deléage, G., & Hallek, M. (1999). Genetic capsid modifications allow efficient re-targeting of adeno- associated virus type 2. *Nature Medicine*, *5*(9). https://doi.org/10.1038/12491

Girod, A., Wobus, C. E., Zádori, Z., Ried, M., Leike, K., Tijssen, P., Kleinschmidt, J. A., & Hallek, M. (2002). The VP1 capsid protein of adeno-associated virus type 2 is carrying a phospholipase A2 domain required for virus infectivity. *Journal of General Virology*, *83*(5). https://doi.org/10.1099/0022-1317-83-5-973

Goeddel, D. V., Heyneker, H. L., Hozumi, T., Arentzen, R., Itakura, K., Yansura, D. G., Ross, M. J., Miozzari, G., Crea, R., & Seeburg, P. H. (1979). Direct expression in Escherichia coli of a DNA sequence coding for human growth hormone. *Nature*, *281*(5732). https://doi.org/10.1038/281544a0

Goldstein, I. J., Winter, H. C., & Poretz, R. D. (1997). Chapter 12 Plant Lectins: tools for the Study of Complex Carbohydrates. In *New Comprehensive Biochemistry* (Vol. 29, Issue PART B). https://doi.org/10.1016/S0167-7306(08)60625-0

Gorbatyuk, O. S., Warrington, K. H., Gorbatyuk, M. S., Zolotukhin, I., Lewin, A. S., & Muzyczka, N. (2019). Biodistribution of adeno-associated virus type 2 with mutations in the capsid that contribute to heparan sulfate proteoglycan binding. *Virus Research*, *274*. https://doi.org/10.1016/j.virusres.2019.197771

Gray, S. J., Nagabhushan Kalburgi, S., McCown, T. J., & Jude Samulski, R. (2013). Global CNS gene delivery and evasion of anti-AAV-neutralizing antibodies by intrathecal AAV administration in non-human primates. *Gene Therapy*, *20*(4). https://doi.org/10.1038/gt.2012.101

Gruh, I., Wunderlich, S., Winkler, M., Schwanke, K., Heinke, J., Blömer, U., Ruhparwar, A., Rohde, B., Li, R. K., Haverich, A., & Martin, U. (2008). Human CMV immediate-early enhancer: A useful tool to enhance cell-type-specific expression from lentiviral vectors. *Journal of Gene Medicine*, *10*(1). https://doi.org/10.1002/jgm.1122

Guy, J., Feuer, W. J., Davis, J. L., Porciatti, V., Gonzalez, P. J., Koilkonda, R. D., Yuan, H., Hauswirth, W. W., & Lam, B. L. (2017). Gene Therapy for Leber Hereditary Optic Neuropathy: Low- and Medium-Dose Visual Results. *Ophthalmology*, *124*(11). https://doi.org/10.1016/j.ophtha.2017.05.016

Hacker, U., & Büning, H. (2011). Optimizing the adeno-associated viral vector system: A brief summary. In *Therapeutic Delivery* (Vol. 2, Issue 8). https://doi.org/10.4155/tde.11.69

Han, S. O., Mahato, R. I., Sung, Y. K., & Kim, S. W. (2000). Development of biomaterials for gene therapy. In *Molecular Therapy* (Vol. 2, Issue 4). https://doi.org/10.1006/mthe.2000.0142

Hansen, J., Qing, K., Kwon, H.-J., Mah, C., & Srivastava, A. (2000). Impaired Intracellular Trafficking of Adeno-Associated Virus Type 2 Vectors Limits Efficient Transduction of Murine Fibroblasts. *Journal of Virology*, *74*(2). https://doi.org/10.1128/jvi.74.2.992-996.2000

Hartono, S. B., Gu, W., Kleitz, F., Liu, J., He, L., Middelberg, A. P. J., Yu, C., Lu, G. Q., & Qiao, S. Z. (2012). Poly-L-lysine functionalized large pore cubic mesostructured silica nanoparticles as biocompatible carriers for gene delivery. *ACS Nano*, *6*(3). https://doi.org/10.1021/nn2039643

Heape, A. M., Boiron, F., & Cassagne, C. (1986). Technique for injection into the sciatic nerve of the mouse for quantitative in vivo metabolic studies. *Analytical Biochemistry*, *155*(1). https://doi.org/10.1016/0003-2697(86)90220-4

Helal, N. A., Osami, A., Helmy, A., McDonald, T., Shaaban, L. A., & Nounou, M. I. (2017). Non-viral gene delivery systems: Hurdles for bench-to-bedside transformation. In *Pharmazie* (Vol. 72, Issue 11). https://doi.org/10.1691/ph.2017.7092

Hermonat, P. L., & Muzyczka, N. (1984). Use of adeno-associated virus as a mammalian DNA cloning vector: Transduction of neomycin resistance into mammalian tissue culture cells. *Proceedings of the National Academy of Sciences of the United States of America*, *81*(20 I). https://doi.org/10.1073/pnas.81.20.6466

Hileman, R. E., Fromm, J. R., Weiler, J. M., & Linhardt, R. J. (1998). Glycosaminoglycan-protein interactions: Definition of consensus sites in glycosaminoglycan binding proteins. In *BioEssays* (Vol. 20, Issue 2). https://doi.org/10.1002/(SICI)1521-1878(199802)20:2<156::AID-BIES8>3.0.CO;2-R

Hoggan, M. D., Blacklow, N. R., & Rowe, W. P. (1966). Studies of small DNA viruses found in various adenovirus preparations: physical, biological, and immunological characteristics. *Proceedings of the National Academy of Sciences of the United States of America*, *55*(6). https://doi.org/10.1073/pnas.55.6.1467

Hollenberg, M. D., Mihara, K., Polley, D., Suen, J. Y., Han, A., Fairlie, D. P., & Ramachandran, R. (2014). Biased signalling and proteinase-activated receptors (PARs): Targeting inflammatory disease. In *British Journal of Pharmacology* (Vol. 171, Issue 5). https://doi.org/10.1111/bph.12544

Hordeaux, J., Wang, Q., Katz, N., Buza, E. L., Bell, P., & Wilson, J. M. (2018). The Neurotropic Properties of AAV-PHP.B Are Limited to C57BL/6J Mice. In *Molecular Therapy* (Vol. 26, Issue 3). https://doi.org/10.1016/j.ymthe.2018.01.018

Hörner, M., Kaufmann, B., Cotugno, G., Wiedtke, E., Büning, H., Grimm, D., & Weber, W. (2014). A chemical switch for controlling viral infectivity. *Chemical Communications*, *50*(71). https://doi.org/10.1039/c4cc03292f

Hory-Lee, F., Russell, M., Lindsay, R. M., & Frank, E. (1993). Neurotrophin 3 supports the survival of developing muscle sensory neurons in culture. *Proceedings of the National Academy of Sciences of the United States of America*, *90*(7). https://doi.org/10.1073/pnas.90.7.2613

Huang, L. Y., Halder, S., & Agbandje-Mckenna, M. (2014). Parvovirus glycan interactions. In *Current Opinion in Virology* (Vol. 7, Issue 1). https://doi.org/10.1016/j.coviro.2014.05.007

Huber, T., Naganathan, S., Tian, H., Ye, S., & Sakmar, T. P. (2013). Unnatural amino acid mutagenesis of GPCRs using amber codon suppression and bioorthogonal labeling. In *Methods in Enzymology* (Vol. 520). https://doi.org/10.1016/B978-0-12-391861-1.00013-7

Huisgen, R. (1963). 1.3-Dipolare Cycloadditionen Rückschau und Ausblick. *Angewandte Chemie*, *75*(13). https://doi.org/10.1002/ange.19630751304

Hutton, L. A., DeVellis, J., & Perez-Polo, J. R. (1992). Expression of p75NGFR trkA, and trkB mRNA in rat C6 glioma and type I astrocyte cultures. *Journal of Neuroscience Research*, *32*(3). https://doi.org/10.1002/jnr.490320309

Jensen, T. S., Baron, R., Haanpää, M., Kalso, E., Loeser, J. D., Rice, A. S. C., & Treede, R. D. (2011). A new definition of neuropathic pain. In *Pain* (Vol. 152, Issue 10). https://doi.org/10.1016/j.pain.2011.06.017

john wiley, & sons Ltd. (2017). Gene Therapy Clinical Trials Worldwide. In *The Journal of Gene Medicine*.

Johnson, J. S., & Samulski, R. J. (2009). Enhancement of Adeno-Associated Virus Infection by Mobilizing Capsids into and Out of the Nucleolus. *Journal of Virology*, *83*(6). https://doi.org/10.1128/jvi.02309-08

Juliano, R. L. (2016). The delivery of therapeutic oligonucleotides. In *Nucleic Acids Research* (Vol. 44, Issue 14). https://doi.org/10.1093/nar/gkw236

Kawabata, K., Takakura, Y., & Hashida, M. (1995). The Fate of Plasmid DNA After Intravenous Injection in Mice: Involvement of Scavenger Receptors in Its Hepatic Uptake. *Pharmaceutical Research: An Official Journal of the American Association of Pharmaceutical Scientists*, *12*(6). https://doi.org/10.1023/A:1016248701505

Kelly, J. J., Moore, T. M., Babal, P., Diwan, A. H., Stevens, T., & Thompson, W. J. (1998). Pulmonary microvascular and macrovascular endothelial cells: Differential regulation of Ca2+ and permeability. *American Journal of Physiology - Lung Cellular and Molecular Physiology*, *274*(5 18-5). https://doi.org/10.1152/ajplung.1998.274.5.l810

Keppler, A., Gendreizig, S., Gronemeyer, T., Pick, H., Vogel, H., & Johnsson, K. (2003). A general method for the covalent labeling of fusion proteins with small molecules in vivo. *Nature Biotechnology*, *21*(1). https://doi.org/10.1038/nbt765

Khan, N., & Smith, M. T. (2015). Neurotrophins and neuropathic pain: Role in pathobiology. *Molecules*, *20*(6). https://doi.org/10.3390/molecules200610657

Kolb, H. C., Finn, M. G., & Sharpless, K. B. (2001). Click Chemistry: Diverse Chemical Function from a Few Good Reactions. In *Angewandte Chemie - International Edition* (Vol. 40, Issue 11). https://doi.org/10.1002/1521-3773(20010601)40:11<2004::AID-ANIE2004>3.0.CO;2-5

Kress, M., Hüttenhofer, A., Landry, M., Kuner, R., Favereaux, A., Greenberg, D., Bednarik, J., Heppenstall, P., Kronenberg, F., Malcangio, M., Rittner, H., Üçeyler, N., Trajanoski, Z., Mouritzen, P., Birklein, F., Sommer, C., & Soreq, H. (2013). microRNAs in nociceptive circuits as predictors of future clinical applications. In *Frontiers in Molecular Neuroscience* (Vol. 6, Issue OCT). https://doi.org/10.3389/fnmol.2013.00033

Kreuger, J., & Kjellén, L. (2012). Heparan Sulfate Biosynthesis: Regulation and Variability. *Journal of Histochemistry and Cytochemistry*, *60*(12). https://doi.org/10.1369/0022155412464972

Kumar, V., Gupta, A. K., Shukla, R. K., Tripathi, V. K., Jahan, S., Pandey, A., Srivastava, A., Agrawal, M., Yadav, S., Khanna, V. K., & Pant, A. B. (2020). Author Correction: Molecular Mechanism of Switching of TrkA/p75NTR Signaling in Monocrotophos Induced Neurotoxicity. *Scientific Reports*, *10*(1). https://doi.org/10.1038/s41598-020-63175-5

Lambiase, A., Bracci-Laudiero, L., Bonini, S., Bonini, S., Starace, G., D'Elios, M. M., De Carli, M., & Aloe, L. (1997). Human CD4+ T cell clones produce and release nerve growth factor and express high-affinity nerve growth factor receptors. *Journal of Allergy and Clinical Immunology*, *100*(3). https://doi.org/10.1016/S0091-6749(97)70256-2

Laughlin, C. A., Jones, N., & Carter, B. J. (1982). Effect of deletions in adenovirus early region 1 genes upon replication of adeno-associated virus. *Journal of Virology*, *41*(3). https://doi.org/10.1128/jvi.41.3.868-876.1982

Le Pichon, C. E., & Chesler, A. T. (2014). The functional and anatomical dissection of somatosensory subpopulations using mouse genetics. In *Frontiers in Neuroanatomy* (Vol. 8, Issue APR). https://doi.org/10.3389/fnana.2014.00021

Ledsgaard, L., Kilstrup, M., Karatt-Vellatt, A., McCafferty, J., & Laustsen, A. H. (2018). Basics of antibody phage display technology. In *Toxins* (Vol. 10, Issue 6). https://doi.org/10.3390/toxins10060236

Lee, G. K., Maheshri, N., Kaspar, B., & Schaffer, D. V. (2005). PEG conjugation moderately protects adeno-associated viral vectors against antibody neutralization. *Biotechnology and Bioengineering*, *92*(1). https://doi.org/10.1002/bit.20562

Letrou-Bonneval, E., Chèvre, R., Lambert, O., Costet, P., André, C., Tellier, C., & Pitard, B. (2008). Galactosylated multimodular lipoplexes for specific gene transfer into primary hepatocytes. *Journal of Gene Medicine*, *10*(11). https://doi.org/10.1002/jgm.1212

Li, C., & Samulski, R. J. (2020). Engineering adeno-associated virus vectors for gene therapy. In *Nature Reviews Genetics* (Vol. 21, Issue 4). https://doi.org/10.1038/s41576-019-0205-4

Liechtenstein, T., Perez-Janices, N., & Escors, D. (2013). Lentiviral vectors for cancer immunotherapy and clinical applications. In *Cancers* (Vol. 5, Issue 3). https://doi.org/10.3390/cancers5030815

Liu, Y., Mounkes, L. C., Liggitt, H. D., Brown, C. S., Solodin, I., Heath, T. D., & Debs, R. J. (1997). Factors influencing the efficiency of cationic liposome-mediated intravenous gene delivery. *Nature Biotechnology*, *15*(2). https://doi.org/10.1038/nbt0297-167

Liuzzi, A., Angeletti, P. U., & Levi-Montalcini, R. (1965). METABOLIC EFFECTS OF A SPECIFIC NERVE GROWTH FACTOR (NGF) ON SENSORY AND SYMPATHETIC GANGLIA: ENHANCEMENT OF LIPID BIOSYNTHESIS. *Journal of Neurochemistry*, *12*(8). https://doi.org/10.1111/j.1471-4159.1965.tb06784.x

Loberg, R. D., Tantivejkul, K., Craig, M., Neeley, C. K., & Pienta, K. J. (2007). PAR1-mediated RhoA activation facilitates CCL2-induced chemotaxis in PC-3 cells. *Journal of Cellular Biochemistry*, *101*(5). https://doi.org/10.1002/jcb.21252

Logunov, D. Y., Dolzhikova, I. V., Shcheblyakov, D. V., Tukhvatulin, A. I., Zubkova, O. V., Dzharullaeva, A. S., Kovyrshina, A. V., Lubenets, N. L., Grousova, D. M., Erokhova, A. S., Botikov, A. G., Izhaeva, F. M., Popova, O., Ozharovskaya, T. A., Esmagambetov, I. B., Favorskaya, I. A., Zrelkin, D. I., Voronina, D. V., Shcherbinin, D. N., … Gintsburg, A. L. (2021). Safety and efficacy of an rAd26 and rAd5 vector-based heterologous prime-boost COVID-19 vaccine: an interim analysis of a randomised controlled phase 3 trial in Russia. *The Lancet*, *397*(10275). https://doi.org/10.1016/S0140-6736(21)00234-8

Luo, Y., Zhang, B., Whent, M., Yu, L. L., & Wang, Q. (2011). Preparation and characterization of zein/chitosan complex for encapsulation of α-tocopherol, and its in vitro controlled release study. *Colloids and Surfaces B: Biointerfaces*, *85*(2). https://doi.org/10.1016/j.colsurfb.2011.02.020

Machida, T., Dohgu, S., Takata, F., Matsumoto, J., Kimura, I., Koga, M., Nakamoto, K., Yamauchi, A., & Kataoka, Y. (2017). Role of thrombin-PAR1-PKCθ/δ axis in brain pericytes in thrombin-induced MMP-9 production and blood–brain barrier dysfunction in vitro. *Neuroscience*, *350*. https://doi.org/10.1016/j.neuroscience.2017.03.026

Maheshri, N., Koerber, J. T., Kaspar, B. K., & Schaffer, D. V. (2006). Directed evolution of adeno-associated virus yields enhanced gene delivery vectors. *Nature Biotechnology*, *24*(2). https://doi.org/10.1038/nbt1182

Makhlof, A., Fujimoto, S., Tozuka, Y., & Takeuchi, H. (2011). In vitro and in vivo evaluation of WGA-carbopol modified liposomes as carriers for oral peptide delivery. *European Journal of Pharmaceutics and Biopharmaceutics*, *77*(2). https://doi.org/10.1016/j.ejpb.2010.12.008

Malmberg, A. B., Brandon, E. P., Idzerda, R. L., Liu, H., McKnight, G. S., & Basbaum, A. I. (1997). Diminished inflammation and nociceptive pain with preservation of neuropathic pain in mice with a targeted mutation of the type I regulatory subunit of cAMP-dependent protein kinase. *Journal of Neuroscience*, *17*(19). https://doi.org/10.1523/jneurosci.17-19-07462.1997

Manno, C. S., Arruda, V. R., Pierce, G. F., Glader, B., Ragni, M., Rasko, J., Ozelo, M. C., Hoots, K., Blatt, P., Konkle, B., Dake, M., Kaye, R., Razavi, M., Zajko, A., Zehnder, J., Nakai, H., Chew, A., Leonard, D., Wright, J. F., … Kay, M. A. (2006). Successful transduction of liver in hemophilia by AAV-Factor IX and limitations imposed by the host immune response. *Nature Medicine*, *12*(3). https://doi.org/10.1038/nm1358

Mashel, T. V., Tarakanchikova, Y. V., Muslimov, A. R., Zyuzin, M. V., Timin, A. S., Lepik, K. V., & Fehse, B. (2020). Overcoming the delivery problem for therapeutic genome editing: Current status and perspective of non-viral methods. In *Biomaterials* (Vol. 258). https://doi.org/10.1016/j.biomaterials.2020.120282

Maude, S. L., Frey, N., Shaw, P. A., Aplenc, R., Barrett, D. M., Bunin, N. J., Chew, A., Gonzalez, V. E., Zheng, Z., Lacey, S. F., Mahnke, Y. D., Melenhorst, J. J., Rheingold, S. R., Shen, A., Teachey, D. T., Levine, B. L., June, C. H., Porter, D. L., & Grupp, S. A. (2014). Chimeric Antigen Receptor T Cells for Sustained Remissions in Leukemia. *New England Journal of Medicine*, *371*(16). https://doi.org/10.1056/nejmoa1407222

McCarty, D. M., Fu, H., Monahan, P. E., Toulson, C. E., Naik, P., & Samulski, R. J. (2003). Adeno-associated virus terminal repeat (TR) mutant generates self-complementary vectors to overcome the rate-limiting step to transduction in vivo. *Gene Therapy*, *10*(26). https://doi.org/10.1038/sj.gt.3302134

McCarty, Douglas M., Young, S. M., & Samulski, R. J. (2004). Integration of adeno-associated virus (AAV) and recombinant AAV vectors. In *Annual Review of Genetics* (Vol. 38). https://doi.org/10.1146/annurev.genet.37.110801.143717

McClure, C., Cole, K. L. H., Wulff, P., Klugmann, M., & Murray, A. J. (2011). Production and titering of recombinant adeno-associated viral vectors. *Journal of Visualized Experiments*, *57*. https://doi.org/10.3791/3348

McDonald, N. Q., Lapatto, R., Rust, J. M., Gunning, J., Wlodawer, A., & Blundell, T. L. (1991). New protein fold revealed by a 2.3-Å resolution crystal structure of nerve growth factor. *Nature*, *354*(6352). https://doi.org/10.1038/354411a0

McGhee, J., Bailey, B., Parton, R. G., Ariotti, N., & Johnston, A. (2016). *Journey to the centre of the cell (JTCC)*. https://doi.org/10.1145/2996376.2996385

McKelvey, L., Shorten, G. D., & O'Keeffe, G. W. (2013). Nerve growth factor-mediated regulation of pain signalling and proposed new intervention strategies in clinical pain management. In *Journal of Neurochemistry* (Vol. 124, Issue 3). https://doi.org/10.1111/jnc.12093

McLaughlin, J. N., Shen, L., Holinstat, M., Brooks, J. D., DiBenedetto, E., & Hamm, H. E. (2005). Functional selectivity of G protein signaling by agonist peptides and thrombin for the protease-activated receptor-1. *Journal of Biological Chemistry*, *280*(26). https://doi.org/10.1074/jbc.M414090200

Melim, C., Jarak, I., Veiga, F., & Figueiras, A. (2020). The potential of micelleplexes as a therapeutic strategy for osteosarcoma disease. In *3 Biotech* (Vol. 10, Issue 4). https://doi.org/10.1007/s13205-020-2142-5

Mével, M., Bouzelha, M., Leray, A., Pacouret, S., Guilbaud, M., Penaud-Budloo, M., Alvarez-Dorta, D., Dubreil, L., Gouin, S. G., Combal, J. P., Hommel, M., Gonzalez-Aseguinolaza, G., Blouin, V., Moullier, P., Adjali, O., Deniaud, D., & Ayuso, E. (2020). Chemical modification of the adeno-associated virus capsid to improve gene delivery. *Chemical Science*, *11*(4). https://doi.org/10.1039/c9sc04189c

Miao, C. H., Thompson, A. R., Loeb, K., & Ye, X. (2001). Long-term and therapeutic-level hepatic gene expression of human factor IX after naked plasmid transfer in vivo. *Molecular Therapy*, *3*(6). https://doi.org/10.1006/mthe.2001.0333

Michelfelder, S., Varadi, K., Raupp, C., Hunger, A., Körbelin, J., Pahrmann, C., Schrepfer, S., Müller, O. J., Kleinschmidt, J. A., & Trepel, M. (2011). Peptide ligands incorporated into the threefold spike capsid domain to re-direct gene transduction of AAV8 and AAV9 in vivo. *PLoS ONE*, *6*(8). https://doi.org/10.1371/journal.pone.0023101

Milone, M. C., & O'Doherty, U. (2018). Clinical use of lentiviral vectors. In *Leukemia* (Vol. 32, Issue 7). https://doi.org/10.1038/s41375-018-0106-0

Modlich, U., Navarro, S., Zychlinski, D., Maetzig, T., Knoess, S., Brugman, M. H., Schambach, A., Charrier, S., Galy, A., Thrasher, A. J., Bueren, J., & Baum, C. (2009). Insertional transformation of hematopoietic cells by self-inactivating lentiviral and gammaretroviral vectors. *Molecular Therapy*, *17*(11). https://doi.org/10.1038/mt.2009.179

Morioka, T., Kalehua, A. N., & Streit, W. J. (1993). Characterization of microglial reaction after middle cerebral artery occlusion in rat brain. *Journal of Comparative Neurology*, *327*(1). https://doi.org/10.1002/cne.903270110

Müller, O. J., Kaul, F., Weitzman, M. D., Pasqualini, R., Arap, W., Kleinschmidt, J. A., & Trepel, M. (2003). Random peptide libraries displayed on adeno-associated virus to select for targeted gene therapy vectors. *Nature Biotechnology*, *21*(9). https://doi.org/10.1038/nbt856

Münch, R. C., Muth, A., Muik, A., Friedel, T., Schmatz, J., Dreier, B., Trkola, A., Plückthun, A., Büning, H., & Buchholz, C. J. (2015). Off-target-free gene delivery by affinity-purified receptor-targeted viral vectors. *Nature Communications*, *6*. https://doi.org/10.1038/ncomms7246

Musatov, S., Roberts, J., Pfaff, D., & Kaplitt, M. (2002). A cis -Acting Element That Directs Circular Adeno-Associated Virus Replication and Packaging . *Journal of Virology*, *76*(24). https://doi.org/10.1128/jvi.76.24.12792-12802.2002

Myers, M. W., & Carter, B. J. (1980). Assembly of adeno-associated virus. *Virology*, *102*(1). https://doi.org/10.1016/0042-6822(80)90071-9

Nayerossadat, N., Ali, P., & Maedeh, T. (2012). Viral and nonviral delivery systems for gene delivery. *Advanced Biomedical Research*, *1*(1). https://doi.org/10.4103/2277-9175.98152

Nicolson, S. C., & Samulski, R. J. (2014). Recombinant Adeno-Associated Virus Utilizes Host Cell Nuclear Import Machinery To Enter the Nucleus. *Journal of Virology*, *88*(8). https://doi.org/10.1128/jvi.02660-13

Niethammer, A. G., Xiang, R., Becker, J. C., Wodrich, H., Pertl, U., Karsten, G., Eliceiri, B. P., & Reisfeld, R. A. (2002). A DNA vaccine against VEGF receptor 2 prevents effective angiogenesis and inhibits tumor growth. *Nature Medicine*, *8*(12). https://doi.org/10.1038/nm794

Nieuwenhuis, B., Haenzi, B., Hilton, S., Carnicer-Lombarte, A., Hobo, B., Verhaagen, J., & Fawcett, J. W. (2021). Optimization of adeno-associated viral vector-mediated transduction of the corticospinal tract: comparison of four promoters. *Gene Therapy*, *28*(1–2). https://doi.org/10.1038/s41434-020-0169-1

Ning, X., Guo, J., Wolfert, M. A., & Boons, G. J. (2008). Visualizing metabolically labeled glycoconjugates of living cells by copper-free and fast huisgen cycloadditions. *Angewandte Chemie - International Edition*, *47*(12). https://doi.org/10.1002/anie.200705456

Nocchi, L., Portulano, C., Franciosa, F., Doleschall, B., Panea, M., Roy, N., Maffei, M., Gargano, A., Perlas, E., & Heppenstall, P. A. (2019). Nerve growth factor-mediated photoablation of nociceptors reduces pain behavior in mice. *Pain*, *160*(10). https://doi.org/10.1097/j.pain.0000000000001620

Nonnenmacher, M., & Weber, T. (2012). Intracellular transport of recombinant adeno-associated virus vectors. In *Gene Therapy* (Vol. 19, Issue 6). https://doi.org/10.1038/gt.2012.6

Nonnenmacher, Mathieu, & Weber, T. (2011). Adeno-associated virus 2 infection requires endocytosis through the CLIC/GEEC pathway. *Cell Host and Microbe*, *10*(6). https://doi.org/10.1016/j.chom.2011.10.014

O'Shea, C. C., Johnson, L., Bagus, B., Choi, S., Nicholas, C., Shen, A., Boyle, L., Pandey, K., Soria, C., Kunich, J., Shen, Y., Habets, G., Ginzinger, D., & McCormick, F. (2004). Late viral RNA export, rather than p53 inactivation, determines ONYX-015 tumor selectivity. *Cancer Cell*, *6*(6). https://doi.org/10.1016/j.ccr.2004.11.012

Opie, S. R., Warrington, K. H., Agbandje-McKenna, M., Zolotukhin, S., & Muzyczka, N. (2003). Identification of Amino Acid Residues in the Capsid Proteins of Adeno-Associated Virus Type 2 That Contribute to Heparan Sulfate Proteoglycan Binding. *Journal of Virology*, *77*(12). https://doi.org/10.1128/jvi.77.12.6995-7006.2003

Park, J. H., & Park, H. J. (2017). Botulinum toxin for the treatment of neuropathic pain. In *Toxins* (Vol. 9, Issue 9). https://doi.org/10.3390/toxins9090260

Perabo, L., Büning, H., Kofler, D. M., Ried, M. U., Girod, A., Wendtner, C. M., Enssle, J., & Hallek, M. (2003). In vitro selection of viral vectors with modified tropism: The adeno-associated virus display. *Molecular Therapy*, *8*(1). https://doi.org/10.1016/S1525-0016(03)00123-0

Pereira, D. J., McCarty, D. M., & Muzyczka, N. (1997). The adeno-associated virus (AAV) Rep protein acts as both a repressor and an activator to regulate AAV transcription during a productive infection. *Journal of Virology*, *71*(2). https://doi.org/10.1128/jvi.71.2.1079-1088.1997

Pillay, S., Meyer, N. L., Puschnik, A. S., Davulcu, O., Diep, J., Ishikawa, Y., Jae, L. T., Wosen, J. E., Nagamine, C. M., Chapman, M. S., & Carette, J. E. (2016). An essential receptor for adeno-associated virus infection. *Nature*, *530*(7588). https://doi.org/10.1038/nature16465

Plank, C., Scherer, F., Schillinger, U., Bergemann, C., & Anton, M. (2003). Magnetofection: Enhancing and targeting gene delivery with superparamagnetic nanoparticles and magnetic fields. *Journal of Liposome Research*, *13*(1). https://doi.org/10.1081/LPR-120017486

Plattner, V. E., Wagner, M., Ratzinger, G., Gabor, F., & Wirth, M. (2008). Targeted drug delivery: Binding and uptake of plant lectins using human 5637 bladder cancer cells. *European Journal of Pharmaceutics and Biopharmaceutics*, *70*(2). https://doi.org/10.1016/j.ejpb.2008.06.004

Pontarollo, G., Mann, A., Brandão, I., Malinarich, F., Schöpf, M., & Reinhardt, C. (2020). Protease-activated receptor signaling in intestinal permeability regulation. In *FEBS Journal* (Vol. 287, Issue 4). https://doi.org/10.1111/febs.15055

Potter, H., & Heller, R. (2018). Transfection by electroporation. *Current Protocols in Molecular Biology*, *2018*. https://doi.org/10.1002/cpmb.48

Pringle, I. A., Hyde, S. C., & Gill, D. R. (2009). Non-viral vectors in cystic fibrosis gene therapy: Recent developments and future prospects. In *Expert Opinion on Biological Therapy* (Vol. 9, Issue 8). https://doi.org/10.1517/14712590903055029

Ramamoorth, M., & Narvekar, A. (2015). Non viral vectors in gene therapy - An overview. In *Journal of Clinical and Diagnostic Research* (Vol. 9, Issue 1). https://doi.org/10.7860/JCDR/2015/10443.5394

Rogers, G. L., Martino, A. T., Aslanidi, G. V., Jayandharan, G. R., Srivastava, A., & Herzog, R. W. (2011). Innate immune responses to AAV vectors. *Frontiers in Microbiology*, *2*(SEP). https://doi.org/10.3389/fmicb.2011.00194

Roque, A. C. A., Lowe, C. R., & Taipa, M. Â. (2004). Antibodies and genetically engineered related molecules: Production and purification. In *Biotechnology Progress* (Vol. 20, Issue 3). https://doi.org/10.1021/bp030070k

Rosano, G. L., & Ceccarelli, E. A. (2014). Recombinant protein expression in Escherichia coli: Advances and challenges. In *Frontiers in Microbiology* (Vol. 5, Issue APR). https://doi.org/10.3389/fmicb.2014.00172

Rose, J. A., Berns, K. I., Hoggan, M. D., & Koczot, F. J. (1969). Evidence for a single-stranded adenovirus-associated virus genome: formation of a DNA density hybrid on release of viral DNA. *Proceedings of the National Academy of Sciences of the United States of America*, *64*(3). https://doi.org/10.1073/pnas.64.3.863

Rowe, W. P., Huebner, R. J., Gilmore, L. K., Parrott, R. H., & Ward, T. G. (1953). Isolation of a Cytopathogenic Agent from Human Adenoids Undergoing Spontaneous Degeneration in Tissue Culture. *Proceedings of the Society for Experimental Biology and Medicine*, *84*(3). https://doi.org/10.3181/00379727-84-20714

Rutledge, E. A., & Russell, D. W. (1997). Adeno-associated virus vector integration junctions. *Journal of Virology*, *71*(11). https://doi.org/10.1128/jvi.71.11.8429-8436.1997

Ryan, J. H., Zolotukhin, S., & Muzyczka, N. (1996). Sequence requirements for binding of Rep68 to the adeno-associated virus terminal repeats. *Journal of Virology*, *70*(3). https://doi.org/10.1128/jvi.70.3.1542-1553.1996

Rybniker, J., Nowag, A., Janicki, H., Demant, K., Hartmann, P., & Buning, H. (2012). Incorporation of Antigens into Viral Capsids Augments Immunogenicity of Adeno-Associated Virus Vector-

Based Vaccines. *Journal of Virology*, *86*(24). https://doi.org/10.1128/jvi.01708-12

Sadler, K. E., & Stucky, C. L. (2019). Neuronal transient receptor potential (TRP) channels and noxious sensory detection in sickle cell disease. In *Neuroscience Letters* (Vol. 694). https://doi.org/10.1016/j.neulet.2018.11.056

Sakarya, O., Armstrong, K. A., Adamska, M., Adamski, M., Wang, I. F., Tidor, B., Degnan, B. M., Oakley, T. H., & Kosik, K. S. (2007). A Post-Synaptic Scaffold at the Origin of the Animal Kingdom. *PLoS ONE*, *2*(6). https://doi.org/10.1371/journal.pone.0000506

Sanftner, L. M., Sommer, J. M., Suzuki, B. M., Smith, P. H., Vijay, S., Vargas, J. A., Forsayeth, J. R., Cunningham, J., Bankiewicz, K. S., Kao, H., Bernal, J., Pierce, G. F., & Johnson, K. W. (2005). AAV2-mediated gene delivery to monkey putamen: Evaluation of an infusion device and delivery parameters. *Experimental Neurology*, *194*(2). https://doi.org/10.1016/j.expneurol.2005.03.007

Sanlioglu, S., Benson, P. K., Yang, J., Atkinson, E. M., Reynolds, T., & Engelhardt, J. F. (2000). Endocytosis and Nuclear Trafficking of Adeno-Associated Virus Type 2 Are Controlled by Rac1 and Phosphatidylinositol-3 Kinase Activation. *Journal of Virology*, *74*(19). https://doi.org/10.1128/jvi.74.19.9184-9196.2000

Sanmiguel, J., Gao, G., & Vandenberghe, L. H. (2019). Quantitative and digital droplet-based AAV genome titration. In *Methods in Molecular Biology* (Vol. 1950). https://doi.org/10.1007/978-1-4939-9139-6_4

Sarasola, E., Rodríguez, J. A., Garrote, E., Arístegui, J., & García-Barcina, M. J. (2011). A short in-frame deletion in NTRK1 tyrosine kinase domain caused by a novel splice site mutation in a patient with congenital insensitivity to pain with anhidrosis. *BMC Medical Genetics*, *12*. https://doi.org/10.1186/1471-2350-12-86

Savić, N., & Schwank, G. (2016). Advances in therapeutic CRISPR/Cas9 genome editing. In *Translational Research* (Vol. 168). https://doi.org/10.1016/j.trsl.2015.09.008

Schuster, D. J., Dykstra, J. A., Riedl, M. S., Kitto, K. F., Belur, L. R., Scott McIvor, R., Elde, R. P., Fairbanks, C. A., & Vulchanova, L. (2014). Biodistribution of adeno-associated virus serotype 9 (AAV9) vector after intrathecal and intravenous delivery in mouse. *Frontiers in Neuroanatomy*, *8*(JUN). https://doi.org/10.3389/fnana.2014.00042

Schwab, M. E., Javoy-Agid, F., & Agid, Y. (1978). Labeled wheat germ agglutinin (WGA) as a new, highly sensitive retrograde tracer in the rat brain hippocampal system. *Brain Research*, *152*(1). https://doi.org/10.1016/0006-8993(78)90140-3

Schwarz, R. E., Wojciechowicz, D. C., Picon, A. I., Schwarz, M. A., & Paty, P. B. (1999). Wheatgerm agglutinin-mediated toxicity in pancreatic cancer cells. *British Journal of Cancer*, *80*(11). https://doi.org/10.1038/sj.bjc.6690593

Seisenberger, G., Ried, M. U., Endreß, T., Büning, H., Hallek, M., & Bräuchle, C. (2001). Real-time single-molecule imaging of the infection pathway of anadeno-associated virus. *Science*, *294*(5548). https://doi.org/10.1126/science.1064103

Sexton, J. E., Cox, J. J., Zhao, J., & Wood, J. N. (2018). The Genetics of Pain: Implications for Therapeutics. In *Annual Review of Pharmacology and Toxicology* (Vol. 58). https://doi.org/10.1146/annurev-pharmtox-010617-052554

Sharon, D., & Kamen, A. (2018). Advancements in the design and scalable production of viral gene transfer vectors. In *Biotechnology and Bioengineering* (Vol. 115, Issue 1). https://doi.org/10.1002/bit.26461

Shaw, K. L., & Kohn, D. B. (2011). A Tale of Two SCIDs. *Science Translational Medicine*, *3*(97). https://doi.org/10.1126/scitranslmed.3002594

Shen, S., Bryant, K. D., Brown, S. M., Randell, S. H., & Asokan, A. (2011). Terminal n-linked galactose is the primary receptor for adeno-associated virus. *Journal of Biological Chemistry*, *286*(15). https://doi.org/10.1074/jbc.M110.210922

Shinohara, Y., Hasegawa, Y., Kaku, H., & Shibuya, N. (1997). Elucidation of the mechanism enhancing the avidity of lectin with oligosaccharides on the solid phase surface. *Glycobiology*, *7*(8). https://doi.org/10.1093/glycob/7.8.1201

Sibbald, B. (2001). Death but one unintended consequence of gene-therapy trial. *CMAJ : Canadian Medical Association Journal = Journal de l''Association Medicale Canadienne*, *164*(11).

Sillitoe, R. V. (2016). Mossy Fibers Terminate Directly Within Purkinje Cell Zones During Mouse Development. *Cerebellum*, *15*(1). https://doi.org/10.1007/s12311-015-0712-6

Singh, D., Ambroise, A., Haicour, R., Sihachakr, D., & Rajam, M. V. (2014). Increased resistance to fungal wilts in transgenic eggplant expressing alfalfa glucanase gene. *Physiology and Molecular Biology of Plants*, *20*(2). https://doi.org/10.1007/s12298-014-0225-7

Sisignano, M., Parnham, M. J., & Geisslinger, G. (2019). Novel Approaches to Persistent Pain Therapy. In *Trends in Pharmacological Sciences* (Vol. 40, Issue 6). https://doi.org/10.1016/j.tips.2019.04.003

Sonntag, F., Kother, K., Schmidt, K., Weghofer, M., Raupp, C., Nieto, K., Kuck, A., Gerlach, B., Bottcher, B., Muller, O. J., Lux, K., Horer, M., & Kleinschmidt, J. A. (2011). The Assembly-Activating Protein Promotes Capsid Assembly of Different Adeno-Associated Virus Serotypes. *Journal of Virology*, *85*(23). https://doi.org/10.1128/jvi.05359-11

Sonntag, Florian, Bleker, S., Leuchs, B., Fischer, R., & Kleinschmidt, J. A. (2006). Adeno-Associated Virus Type 2 Capsids with Externalized VP1/VP2 Trafficking Domains Are Generated prior to Passage through the Cytoplasm and Are Maintained until Uncoating Occurs in the Nucleus. *Journal of Virology*, *80*(22). https://doi.org/10.1128/jvi.01056-06

Su, Y., Sun, B., Gao, X., Dong, X., Fu, L., Zhang, Y., Li, Z., Wang, Y., Jiang, H., & Han, B. (2020). Intranasal Delivery of Targeted Nanoparticles Loaded With miR-132 to Brain for the Treatment of Neurodegenerative Diseases. *Frontiers in Pharmacology*, *11*. https://doi.org/10.3389/fphar.2020.01165

Szok, D., Tajti, J., Nyári, A., & Vécsei, L. (2019). Therapeutic Approaches for Peripheral and Central Neuropathic Pain. In *Behavioural Neurology* (Vol. 2019). https://doi.org/10.1155/2019/8685954

Taghian, T., Marosfoi, M. G., Puri, A. S., Cataltepe, O. I., King, R. M., Diffie, E. B., Maguire, A. S., Martin, D. R., Fernau, D., Batista, A. R., Kuchel, T., Christou, C., Perumal, R., Chandra, S., Gamlin, P. D., Bertrand, S. G., Flotte, T. R., McKenna-Yasek, D., Tai, P. W. L., … Gray-Edwards, H. L. (2020). A Safe and Reliable Technique for CNS Delivery of AAV Vectors in the Cisterna Magna. *Molecular Therapy*, *28*(2). https://doi.org/10.1016/j.ymthe.2019.11.012

Tang, H., Kuhen, K. L., & Wong-Staal, F. (1999). Lentivirus replication and regulation. In *Annual Review of Genetics* (Vol. 33). https://doi.org/10.1146/annurev.genet.33.1.133

Thi, T. T. H., Pilkington, E. H., Nguyen, D. H., Lee, J. S., Park, K. D., & Truong, N. P. (2020). The importance of Poly(ethylene glycol) alternatives for overcoming PEG immunogenicity in drug delivery and bioconjugation. In *Polymers* (Vol. 12, Issue 2). https://doi.org/10.3390/polym12020298

Thomas, C. E., Storm, T. A., Huang, Z., & Kay, M. A. (2004). Rapid Uncoating of Vector Genomes Is the Key toEfficient Liver Transduction with Pseudotyped Adeno-Associated VirusVectors. *Journal of Virology*, *78*(6). https://doi.org/10.1128/jvi.78.6.3110-3122.2004

Tian, G., Liu, J., Zhou, J. S. R., & Chen, W. (2009). Multiple hepatic arterial injections of recombinant adenovirus p53 and 5-fluorouracil after transcatheter arterial chemoembolization for unresectable hepatocellular carcinoma: a pilot phase II trial. *Anti-Cancer Drugs*, *20*(5). https://doi.org/10.1097/cad.0b013e32832a2df9

Tolmachov, O. (2009). Designing plasmid vectors. *Methods in Molecular Biology*, *542*. https://doi.org/10.1007/978-1-59745-561-9_6

Trapani, I. (2019). Adeno-associated viral vectors as a tool for large gene delivery to the retina. *Genes*, *10*(4). https://doi.org/10.3390/genes10040287

Ugolini, G., Marinelli, S., Covaceuszach, S., Cattaneo, A., & Pavone, F. (2007). The function neutralizing anti-TrkA antibody MNAC13 reduces inflammatory and neuropathic pain. *Proceedings of the National Academy of Sciences of the United States of America*, *104*(8). https://doi.org/10.1073/pnas.0611253104

Vaillancourt, M. T., Atencio, I., Quijano, E., Howe, J. A., & Ramachandra, M. (2005). Inefficient killing of quiescent human epithelial cells by replicating adenoviruses: Potential implications for their use as oncolytic agents. *Cancer Gene Therapy*, *12*(8). https://doi.org/10.1038/sj.cgt.7700840

Van Der Want, J. J. L., Klooster, J., Nunes Cardozo, B., De Weerd, H., & Liem, R. S. B. (1997). Tract-tracing in the nervous system of vertebrates using horseradish peroxidase and its conjugates: Tracers, chromogens and stabilization for light and electron microscopy. *Brain Research Protocols*, *1*(3). https://doi.org/10.1016/S1385-299X(96)00042-6

Vance, K. M., Rogers, R. C., & Hermann, G. E. (2015). PAR1-activated astrocytes in the nucleus of the solitary tract stimulate adjacent neurons via NMDA receptors. *Journal of Neuroscience*, *35*(2). https://doi.org/10.1523/JNEUROSCI.3105-14.2015

Vesa, J., Kruttgen, A., & Shooter, E. M. (2000). p75 Reduces TrkB tyrosine autophosphorylation in response to brain-derived neurotrophic factor and neurotrophin 4/5. *Journal of Biological Chemistry*, *275*(32). https://doi.org/10.1074/jbc.M001641200

Von Banchet, G. S., & Schaible, H. G. (1999). Localization of the neurokinin 1 receptor on a subset of substance P-positive and isolectin B4-negative dorsal root ganglion neurons of the rat. *Neuroscience Letters*, *274*(3). https://doi.org/10.1016/S0304-3940(99)00719-3

Wälchli, T., Mateos, J. M., Weinman, O., Babic, D., Regli, L., Hoerstrup, S. P., Gerhardt, H., Schwab, M. E., & Vogel, J. (2015). Quantitative assessment of angiogenesis, perfused blood vessels and endothelial tip cells in the postnatal mouse brain. *Nature Protocols*, *10*(1). https://doi.org/10.1038/nprot.2015.002

Wang, D., Wang, K., & Cai, Y. (2020). An overview of development in gene therapeutics in China. In *Gene Therapy* (Vol. 27, Issues 7–8). https://doi.org/10.1038/s41434-020-0163-7

Wang, K., Guan, T., Cheresh, D. A., & Nemerow, G. R. (2000). Regulation of Adenovirus Membrane Penetration by the Cytoplasmic Tail of Integrin β5. *Journal of Virology*, *74*(6). https://doi.org/10.1128/jvi.74.6.2731-2739.2000

Warrington, K. H., Gorbatyuk, O. S., Harrison, J. K., Opie, S. R., Zolotukhin, S., & Muzyczka, N. (2004). Adeno-Associated Virus Type 2 VP2 Capsid Protein Is Nonessential and Can Tolerate Large Peptide Insertions at Its N Terminus. *Journal of Virology*, *78*(12). https://doi.org/10.1128/jvi.78.12.6595-6609.2004

Wei, F., McConnell, K. I., Yu, T. K., & Suh, J. (2012). Conjugation of paclitaxel on adeno-associated virus (AAV) nanoparticles for co-delivery of genes and drugs. *European Journal of Pharmaceutical Sciences*, *46*(3). https://doi.org/10.1016/j.ejps.2012.02.022

Weiss, B., Nitschko, H., Ghattas, I., Wright, R., & Schlesinger, S. (1989). Evidence for specificity in the encapsidation of Sindbis virus RNAs. *Journal of Virology*, *63*(12). https://doi.org/10.1128/jvi.63.12.5310-5318.1989

Wiesmann, C., & De Vos, A. M. (2001). Nerve growth factor: Structure and function. In *Cellular and Molecular Life Sciences* (Vol. 58, Issues 5–6). https://doi.org/10.1007/PL00000898

Wilmott, P., Lisowski, L., Alexander, I. E., & Logan, G. J. (2019). A User's Guide to the Inverted Terminal Repeats of Adeno-Associated Virus. *Human Gene Therapy Methods*, *30*(6). https://doi.org/10.1089/hgtb.2019.276

Wold, W., & Toth, K. (2014). Adenovirus Vectors for Gene Therapy, Vaccination and Cancer Gene Therapy. *Current Gene Therapy*, *13*(6). https://doi.org/10.2174/1566523213666131125095046

Wooddell, C. I., Reppen, T., Wolff, J. A., & Herweijer, H. (2008). Sustained liver-specific transgene expression from the albumin promoter in mice following hydrodynamic plasmid DNA delivery. *Journal of Gene Medicine*, *10*(5). https://doi.org/10.1002/jgm.1179

Woolf, C. J., Safieh-Garabedian, B., Ma, Q. P., Crilly, P., & Winter, J. (1994). Nerve growth factor contributes to the generation of inflammatory sensory hypersensitivity. *Neuroscience*, *62*(2). https://doi.org/10.1016/0306-4522(94)90366-2

Wu, J., Davis, M. D., & Owens, R. A. (1999). Factors Affecting the Terminal Resolution Site Endonuclease, Helicase, and ATPase Activities of Adeno-Associated Virus Type 2 Rep Proteins. *Journal of Virology*, *73*(10). https://doi.org/10.1128/jvi.73.10.8235-8244.1999

Wu, P., Xiao, W., Conlon, T., Hughes, J., Agbandje-McKenna, M., Ferkol, T., Flotte, T., & Muzyczka, N. (2000). Mutational Analysis of the Adeno-Associated Virus Type 2 (AAV2) Capsid Gene and Construction of AAV2 Vectors with Altered Tropism. *Journal of Virology*, *74*(18). https://doi.org/10.1128/jvi.74.18.8635-8647.2000

Wu, Y., Mei, T., Jiang, L., Han, Z., Dong, R., Yang, T., & Xu, F. (2019). Development of versatile and flexible sf9 packaging cell line-dependent onebac system for large-scale recombinant adeno-associated virus production. *Human Gene Therapy Methods*, *30*(5). https://doi.org/10.1089/hgtb.2019.123

Xiao, G., & Gan, L. S. (2013). Receptor-mediated endocytosis and brain delivery of therapeutic

biologics. In *International Journal of Cell Biology*. https://doi.org/10.1155/2013/703545

Xiao, W., Chirmule, N., Berta, S. C., Gao, G., Wilson, J. M., & Cullough, B. M. C. (1999). Gene Therapy Vectors Based on Adeno-Associated Virus Type 1 Gene Therapy Vectors Based on Adeno-Associated Virus Type 1. *Journal of Virological Methods*, *73*(5).

Xie, Q., Bu, W., Bhatia, S., Hare, J., Somasundaram, T., Azzi, A., & Chapman, M. S. (2002). The atomic structure of adeno-associated virus (AAV-2), a vector for human gene therapy. *Proceedings of the National Academy of Sciences of the United States of America*, *99*(16). https://doi.org/10.1073/pnas.162250899

Yan, Z., Lei-Butters, D. C. M., Zhang, Y., Zak, R., & Engelhardt, J. F. (2007). Hybrid adeno-associated virus bearing nonhomologous inverted terminal repeats enhances dual-vector reconstruction of minigenes in vivo. *Human Gene Therapy*, *18*(1). https://doi.org/10.1089/hum.2006.128

Yang, Q., Mamounas, M., Yu, G., Kennedy, S., Leaker, B., Merson, J., Wong-Staal, F., Yu, M., & Barber, J. R. (1998). Development of novel cell surface CD34-targeted recombinant adenoassociated virus vectors for gene therapy. *Human Gene Therapy*, *9*(13). https://doi.org/10.1089/hum.1998.9.13-1929

Yang, S., Xiao, Y., Kang, D., Liu, J., Li, Y., Undheim, E. A. B., Klint, J. K., Rong, M., Lai, R., & King, G. F. (2013). Discovery of a selective NaV1.7 inhibitor from centipede venom with analgesic efficacy exceeding morphine in rodent pain models. *Proceedings of the National Academy of Sciences of the United States of America*, *110*(43). https://doi.org/10.1073/pnas.1306285110

Yardeni, T., Eckhaus, M., Morris, H. D., Huizing, M., & Hoogstraten-Miller, S. (2011). Retro-orbital injections in mice. In *Lab Animal* (Vol. 40, Issue 5). https://doi.org/10.1038/laban0511-155

Yin, H., Kanasty, R. L., Eltoukhy, A. A., Vegas, A. J., Dorkin, J. R., & Anderson, D. G. (2014). Non-viral vectors for gene-based therapy. In *Nature Reviews Genetics* (Vol. 15, Issue 8). https://doi.org/10.1038/nrg3763

Yoshihara, Y. (2010). Visualization of selective transsynaptic neural pathways using a genetic method. *Brain and Nerve*, *62*(3).

Zhang, C., Yao, T., Zheng, Y., Li, Z., Zhang, Q., Zhang, L., & Zhou, D. (2016). Development of next generation adeno-associated viral vectors capable of selective tropism and efficient gene delivery. *Biomaterials*, *80*. https://doi.org/10.1016/j.biomaterials.2015.11.066

Zhang, Q., Zheng, Y. W., Coughlin, S. R., & Shu, X. (2018). A rapid fluorogenic GPCR–β-arrestin interaction assay. *Protein Science*, *27*(4). https://doi.org/10.1002/pro.3385

Zhang, R., Cao, L., Cui, M., Sun, Z., Hu, M., Zhang, R., Stuart, W., Zhao, X., Yang, Z., Li, X., Sun, Y., Li, S., Ding, W., Lou, Z., & Rao, Z. (2019). Adeno-associated virus 2 bound to its cellular receptor AAVR. *Nature Microbiology*, *4*(4). https://doi.org/10.1038/s41564-018-0356-7

Zhu, F. C., Li, Y. H., Guan, X. H., Hou, L. H., Wang, W. J., Li, J. X., Wu, S. P., Wang, B. Sen, Wang, Z., Wang, L., Jia, S. Y., Jiang, H. D., Wang, L., Jiang, T., Hu, Y., Gou, J. B., Xu, S. B., Xu, J. J., Wang, X. W., … Chen, W. (2020). Safety, tolerability, and immunogenicity of a recombinant adenovirus type-5 vectored COVID-19 vaccine: a dose-escalation, open-label, non-randomised, first-in-human trial. *The Lancet*, *395*(10240). https://doi.org/10.1016/S0140-6736(20)31208-3

Zylka, M. J. (2005). Nonpeptidergic circuits feel your pain. In *Neuron* (Vol. 47, Issue 6). https://doi.org/10.1016/j.neuron.2005.09.003